Tove Anette Haug

Dissolution and carbonation of mechanically activated olivine

- Investigating CO_2 sequestration possibilities

Thesis for the degree of Philosophiae Doctor

Trondheim, March 2010

Norwegian University of Science and Technology
Faculty of Engineering Science and Technology
Department of Geology and Mineral Resources Engineering

NTNU
Norwegian University of
Science and Technology

NTNU
Norwegian University of Science and Technology

Thesis for the degree of Philosophiae Doctor

Faculty of Engineering Science and Technology
Department of Geology and Mineral Resources Engineering

ISBN 978-82-471-1960-0 (printed ver.)
ISBN 978-82-471-1961-7 (electronic ver.)
ISSN 1503-8181

Doctoral theses at NTNU, 2010:5

Printed by NTNU-trykk

"The impossible cannot have happened, therefore the impossible must be possible in spite of appearances"

Agatha Christie, 1934

Preface and acknowledgements

The work presented in this thesis was mainly carried out at the Department of Geology and Mineral Resources Engineering (IGB) at the Norwegian University of Science and technology (NTNU) and the Institute for Energy Technology (IFE), a research institute for energy and nuclear technology in Norway, during the period of 2005 -2009. In addition 6 months were spent at Los Alamos National Laboratory during the fall of 2006. The PhD work was a part of the project "From Waste to Value", a collaboration project between IFE, IGB and NGU where utilization of CO_2 combined with mineral resources were the main focus.

The main objective of the PhD was to evaluate how energy-intensive milling influences the carbonation properties of olivine and evaluate the possibility of energy intensive milling as a pre-treatment method for ex-situ mineral carbonation. Financial support was retrieved from The Norwegian Research Council, the Department of Geology and Mineral Resources Engineering, and final support from Institute for Energy Technology (IFE). Supervisors have been Associate Professor Rolf Arne Kleiv (IGB), Professor Knut Lyng Sandvik (IGB) and Dr. Ingrid Anne Munz (IFE).

I will address a sincere thanks to all my supervisors, Associate Professor Rolf Arne Kleiv, Professor Knut Lyng Sandvik and Dr. Ingrid Anne Munz for giving me the opportunity to explore the relatively new research field of CO_2 storage, and their contribution of many hours of editing and commenting of manuscripts. Many ideas have been discussed discharged, reformulated, changed and rewritten during the course of the PhD work. Without your excellent help, the final version of my thesis would never have been born. Thank you, Rolf Arne, for taking the challenge of being a main supervisor for the first time. You did an excellent job for me and Professor Knut Lyng Sandvik. Great thanks is also send to John P. Kaszuba for making it possible for me to visit Los Alamos National Laboratory, USA and all the experiences included in a stay abroad. There I met J. William Carey who has been very kind and helped me with my modelling and language editing in parts of this thesis.

All my friends and colleagues deserve a sincere Thank You as well because of all positive support and technical and absolutely non-technical discussions. Sometimes the best a PhD-candidate can experience is homemade dinner after a long day at work without anything else to discuss than the latest gossip.

At last, but not least I will send my largest appreciation to my dear family: My parents for always believing in me, Ine and Birgitta for making dinner, coming for bike rides and giving me a roof over my head when necessary during these years, and Hans Edvard for being exceptionally patient with me and never giving up on my behalf. Now it is my turn to support your writing. Thank you!

Trondheim, September 2009

Anette Haug

Summary

Mineral carbonation used for CO_2 sequestration faces three main challenges: increasing the overall carbonation rate, handle large amounts of feedstock and products, and developing a practical process with commercially acceptable energy consumption.

High intensity milling, also called mechanical activation, has been found to increase the extraction rate of metals in the metallurgical industry. The focus of this PhD study has been the use of mechanical activation as a pre-treatment method within mineral carbonation as applied to CO_2 sequestration. Olivine was chosen due to the availability of this mineral in Norway. Experiments were conducted to determine how mechanical activation changed the specific surface area, particle size distribution and the crystallinity; and to explore how milling conditions and material characteristics were correlated with increased dissolution rates and increased extent of carbonation. A planetary mill was used in all experiments in addition to a laboratory ball mill, a pilot scale Hicom mill and a pilot scale Szegvari attritor when mechanical activation was evaluated for implementation within mineral carbonation. Finally the energy consumption during milling was evaluated in the context of CO_2 sequestration.

Over 60 olivine samples were prepared by milling including duplicates. Two dissolution experiments were performed, one at room conditions with 0.01 M HCl and one at 128 °C and 150 bar of CO_2. The specific dissolution rates of mechanically activated samples increased up to three orders of magnitude compared to an unactivated reference sample. Crystallinity as calculated from X-ray diffractograms was the material parameter with the best correlation with the measured dissolution rates. Specific surface area was only correlated to dissolution rates for samples with relatively high crystallinity. The particle size distribution was not correlated with the measured dissolution rates. Neither the dissolution rates nor the material characteristics were directly correlated with the extent of carbonation observed in the direct carbonation experiments at 185 °C and 115 bar of CO_2. The dissolution rates and crystallinity were partially correlated with the extent of carbonation obtained in the direct

carbonation experiments performed at 128 °C and 150 bar of CO_2. The interpretation was that in the 185 °C and 115 bar experiments, the extent of carbonation was mainly limited by precipitation kinetics of magnesite and silica, and was probably not limited by either the dissolution rate or olivine material properties.

The recognition of the importance of magnesite precipitation kinetics as an important factor of direct olivine carbonation has implications for the choice of pre-treatment methods and the design of the carbonation process used for CO_2 sequestration. To optimize the direct carbonation reaction the dissolution rate can only be increased to a certain level. Then the magnesite precipitation rate has to be increased by manipulating the saturation indices, the reaction conditions and the precipitation mechanisms. At conditions where the precipitation kinetics are important, the least energy consuming milling alternative can be used since the additional energy does not contribute to the carbonation rate. The ball mill was shown to be a good option.

To take advantage of the observed increase in the dissolution rates, the carbonation process can be divided into two or more steps in an indirect carbonation process. The first step is dissolution and the second, and possibly subsequent steps, are precipitation of secondary minerals. Dividing dissolution and precipitation into two process steps introduces increased requirements for equipment, and the optimization of mass flows and saturation indices has to take into account unwanted precipitation and equilibrium restrictions. Indirect carbonation using mechanically activated samples with a high dissolution rate can be a viable option within CO_2 sequestration, but the challenges of precipitation kinetics and energy consumption have yet to be solved.

Table of contents

Note on contributions

Paper I: Energy intensive milling of olivine used for CO_2 storage

Haug, T.A., Munz, I.A., Kihle, J., Kaszuba, J.P., and Carey, J.W.

This paper was written by T.A. Haug. The laboratory work was divided into two parts. The first part was milling of olivine in a planetary mill, and this work was performed by the candidate. The second part was flow-through experiments performed together with J. Kihle at Institute for Energy Technology. J.P. Kaszuba organized the analytical work performed on the flow-through residuals, and participated together with J.W. Carey to discussions and interpretations related to the geochemical reactions.

Paper II: Dissolution of mechanically activated olivine in hydrochloric acid - investigating leaching properties for carbonation purposes used for CO_2 storage

Haug, T.A., Kleiv, R.A. and Munz, I.A.

T.A. Haug performed the laboratory work after joint planning of the methods with R.A. Kleiv. Then the manuscript was written by the candidate, and thoroughly revised both by R.A. Kleiv and I.A. Munz, also contributing to the discussion and interpretation of the results and evaluating the importance of each result.

Paper III: Carbonation of mechanically activated olivine

Haug, T.A., Munz, I.A., Kleiv, R.A, Kaszuba, J.P. and Carey, J.W.

The manuscript was written by T.A. Haug. R.A. Kleiv helped with the choice of milling parameters and the revision of the manuscript. I.A. Munz contributed with extensive reading of drafts and comments regarding calculations, structure and content. J.P. Kaszuba helped planning the experiments and making the equipment available at LANL. J.W. Carey was helpful with the implementation of CO2 phases in PHREEQCi and some comments on the experiments and the final draft.

Paper IV: The importance of grinding solutions for mineral carbonation concepts

Haug, T.A., Kleiv, R.A. and Munz, I.A.

The final idea of this paper was found after several discussions between T.A. Haug, R.A. Kleiv and I.A. Munz. T.A. Haug performed the laboratory work and the main writing of the manuscript. Kleiv and Munz revised and commented the manuscript.

Abbreviations

Abbreviation	Explanation
AGU	American Geophysical Union
AWL	Accelerated Weathering of Limestone
BET	Method developed by Stephen Brunauer, Paul H. Emmett and Edward Teller for specific surface area measurements
C-1 and C-2	Name of carbonation experiment type 1 and 2
CCS	Carbon Capture and Storage
D-0 through D-3	Name of dissolution experiments type 0 through 3
IFE	Institute for Energy Technology
IGB	Department of Geology and Mineral Resources Engineering
IPCC	Intergovernmental panel of Climate Change
LANL	Los Alamos National Laboratory
NGU	Norwegian Geological Survey
NTNU	Norwegian University of Science and Technology
PCC	Precipitate Calcium Carbonate
PHREEQCi	Geochemical modelling program name, abbreviated from pH, redox and equilibrium, programmed with C language. i stands for interactive
SEM	Scanning Electron Microscope
SIP	Strategic institute program, founding program from the Norwegian research council.
SSA	Specific surface area
TC	Total carbon content based on weight [%]
XRD	X-ray diffraction
XRF	X-ray fluorescence

List of Figures

List of Tables

Part 1

Chapter 1. Introduction

1.1 General introduction

Mineral carbonation as an option for CO_2 storage has been proposed by several including Seifritz (1990) and Lackner *et al.* (1995). Ex-situ mineral carbonation is carbonation performed in an industrial plant, in contrast to in-situ carbonation where CO_2 is injected into geological formations. The chemical reactions leading to long-term storage of carbon dioxide are called CO_2 sequestration. Ex-situ mineral carbonation as CO_2 storage introduces an extra energy penalty during heat and power production if the CO_2 emitted must be stored. This energy penalty includes the energy required by mining the feedstock, transport of the feedstock, transport of the products, and the process energy. This energy consumption converted into costs has been studied for several minerals and industrial waste materials (e.g. Gerdemann *et al.*, 2007, Huijgen *et al.*, 2007, Huijgen *et al.*, 2005, Stolaroff *et al.*, 2005, Wu *et al.*, 2001) and the cost is still too high. Today the pre-treatment and/or the carbonation process is to energy consuming compared to the price of energy and the upper limit of CO_2 storage costs from an commercial point of view. Pre-treatment and process design therefore has to

be developed further. Several methods have been investigated to increase the total carbonation reaction and at the same time minimize the energy consumption. These methods include heat activation (McKelvy *et al.*, 2004), chemical activation (Maroto-Valer *et al.*, 2005), grinding (Summers *et al.*, 2005), additives in the reaction fluid and elevated process temperatures and pressures (O'Connor *et al.*, 2002).

Every mineral carbonation process will to a certain extent involve milling to reach a given particle size or a specific surface area of the material. Energy intensive milling, also called mechanical activation, changes the character of the material beyond reduced particle size and increased surface area (Tkáčová, 1989). Mechanical activation belongs to the science of mechanochemistry which is defined below:

"*Mechanochemistry is a branch of chemistry which is concerned with chemical and physico-chemical changes of substances of all states of aggregation due to the influence of mechanical energy"* (Baláž, 2008)

The elementary physical and chemical processes which take place during the straining of solids and which results in their mechanical activation is the basis for the theoretical study of mechanochemistry (Tkáčová, 1989). When the particles collide during mechanical activation, the impact force and the changes in the crystal lattice can produce local temperatures of 10.000 K (Baláž, 2008). The observed changes in the material properties resulting from the mechanical activation have been found to be very important for dissolution properties of minerals (Eggleston *et al.*, 1989, Sangwal, 1982), and may be one out of several ways of making mineral carbonation more attractive as a part of the solution for efficient CO_2 storage.

A range of minerals including wollastonite, olivine and serpentine, has been evaluated (Kojima *et al.*, 1997, McKelvy *et al.*, 2004, O'Connor *et al.*, 1999, Teir *et al.*, 2005), and silicates containing Ca, Mg and Fe can be considered as feedstock because these elements form stable carbonates. In a geological context a high density of relevant minerals are found within the ultramafic and mafic rocks containing large amounts of Mg and Fe. Norway has vast resources of olivine and other suitable minerals. Olivine is well

suited for laboratory experiments and large scale mineral carbonation and was therefore chosen as the mineral used in this PhD work. Norwegian olivine production was estimated to be 2.6 million tons in 2008 (NGU and Bergvesenet, 2009) and several deposits exceed 100 million tons (Roberts, 2008), and hopefully the findings for olivine milling and carbonation can be transferred into a general mineral carbonation context.

1.2 PhD project background and funding

The PhD was a part of the strategic institute program (SIP) "From waste to value: New industrial process for mineral dressing by use of CO_2 (158916/I30)". Institute for Energy Technology, Department of Geology and Mineral Resources Engineering at the Norwegian University of Science and Technology (NTNU), and Norwegian Geological Survey (NGU) were the main collaborating partners. The program was funded by the Research Council of Norway. Main objectives of the strategic institute program were to explore the aspects and possibilities of using CO_2 to increase the value of different industrial mineral resources. The project assessed the technical, economical, and environmental feasibility of using CO_2 in mineral processing. The intentions were to improve the quality and recovery percentage of the present products, and to develop new value added products by the reduction of waste. The program focused on the possibility of industrial use of CO_2 for reaction with silicates to form carbonates and improved silica products. A main challenge was to increase the overall reaction rate between the minerals including mineral dissolution and precipitation. Project manager was section head Ingrid Anne Munz at IFE and project period was 01.01.2004 until 31.12.2007.

The SIP included one doctoral fellowship resulting in this thesis. Main supervisor was Professor Knut Lyng Sandvik at the Department of Geology and Mineral Resources Engineering from 01.01.2005 until 01.04.2007, replaced by Associate Professor Rolf Arne Kleiv from 01.04.2007 and to the end of the fellowship. Sandvik continued as a co-supervisor after 01.04.2007. Ingrid Anne Munz was a co-supervisor the entire PhD period. The PhD fellowship exceeded the main program period mainly due to the initiation one year after program start, and also because of one year of

teaching duties at the Department of Geology and Mineral Resources Engineering.

1.2.1 International cooperation

Anette Haug visited Los Alamos National Laboratory (LANL) from June 2006 until December 2006 to obtain international experience and increase the collaboration between the SIP and the important network of scientists working with mineral sequestration. Main supervisor at LANL was John P. Kaszuba at the Isotope and Nuclear Chemistry Group at Chemistry Division. He is now employed at the Department of Geology and Geophysics at the University of Wyoming. Co–mentor was J. William Carey at the Hydrology, Geochemistry, and Geology group at LANL.

The work performed at LANL consisted of mineral characterization, geochemical interpretation of dissolution experiments, planning and performing a direct carbonation experiment, and participation with a poster presentation at the American Geophysics Union (AGU) conference in San Francisco, December 2006.

1.3 Aim and scope of the PhD study

The PhD results were meant to supplement the mineral carbonation research field with research related to the milling step in a carbonation process. Main focus was on mechanical activation with a laboratory planetary mill, and dissolution and carbonation of the milled samples. The energy consumption during a carbonation process has not been evaluated, only energy consumption during milling has been estimated. Key objectives were:

1. Describe the effect of mechanical activation on olivine particle size, specific surface area and bulk crystallinity calculated from X-ray diffractograms.
2. Describe how the particle size, specific surface area and bulk crystallinity calculated from X-ray diffractograms correlate to obtained olivine dissolution kinetics and conversion degrees.
3. Indicate large scale energy consumption during mechanical activation of olivine, and evaluate the possibility of using mechanical activation in a large scale CO_2 sequestration plant based on olivine carbonation.

1.4 PhD work overview

Emphasis has been put into experimental work and material characterization, and detailed information about the effect on olivine as a consequence of mechanical activation was the initial focus. Main analysis techniques were particle size distributions, specific surface areas and changes in crystallinity measured by X–ray diffraction. X–ray fluorescence was used to determine the chemical composition of the samples, often influenced by mill contamination due to ball/mill wear during milling. A laboratory planetary mill was used for most of the experiments, but a selection of mills was included in an effort to compare the similarities and differences between the mills in a practical context for possible scale-up. Figure 1.1 shows a flow sheet describing the development of the thesis focus following the black arrows. The uppermost box represents the initial focus.

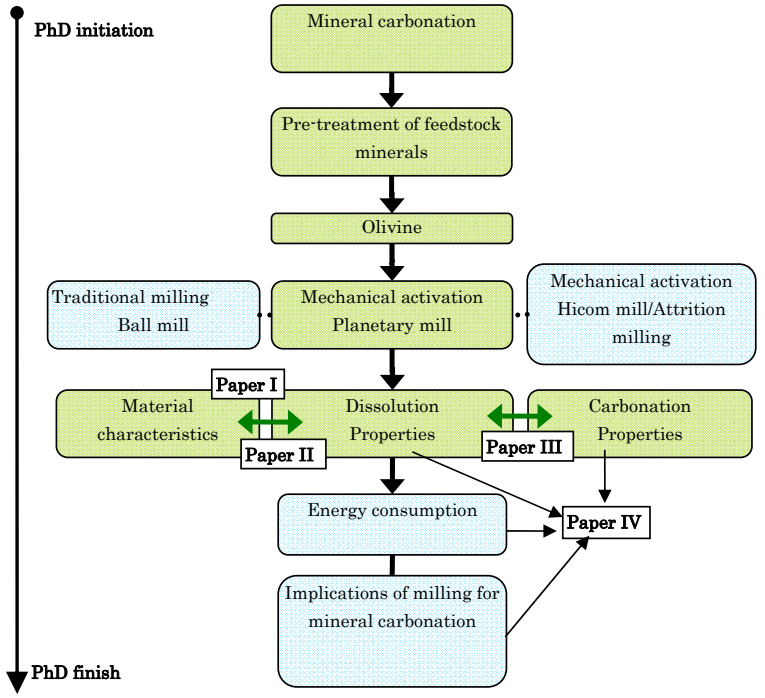

Figure 1.1 Flow sheet of the development of the PhD focus and research. Main focus has been paid to the topics in green boxes and some attention has been paid to the light blue boxes. The papers included in the thesis are shown in the flow sheet to illustrate the focus of each paper.

Aqueous olivine carbonation consists of two main reaction steps, dissolution and precipitation. These two steps can be performed separately or simultaneously. Since olivine dissolution comes prior to the carbonation, dissolution experiments were performed to relate material characteristics to the dissolution rates and rate constants. The results from the material characterization and dissolution experiments were used together to design two carbonation experiments. Analyses of residual materials, fluid composition and geochemical modelling with PHREEQCi were used to interpret the geochemical reactions.

The overall purpose was to evaluate the usefulness of mechanical activation as a pre–treatment method for carbonation processes, hence the final experimental work focused on the total picture of energy consumption during milling, related to how well the different milled samples were suited for a possible carbonation process. The total energy consumption from mineral resource to final chemical products is not included.

1.5 Outline of the thesis

This thesis consists of three parts. **Part 1** is an introduction, overview, and a general discussion which includes an overall conclusion of the PhD project. The focus of Part 1 contains a brief introduction to the scientific fields incorporated in the papers describing the experiments performed, summary of all papers, and the results of all papers discussed together. This discussion was the basis for the overall conclusions.

Part 2 is the assemblage of the four papers included in this thesis. Paper I was written for a mineral processing conference in January 2007, and is the earliest PhD–work included. Main objective of Paper I was to describe how mechanical activation affects the material characteristics of olivine when milled in a planetary mill. The three remaining papers were all written the last year of the PhD work. They were based on the material characteristics found in Paper I relevant for dissolution and carbonation. Paper II deals with the correlation between the material characteristics resulting from mechanical activation with a planetary mill and dissolution in hydrochloric acid. Paper III discusses the carbonation reaction of the mechanically activated samples used in Paper II with a focus of mass balances, conversion degree and dissolution rates compared to precipitation

rates. The dissolution kinetics and carbonation rate was studied experimentally for samples from four different mills including the planetary mill, and the energy consumption during milling was measured. The experimental data and maximum size of the four mills are indicated in Paper IV and the applicability of these mills in a carbonation context is commented. **Part 3** is the appendix containing an example of crystallinity calculation, summary of particle size distributions of relevant samples, and selected PHREEQCi modelling scripts.

Chapter 2. Background

2.1 CO_2 storage

Reactions between CO_2 and a vast number of minerals have been observed in many geological environments, and such processes leads to precipitation of carbonates over the geological time scale. A weathering reaction between silicates and atmospheric CO_2 with subsequent carbonate precipitation has been proposed as the great CO_2 sink when the earth was relatively young and the atmosphere contained much more CO_2 than today (Kojima *et al.*, 1997). However, not all carbonates are stable at the earth's surface, but calcite, magnesite and siderite are stable. The knowledge about the reactions between minerals and CO_2 has led to the suggestion that there is a potential of these observed weathering and carbonation reactions as CO_2 storage (Seifritz, 1990) and industrial reactions (Munz *et al.*, 2005, Song, 2006).

The research field of CO_2 storage is vast and includes many aspects. The technology of carbon capture and storage, often referred to as CCS, is multidisciplinary and includes various chemical, physical and practical aspects, energy consumption, and environmental and economical

considerations. The IPCC special report on Carbon dioxide Capture and Storage (IPCC, 2005) reviews the overall technology until 2005 and is summarized in the following text.

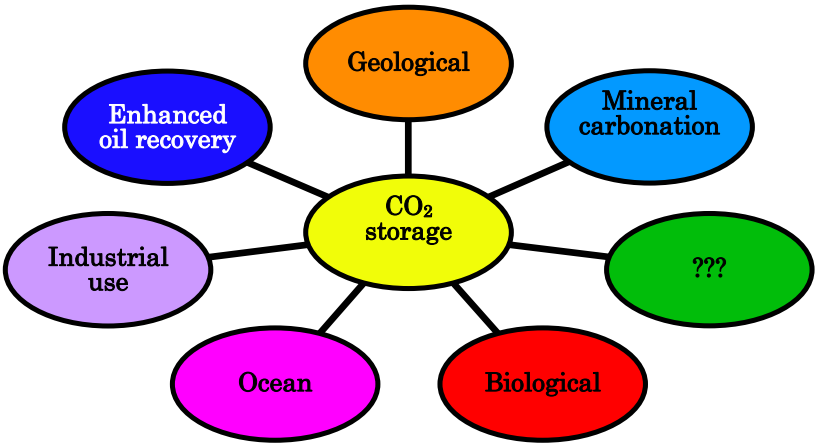

Figure 2.1 Main options of CO_2 storage alternatives (IPCC, 2005).

An illustration of possible ways of storing CO_2 is presented in Figure 2.1. As a consequence of the environmental concern about the emissions of greenhouse gases to the atmosphere, and especially CO_2 due to the large amount emitted, several ideas CO_2 use and storage have been discussed without reaching one specific final solution to the problem. Geological storage indicates injection of CO_2 into trapping geological structures as deep aquifers, oil reservoirs or coal beds. Enhanced oil recovery (EOR) takes advantage of the injected CO_2 to increase the net production of oil or gas from a reservoir, or possibly influence the use of coal beds. Storage of CO_2 at large depths in the ocean has been partially abandoned because of the high risks of leakage due to ocean currents and earthquakes. A new option of this alternative is to inject the CO_2 into the sea bottom sediments and hence make the CO_2 less mobile and possibly initiate mineral reactions, and by that stabilization.

The reaction between minerals and CO_2 happening during geological storage is being developed as an industrial process as well and is addressed as industrial mineral carbonation. Three main obstacles to overcome for ex-situ mineral carbonation is the reaction rate between the minerals and CO_2, the large amounts of CO_2 and solids needed to be mined, transported and

stored together with the challenge of low energy consumption. Mineral carbonation is described in more detail in the next chapter.

Carbonation reactions have been and are studied today for more reasons than exclusively CO_2 storage. In the processing industry CO_2 can be used as a leaching agent to retrieve and differentiate the metals in a mineral ore or be used in products containing carbon. Dissolution, precipitation and possibly separation may create enhanced products or new products. Good examples are precipitated calcium carbonate (PCC) and magnesium carbonate normally produced from heating and decomposition of naturally occurring carbonates. Calcium carbonates can be used in the paper industry as fillers. The silica residue may have potential applications e.g. in the cosmetic industry and as fillers in tires, and waste dumps are not the only option. The total amounts of products following large scale mineral carbonation will however produce so large quantities of solids that the marked for any by product will very likely be flooded if every process results in high quality products.

The last option in Figure 2.1 is "???". Science and development of technology can often take unexpected turns, and that may be important for CO_2 storage, i.e. the possibilities within biological activity are at least one possible additional way of CO_2 storage, and others may be found. CO_2 storage includes the aspect of growth of biological material, where algae producing H_2 and captures CO_2 (Skjånes *et al.*, 2007) is an example, and possibly biologically increased carbonate precipitation. Lackner *et al.* (2003) concludes that geological storage and possibly mineral carbonation are valuable options within the portfolio of CO_2 storage possibilities. The final solution will most likely be a portfolio of alternatives applicable dependent of the emission sources of CO_2 and capture and transport technology adjusted to local and regional opportunities.

2.2 Mineral carbonation

Mineral carbonation in an ex–situ storage or industrial chemistry perspective includes several important chemical considerations. The overall goal is to overcome the main challenges of slow reaction rates and possibly obtain useful products, and at the same time minimize the energy consumption of the reaction and minimize the costs. Several reviews

summarize the state of the art (i.e. Huijgen and Comans, 2003, Huijgen and Comans, 2005, IPCC, 2005, Sipilä *et al.*, 2008). The principal reaction of mineral CO_2 sequestration is given in equation 1 which is an exothermic reaction.

$$Ca/Mg/Fe\text{-}Silicate_{(s)} + CO_{2(g)} \rightarrow (Ca/Mg/Fe)CO_{3(s)} + SiO_{2(s)} \quad (1)$$

A number of attempts have been made to design a mineral carbonation process and Figure 2.2 shows an overview of possible carbonation alternatives. There are two basically different approaches to mineral carbonation, direct carbonation and indirect carbonation. During direct aqueous carbonation CO_2 and mineral reacts as equation 1 in one single reaction step. Precipitation is performed in the same reactor as the dissolution occurs. Typical additives are acids or complexing agents solved in water. If the reaction is divided into two or more steps, indirect carbonation is performed where dissolution and precipitation does not occur in the same reactor. Aqueous carbonation (direct or indirect) seems to be the most promising alternative with the largest research effort the last ten years (Huijgen and Comans, 2005, Sipilä *et al.*, 2008).

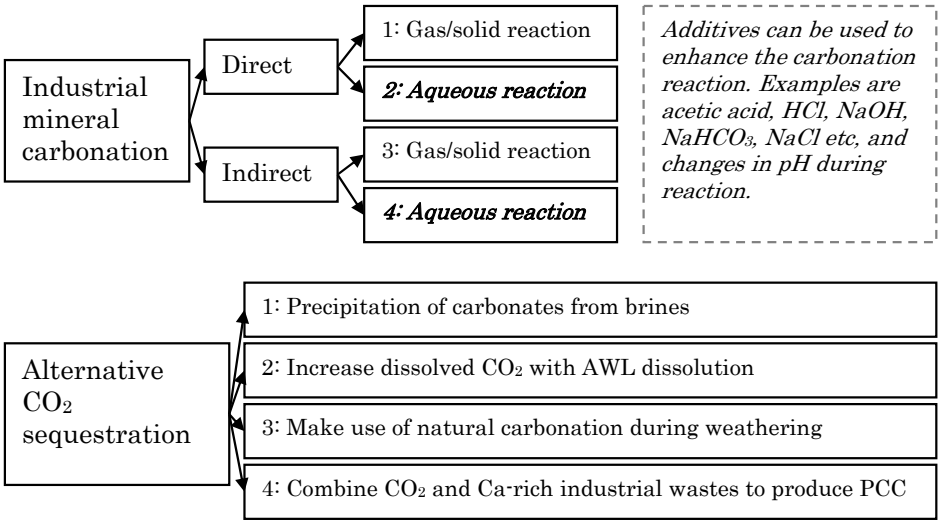

Figure 2.2 Overview of possible mineral carbonation routes (modified from Sipilä *et al.*, 2008). Mineral carbonation options used in experiments relevant for this PhD thesis are marked with bold and italic. Option 4 under industrial mineral carbonation was only studied in laboratory scale for the dissolution step, and not the precipitation step.

At alkaline conditions and high temperatures magnesite precipitation is favoured. Olivine dissolution favour high temperatures and low pH, but at high temperatures the pH also increases if carbonic acid is the only acid present. Hence, the magnesite precipitation behaves in the opposite way of the favourable olivine dissolution conditions regarding pH. Optimum reaction conditions are difficult to predict due to the complexity of the carbonation system. The slowest reaction determines the overall reaction rate, but the slowest partial reaction is dependent on the chosen reaction conditions as well. If direct carbonation is chosen, dissolution and precipitation kinetics has to be optimized together, but with a multiple step process, each step can be adjusted separately. Sipilä *et al.* (2008) concluded in their review that separating the dissolution step from the precipitation step probably is the most reasonable way to go and hence avoiding balancing two opposite reactions, despite the additional investment costs, challenges with mass balance and equilibrium considerations.

The last main carbonation alternative noted is "Alternative CO_2 sequestration" and includes the use of CO_2 in processes not directly linked to the two preceding categories, but they have some common technical aspects. Brines, highly saline waters being a waste product from the production of oil and gas, contain large amounts of elements possible to utilize for the precipitation of carbonates. AWL is accelerated weathering of limestone imitating dissolution of carbonate and produces a solution enriched in bicarbonate with a net reduction of gaseous CO_2 (Rau *et al.*, 2007). The simplest alternative is very close to the natural carbonation silicates. Just spreading Mg/Ca/Fe–rich minerals, for example olivine, on the ground and let it react with the surrounding CO_2 and possibly seawater without any processing plant or high investment costs. The last alternative has been evaluated to be a niche supplement to CCS more than a large scale alternative (Hangx and Spiers, 2009). The knowledge about precipitated calcium carbonate (PCC) can be utilized to optimize the products from the carbonation processes.

2.2.1 Aqueous carbonation chemistry

Limiting the chemical description to industrial mineral carbonation without additives, there is a set of important partial reactions which has to be

considered. Equation 1 is the overall general carbonation reaction, but when studying the carbonation reaction in detail, the carbonation reaction is complex. There are three general reactions including the dissolution of CO_2 in water (equation 2) creating dissociated carbonic acid and resulting in a lowered pH. This acid is dissolving the chosen mineral and the compounds in the resulting solution can result in precipitation either directly or in a subsequent step if preferred. As an illustration the dissolution of CO_2 and the dissolution of Mg–rich olivine through acid consumption (equation 3) and precipitation (equation 4) are shown in the following reactions.

$$CO_2 + H_2O \leftrightarrow H_2CO_3 \leftrightarrow HCO_3^- + H^+ \leftrightarrow CO_3^{2-} + H^+ \quad (2)$$

$$Mg_2SiO_4 + 4H^+ \rightarrow 2Mg^{2+} + H_4SiO_4 \quad (3)$$

$$Mg^{2+} + CO_3^{2-} \leftrightarrow MgCO_3 \quad (4)$$

The net aqueous carbonation reaction where water is excluded since it only has a catalytical effect, then becomes as described in equation 5.

$$Mg_2SiO_4 + CO_2 \rightarrow 2MgCO_3 + SiO_2 \quad (5)$$

Several papers have been devoted to describe the carbonation of olivine together with serpentine and other relevant minerals. (i.e. Alexander *et al.*, 2007, Bearat *et al.*, 2006, Bearat *et al.*, 2002, Carey *et al.*, 2003, Chen *et al.*, 2006, Gerdemann *et al.*, 2007, Giammar *et al.*, 2005, Guthrie Jr *et al.*, 2001, Huijgen and Comans, 2003, Huijgen *et al.*, 2007, Jadhav *et al.*, 2002, Jia *et al.*, 2004, Kalinkin *et al.*, 2003, Kleiv *et al.*, 2006, Lackner *et al.*, 1995, Lichtner *et al.*, 2003, Maroto-Valer *et al.*, 2005, McKelvy *et al.*, 2004, O'Connor *et al.*, 1999, O'Connor *et al.*, 2002, Park and Fan, 2004, Park *et al.*, 2003, Summers *et al.*, 2005, Wu *et al.*, 2001, Zevenhoven and Kavaliauskaite, 2004, Zevenhoven *et al.*, 2008).

Lackner *et al.* (1995) have made a summary of the thermodynamically properties of relevant substances and minerals relevant for the carbonation reaction. Thermodynamically the total carbonation reaction occurs spontaneously and creates varying amounts of heat dependent of the chosen mineral and reaction temperature, but there are problems with slow or not favourable intermediate partial reactions heavily influencing the measured carbonation rates. The reaction rates can be

manipulated with changes is the temperature (T), the pressure (P), the pH, additives or pre-treatment of the feedstock material. These five factors influence the dissolution rate of CO_2 in the reaction solution, the dissolution rate of the mineral and the precipitation rate. The pre–treatment aims at increasing the dissolution rate by increasing the specific surface area, make the material more amorphous, increase the porosity or change the overall properties in some other way by making the material less stable.

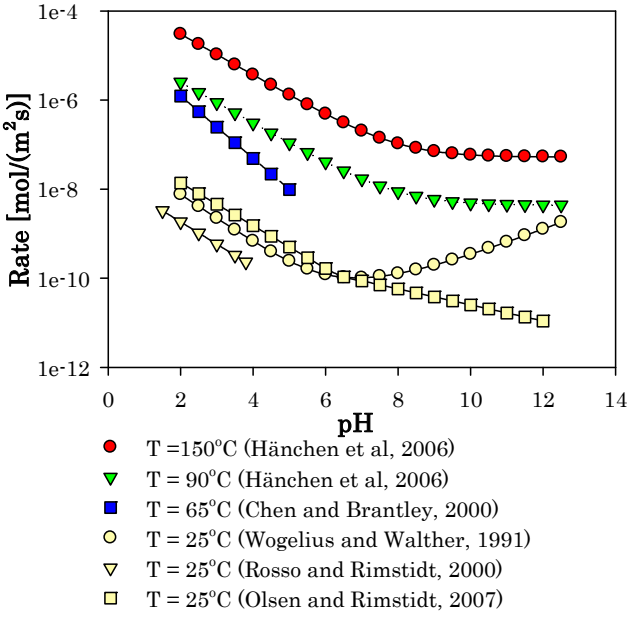

Figure 2.3 Olivine dissolution rates in a dilute solution as a function of pH, 4 temperatures.

The three main reactions listed as equation 2 and 3 are dependent of T, P and pH. Equation 4 is also dependent on T and P, and indirectly on pH since the carbonate equilibrium is dependent on pH. In the following text these important reactions and dependence of process conditions are discussed for olivine starting with the influence of pH on olivine dissolution rates at different temperatures in Figure 2.3. Figure 2.3 shows olivine dissolution at temperatures from 25 °C to 150 °C at ambient pressure and the experiments were performed with HCl or NaOH or LiOH to obtain the wanted pH. Olivine dissolution rates at pH below 8 are relatively well documented, but the uncertainties above pH = 8, are large. The difference between the three different rate models for 25 °C indicates some of the

variations possible to observe. Low pH gives the highest dissolution rates, and the rate increases with temperature.

The rates presented here are only valid for the conditions they are calculated for, and the presence of high CO_2 concentrations at high pH values can inhibit the reaction rate and organic acids can increase the dissolution rate compared to HCl (Hänchen *et al.*, 2006, Wogelius and Walther, 1991). Other additives and high solution concentrations can be very important as well. Mg and Al concentrations are probably not important for the dissolution of olivine (Chen and Brantley, 2000). Giammar *et al.* (2005) indicated that the concentration of Si in the reaction fluid was controlled by the equilibrium of amorphous silica. During extensive dissolution of olivine an Mg – depleted layer may be formed (Bearat *et al.*, 2006, Pokrovsky and Schott, 2000), or a silica layer resulting from precipitation (Giammar *et al.*, 2005, O'Connor *et al.*, 2002), which both can be inhibiting the olivine dissolution rate. Iron from olivine may form oxyhydroxides on the olivine surface as well (Giammar *et al.*, 2005).

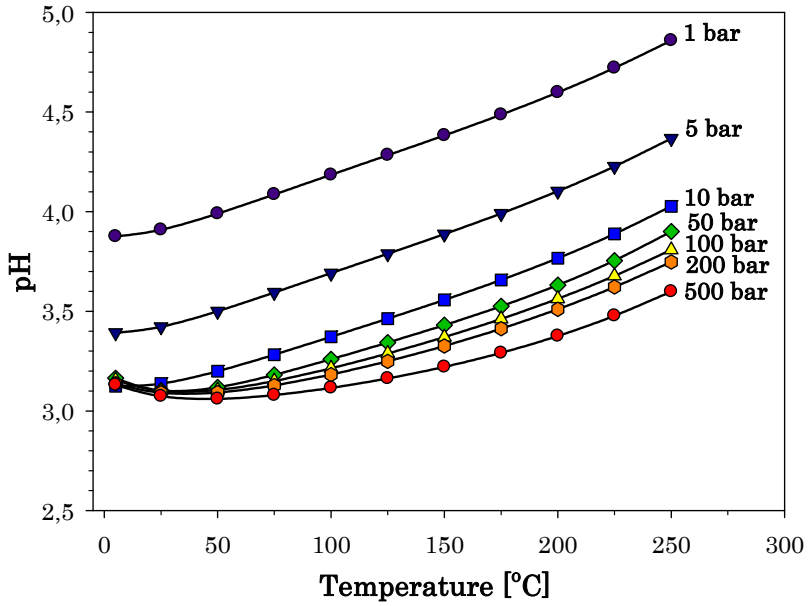

Figure 2.4 Effect of the CO_2 pressure and temperature on pH when CO_2 dissolves in pure water. Modelled with PHREEQCi

Aqueous carbonation using only olivine, water and carbon dioxide, is dependent of the pH (Figure 2.4) caused by dissociation of the carbonic acid,

the relative concentrations of the carbonate species (Figure 2.5) from equation 2, and the total amount of dissolved CO_2 (Figure 2.6). pH, temperature and pressure are included in the figures when relevant.

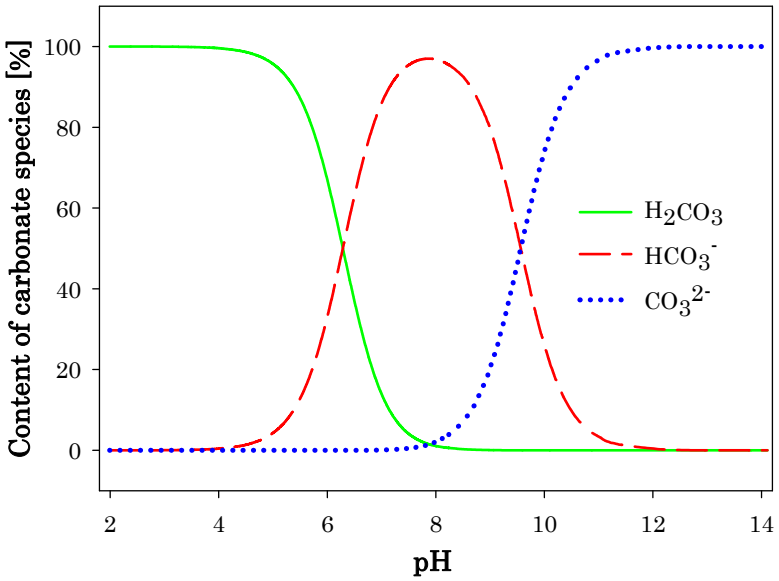

Figure 2.5 Carbonate species calculated with 25 °C, a CO_2 pressure of 1 bar and initially pure water.

The choice of pressure and temperature for the carbonation reaction is not straight forward. Low pH increases the dissolution rate of olivine, but reduces the precipitation of carbonates. Low pH is obtained at high pressures when mixing water and CO_2, but above 50 – 100 bars, the effect on pH of an additional pressure increase is limited. This pH is the initial reaction pH and will increase during dissolution of olivine. The final pH is very dependent on the process design and liquid/solid ratios. The distribution of the concentrations of $H_2CO_3^{*(1)}$, HCO_3^- and CO_3^{2-} which are very dependent of pH is important for the saturation of magnesite which has to be achieved during direct carbonation and avoided in the first step of indirect carbonation. Figure 2.5 shows how these species are distributed at different pH. If no other acid or base is added, the pH normally will be between 3 and 5 for relevant P and T, and HCO_3^- will be the dominating species in the solution.

[1] $H_2CO_3^* = H_2CO_3 + CO_{2(aq)}$

Precipitation is governed by two mechanisms, nucleation and crystal growth. Depending on suitable precipitation sites and degree of super saturation one of the two mechanisms is dominating. If suitable surfaces are available, here carbonate particle surfaces are the best option, crystal growth will happen on the existing surfaces. When the initial precipitation from the solution happens directly on surfaces, the precipitation is limited by crystal growth, otherwise nucleation is most important. If no surfaces are available, nucleation is important in the beginning, but gradually crystal growth will be more important as the precipitated mass is increasing. Recognition of the precipitation mechanisms in each given mineral carbonation process is important of two reasons. Firstly, if precipitation occurs onto the feedstock grains the dissolution rate can be reduces, and secondly intergrown particles are difficult to separate compared to free particles.

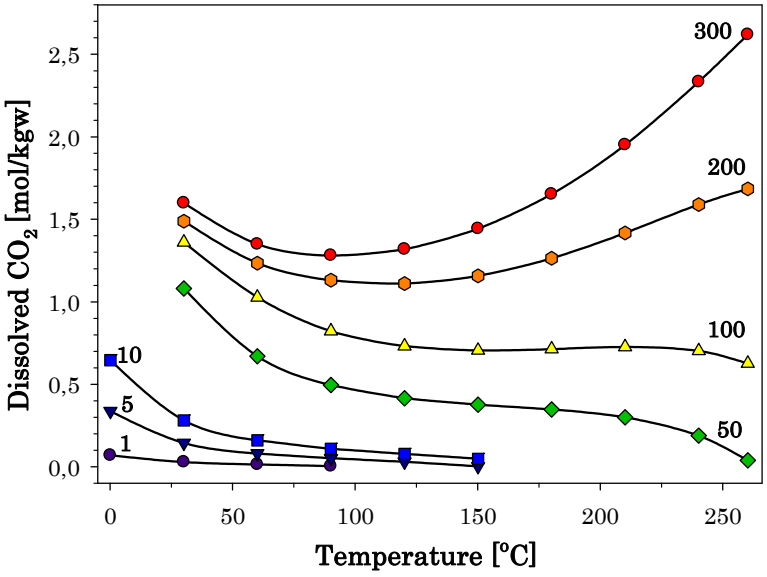

Figure 2.6 Total CO_2 solubility in pure water at different CO_2 pressures and temperatures (tabulated data from Duan and Sun, 2003). Numbers related to each line in the graph represents the CO_2 pressure from 1 bar to 300 bars.

The literature published about magnesite precipitation (geology) or magnesium carbonate (chemistry) is normally descriptive of when precipitation occurs (Giammar *et al.*, 2005, Hänchen *et al.*, 2008, Sheila and

Khangaonkar, 1989, Teir *et al.*, 2007), more than a quantitative description of the precipitation rate (Pokrovsky, 1998). An explanation for the lack of precipitation kinetics is the complexity of magnesite precipitation reaction (Hänchen *et al.*, 2008).

2.3 Conventional comminution

The knowledge about valuable minerals and metals in rocks and sedimentary deposits has been so essential that the human history timeline have been named after the dominating resources; stone age, bronze age and iron age. Today a vast amount of minerals and metals are extracted from the earth and used daily. Mineral processing includes the technology extending from the transport of rock fragments after blasting until the valuable minerals are liberated and separated from the waste minerals. An overview of mineral processing is given in several books (Austin *et al.*, 1984, Sandvik *et al.*, 1999, Weiss, 1985, Wills and Napier-Munn, 2005).

Minerals are homogeneous, natural occurring, solid, inorganic substances with a defined crystal structure, a defined chemical composition or constant chemical and physical properties. Hard rocks are constituted of several minerals and have to crushed and ground to liberate a wanted mineral and then separate the valuable mineral form the gauge minerals. The technology concerned with particle size reduction until a defined particle size, often related to the size of mineral grains, is called comminution. A short introduction to conventional comminution is presented here without further references to the mentioned works. Other references are included when needed. Mineral processing includes a typical sequence of steps as shown in Figure 2.7.

Figure 2.7 Generalized mineral processing flow sheet

Comminution takes place in a sequence of crushing and grinding stages because it is practically impossible in one step to reduce the particle

size from 1 m as can be found for blocks in the mining pit to < 300 μm which can be necessary to liberate valuable mineral grains. A reduction ratio can be defined to be the ratio between the maximum particle size entering to the maximum particle size leaving the crusher and reduction ratios of the crushing stages are from three to six in each stage. Crushing is normally performed on dry materials by compression of hard crystalline rocks between rigid surfaces or by impact against surfaces in a fixed motion path more used for brittle or loose rocks. Typical examples of compression equipment are jaw crushers, where Figure 2.8A represents a cross section, and cone crushers. The barmac crusher is a modern impact crusher.

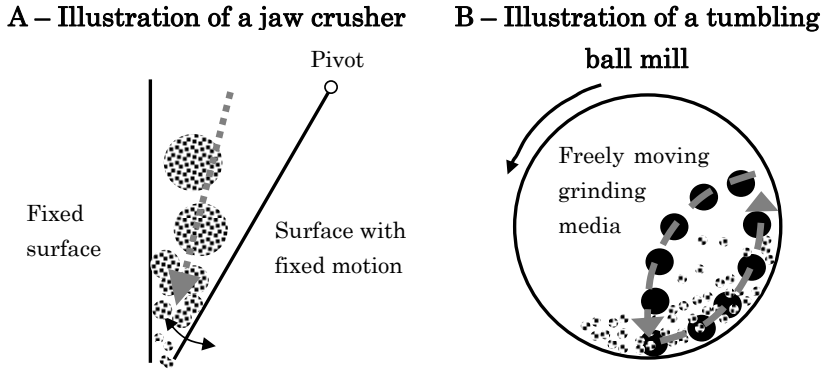

Figure 2.8 Illustration of crushing (A – jaw crusher) and grinding (B – ball mill).

In contrast to crushing, grinding (milling) is accomplished by abrasion and impact of the ore by the free motion of unconnected grinding media such as rods, balls, or pebbles. Dry grinding has limited applications and most grinding is performed wet, creating a slurry of dispersed particles in water. Additives, as dispersing agents, can be used to inhibit flocculation of the particles. Tumbling ball mills rotates around a horizontal axis, where Figure 2.8B illustrates a cross section of a ball mill including the movement direction, are common within commercial grinding. Typical size reduction of particles is from 5 mm – 250 mm to a size to between 40 μm and 300 μm. These mills are restricted by the fact that at high rotational speeds, the mill charge will be centrifuging, and no grinding will occur. Stirred mills (attritors) are ball mills with a stirring device in the centre and do not have an upper limit for the speed due to the construction of the mill where the

stirring devise can rotate as fast as allowed by the equipment strength. Attritors can operate with smaller media sizes than tumbling mills, therefore they are more suited for fine grinding purposes than ball mills. Stirred mills find application in fine (15-40 μm) and ultra-fine (<15 μm) grinding, also called micronizing.

The final particle size is dependent on the rock, the grain size in the rock, the chosen mill, size of grinding media, weight distribution of grinding media and grinding time. The choice of mills and operational settings are increasingly important when the desired particle size is reduced, and normally smaller balls are used to produce smaller particles (Stražišar and Runovc, 1996). The desired particle size distribution is normally defined by the liberation of the wanted mineral or the application of the ground product, whether it is a metallurgical process extracting gold, carbonates used as paper filler or crushed stone for road construction etc.

2.4 Grinding energy

2.4.1 Mill power

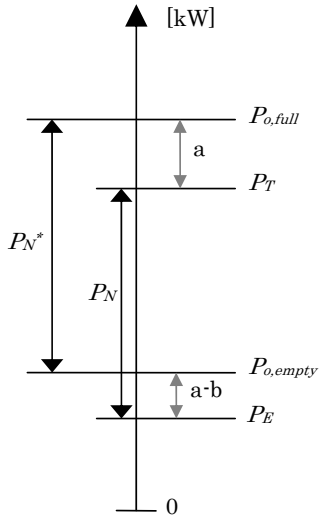

$P_{o,empty}$: Operational power, empty load
$P_{o,full}$: Operational power, full load
P_E : Power used to rotate mill, excluding friction and transmission loss when empty
P_T : Power used to rotate mill, excluding friction and transmission loss when full
P_N : True net power delivered from mill to mill charge
P_N^* : Estimated net power delivered from mill to mill charge using power measurements
a : Power loss due to motor inefficiencies and friction loss in transmission at full load
b : Reduction in power loss because of reduced load when empty

Figure 2.9 Definition of power terms relevant for mill power and mill energy calculations.

The total measured power draw from the power grid, also called the operational power P_o, consists of the power used for rotation of the mill including all the power losses due to inefficiencies in the motor and the

transmission of the power from the motor to the mill. These power losses are determined by the mill and motor design, and are influenced by the mill load. A higher mill load will give rise to higher power losses. Figure 2.9 shows how the power measurements of a mill are related to the power transmitted to the mill charge. No direct numbers are put into Figure 2.9 because all values are mill specific, and the ratio between the parameters varies.

Two parameters from Figure 2.9 are normally used when discussing the power draw of mills. The first, $P_{o,full}$ represents the total power use of the mill and hence is the relevant parameter when discussing the overall economy of a milling operation. Secondly, P_N is the net power transmitted to the charge and hence influences the resulting grinding product. For practical purposes P_N is calculated by equation 6. The only difference between P_N and P_N^* is the change in power loss due to the change in total weight of the mill from full load to empty mill, which can be difficult to determine. The magnitude of this additional loss, b, is assumed to be negligible compared to P_N.

$$P_N \approx P_N^* = P_{o,full} - P_{o,empty} \tag{6}$$

Heating of the mill, production of sound, creation of new surfaces, particle size reduction and changes in crystallinity are all contributing to P_N, and only a fraction of 0.6 % to 3 % of P_N has been estimated to be available for the physical breaking of the particles (Lynch, 1977, Wills and Napier-Munn, 2005).

2.4.2 Estimating energy consumption during milling

Not only the power draw is significant, but the total and net energy used to produce a given amount of material with a set of specific properties is an important parameter. There are several challenges trying to relate energy consumption to material properties like particle size and surface area. An empty mill consumes energy, water in the mill influence the mill charge movement, the stabilization of the mill is important, energy is lost due to the efficiency of the motor and mill mechanics, the particles are heated, elastic deformation can occur and so on (Lynch, 1977). In addition to the general considerations for energy loss, the choice of mill and the mill

size play an important role when trying to measure and calculate the mills energy consumption.

Energy consumption is considered to be some function related to the initial and final particle size. Several empirical equations have been developed to estimate the energy needed to reach a certain particle size, and Lynch(1977) has given an overview of the relationships dedicated to Rittinger, Bond and Kick valid for different ranges of particles. The net milling energy can be estimated for ball mills with the formula of Bond if particle sizes of feedstock and product are known. Bond's work index formula, equation 7, is the most common equation used (Wills and Napier-Munn, 2005). Bond's work index, W_i, is material specific and found with a standardized laboratory test (Bond, 1961a, Bond, 1961b). W_i is defined to be the net specific energy needed to grind a mineral from an assumed infinite size to d_{80} = 100 μm in a ball mill using the particle size, where d_{80} represents the particle size where 80% of the sample is smaller than the given value. d_{80} of the feedstock and the mill product are used together with W_i as input parameters in the formula. For accurate energy consumption, direct measurements are the best option.

$$W_N = 10 \cdot W_i \left(\frac{1}{\sqrt{d_{80,product}}} - \frac{1}{\sqrt{d_{80,feed}}} \right) \tag{7}$$

2.4.3 Energy calculations

P_O and P_N, together will milling time, t, and the sample mass during milling, m, are the main parameters needed when performing energy consumption calculations. The formulas described here are used for batch processes, but the same relationship exists for continuous milling, but in that case mass is divided by time, giving the mass flow. "Total" indicates a parameter relevant for the overall energy consumption of the milling process, while "net" parameters are related to the energy consumption used to change the material properties. In a batch process, the net specific mechanical work exerted by the mill charge, W_N, is described in equation 8. Total specific energy consumption of the mill, W_O is found by replacing P_N by P_O.

$$W_N = \frac{P_N}{m} \cdot t \tag{8}$$

$$\text{Energetic efficiency} = \frac{P_N}{P_o} \cdot 100\% = \frac{W_N}{W_o} \cdot 100\% \tag{9}$$

$$I = \frac{P_N}{m} \tag{10}$$

The ratio between net and total energy consumption is defined to be the energetic efficiency, calculated by equation 9. Generally large scale mills have better energetic efficiencies than laboratory– and pilot scale mills and low intensity mills have higher values than high intensity mills. Large scale ball mills have an energetic efficiency of approximately 90 % (Kheifets and Lin, 1996) to 95 % (Musa and Morrison, 2009), while for planetary mills a rule is 60 %-70 % (Kheifets and Lin, 1996). These energetic efficiencies must not be confused with the energy purely used for breaking of the particles as mentioned in chapter 2.4.1.

A comparison of products produced with different W_N, or in different mills or with different settings, can tell us how efficiently the available energy have been utilised to achieve the resulting material characteristics. A large W_N can have a small effect on the material and vice versa. The energy intensity is important in addition to the energy consumption. The net energy intensity can be expressed as shown in equation 10. If P_N is replaced by P_O, the total energy intensity is found. Variation in the intensity can result in changes in the output characteristics, despite the same net specific energy consumption.

2.4.4 Measurements

Power measurements are essential when performing energy calculations. Continuous logging of the power draw from an empty laboratory mill will show how the power draw decreases simultaneously as the motor and mill parts are warmed up during motion. Obtaining the most realistic measurements of the power draw required to produce a sample needs to take into the effect of a cold or a warm mill. The mill has to be run for a necessary amount of time to become warm. This warm up period can be

found by logging the power draw continuously during an initial warm up test period. From this curve the necessary warm up period can be found.

Another aspect during power draw is the effect of decreasing particle size of the sample inside the mill. During milling the particle size decreases and the motion of the steel balls may change and be damped by the surrounding sample. The effects of mill heat and sample influence are best taken into account when the power draw is measured several times during a batch and for the same duration as the batch, preferably the batch that produces the given sample. The mill is run empty to measure $P_{o,empty,}$ and $P_{o,full}$ can be measured when the chosen batch is run. Mill intensity and energy consumption can then be calculated with equations 6, 8 and 10.

2.5 Mechanical activation

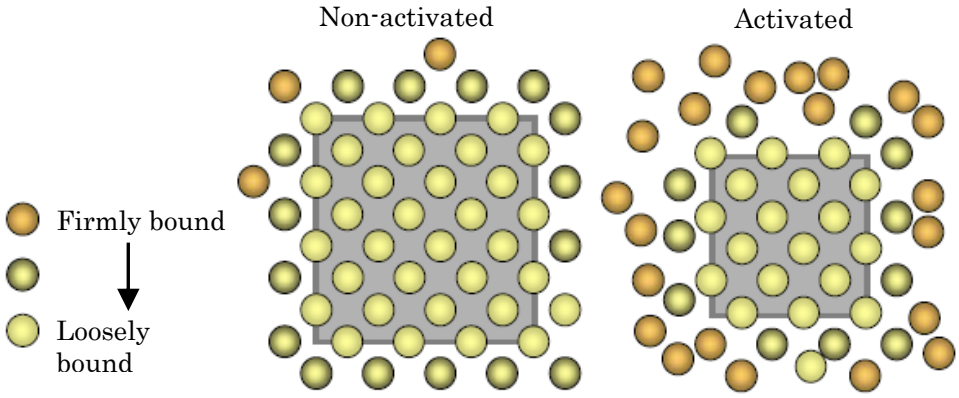

Figure 2.10 A conceptual two dimensional illustration of the arrangement of atoms prior to and after mechanical activation (Kleiv, 2007).

Chemical reactions as an effect of introducing mechanical energy were documented as early as 1882 by M. Carey Lea (Historical review by Baláž, 2000). The following description of mechanical activation is based on three important books written by Tkáčová (1989) and Baláž (2000, 2008) and further details are found within them. Additional references are mentioned when necessary. Mechanical activation can be described as very intensive milling, and changes the character of a material beyond reduced particle size and increased surface area. Mechanical activation can be seen as an extension of fine grinding from a mineral processing point of view, where

the primary aim is to achieve a more reactive product, rather than a further decrease in particle size or mineral liberation, through mechanically induced structural or chemical modifications.

Primary effects of mechanical activation are a decrease in particle size, an increase of surface area, an increase in internal and surface energy, and a decrease of the coherence energy of the solids. These effects can partially be detected directly by specific surface area measurements and calculation of crystallinity or indirectly by changes in reactivity. *Secondary* processes as aggregation, adsorption and recrystallization can occur during and after grinding has taken place. Figure 2.10 illustrates the effect of mechanical activation on a crystal lattice, and the crystallinity obtained after alteration, can be estimated (Baláž, 2000, Ohlberg and Strickler, 1962). Chapter 2.6.3 describes the crystallinity calculation from an X-ray diffractogram. During and after activation the crystal lattice is not in equilibrium and the excess energy caused by disordering contributes to lowering the activation energy of any following reaction of the material (Tkáčová, 1989, Tromans and Meech, 2001). However, the effect of mechanical activation is time dependent as indicated by Figure 2.11.

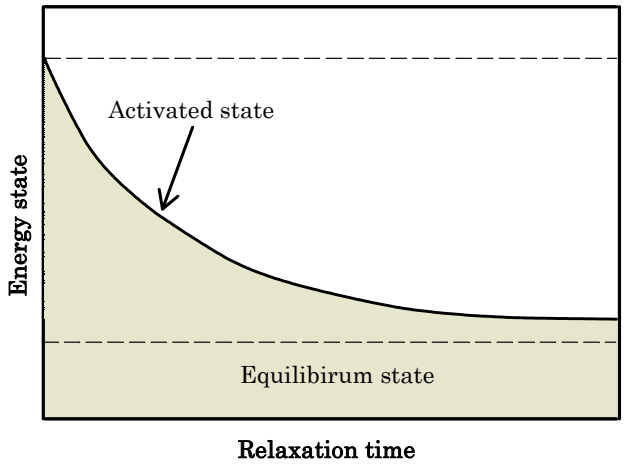

Figure 2.11 Illustration of how the increase in material energy decreases in a mechanically activated material and approaches equilibrium with time.

The mills used for mechanical activation have several times higher energy intensity than conventional tumbling mills and typical mills are planetary mills, vibratory mills, stirred ball mills (attritor), pin mills and

rolling mills. Within the grinding technology, mechanical activation is a pre-treatment option normally used for two purposes, mechanically alloying or increasing the leachability of metal ores in the hydrometallurgical industry. Here leachability indicates the ability to dissolve metal from the constituents of a metal ore. Hoberg and Götte (1985) found that the effect of mechanical activation on the leaching rate of columbite, decreased with increased dissolution as a consequence of decreasing activation of the residual solids. The effects on material properties such as favourable structure or composition of the surfaces can be taken advantages of within adsorption, catalysis and mineral synthesis.

2.6 Fundamental analyses of activated materials

Three parameters have been of particular interest during this PhD work when characterizing mechanically activated materials: the particle size, the specific surface area and the degree of structural disorder. Normally these three material properties are analysed with respectively laser diffraction, BET analysis and X–ray diffraction. The laser diffraction and BET analysis equipment interpret the measurements automatically and gives the results directly in a volume% versus particle size [μm] and specific surface area [m^2/g]. Each of these analytical techniques is trying to describe a material property, but simplifications in the apparatus and the used equations introduce some possible discrepancies between the measured values and the true values. In chapter 2.6.1 through 2.6.3 relevant analytical techniques are described, including possible uncertainties introduced by the technique. Porosity can also be important, but has not been included.

2.6.1 Laser diffraction

The method is based on diffraction of a laser beam when passing through a fluid with dispersed particles. When the light hits a particle, the light is diffracted. As the particle size increases the angle of diffraction decreases. This is an indirect method where the particle size is an interpretation of the diffraction pattern. Agglomeration due to e.g. van der Waals forces and electrostatic forces of the dispersed particles are normally avoided by adding a dispersing agent to the dispersion. Mechanically

activated samples may have charged surfaces due to the rapidly broken crystal bonds, and the fines are mechanically alloyed due to the mechanical impact and this may create agglomerates may not be possible to disintegrate by ultrasound and the dispersing agent. The result is that the particle sizes are overestimated. Another disadvantage of this method is that the diffraction pattern does not reveal anything about the particle shape and the existents of aggregates in the initial materials. Aggregates will be interpreted as large particles instead of several small particles. Irregular shaped minerals, with asbestos as a good example, will diffract the light differently depending on the orientation. Hence, the particle size distribution will appear broader than results measured by sieves, microscopy or other techniques (Snilsberg, 2008).

2.6.2 BET analysis

Specific surface analysis by the BET – analysis was developed by Stephen Brunauer, Paul Hugh Emmet and Edward Teller who published an article about the BET theory in 1938 (Brunauer *et al.*, 1938). The measurement is based on gas adsorption onto the surface area of the particles. Surfaces of porous and complex particles can be measured as long as the pores and cracks are larger than the gas molecules. This adsorption is performed close to the boiling point of the gas, and at that condition the area covered by each gas molecule is known with a large degree of certainty. Allowing several monomolecular layers to form, measure the amount of gas adsorbed and interprets the results with the BET theory about multilayer adsorption, makes it possible to estimate the specific surface area of a solid sample.

BET measurements of mechanically activated materials does not reveal the amount of steps and kink sites on the surfaces and within fractures of the materials. Hence materials with the same specific surface area may have very different surface topographies.

2.6.3 XRD

X-ray powder diffraction (XRD) has a main application within detection of crystalline minerals. To some extent also quantification can be made, if standardized and calibrated methods have been developed. A carefully prepared sample is exposed to monochromatic X-rays, and due to

varying lattice distances in different minerals, the rays are diffracted differently depending on the given minerals. Each mineral have a set of distinct refraction angles. The structure of a real mineral will affect the measurement with several factors as microstructure, chemical composition, phase boundaries, grain sizes, crystallographic orientation, grain boundaries, dislocations and point defects etc (Baláž, 2000).

When XRD is used to analyse mechanically activated samples, changes in the crystallinity can be detected. Due to deformation and breakage of crystal bond, the refracted rays will become more dispersed since the lattice distances have been exposed to elastic and plastic deformation caused by milling. The number of rays measured at the same angle will decrease, and several rays will be detected in the close surrounding of a distinct angel of a given minerals. If the angle, referred to as 2 theta, is plotted versus the frequency of rays counted for each angle, the resulting graph is a XRD diffractogram. There are several observable features in an X-ray diffractogram when the crystallinity decreases. The background level increases and the peaks get lower and wider. Crystallinity calculated from an XRD - diffractogram, C_{XRD}, of a milled sample can be calculated by measuring the average background levels, B_o and B_i, and the integral peak areas, I_o and I_i, above the background level for all samples, using equation 11. Indices i and o refers respectively to a mechanically activated sample, and the original sample representing a 100% crystalline material.

$$C_{XRD} = \frac{I_i}{I_o}\frac{B_o}{B_i}\cdot 100\% \qquad (11)$$

C_{XRD} is a bulk property for a given material and summarizes the effects of particle size distributions where fines are very important, the crystallite sizes and the deformation of the crystal lattice. See appendix A1 for an example of the calculation. C_{XRD} represents a value combining the effect of decreasing crystallite size, strain and amorphization, and can also be influenced by changes in the particle sizes due to milling if the mechanically activated material contains large amounts of fines.

Chapter 3. Key experiments – overview and main purposes

Over sixty olivine samples have been prepared by milling from one original olivine sand quality, and dissolution and carbonation properties have been investigated. In the following text an overview of the experiments are given and the main purposes of the experiments are presented. Additional experimental details can be found in the papers.

There were two main purposes behind all the milling solutions. The first purpose was to describe the effect of milling parameters on the obtained olivine characteristics as specific surface area, particle size distribution and crystallinity. The second purpose was to evaluate how the differently milled samples behaved during dissolution or direct carbonation and how these reactions were related to the material characteristics and energy consumption during milling. All the experiments included in this thesis are summarized in Table 3.1 and all milling combinations are described in chapter 3.1 and summarized in Table 3.2. Two dissolution experiments were used (experiment D-0, experiments D-1/D-2/D-3) where the second design included different acid volumes and olivine sample

masses. Two designs of direct carbonation experiments were performed as well (C-1 and C-2).

Table 3.1 Specific data for the dissolution experiments marked with a D, and the carbonation experiments marked with C.

Exp. type[2]	Number of valid exp.	Volume	Mass of olivine [g]	Temp [°C]	Pressure [bar]	Duration	Stirring	Mills used to prepare samples[3]	Papers including the experiments
D-0	5	Continuous flow	0.1-1.4	128	150 CO_2	18-72 h	Yes	PM	I
D-1	22	500 ml HCl 0.01 M	0.5	21.5	1 air	1-24 h	500 [RPM]	ALL	II/IV
D-2	3	2000 ml HCl 0.01 M	2.0	21.5	1 air	2-24 h	750 [RPM]	PM	II
D-3	15	500 ml HCl 0.01 M	2.0	21.5	1 air	1-24 h	500 [RPM]	ALL	II/IV
C-1	20	3 g DI H_2O	0.5	128	150 CO_2	1-45 min	No	PM	III
C-2	23	50 ml DI H_2O	7.5	185	115 CO_2	2/18 h	Yes	ALL	III/IV

3.1 Milling

Milling was mainly performed in a high intensity laboratory Fritsch Pulverisette Planetary Mono Mill 6. Samples prepared in this mill were used in all experimental designs. In Paper IV, three other mills, a laboratory ball mill, a Hicom 15 mill, and a Szegvari Attritor 1SDG were used in addition to the planetary mill. All four mills are shown in Figure 3.1. The largest differences between the mills were the movements and rotational speeds. The speeds described here are given for the actual mills used in the experiments, but the movement descriptions are general for the given types of mills.

A ball mill rotates around a horizontal axis with steel balls moving freely within the chamber. The ball mill used could only be operated at a constant speed of 75 RPM. The ball mill speed is in general limited by the critical speed where the mill charge starts to centrifuge. The chamber of the attritor does not rotate, but a stirrer within the chamber rotates around a

[2] Experiment numbers referrer to the numbering used in the Papers II, III and IV. The experiment in Paper I is named D-O here, but does not have a name in the paper.
[3] PM = planetary mill, ALL = Planetary mill, attritor, Hicom mill and ball mill. All mills are described in chapter 3.1.

vertical axis (Goodson, 1985) up to 600 RPM. The chamber of the planetary mill rotates around a vertical axis simultaneously as the chamber rotates in a larger circle, thereby imitating a planetary movement. Maximum speed of the planetary mill is 600 RPM. The Hicom mill uses a nutating motion to generate centrifugal accelerations (Hoyer, 1992, Hoyer *et al.*, 2001) with a maximum RPM of 1200. The movement is comparable to rotating a bottle with one hand in horizontal circles around a vertical axis with the largest distance to the axis at the bottom. Freely moving steel balls are used in all four mills.

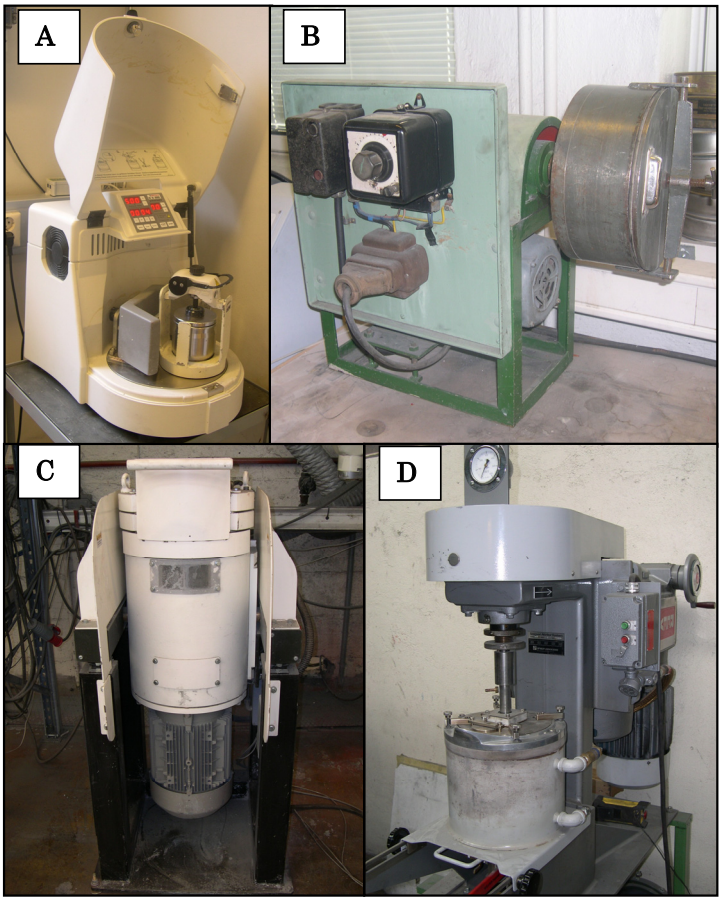

Figure 3.1 A: Planetary mill, B: Laboratory ball mill, C: Hicom mill, and D: Attritor.

Table 3.2 summarized the mills and milling parameters for all types of samples prepared. Some steel ball charges consisted of two sizes, indicated as Part I and Part 2 used simultaneously. A total of 13

combinations of mills, water addition and milling durations were used for the planetary mill, 2 samples were prepared in the attritor and the Hicom mill, and 4 samples in the ball mill. Paper I and Paper II presents the results of changing the milling duration, water addition and mill atmosphere for the planetary mill. Paper IV investigates the effect of different mills and mill intensities. Particle size distribution, specific surface area and crystallinity were obtained for all samples.

Table 3.2 Milling parameters[4]

Material name	Mill	Atmosphere	RPM	Milling time [min]	Water addition [ml]	Mass olivine [g]	Used in paper	Part 1 Steel balls		Part 2 Steel balls	
								[mm]	[g]	[mm]	[g]
P_N10minDry	Planetary mill	N_2	500	10	0	20	I	10	640	0	0
P_N30minDry	Planetary mill	N_2	500	30	0	20	I	10	640	0	0
P_N60minDry	Planetary mill	N_2	500	60	0	20	I	10	640	0	0
P10minDry	Planetary mill	Air	500	10	0	20	I/II/III/IV	10	640	0	0
P30minDry	Planetary mill	Air	500	30	0	20	I/II	10	640	0	0
P60minDry	Planetary mill	Air	500	60	0	20	I/II/III/IV	10	640	0	0
P90minDry	Planetary mill	Air	500	90	0	20	II	10	640	0	0
P10minW10%	Planetary mill	Air	500	10	2	20	I/II/III	10	640	0	0
P30minW10%	Planetary mill	Air	500	30	2	20	I/II/III	10	640	0	0
P60minW10%	Planetary mill	Air	500	60	2	20	I/II/III	10	640	0	0
P10minWet	Planetary mill	Air	500	10	100	20	II/III/IV	10	640	0	0
P30minWet	Planetary mill	Air	500	30	100	20	II	10	640	0	0
P60minWet	Planetary mill	Air	500	60	100	20	I/II/III/IV	10	640	0	0
A10minWet	Attritor	Air	350	10	1200	800	IV	6	16000	0	0
A60minWet	Attritor	Air	350	60	1200	800	IV	6	16000	0	0
B2hDry	Ball mill	Air	75	120	0	750	IV	19.1	250	9.5	750
B8hDry	Ball mill	Air	75	480	0	750	IV	19.1	250	9.5	750
B2hWet	Ball mill	Air	75	120	1200	750	IV	19.1	250	9.5	750
B8hWet	Ball mill	Air	75	495	1200	750	IV	19.1	250	9.5	750
H1minDry	Hicom mill	Air	900	1	0	1000	IV	9	2011	5	10000
H5minDry	Hicom mill	Air	900	5	0	1000	IV	9	2011	5	10000

[4] Sample names used in Paper I are unfortunately not consistent with the nomenclature in the table. In Paper I wet indicates in fact W10% milling. In Paper II and III the letter P is excluded in front of the sample name since only the planetary mill was used in the experiments described there.

3.2 Dissolution and carbonation

Dissolution experiments were performed to differentiate between the mechanically activated samples without being significantly affected by precipitation, and direct carbonation experiments were performed to evaluate how suited the milled olivine samples were for direct carbonation.

3.2.1 D-0: Flow-through dissolution at 128 °C /150 bar of CO_2

An illustration of the experimental set-up of experiment D-0 is given in Figure 3.2. Flow-through dissolution experiments were performed on three mechanically activated olivine samples and two experiments on a reference sample. The autoclave contained 50 ml and solution samples were taken at regular intervals, and conductivity was logged continuously. Qualitative descriptions of the solid residues were performed using XRD and SEM.

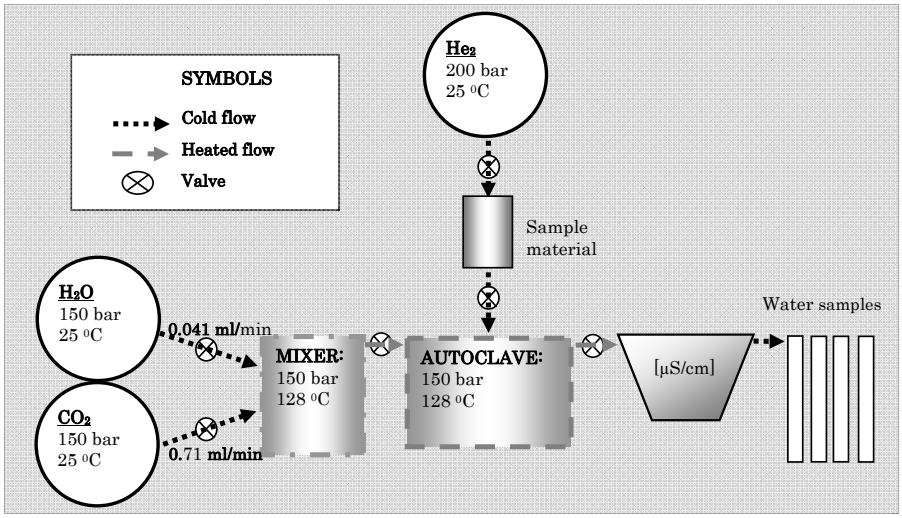

Figure 3.2 D-0 : Carbonation design using pressurized CO_2 and a supercritical fluid extractor.

This experimental set-up was not used further. The mechanically activated samples had very low particle size distributions and problems arose when these sample were entering the autoclave and some of the samples remained in the sample container. This amount was measured, but included uncertainties related to the sample collection within the container.

3.2.2 D-1, D-2 and D-3: Batch dissolution at 22 °C / 1 bar of air

A simple batch experiment, with the varieties of D-1, D-2-and D-3, was developed to be able to run many dissolution experiments with differently milled samples. A pH of approximately 2 was chosen to achieve a reasonable reaction rate of olivine and still operate with a diluted acid resembling the conditions with carbonic acid. Figure 3.3A shows the magnetic stirrer designed to avoid abrasion between the magnetic stirrer, the bottom and settled particles. Figure 3.3B shows an ongoing experiment.

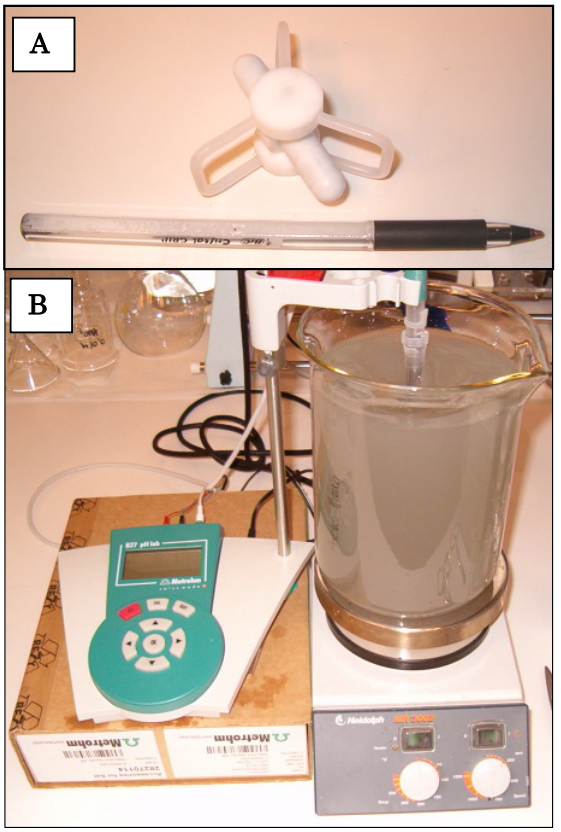

Figure 3.3 D-1, D-2, D-3: Dissolution in 0.01 M HCl. A: Magnetic stirrer, B: Experiment.

Dissolution of olivine consumes acid and therefore pH was chosen as a convenient continuous reaction parameter. All experiments were performed in room temperature and pressure. During each experiment pH was logged automatically, initially with short intervals and then longer intervals when the pH change slowed down. At the end of each experiment a water sample

was taken and analysed to verify the calculated concentrations based on pH. Some selected samples from the D-1 experiments were used in the D-2 experiments to obtain enough residual material for specific surface analyses, particle size distributions and XRD analyses, and thereby be able to compare the initial properties of the samples to the properties of the solid residues (Paper II).

These dissolution experiments were performed in two series where the first series was samples milled in the planetary mill (Paper II), whereas the second series consisted of chosen samples from Paper II and the samples milled in different mills (Paper IV). The results of the dissolution experiments in Paper II were used to study the relationship between material characteristics and dissolution rates. Some of the main results form Paper II regarding dissolution rates where then included in Paper III to enlighten the difference between dissolution results and the direct carbonation results. The results from the second series with different mills were used to compare the effect of the different mills on dissolution, the connection to direct carbonation results, and practical aspects of milling, dissolution and carbonation.

3.2.3 C-1: Direct carbonation at 128 °C / 150 bar of CO_2

Four differently milled samples were prepared in the planetary mill and used in a direct carbonation experiment called C-1. The C-1 experiment was initially planned to evaluate how mechanically activated olivine dissolved in carbonic acid. The experiments were modelled with PHREEQCi prior to the laboratory work with dissolution kinetics for non-activated olivine. Saturation was not reached for either olivine or any Mg containing carbonate within the planned experimental durations. The large increases in dissolution rates influenced the reaction to such an extent that precipitation also occurred. Therefore the experiments were both dissolution and carbonation experiments and not pure dissolution experiments as estimated from the geochemical model.

Figure 3.4 is an illustration of the experimental set-up. The total volume of the reaction fluid was collected after each experiment and analysed for relevant elements, three thin sections were prepared of solid residues from three duplicate experiments, and the final 17 solid residues

were analysed for total carbon content (TC). Due to solid residue masses of maximum 0.5 g, no other analyses were performed. The carbonation results from these experiments were included in Paper III together with results from the C-2 experiments.

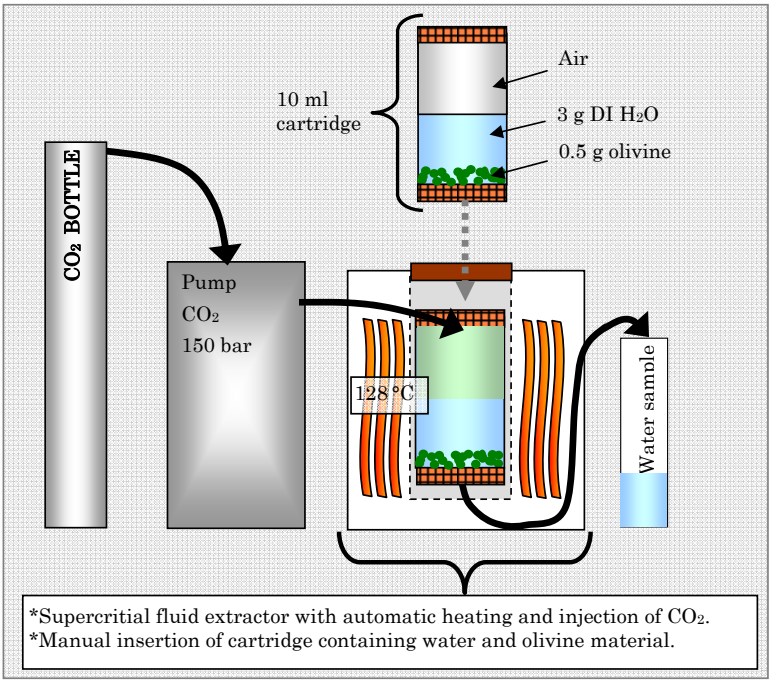

Figure 3.4 C-1: Direct carbonation experiment performed at 128 °C and 150 bar of CO_2.

3.2.4 C-2: Direct carbonation at 185 °C / 115 bar of CO_2

The purpose of the C-2 experiments was to carbonate differently milled olivine samples with a medium carbonation degree after 2 h of reaction, and approaching maximum carbonation after 18 h. Direct carbonation was performed in an experimental set-up with 4 simultaneously run autoclaves (Figure 3.5A). All batches were run with a continuous supply of supercritical CO_2. Constant pressure and constant temperature were used in the experiments. Heating, temperature measurements, pressurizing and pressure measurements were separately associated with each autoclave and logged (Figure 3.5B). Figure 3.5C shows the overall experimental setup. The autoclaves were able to run at different temperatures, but the pressure could not be adjusted individually with the exception of a valve attached to

each autoclave making it possible to separately close each autoclave from the pressurized system. In addition to the defined reaction time, heating took approximately 0.5 h and cooling 1.5 h. Pressurizing and depressurizing took about 3-5 min after the correct temperature was achieved.

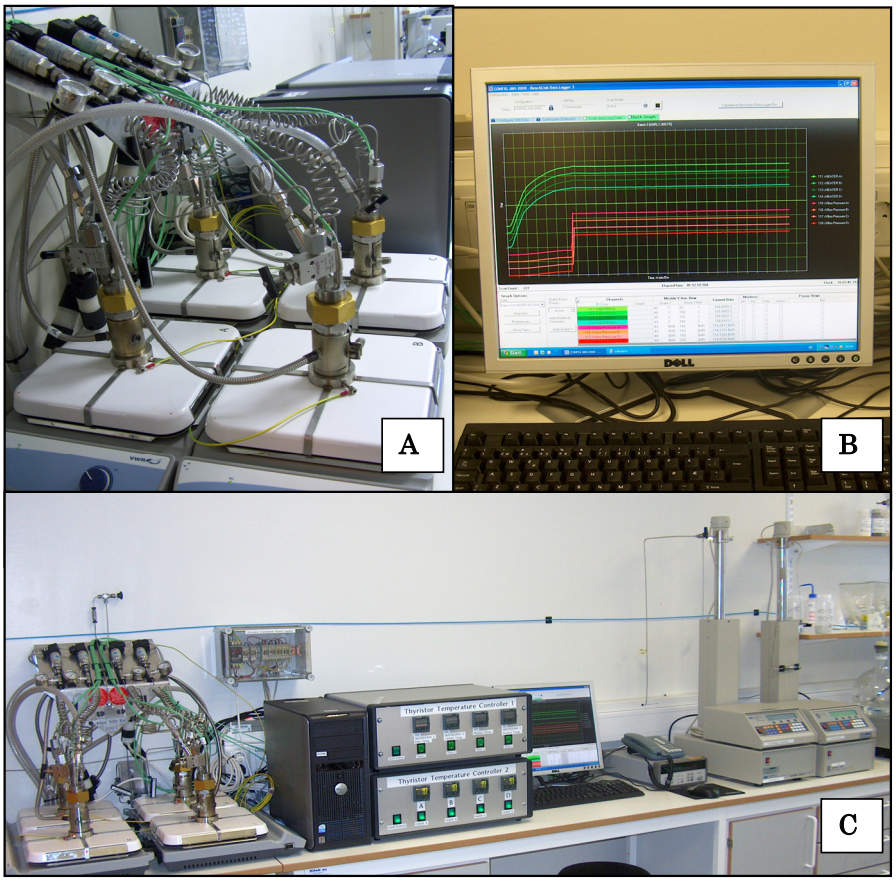

Figure 3.5 C-2 : A: 4 autoclaves ready for heating and pressuring, B: Example of continuous log of P and T, C: Autoclaves, heat controllers, display of computer log, and pumps (from left to right).

After terminating an experiment, pH was measured in the degassed solution, a water sample was filtered with a syringe to remove fines, and the residual solution and solid residue was filtered with a vacuum pump and dried in air. The water chemistry was analysed and the solid reaction residues were analysed for TC. Thin sections were prepared from the solid reaction residues after 2 h and 18 h reaction of the initial samples with

minimum crystallinity, maximum specific surface area and minimum activation. Particle size distributions were found for the same residues used in the preparation of thin-sections.

The results from the experiment C-2 were used together with the results from experiment C-1 and described in Paper III. In addition to the samples from the planetary mill, two samples milled in the laboratory ball mill and one sample from the Hicom mill and the attritor were carbonated. The results for the four mills are presented in Paper IV together with dissolution experiments of the corresponding materials.

Chapter 4. Summary of papers

4.1 Paper I

Haug, T.A., Munz, I.A., Kihle, J., Kaszuba, J.P., and Carey, J.W., 2007, Energy intensive milling of olivine used for CO_2 storage. In *Proc. Conference in Mineral Processing 6. - 7. February 2007*, Luleå, Sweden, 91-98

The attention in this paper was paid to experimental work related to the possibility of using mechanical activation as a pre-treatment method for olivine carbonation. A laboratory planetary mill was used to mill olivine, and the milled samples were analysed to find the specific surface area, the particle size distribution and X-ray diffractograms. 4 selected samples were used in 5 flow-through dissolution experiments with water and CO_2. The focus was on changes in the material characteristics due to mechanical activation, and stoichiometry and changes in mineral composition due to dissolution. Mechanical activation with the addition of 10 wt% water resulted in increased specific surface areas with milling time with the maximum value of 47 m^2/g obtained after 60 min, while dry milling had a maximum specific surface area of 4.2 m^2/g after approximately 10 min. The crystallinity was observed to decrease with prolonged activation both for dry

milling and milling with 10 wt% water. The mineral composition did not change during milling, but the solid dissolution residues had obtained a dark red/brown colour, and goethite or hematite may have been formed. The relative content of olivine compared to the other minerals present, was reduced after dissolution.

4.2 Paper II

Haug, T.A., Kleiv, R.A., and Munz, I.A., 2009, Dissolution of mechanically activated olivine in hydrochloric acid - investigating leaching properties for carbonation purposes (in review), Journal of Applied Geochemistry

The main focus of this paper was to study how the material characteristics of olivine changed during milling in a laboratory planetary mill, and investigate the effect of mechanical activation on the dissolution rate constant. Dissolution experiments with 0.01 M HCl solution was performed at room temperature and pressure. Mechanical activation as a pre-treatment method was found to enhance the initial specific reaction rates with approximately 3 orders of magnitude. The samples milled dry had the lowest specific surface areas (< 4 m^2/g), but had the largest rate constants. The measured particle size distributions could not explain the rate constants found, but the specific surface area gave a nice trend versus dissolution for samples milled wet and the samples milled with 10 wt% water. The crystallinity, calculated from X-ray diffractograms, was the material parameter with the best fit for the observed differences in the specific rate constants. Wet milling does not have the same maximum reaction rate as dry milling, but wet milling might be easier to implement into a wet carbonation process.

4.3 Paper III

Haug, T.A., Kleiv, R.A., Munz, I.A., Kaszuba, J.P., and Carey, J.W., (manuscript September 2009), Carbonation of mechanically activated olivine, Trondheim, Norwegian University of Science and Technology.

The main objective was to evaluate the efficiency of increasing the dissolution rate versus an obtained carbonation degree. A laboratory planetary mill was used as a pre-treatment method to produce 6 variations

of olivine samples with varying dissolution rates. Two carbonation experiments were performed, respectively with reaction durations from 1 – 45 min at 128 °C and 150 bar, and 2 h and 18 h at 185 °C and 115 bar. A maximum conversion of more than 95 % was obtained after 18 h of reaction at 185 °C and 115 bar for wet milled samples. Comparison of the conversion values to earlier dissolution rates for the same materials indicate that the dissolution rate governed the conversion rate when the conversion was below ~ 10 % at 128 °C and 150 bar, whereas with conversion approaching maximum values at 185 °C and 115 bar the rate was governed by precipitation kinetics. To maximize the advantage of mechanical activation carbonation can be performed in two steps. First step is dissolution, and the second step is precipitation. Dividing dissolution and precipitation into two steps can create more opportunities for optimization of the carbonation process, but will probably require more equipment then necessary with direct carbonation. In addition precipitation of minerals in the first step has to be kept at a minimum by controlling the concentrations of solved elements.

4.4 Paper IV

Haug, T.A., Munz, I.A., and Kleiv, R.A., (manuscript September 2009) The importance of grinding solutions for mineral carbonation concepts, Trondheim, Norwegian University of Science and Technology

The motive of this paper was to use a dissolution experiment and a direct carbonation experiment to evaluate if four mills with varying milling intensity produced samples possible to use in a CO_2 sequestration process. The specific reaction rates of the samples and the energy consumption during sample production was included and compared. Finally the maximum sizes of these mills were obtained from several manufacturers and compared to a probable mass flow in a 100 MW gas power plant. Olivine samples were prepared in a ball mill, a Hicom mill, an attritor and a planetary mill. Dissolution of olivine samples was performed at room temperature and pressure in 0.01 M HCl and carbonation was performed at 185 °C and 115 bar of CO_2 pressure. Planetary mills are too energy consuming for the purpose of CO_2 storage, but obtained the largest change in material properties and dissolution rates compared to the other mills.

Wet milling in ball mills are most suited for direct carbonation since the additional energy consumption of high intensity mills were not reflected in the carbonation results. If the carbonation reaction is divided into two steps, first dissolution then precipitation as a subsequent step, the results indicate that the commercially available attritors or Hicom mills are possibly both large enough and obtain sufficient increase in the dissolution rate of olivine. For indirect carbonation to become an option for CO_2 sequestration, the potential challenges of avoiding precipitation during transport from step 1 to step 2 must be evaluated and solved.

Chapter 5. General discussion

Mechanical activation has been used as pre-treatment of olivine with the purpose of investigating changes in material characteristics and how easily these materials dissolve and reacts with CO_2 to form carbonates. All the experimental efforts were aiming at the utilization of mechanical activation for mineral carbonation and possibly CO_2 sequestration. In the following discussion, the implications and consequences of the results presented in the articles and during the PhD work are summarized and evaluated in the practical context of olivine characteristics, energy consumption, mineral carbonation and mineral processing.

5.1 Olivine characteristics

5.1.1 Milling energy and conditions

Figure 5.1 is an illustration of how the obtained material characteristics of olivine depended on the joint effect of mill intensity, mill choice and estimated large scale net energy consumption W_N (Paper IV). The Hicom mill and the ball mill had W_N in the same range, but the Hicom mill

obtained smaller particles, lower crystallinity and higher SSA than the ball mill, indicating that the mill intensity was important for the outcome.

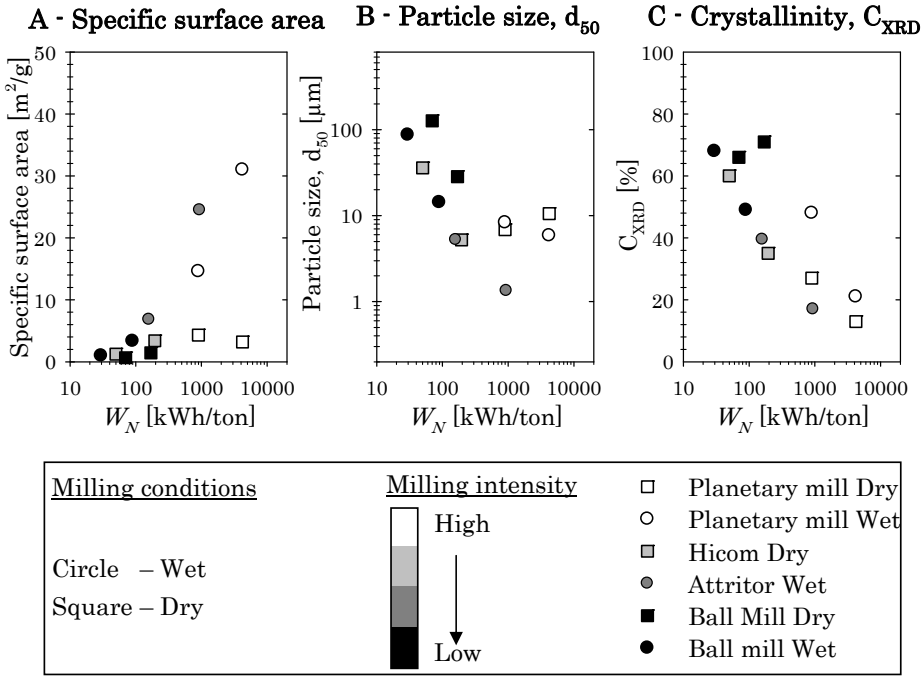

Figure 5.1 Plots of the effect of net energy consumption on material characteristics. Type of mill, water addition and mill intensity are included.

The effect on the material after reaching a critical particle size is probably dependent on the impact force, and therefore on the mill intensity. The observation of decreasing crystallinity can be explained by the fact that the particle size decreases initially during milling, but after obtaining some critical size, the additional grinding energy will accumulate at the surface of the material or in the bulk volume resulting in amorphization (Boldyrev and Tkáčová, 2000). The crystallinity calculation (described in chapter 2.6.3) does not distinguish between small crystals in a matrix, extremely fine grained particles or truly amorphous materials (Baláž, 2000, Baláž, 2008, Tkáčová, 1989). The combination of these three properties of an olivine sample might explain why the crystallinity calculated from XRD analyses has the best correlation with the energy consumption, since the destruction of the crystals were related to the intensity and so is the particle size reduction with following aggregation.

Water can act as a surfactant in the mill and inhibit the creation of aggregates and agglomerates. Therefore can wet milling of olivine create large surface areas reaching 31 m^2/g after 60 min in the planetary mill (Figure 5.1A) while dry milling only obtained 4.3 m^2/g after 10 min in the same mill. Milling with the addition of 10 wt% water in the planetary mill created powders that looked like dry milled powders, but obtained even higher surface areas, up to 47 m^2/g after 60 min (Paper II), than the wet milled samples. The three samples milled with 10 wt% water is not included in Figure 5.1 because the power consumption was not measured, but are shown in Figure 5.2 and is relevant for the discussion of combinations of material properties later in this chapter. Increased energy consumption reduced in general the particle size of the finest 10 % of the samples from all mills, but the planetary mill was not as efficient as the attritor (Figure 5.1B), despite the much larger amount of energy used. One explanation might be aggregation due to a higher milling intensity.

The planetary mill caused the largest effect on all three material characteristics, but is the definitely the most energy consuming mill with an estimated intensity of 5000 kW/ton where the intensity illustrates how energy intensive the mill is. The Hicom mill and the attritor are the most efficient mills of reducing the particle size and decreasing the crystallinity. When it comes to the specific surface area, the attritor is the most efficient mill.

5.1.2 Measured characteristics and analytical techniques

Figure 5.2A, B and C show how different combinations of the olivine characteristics can be obtained by the mill choice and the use of water or not. Low C_{XRD} and high SSA are obtained with the planetary mill, while the smallest changes are obtained from the ball mill. The relationships found in Figure 5.2B and C show how the samples milled in the planetary mill have apparently higher d_{10} compared to both C_{XRD} and SSA and the other mills and illustrates the changes in the particles due to mechanical activation. Particle size distributions of the samples are given in Appendix 2.

$$\mathrm{SSA} = \frac{A}{m} = \frac{4\pi r^2}{\frac{4}{3}\pi r^3 \cdot \rho} = \frac{6}{d \cdot \rho} \tag{12}$$

For a material with varying particle sizes the surface area of the sample can be calculated by summarizing the surface areas of several particle sizes combined with the wt% of the given size. Fines below approximately 10 µm will dominate the total sum.

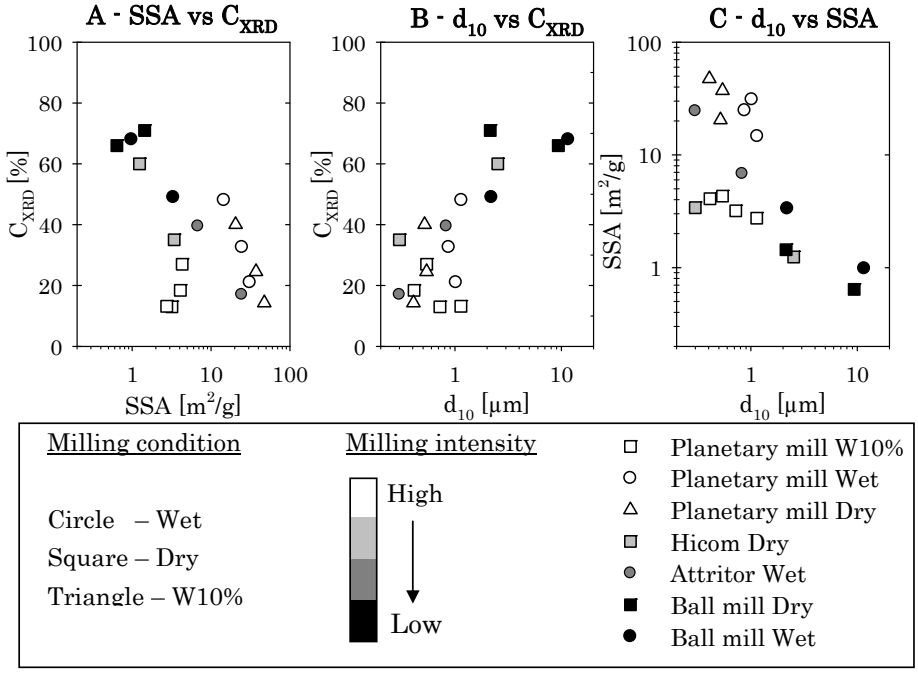

Figure 5.2 Correlation between the three main material characteristics particle size, specific surface area and crystallinity represented by C_{XRD}. Type of mill, water addition and mill intensity are included.

Two pictures taken with SEM of the olivine sample milled without water for 60 min in the planetary mill is shown in Figure 5.3 to illustrate the complex surface and texture of olivine found in mechanically activated materials (Baláž *et al.*, 2008). Large agglomerates of particles < 1 µm (Figure 5.3 left) with high binding forces will be interpreted as one large particle during particle size analyses.

Analytical uncertainties for both the particle size analysis and the specific surface area analysis will influence the correlation shown in Figure 5.2C. The lower limit of the particle size distribution analysis was 0.02 µm and no material had measurable amounts of fines below 0.04 µm. If a

sample was 100% 0.04 µm spherical particles, the resulting SSA would have been 45 m^2/g, which illustrates that the measured surface areas cannot solely be explained by the measured particle sizes, since the particles were much larger than 0.04 µm and the surface area was within the same order of magnitude. The agglomerates will have higher surface areas than smoother particles due to the complex surface area and the XRD analysis will reflect the low crystallite sizes, despite the seemingly coarser particles. This is why the correlations between particle size and SSA, and particle size and C_{XRD} have large variations in Figure 5.2. The surface area measurements are affected by the formation of aggregates and surface topography.

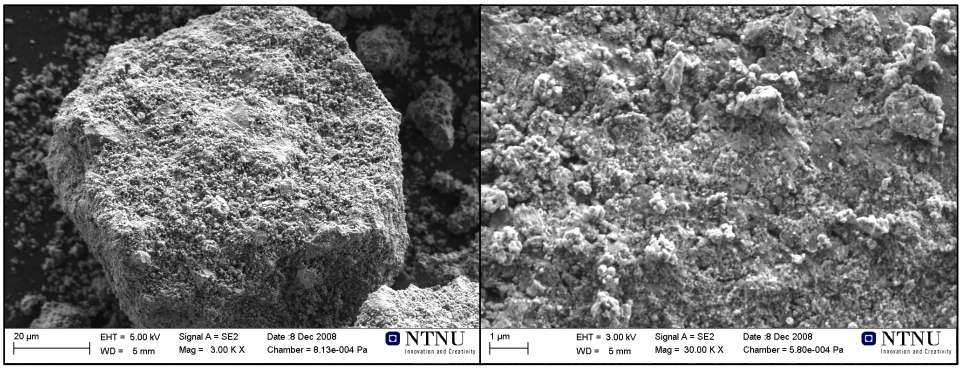

Figure 5.3 Illustration of an olivine sample after 60 min of dry milling in the planetary mill.

In Figure 5.4 specific surface area measurements are plotted versus age of the sample at the point in time when analysed. Only olivine samples from the planetary mill produced with dry milling or with 10 wt% of water were analysed several times. Some measurements have been performed on the sample, and some are from samples produced the same way. Nevertheless, there is a slight decrease with age of the samples except the samples milled dry for 30 min (Figure 5.4A). Secondary processes as aggregation, adsorption and recrystallization (Baláž, 2008) have probably influenced the materials and resulted in the decrease in specific surface area. The simplifications during material property analyses made the interpretation of the differences between the milling conditions and mills more difficult than expected. Inclusion of more advanced analytical methods would probably have contributed to additional understanding of the changes

in the material characteristics. Several analytical methods suitable for mechanically activated minerals are found in the book written by Baláž (2008).

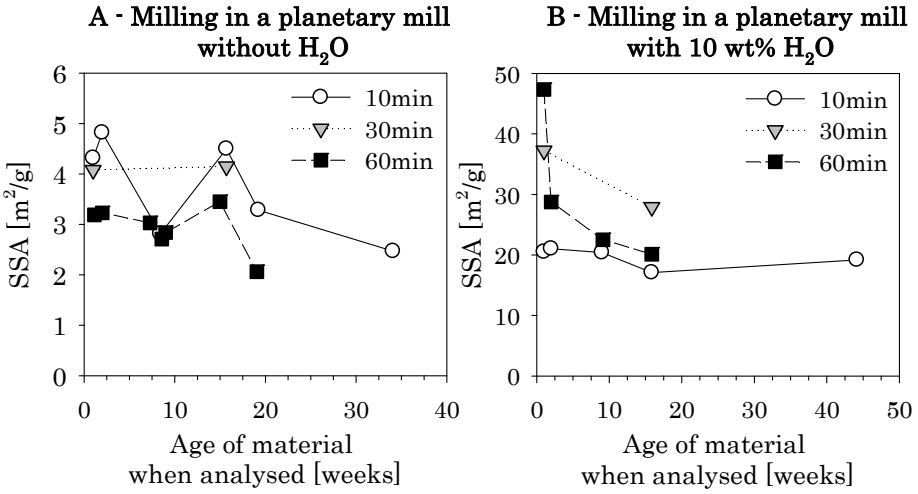

Figure 5.4 Illustration of aging effects and reproducibility of BET measurements.

5.2 Mineral carbonation

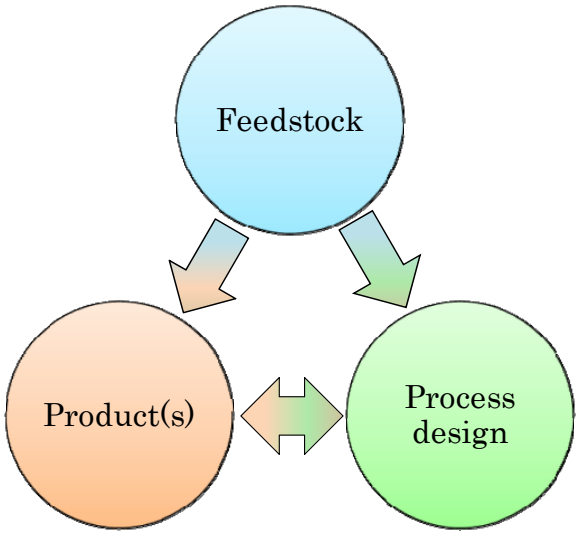

Figure 5.5 Defining parameters relevant for mineral carbonation

Mineral carbonation used for CO_2 storage are restricted by the availability of feedstock minerals, the total energy consumption of mining – pre-treatment – carbonation – storage or transport to market, and the total cost of investment and maintenance. To meet these three requirements the type of feedstock, the process design and the possible product quality has to be evaluated together due to the mutual dependency as illustrated in Figure 5.5. After choosing feedstock mineral, an evaluation of possible valuable products can be made, and a decision whether or not to use direct carbonation has to be done.

5.2.1 Feedstock

It is beneficial to the overall CO_2 storage concept if the feedstock mineral resources have a relative closeness to the point source of CO_2, since extra transport of the feedstock increases the costs and the CO_2 emissions. In general many minerals with a focus on Ca, Mg and Fe containing silicates, have been considered as feedstock because these elements form stable carbonates (Kojima *et al.*, 1997, McKelvy *et al.*, 2004, O'Connor *et al.*, 1999, Teir *et al.*, 2005, Wu *et al.*, 2001). The choice of feedstock mineral must be performed separately for each relevant CO_2 storage case and is defined by the regional geology. The chosen mineral(s) are determining for the following chemical reactions, and the possibilities within types of products and process design due to the variations in the chemical properties and reactions involved.

5.2.2 Olivine dissolution residues

Pictures of selected solid residues from the flow-through dissolution with carbonic acid at 128 °C and 150 bar (Paper I) and solid residues from dissolution at room temperature and pressure with 0.01 M HCl (Paper II) are shown in Figure 5.6. The studies of the dissolution residues showed how some of the texture from the mechanical activation was preserved even after extensive dissolution (Figure 5.6A). Solid residues after dissolution of samples milled in the planetary mill, regardless of experiment type, was the observation of aggregates/agglomerates as found in the lower part of Figure 5.6A. This observation shows that the initial agglomerate are dissolved at the same time as the texture is preserved. The preservation of the textures

indicated that the dissolution rates resulting from the mechanical activation probably will be important for the overall dissolution rate. This observation is very important in the planning of processes when mechanical activation is used. The preservation was most obvious for samples milled dry in the planetary mill. Dissolution residues after samples milled wet and W10% contained olivine grains with typical crystalline appearance (Upper part of Figure 5.6A). The observation of aggregate textures in the dissolution residues shows how the aggregates not are some superficial property of the mechanically activated olivine, but whole particles might contain this texture.

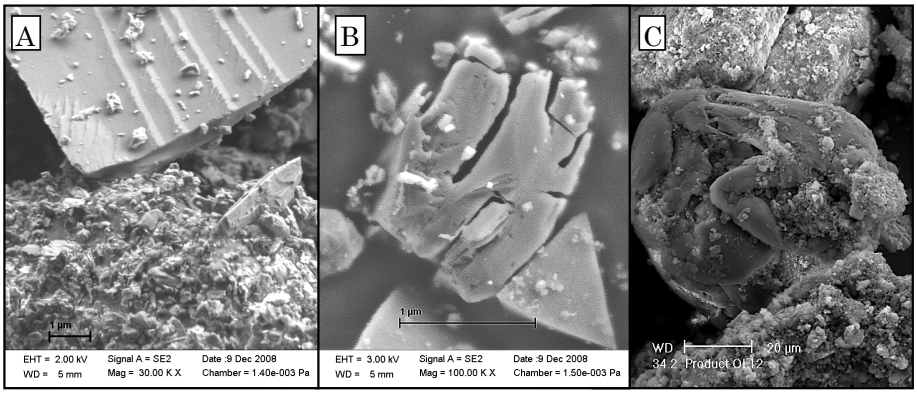

Figure 5.6 Illustration of the diversity of features observed in solid dissolution residues. A – Aggregates and olivine crystals (experiment D-3 with P60minWet), B – Dissolution along fractures of nanometre-scale (experiment D-3 with P60minWet), C – Iron rich phase on centre grain (experiment D-0 with P60minDry).

The shrinking core model (SCM) can be applied during dissolution modelling to calculate the surface area available by accounting for the loss of mass during dissolution. This model did not fit the specific surface area measurement of three differently milled and dissolved olivine samples (Paper II). SCM simplifies the particle to be spherical or cubical and having homogeneous dissolution properties. Theoretically, using the shrinking core model, the specific surface areas of the D-1 and D-3 experiments (Paper II) should have increased with about 20 %, but the reductions were 41 % and 55 % respectively for the P10minW10% sample and the P60minWet sample. The P60minDry sample increased, but instead of a 20 % increase, the surface area increased from 3.2 m^2/g to 44.2 m^2/g, resulting in an over 10

times higher specific surface area at the end of the experiment than in the beginning.

A large increase in specific surface area can be explained by the aggregates breaking up and the creation of fractures as shown in Figure 5.6B indicating direction dependent dissolution. Direction dependent dissolution have been observed for olivine (Awad *et al.*, 2000) and may have been enhanced by mechanical stress as a result of milling and varying mechanical strength dependent of the crystal structure. In summary the shrinking core model as discussed in Paper II is not suitable to describe changes in the specific surface areas for mechanically activated olivine, and this probably applies to other minerals as well.

An important question during dissolution, and relevant for large scale mineral carbonation as discussed in the next chapter, is the presence of iron. Iron contaminating magnesite reduces the purity of the product, iron-phases precipitating during dissolution can slow down the dissolution rate, but on the other hand, iron rich phases can become a valuable product. The olivine used in all experiments contained approximately 7 wt% Fe_2O_3, and the contaminating steel also contained significant amounts of iron (Paper II). In the dissolution residues the only observation of an iron rich phase (Figure 5.6C) was from the flow through dissolution experiment performed at 128 °C and 150 bar. No comparable phases were found in the experiments performed at room conditions with the analysis performed (Paper II), and the difference between these results is probably related to the reaction conditions. The importance of iron and reaction mechanisms has to be investigated further.

5.2.3 Carbonation products

The overall chemical composition is mainly dependent of the feedstock chemistry, but the quality, purity and composition of the products (precipitated secondary minerals) are governed by the process conditions and design. In the case of silicates as feedstock, Ca, Mg and Fe containing carbonates can be the main product and silica can then be an important by-product together with for instance Al, Cr, Fe, K, Mn, and Na or other valuable minerals or elements.

The amounts of products from a mineral carbonation plant are vast, and valuable ways of using the products will increase the potential of implementing mineral carbonation as a CO_2 storage alternative. For each ton of CO_2 stored at least 2.6 tons of products are created with the assumption of 100 % conversion of 100 % Mg-olivine. Lower conversion grade and lower contents of carbonate forming elements in the feedstock will increase the mass of products. An estimated worldwide energy related CO_2 emissions of 31 gigatons in 2010 (EIA, 2009) will result in a minimum of 80 gigatons of products if only ex-situ olivine carbonation is used for CO_2 storage. Mineral carbonation cannot be the only CO_2 storage alternative, but it is an option for power plants with large resources of suitable feedstock minerals in the proximity of the plant. A 100 MW power plant is estimated to emit 480 kton/yr of CO_2 (Huijgen *et al.*, 2007) and assuming 100 % olivine with 100 % conversion, this results in annual productions of carbonation products of 1200 kton/year. In comparison a total of 2600 kton of olivine were mined in Norway in 2008 (NGU and Bergvesenet, 2009), hence the amount of solid products from a 100 MW power plant is possible to handle and may have some market value with an optimized carbonation process design.

The direction carbonation approach results in a solid product that consists of a mixture of secondary minerals. Products of direct carbonation can for example be used as fillers when the material does not contain any harmful constituents or the material can be dumped in a land fill or in closed mines. Dividing the carbonation process into several steps with differentiated process conditions, introduces the possibility of separating the precipitation steps and creating one or more valuable products with specified characteristics. The latter solution on the other hand consumes more energy than direct carbonation and costs more. The value of the bi-products has to balance the additional costs and the energy consumption and cannot in total produce more CO_2 than stored.

Olivine dissolution and direct olivine carbonation gave some indications of typical reaction products. In the flow-through experiments (D-0) at 128 °C and 150 bar (Paper I) no precipitation was planned, but iron precipitation was observed as a dark brown surface on the residual olivine material after dissolution was terminated. X-ray diffraction of the residuals

revealed the possibility of having precipitated hematite or goethite. This was not observed in the dissolution experiments performed at room conditions (Paper II) or in the batch carbonation experiments at 185 °C and 115 bar (Paper III). These varying results show how the product composition is very dependent on the process conditions, and the removal of dissolved substances.

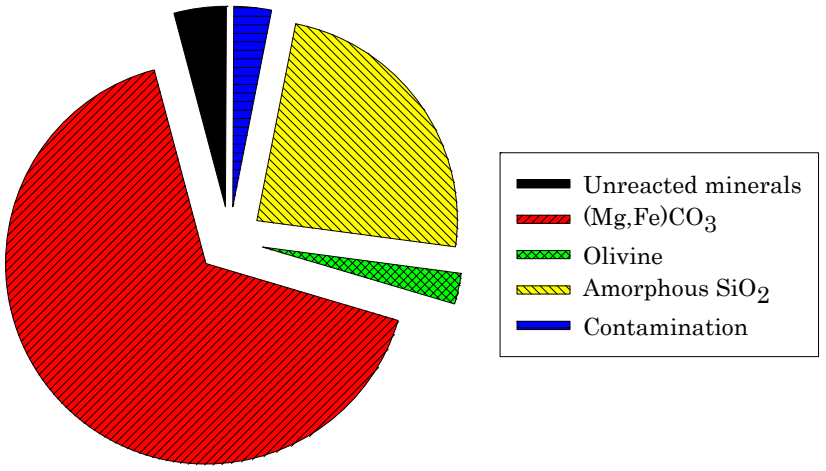

Figure 5.7 Example of a product composition after direct carbonation at 185 °C and 18 h of the P10minWet olivine sample. Obtained conversion was 95 mol%.

The direct carbonation experiments of olivine showed that for conversion above 95 % the product was estimated to contain over 24 wt% of silica as indicated in Figure 5.7. Very small amounts of material were solved in the fluid phase of the experiment, and most of the main precipitates were silica and magnesite (Paper III). The products also contained contamination obtained during milling and remains of unconverted minerals, which both will be a varying problem in all carbonation processes.

5.2.4 Implications of results for a carbonation process

The efficiency of a carbonation process is dependent on the dissolution rate and the precipitation rate being optimized. This can be done in a direct carbonation process where dissolution and precipitation happens at the same conditions or in a two step process where the conditions can be

adjusted separately. Carbonation involves dissolution of CO_2 in water, dissolution of feedstock mineral, and precipitation of carbonates. The optimization is done by combining the right pre-treatment, process temperature, CO_2 pressure and liquid/solid ratio. If milling is chosen as the main pre-treatment option, more than the measured specific surface area and particle size has to be taken into account as showed by the lack of correlation between particle size and specific surface area and dissolution/carbonation (Paper II, Paper III and Paper IV). To determine the best pre-treatment, the process conditions and milling solution has to be evaluated together.

Chen *et al.* (2006) studied key parameters affecting direct carbonation and found two principal reactions; dissolution of the feedstock and precipitation of carbonate from the solution. The governing reaction depends of the process conditions. Huijgen *et al.* (2006) described the carbonation of wollastonite, $CaSiO_3$, and found it to be dependent on the dissolution rate at low temperatures and pressures, while at temperatures above approximately 200 °C the reaction became pressure dependent because the activity of the (bi)carbonate ion was reduced and nucleation and crystal growth became the dominating reaction step. These two regimes are likely to be valid for olivine as well with slightly different temperatures and pressures dividing the reaction regimes, determined by olivine dissolution rates and precipitation rates of Mg-carbonates instead of Ca-carbonates. With the large increases in dissolution rate of olivine as obtained by mechanical activation, the rate liming step became magnesite precipitation at 185 °C and 115 bar of CO_2, but with decreased temperature and increased pressure at 128 °C and 150 bar of CO_2 dissolution is possibly the rate limiting reaction (Paper III, Paper IV). Increasing the dissolution rate with two to three orders of magnitude alters the balance between the dissolution kinetics and the precipitation kinetics when performing direct carbonation. Since the dissolution rate of olivine has been increased drastically, the process conditions of direct carbonation can be changed to increase the precipitation rate with good margins of making the dissolution rate the rate limiting step.

An upper energy consumption limit for pre-treatment and carbonation reactions for mineral carbonation as CO_2 storage was estimated

to be 500 kWh/ton of feedstock (Paper IV). Initial assumptions of the calculations were the energy produced by a 100 MW gas power plant, where the net amount of CO_2 produced was equal the amount of CO_2 bound in the carbonation process (Paper IV). The planetary mill obtained the largest increase in olivine dissolution rates compared to the ball mill, Hicom mill and the attritor, but the estimated total energy consumption of commercial planetary milling exceeded 1000 kWh/ton after 10 min of milling excludes this mill as pre-treatment for CO_2 storage purposes (Paper IV). Even though the planetary mill is not suited for carbonation processes, the high dissolution rates possible to obtain were useful in laboratory experiments with the rapid dissolution and following rapid saturation of secondary minerals in the fluid. The effect on dissolution rate can probably be used to study dissolution/precipitation reactions of other minerals as well. The Hicom mill or the attritor may be possible to use if the carbonation process is divided into two steps or direct carbonation is performed at conditions where dissolution is the rate limiting step. Process conditions where precipitation is the rate limiting reaction cannot take advantage of the increased dissolution rate resulting from mechanical activation. Therefore are ball mills most suited as the grinding solution due to the low energy consumption (Paper IV).

With a simple carbonation system containing only olivine, CO_2 and water, the olivine dissolution rate is dependent on the pH resulting from the dissolution and dissociation of CO_2. The olivine dissolution rate increases with increasing temperature and decreasing pH, but with CO_2 as the only source of acid, a compromise between low pH at low temperatures, and an increase in the dissolution rate due to higher temperatures has to be made. Increasing the CO_2 pressure can to some extent counteract the effects of temperature on CO_2 dissolution. To complicate the overall carbonation mechanisms even further, magnesite precipitation has been found to increase with increasing temperature, in experiments studying precipitation until approximately 200 °C.

The amount of dissolved CO_2 in pure water increases with pressure. The solubility varies from less than 0.1 mol/kgw at 1 bar and temperatures between 25 °C and 260 °C to 2.6 mol/kgw at 260 °C. The solubility decreases with temperature as long as the pressure is below 100 bar, and for 200 bar

and higher the dissolution decreases to a minimum dissolution of 1.1-1.3 mol/kgw at approximately 100 °C to 150 °C with the pressures of 200 bar or 300 bar (Figure 6 chapter 2.2). For temperatures between 5 °C and 250 °C and CO_2 pressures between 10 bar and 500 bar, pH was estimated with PHREEQCi (Figure 5 chapter 2.2) to be relatively constant from 5 °C to 50 °C e at 3.1 – 3.2, and at higher temperatures the pH increases, but as the amount of CO_2 solved increases, the pH decreases with increasing temperature.

It may be possible to obtain up to a two order increase in the dissolution rate by optimization the milling solution in a Hicom mill or an attritor, and keep the energy consumption below the maximum limit. Dry milling was in general more efficient to increase the dissolution rate, but wet milling may be the most practical solution in an aqueous carbonation process. To make milling the main pre-treatment choice, the energy consumption during milling not only has to be lower than the upper limit, it has to be decreased to such a level that the power plant is economical feasible without to high energy penalty due to the total mineral carbonation process. With the energy efficiencies of high intensity mills today and the energy consumption necessary to obtain significant increases in the dissolution rates, these mills are probably not a good choice before the mill technology makes them even more efficient.

Choosing a two-step carbonation process solves the problem with optimization of dissolution and precipitation simultaneously, but introduces the possibility of precipitation occurring in the dissolution step if the process is not designed correctly. The solubility and precipitation kinetics of solved secondary minerals limits the maximum concentration of solved elements in the solution. This can result in very large volumes of fluids if the solubility is very low under the chosen conditions. The dissolution process can in general be optimized by a relatively high temperature and at the same time minimizing the pH. For pressures above 10 bar, pH is in the order of 3.1 – 3.3 as long as the temperature is below 250 °C. Main precipitate is carbonates: therefore the precipitation step is optimized for carbonate not silica or other possible minerals. In the case where several valuable constituents are going to be recovered, multiple precipitation steps are possible or separation after precipitation if the minerals are not intergrown.

Indirect carbonation can become an option if the challenges with liquid/solid ratios and precipitation kinetics can be solved.

A brief evaluation of the precipitated magnesite grains from the experiment at 185 °C and 115 bar (Paper III) indicated that the final size and shape of the grains may be related to the initial olivine material properties and the saturation of magnesite. The fastest dissolving sample obtained the smallest and least euhedral magnesite grains, and the grain shape did not change significantly from 2 h of carbonation to 18 h of carbonation. For the least altered olivine sample and the sample with the highest surface area the crystals were more developed and increased in size with carbonation duration (Paper III). Hence, the choice of pre-treatment may be important for the precipitation rate and the material characteristics of the precipitated product as well as the dissolution rate.

5.3 Mechanical activation as a pre-treatment method

The main advantages of the energy intensive mills are the rapid reduction of the particle size, the increase in surface area or the alteration of the crystal lattice. Even though the milling conditions described in Paper IV were not optimized, it took 10 min to reach a d_{10} = 7 μm in the planetary mill, while the ball mill used 8 h to achieve a d_{10} = 14 μm. These rapid changes of a high energy mill reduce the requirements of the mill dimension, or increase the possible mass flow for a given mill volume. Another advantage of mechanical activation is the wider range of material properties possible to obtain because the result is to some extent dependent on the mill intensity (Paper IV). Good examples are materials with a large reduction in crystallinity (dry milling – Paper II), relatively high specific surface areas (wet milling – Paper II), alloys of different compounds (Baláž, 2003), flotation properties (Baláž, 2008), and influence on leaching properties of metal ores (Baláž, 2003) or rock flour fertilizers (Kleiv and Thornhill, 2007) and so on. The application of mechanical activation can be appropriate if large changes in properties are required to make a process economical feasible. A Hicom mill has for instance been used with good

results to liberate diamonds (Nesbit *et al.*, 2001) taking advantage of the difference in hardness between the gauge and the diamonds.

During the PhD work an increase in dissolution rate of approximately three orders of magnitude was observed for olivine. If comparable increases can be obtained for other materials, then mechanical activation can be applied where dissolution properties are important. Milling of olivine in a nitrogen atmosphere inhibits the formation of aggregates (Paper I) and therefore the particle size distribution is significantly smaller than for milling in air. One intriguing observation was how the effect of milling in the planetary mill with the addition of 10 wt% water resulted in higher surface areas than both dry and wet milling, and at the same time the crystallinity reduction was comparable to dry milling. The use of water vapour may consequently be an intermediate grinding solution between wet and dry milling resulting in material properties not possible to obtain in any other way.

A technical disadvantage of mechanical activation can be the production of contamination during milling. Contamination changes the chemical composition of the milled materials, may affect subsequent chemical reactions, and increases the maintenance costs. One way of quantifying the amount of contamination is shown in Appendix 3. Higher quality steel can be used, but then the investment costs may increase instead. Practical experiments and calculations have to be performed for each separate case to determine the best balance between investments and maintenance costs and the effect on material properties and subsequent reactions.

In any commercial process, the main concern is economics, and for the choice of pre-treatment this is translated into the question of investment costs and operating costs. The operating costs are a combination of power draw and replacement of worn out equipment parts. Only the power draw and energetic efficiency of a planetary mill, Hicom mill, an attritor and a ball mill was investigated. The energy consumption is the largest restriction concerning mechanical activation as a pre-treatment method and the maximum allowable energy consumption is in most cases dependent of the earning potential of the obtained product. The energy consumption of energy intensive mills is in general much higher than conventional low intensity

milling (Paper IV) and the energy efficiency is lower as well (Paper IV). If the only requirement of the milled product is size reduction within conventional sizes, mechanical activation is too energy consuming and conventional ball mills are most likely the best choice. The applicability of the high energy mills increases with specified requirements of the milled materials and the sale values of the products.

5.4 Applicability of PHREEQCi

The geochemical modelling program PHREEQCi version 2 (Parkhurst and Appelo, 1999) was used to model olivine dissolution, olivine carbonation and saturation indices of relevant minerals in water samples from dissolution and carbonation experiments. Dissolution mimicking the batch dissolution experiment in HCl at room temperature and pressure was modelled by the implementation of the Arrhenius rate law, but the comparison of the model with the experimental data showed that the rate law and olivine specific parameters did not fit the experimental data. The dissolution kinetics was then adjusted by manipulating the rate expression based on corrections determined from the experimental data (Paper III). Appendix 4A is a script showing an olivine dissolution model with adjustments of the kinetics. There were no problems with implementation of different empirical rate formulas (Paper II and Paper III), but automatic regression of the empirical time series data was not possible in PHREEQCi.

PHREEQCi Geochemical modeling program
Developed by USGS
Available as Freeware (September 2009);
http://wwwbrr.cr.usgs.gov/projects/GWC_coupled/phreeqci/

Main appclications Low-temperature aqueous geochemistry calculations

1. Speciation and saturation-index calculations
2. Batch-reaction, transport calculations, kinetic reactions
3. Inverse modeling: finds sets of mineral and gas mole transfers that account for differences in composition between waters

Figure 5.8 PHREEQCi: Summary of program applications

The main challenges in the modelling of the flow-through and batch experiments were to implement realistic temperature and pressure dependencies of olivine dissolution kinetics, CO_2 solubility and $CO_{2(aq)}$ dissociation since PHREEQCi was developed for naturally occurring groundwater systems. User defined expressions for the dissolution and dissociation of CO_2 were implemented in the carbonation models (Paper III) to better simulate the carbonation reaction, and olivine kinetics were found for the given conditions. The user defined phases overrides the general expressions from large databases used by PHREEQCi. Appendix 4B is a PHREEQCi script combining dissolution and precipitation where CO_2 has been given adjusted thermodynamic data at 150 bar.

Modelling of saturation indices based on water sample chemistry was the last application PHREEQCi was used for. Many of the substances included in the larger databases are probably valid for higher temperatures, but this was substance specific. A script for modelling saturation indices (SI) is presented in Appendix 4C including a user defined CO_2 phases, and two water samples. Saturation indices are easy to model if the concentrations of all constituents are known. Appendix 4C includes a description of how the lack of anion analyses was handled, with a special focus on bicarbonate.

The three types of PHREEQCi models concerned about dissolution, saturation indices and carbonation introduced the valuable possibility to compare the obtained results from the PhD work to other published olivine data at different conditions. Together with a better understanding of the changed kinetics due to mechanical activation, an evaluation of changed input parameters was possible without actually performing new experiments.

Chapter 6. Conclusions

Simple dissolution experiments of milled olivine samples with pH as the main chemical parameter indicated clearly the effect of mill choice and milling conditions. Dry milling, high intensity milling and increased milling duration resulted in the highest dissolution rate constants. The rate constants decreased with dissolution degree and this decrease can be attributed to the dissolution of the most activated parts of the milled samples.

The rate constant k at 5 % dissolution varied from $5 \cdot 10^{-8}$ [mol/m^{2}s] for the sample milled dry in a laboratory ball mill to 10^{-4} [mol/m^{2}s] for the sample milled dry for 90min in a laboratory planetary mill. The reference sample was difficult to measure due to slow reaction, but was estimated to be 10^{-8} [mol/m^{2}s]. Published olivine rates are on the order of 10^{-7} [mol/m^{2}s]. The comparison of the rates indicates that mechanical activation increased the rate constant by approximately three orders of magnitude compared to the published rate constants, including the uncertainties introduced by differences in experimental design. Laser diffraction, BET and XRD were the main analytical methods to describe the mechanically activated olivine samples. These methods gave relatively good bulk descriptions, but had

limited applicability to describe the changes in the physical and chemical properties occurring at the nano scale due to mechanical activation. To obtain these details, more advanced methods have to be used in the future.

Increased energy consumption during milling resulted in increased changes in the material characteristics compared to the original olivine. High mill intensities resulted in lower crystallinity than low intensity milling when the total energy consumption was constant. The only general trends regarding material characteristics and milling solutions were that wet milled samples had smaller particles relative to the specific surface area than the dry milled samples, and that dry milling was more efficient of reducing the crystallinity than both wet milling and milling with the addition of 10 wt% water. Of the three main material characteristics investigated (surface area, particle size distribution and crystallinity), the strongest correlation was found between the rate constant and the crystallinity. This indicates that changes in the crystal lattice and decreased crystallite sizes were the main causes of the rate constant increase beyond the contribution of specific surface area. For the more crystalline samples, the total dissolution rate [mol/s] correlated well with both the measured specific surface areas and the crystallinity

Even though the planetary mill obtained the highest dissolution rates, this mill is far too energy intensive for CO_2 sequestration purposes with an estimated total large scale energy consumption of ≈ 7000 kWh/ton after 60 min of milling. If mills are going to be used to increase the dissolution rate by mechanical activation, the Hicom mill and the attritor are possible choices among the mills studied. They cannot be ruled out before more extensive research has been performed. The commercially available sizes of these two mills, if several are used, are large enough to handle the mass flow of a mineral carbonation plant serving a 100 MW gas power plant.

Two types of direct carbonation experiments were performed to evaluate whether or not mechanical activation increase the carbonation reaction rate. The first experiment had short reaction durations of 1 min to 45 min at 128 °C and 150 bar (C-1), and the second had durations of 2 h and 18 h at 185 °C and 115 bar (C-2). The results from the C-1 experiments revealed that the extent of carbonation correlated well with the observed

dissolution rates, while for the C-2 experiment, neither the dissolution rates nor any of the material characteristics measured correlated with the observed extent of carbonation. The explanation suggested for the C-2 experiments is that precipitation kinetics of magnesite and not dissolution rates of olivine or the olivine characteristics are responsible for the observed range of carbonation degrees. The C-1 experiments may have been influenced by these precipitation kinetics, but the dissolution rate dominated the carbonation within the short reaction durations used.

The recognition of the importance of precipitation kinetics of secondary minerals as an important factor of direct olivine carbonation has implications for the choice of pre-treatment methods and the design of the carbonation process used for CO_2 sequestration. In direct carbonation experiments the challenge is to optimize the dissolution reaction at the same time as the carbonation reaction is optimized. At conditions where the precipitation kinetics is important, the less energy consuming milling alternative can be used, and the ball mill is a very good option.

To take advantage of the observed increase in the dissolution rates, an indirect carbonation process can be used by dividing the process into two or more steps. The first step is dissolution and the second, and possibly subsequent steps, are then precipitation of secondary minerals. This separation of the carbonation may introduce new aspects to the reactor design as for instance increased requirements for equipment and the challenge to preserve the dissolved minerals in solution until the precipitation reactor is reached. Indirect carbonation can be an option within CO_2 sequestration, but then the challenges of a multistep carbonation process have to be studied and solved with further research.

Chapter 7. Suggestions and recommendations

Several possibilities of experimental improvements were found after interpretation and discussing the experimental data, and many intriguing ideas were revealed during the PhD work. In the following text possible improvements of the work done and new research topics are presented.

7.1 Improvement of experiments

Two comments can be made regarding the milling contamination and the dissolution experiment described in chapter 3.2.2. Contamination diluted the olivine sample and the measured material characteristics represented an average of both the characteristics of olivine and the contamination. The importance of contamination increases with increasing amount of contamination. The influence of new chemical constituents might have been important for the dissolution and carbonation reactions, and further knowledge about this can be important.

Another remark is relevant for the dissolution experiments and concerns the quality of the water samples compared to the calculations

based on the measured pH. Water samples were only taken at the end of each experiment where pH in most cases had reached more than 3. Above pH = 3 the dissolution calculations based on pH change could only be compared to the water sample chemistry to a limited extent since pH was influenced by reactions not included in the calculation. To improve the verification of the calculations from the water samples, several water samples should have been taken during each experiment.

7.2 Research ideas succeeding the PhD work

7.2.1 Mineral processing

The first important observation regarding milling conditions and material characteristics was the observation of the effect of 10 wt% water as grinding aid and can be studied further. 10 wt% water obtained the highest measured specific surface area at the same time as the crystallinity was reduced significantly. Even though the crystallinity was almost as low as for dry milling, the dissolution rates were not the same. One possible explanation is that the calculated crystallinity does not distinguishing between for example the effects of crystallite size and strain in the crystal lattice and the size and amounts of fines. The cause of the crystallinity reduction can be very relevant for the interpretation of dissolution and carbonation results and needs more research.

Another relevant feature of mechanically activated materials are the aging effects due to secondary processes related to relaxing of microstrain and energetic unstable bonds within the mechanically activated samples. The result can be changes in the crystallinity, particle size and specific surface over time and loss of the effect of mechanical activation. Measurements over time can be performed to describe how much and how fast these changes occurs. The results are relevant for the choice of storage and storage time of the materials. An additional practical issue within mechanical activation is to study the milling efficiency of several mills with a special focus on the Hicom mill and the attritor. The energy consumption can be compared to obtained changes in material characteristics with the purpose of energy optimizing.

7.2.2 Mineral dissolution and carbonation

Batch dissolution experiments with a higher liquid/solid ratio than used in Paper III and IV can be used to improve the initial resolution of the pH measurements, which is important for the most reactive materials. In addition to changing the liquid/solid ratio, variation of the magnetic stirrer speed will indicate if the dissolution reaction is surface controlled or diffusion controlled. The effects of the stirring speed are probably dependent on the milling solution. Significant amounts of contamination were observed during the dissolution experiments as a dark material attached to the magnetic stirrer and was extensive, approaching 18 % at its most. The influence of contamination on dissolution and carbonation reactions should be attended to with the main questions being: Is the steel inert, and does the contamination particles influence the reactions?

In the extension of the batch experiments, flow-through dissolution experiments with constant pH should be performed. The use of water samples as the main output of the reaction instead of pH eliminates the influence of changing pH on the dissolution kinetics, and the water samples eliminates simplification errors in the concentrations found by pH calculations. Another advantage of the flow-through dissolution experiments is the avoidance of saturation and precipitation of secondary minerals. One more advantage when performing experiments far from saturation is the possibility to study how dissolution rates changes with dissolution degree. Paper II suggest that the material characteristics, and as a result the dissolution rate as well, changes with dissolution degree. Therefore are flow-through experiments far from saturation very suited to study the change in dissolution together with a strict control over the material properties at varying dissolution degrees. Flow-through experiments can be performed with carbonic acid or HCl. Pressurized CO_2 dissolved in water is closer to a commercial process than HCl, but HCl is more practical in a laboratory context when many experiments need to be performed.

A detailed study of particle shape and size, etch pits and surface area changes during dissolution may be valuable. These results give information of the dissolution mechanisms of mechanically activated olivine. There are possibly differences between the different combinations of milling parameters in how the pits and shapes develop during dissolution. In Paper

III and IV there were indications of magnesite precipitation being the rate limiting step in extensive carbonation. A further investigation of the precipitation kinetics and mechanisms of Mg-carbonates during direct carbonation is very valuable. Special attention should be paid to where and how the precipitated minerals are found, and how the occurrence corresponds to the material characteristics of the dissolving samples.

7.2.3 Pilot scale experiments?

1) A very interesting pilot scale experiment is to combine a high temperature, a high pressure, super critical CO_2 in excess and high intensity milling in a flow-through design. The chosen milling solution can be based on the PhD results or later performed experiments concerned with optimized milling and carbonation.
2) If energy intensive mills are going to be used within mineral carbonation, the obtained dissolution rates must be taken maximum advantage of. Therefore a pilot scale experiment with a Hicom mill or an attritor, and a two step mineral carbonation process can be tried where dissolution and precipitation is separated. Milling should be optimized before developing this experiment to decrease the energy consumption during milling and still obtain good dissolution results.

References

Alexander, G., Mercedes Maroto-Valer, M. and Gafarova-Aksoy, P., 2007, Evaluation of reaction variables in the dissolution of serpentine for mineral carbonation. Fuel, 86(1-2), 273-281.

Austin, L.G., Klimpel, R.R. and Luckie, P.T., 1984, *Process engineering of size reduction: ball milling*. Society of Mining Engineers, New York.

Awad, A., Koster van Groos, A.F. and Guggenheim, S., 2000, Forsteritic olivine: effect of crystallographic direction on dissolution kinetics. Geochimica Et Cosmochimica Acta, 64(10), 1765-1772.

Baláž, P., 2000, *Extractive Metallurgy of Activated Minerals*. 1st edn. Elsevier Science B.V., Amsterdam.

Baláž, P., 2003, Mechanical activation in hydrometallurgy. International Journal of Mineral Processing, 72(1-4), 341-354.

Baláž, P., 2008, *Mechanochemistry in Nanoscience and Minerals Engineering*. Springer-Verlag Berlin Heidelberg

Baláž, P., Turianicová, E., Fabián, M., Kleiv, R.A., Briančin, J. and Obut, A., 2008, Structural changes in olivine $(Mg,Fe)_2SiO_4$ mechanically

activated in high-energy mills. International Journal of Mineral Processing, 88(1-2), 1-6.

Bearat, H., McKelvy, M.J., Chizmeshya, A.V.G., Gormley, D., Nunez, R., Carpenter, R.W., Squires, K. and Wolf, G.H., 2006, Carbon sequestration via aqueous olivine mineral carbonation: Role of passivating layer formation. Environmental Science & Technology, 40(15), 4802-4808.

Bearat, H., McKelvy, M.J., Chizmeshya, A.V.G., Sharma, R. and Carpenter, R.W., 2002, Magnesium hydroxide dehydroxylation/carbonation reaction processes: Implications for carbon dioxide mineral sequestration. Journal of the American Ceramic Society, 85(4), 742-748.

Boldyrev, V.V. and Tkáčová, K., 2000, Mechanochemistry of solids: past, present, and prospects. Journal of Materials Synthesis and Processing, 8(3/4), 121-132.

Bond, F.C., 1961a, Crushing and grinding calculations Part I. British Chemical Engineering, 6(6), 378-385.

Bond, F.C., 1961b, Crushing and grinding calculations Part II. British Chemical Engineering, 6(8), 543-634.

Brunauer, S., Emmett, P.H. and Teller, E., 1938, Adsorption of gases in multimolecular layers. Journal of the American Ceramic Society, 60(2), 309-319.

Carey, J.W., Rosen, E.P., Bergfeld, D., Chipera, S., Counce, D.A., Snow, M.G., Ziock, H.J. and Guthrie Jr, G.D., 2003, Experimental studies of the serpentine carbonation reaction. In *Proc. The 28th International technical conference on coal utilization & fuel systems*, Clearwater, Florida, 331-340.

Chen, Y. and Brantley, S.L., 2000, Dissolution of forsteritic olivine at 65 °C and 2<pH<5. Chemical Geology, 165(3-4), 267-281.

Chen, Z.Y., O'Connor, W.K. and Gerdemann, S.J., 2006, Chemistry of aqueous mineral carbonation for carbon sequestration and

explanation of experimental results. Environmental Progress, 25(2), 161-166.

Duan, Z.H. and Sun, R., 2003, An improved model calculating CO_2 solubility in pure water and aqueous NaCl solutions from 273 to 533 K and from 0 to 2000 bar. Chemical Geology, 193(3-4), 257-271.

Eggleston, C.M., Hochella, M.F. and Parks, G.A., 1989, Sample preparation and aging effects on the dissolution rate and surface-composition of diopside. Geochimica Et Cosmochimica Acta, 53(4), 797-804.

EIA, 2009, International Energy Annual 2006. (DOE/EIA-0484), Energy Information Administration, USA.

Gerdemann, S.J., O'Connor, W.K., Dahlin, D.C., Penner, L.R. and Rush, H., 2007, Ex situ aqueous mineral carbonation. Environmental Science & Technology, 41(7), 2587-2593.

Giammar, D.E., Bruant, J.R.G. and Peters, C.A., 2005, Forsterite dissolution and magnesite precipitation at conditions relevant for deep saline aquifer storage and sequestration of carbon dioxide. Chemical Geology, 217(3-4), 257-276.

Goodson, R.E., 1985, Energy input monitoruing during attritor milling. International journal of refractory metals & hard materials, 4(2), 70-76.

Guthrie Jr, G.D., Carey, J.W., Bergfeld, D., Byler, D., Chipera, S., Zoick, H.-J. and Lackner, K.S., 2001, Geochemical aspects of the carbonation of magnesium silicates in an aqueous medium. In *Proc. First National Conference on Carbon Sequestration*, NETL, USA, pp.14.

Hangx, S.J.T. and Spiers, C.J., 2009, Coastal spreading of olivine to control atmospheric CO_2 concentrations: A critical analysis of viability. International Journal of Greenhouse Gas Control, 3(6), 757-767.

Hoberg, H. and Götte, J., 1985, The influence of mechanical activation on the kinetics of the leaching process of columbite. International Journal of Mineral Processing, 15(1-2), 57-64.

Hoyer, D.I., 1992, Power consumption in centrifugal and nutating mills. Minerals Engineering, 5(6), 671-684.

Hoyer, D.I., Mulvihill, B.M. and Young, G.J.C., 2001, Hicom attritioning to remove alumina-silicate coatings on ilmenite sand grains. Minerals Engineering, 14(7), 723-731.

Huijgen, W.J.J. and Comans, R.N.J., 2003, Carbon dioxide sequestration by mineral carbonation: Literature Review (ECN-C--03-016), ECN Clean Fossil Fuels 52.

Huijgen, W.J.J. and Comans, R.N.J., 2005, Carbon dioxide sequestration by mineral carbonation: Literature Review (ECN-C--05-022), ECN Clean Fossil Fuels 37.

Huijgen, W.J.J., Comans, R.N.J. and Witkamp, G.-J., 2007, Cost evaluation of CO_2 sequestration by aqueous mineral carbonation. Energy Conversion and Management, 48(7), 1923-1935.

Huijgen, W.J.J., Witkamp, G.J. and Comans, R.N.J., 2005, Mineral CO_2 sequestration by steel slag carbonation. Environmental Science & Technology, 39(24), 9676-9682.

Huijgen, W.J.J., Witkamp, G.J. and Comans, R.N.J., 2006, Mechanisms of aqueous wollastonite carbonation as a possible CO_2 sequestration process. Chemical Engineering Science, 61(13), 4242-4251.

Hänchen, M., Prigiobbe, V., Baciocchi, R. and Mazzotti, M., 2008, Precipitation in the Mg-carbonate system - effects of temperature and CO_2 pressure. Chemical Engineering Science, 63(4), 1012-1028.

Hänchen, M., Prigiobbe, V., Storti, G., Seward, T.M. and Mazzotti, M., 2006, Dissolution kinetics of forsteritic olivine at 90-150 degrees C including effects of the presence of CO_2. Geochimica Et Cosmochimica Acta, 70(17), 4403-4416.

IPCC, 2005, Special report on carbon dioxide capture and storage. Intergovernmental Panel on Climate Change, 371.

Jadhav, R., Zakin, J.L., Fan, L.S. and Park, A.H.A., 2002, Carbonation of Mg-bearing minerals: Kinetic and mechanistic studies. (#C3.12), Department of Chemical Engineering, The Ohio State University, Columbus, 27.

Jia, L.F., Anthony, E.J., Lin, W.G., Ruan, Y.H. and Gora, D., 2004, Carbonation of magnesium silicate minerals: an experimental study. Canadian Journal of Chemical Engineering, 82(6), 1289-1295.

Kalinkin, A.M., Boldyrev, V.V., Politov, A.A., Kalinkina, E.V., Makarov, V.N. and Kalinnikov, V.T., 2003, Investigation into the mechanism of interaction of calcium and magnesium silicates with carbon dioxide in the course of mechanical activation. Glass Physics and Chemistry, 29(4), 410-414.

Kheifets, A.S. and Lin, I.J., 1996, Energy transformations in a planetary grinding mill Part l. General treatment and model design. International Journal of Mineral Processing, 47(1-2), 1-19.

Kleiv, R.A., 2007, Mechanical activation (Lecture), Spring semester. 38.

Kleiv, R.A., Sandvik, K. and Thornhill, M., 2006, Increasing silicate carbonation kinetics by use of mechanical activation. In *Proc. International Mineral Processing Congress*, Istanbul, Turkey

Kleiv, R.A. and Thornhill, M., 2007, Production of mechanically activated rock flour fertilizer by high intensive ultrafine grinding. Minerals Engineering, 20(4), 334-341.

Kojima, T., Nagamine, A., Ueno, N. and Uemiya, S., 1997, Absorption and fixation of carbon dioxide by rock weathering. Energy Conversion and Management, 38(Supplement 1), 461-466.

Lackner, K.S., 2003, A guide to CO_2 sequestration. Science, 300(5626), 1677-1678.

Lackner, K.S., Wendt, C.H., Butt, D.P., Joyce, J.E.L. and Sharp, D.H., 1995, Carbon dioxide disposal in carbonate minerals. Energy, 20(11), 1153-1170.

Lichtner, P.C., Carey, J.W., O'Connor, W.K., Dahlin, D.C. and Guthrie, G.D.J., 2003, Geochemical mechanisms and models of olivine carbonation. In *Proc. In Proceedings of the 28th International Technical Conference on Coal Utilization & Fuel Systems, March 9-13, 2003*

Lynch, A.J., 1977, *Mineral Crushing and Grinding Circuits - Their simulation, optimisation, design and control*. Elsevier scientific publishing company

Maroto-Valer, M.M., Fauth, D.J., Kuchta, M.E., Zhang, Y. and Andresen, J.M., 2005, Activation of magnesium rich minerals as carbonation feedstock materials for CO_2 sequestration. Fuel Processing Technology, 86(14-15), 1627-1645.

McKelvy, M.J., Chizmeshya, A.V.G., Diefenbacher, J., Bearat, H. and Wolf, G., 2004, Exploration of the role of heat activation in enhancing serpentine carbon sequestration reactions. Environmental Science & Technology, 38(24), 6897-6903.

Munz, I.A., Korneliussen, A., Gorset, O., Johansen, H., Kihle, J., Flaathen, T. and Sandvik, K., 2005, Added value of industrial minerals and CO_2 storage: New possibilities for Norwegian mineral industry. In *Proc. The 8th International Cionference on Greenhouse Gas Control Technologies*, Trondheim, Norway, pp.3.

Musa, F. and Morrison, R., 2009, A more sustainable approach to assessing comminution efficiency. Minerals Engineering, 22(7-8), 593-601.

Nesbit, P.Q., Du Toit, G., Mapasa, K. and Feldman, C., 2001, Evaluation of the Hicom 120 mill at Venetia Mine. Minerals Engineering, 14(7), 711-721.

NGU and Bergvesenet, 2009, Mineral ressurser i Norge 2008 (Eng: Mineral resources in Norway 2008). Norwegian Geological Survey (NGU) and Bergvesenet, Trondheim, 44.

O'Connor, W.K., Dahlin, C.L., Turner, P.C. and Walters, R., 1999, Carbon dioxide sequestration by ex-situ mineral carbonation. (DOE/ARC-99-009), Albany Research Center, Albany, Oregon, 14.

O'Connor, W.K., Dahlin, D.C., Rush, G.E., Dahlin, C.L. and Collins, W.K., 2002, Carbon dioxide sequestration by direct mineral carbonation: process mineralogy of feed and products. Minerals & Metallurgical Processing, 19(2), 95-101.

Ohlberg, S.M. and Strickler, D.W., 1962, Determination of percent crystallinity of partly devitrified glass by X-ray diffraction. Journal of the American Ceramic Society, 45(4), 170-171.

Park, A.H.A. and Fan, L.S., 2004, CO_2 mineral sequestration: physically activated dissolution of serpentine and pH swing process. Chemical Engineering Science, 59(22-23), 5241-5247.

Park, A.H.A., Jadhav, R. and Fan, L.S., 2003, CO_2 mineral sequestration: Chemically enhanced aqueous carbonation of serpentine. Canadian Journal of Chemical Engineering, 81(3-4), 885-890.

Parkhurst, D.L. and Appelo, C.A.J., 1999, User's guide to PHREEQC (Version2)—A computer program for speciation, batch-reaction, one-dimensional transport, and inverse geochemical calculations. (99-4259), U.S. Geological Survey Water-Resources Investigations, 310.

Pokrovsky, O.S., 1998, Precipitation of calcium and magnesium carbonates from homogeneous supersaturated solutions. Journal of Crystal Growth, 186(1-2), 233-239.

Pokrovsky, O.S. and Schott, J., 2000, Kinetics and mechanism of forsterite dissolution at 25 degrees C and pH from 1 to 12. Geochimica Et Cosmochimica Acta, 64(19), 3313-3325.

Rau, G.H., Knauss, K.G., Langer, W.H. and Caldeira, K., 2007, Reducing energy-related CO_2 emissions using accelerated weathering of limestone. Energy, 32(8), 1471-1477.

Roberts, J., 2008, Olivine's future in flux. industrial minerals, (494), 40-42.

Sandvik, K., Digre, M. and Malvik, T., 1999, *Oppredning av Primære og Sekundære Råstoffer*. Tapir, Trondheim.

Sangwal, K.K., 1982, Dissolution kinetics of MgO crystals in aqueous acidic salt solutions [dislocation etching]. Journal of Materials Science, 17(12), 3598-3610.

Seifritz, W., 1990, CO_2 disposal by means of silicates. Nature, 345(6275), 486.

Sheila, D. and Khangaonkar, P.R., 1989, Precipitation of magnesium carbonate. Hydrometallurgy, 22(1-2), 249-258.

Sipilä, J., Teir, S. and Zevenhoven, R., 2008, Carbon dioxide sequestration by mineral carbonation. Literature review update 2005 - 2007. (2008 - 1), Åbo Akademi University, Faculty of Technology, Heat Engineering Laboratory.

Skjånes, K., Lindblad, P. and Muller, J., 2007, BioCO_2 - A multidisciplinary, biological approach using solar energy to capture CO_2 while producing H_2 and high value products. Biomolecular Engineering, 24(4), 405-413.

Snilsberg, B. 2008, *Pavement Wear and Airborn Dust Pollution in Norway*. PhD Thesis, Norwegian University of Science and Technology.

Song, C., 2006, Global challenges and strategies for control, conversion and utilization of CO_2 for sustainable development involving energy, catalysis, adsorption and chemical processing. Catalysis Today, 115(1-4), 2-32.

Stolaroff, J.K., Lowry, G.V. and Keith, D.W., 2005, Using CaO- and MgO-rich industrial waste streams for carbon sequestration. Energy Conversion and Management, 46(5), 687-699.

Stražišar, J. and Runovc, F., 1996, Kinetics of comminution in micro- and sub-micrometer ranges. International Journal of Mineral Processing, 44-45 673-682.

Summers, C.A., Dahlin, D.C., Rush, G.E., O'Connor, W.K. and Gerdemann, S.J., 2005, Grinding methods to enhance the reactivity of olivine. Minerals & Metallurgical Processing, 22(3), 140-144.

Teir, S., Eloneva, S. and Zevenhoven, R., 2005, Production of precipitated calcium carbonate from calcium silicates and carbon dioxide. Energy Conversion and Management, 46(18-19), 2954-2979.

Teir, S., Kuusik, R., Fogelholm, C.-J. and Zevenhoven, R., 2007, Production of magnesium carbonates from serpentinite for long-term storage of CO_2. International Journal of Mineral Processing, 85(1-3), 1-15.

Tkáčová, K., 1989, *Mechanical Activation of Minerals*. Elsevier Science Publishers, Amsterdam.

Tromans, D. and Meech, J.A., 2001, Enhanced dissolution of minerals: Stored energy, amorphism and mechanical activation. Minerals Engineering, 14(11), 1359-1377.

Weiss, N.L., 1985, *SME Mineral Processing Handbook*. Society of Mining Engineers of the American Institute of Mining, Metallurgical and Petroleum Engineers, New York.

Wills, B.A. and Napier-Munn, T., 2005, *Wills' Mineral Processing Technology (Seventh Edition) - An Introduction to the Practical Aspects of Ore Treatment and Mineral Recovery* Butterworth-Heinemann, Oxford.

Wogelius, R.A. and Walther, J.V., 1991, Olivine dissolution at 25 °C: Effects of pH, CO_2, and organic-acids. Geochimica Et Cosmochimica Acta, 55(4), 943-954.

Wu, J.C.S., Sheen, J.D., Chen, S.Y. and Fan, Y.C., 2001, Feasibility of CO_2 fixation via artificial rock weathering. Industrial & Engineering Chemistry Research, 40(18), 3902-3905.

Zevenhoven, R. and Kavaliauskaite, I., 2004, Mineral carbonation for long-term CO_2 storage: An exergy analysis. International Journal of thermodynamics, 7(1), 23-31.

Zevenhoven, R., Teir, S. and Eloneva, S., 2008, Heat optimisation of a staged gas-solid mineral carbonation process for long-term CO_2 storage. Energy, 33(2), 362-370.

Part 2

Paper I

Energy Intensive Milling of Olivine used for CO_2 Storage

T. Anette Haug[1*], Ingrid Anne Munz[2], Jan Kihle[2], John P. Kaszuba[3], J. William Carey[3]

[1]*Institutt for geologi og bergteknikk, NTNU, Norway,* [2]*Institutt for energiteknikk, Norway,* [3]*Los Alamos National Laboratory, USA*

[*]*anette.haug@ntnu.no*

Introduction

Since the 80's the environmental concerns have been accelerating, and continuously reaching wider including CO2 emissions contributing to global heating (Markley and Hurley Iii, 1983) One out of several options for safe storage of CO_2 is reacting CO_2 with minerals and create carbonates that are stable and safe to the environment (Schulze et al., 2004). This process is called mineral carbonation (Lackner et al., 1995). On a small scale the process might be used to clean mineral waste from industry. The knowledge of the reactions between minerals and CO_2, mostly as carbonic acid, might be used to treat mineral waste and create less waste or more practical waste. CO_2 treatment of this kind will include dissolution of minerals leading to easier separation of waste material or creation of more stable carbonates.

One out of several minerals with carbonation potential is the magnesium rich variety of olivine is forsterite. In a natural environment olivine will weather in presence of rain water acidified by CO_2 (Schuiling and Krijgsman, 2006). (Teir et al., Lackner et al., McKelvy et al.) The simplified reaction between Mg-rich olivine and CO_2 in geological context can be described as the combination of two reactions. The first reaction is dissolving CO_2 from air in water. The pH will be around 5,6 and dissolved CO_2 will mainly exists as bicarbonate, after dissociation of carbonic acid (Appelo and Postma, 1999). The second reaction is dissolution of olivine with carbon acidic water as described by the simplified equation 1.

$$Mg_2SiO_{4(s)} + 2H^+ + 2HCO_3^- \leftrightarrow 2MgCO_{3(aq)} + H_4SiO_{2(aq)} \quad (1)$$

olivine + acid + bicarbonate ↔ magnesite + silicic acid (dissolved silica)

The described reaction is too slow for industrial purposes. If mineral carbonation is used for carbon capture, there has to be done some treatment of the material or find conditions that enhance the reaction rate to a practical level. One possibility is to change the characteristics of the olivine by pre-treatment and mechanical activation of olivine particles was chosen to improve the dissolution process. Several experiments have been done with silicates containing magnesium with both direct reaction with CO_2 and indirect reaction where CO_2 is dissolved in an aqueous environment and then reaction with the minerals. The aqueous reaction model seems to be the better alternative (Chen et al., 2006, Kojima et al., 1997).

Mechanical activation is a high energy comminution process, using mechanical treatment on a material, to enhance the reactivity beyond the reaction found in non-activated materials. The mills used for mechanical activation have several times higher energy density than conventional tumbling mills. Common types of energy-intensive mills are the non-rotary ball mill, impact mills and planetary mills (Tkáčová, 1989) as well as vibration mills and attritors (Baláž, 2000). During and after activation the crystal lattice is not in equilibrium and the

excess energy caused by disorder contributes to lower the activation energy of any further reaction of the material (Tromans and Meech, 2001). Tromans and Meech (1999) suggested mechanical activation of crystalline particles to increase the numbers of dissolution sites and reduce the particle size to overcome high activation energies for chemical reactions. Important contributors to this increase is deformation, resulting in changes surface topography, broken molecule bonds, increased surface area and decreased particle size (Tkáčová, 1989). The change of each of these characteristics is dependent of the type of mill, milling factors and materials.

The main purpose of this paper is to introduce the idea of mineral carbonation as one of several CO_2 storage methods hopefully combined with mineral waste reactions describing mainly mechanical activation as a pretreatment enhancing the reaction ability, but also highlighting the carbonation reaction as found from dissolution experiments of olivine. From the knowledge regarding reactions between minerals and CO_2, other useful applications of CO_2 can be discovered as well. CO_2 can be used as an industrial chemical to cleanse waste deposits because of its ability to dissolve minerals and form environmentally friendly carbonates. Here olivine is used as the reacting mineral, but with further research, probably other minerals can be used also.

Materials and methods

Materials

The original material used in the mechanical activation and dissolution experiments was olivine foundry sand (ASF 50) from North Cape Minerals dunite deposit at Åheim in Western Norway. The dunite is crushed and sieved and the original material contains forsterite, enstatite, chlorite, talc, amphibole and mica, as identified by XRD[1]. The sand is approximately 90 % by weight pure olivine with the quality Fo_{93}. The chemical composition of the material determined by XRF[2] analysis is presented in Table 1. In standard XRF main element analysis Cu and Ni are not included, but given the mineral composition of this olivine sand, there might be trace amount of both elements. Ni (NiO) and Cr (Cr_2O_3) has been detected in comparable olivine material earlier, 0.3 wt% for both from XRF analysis (Kleiv and Thornhill, 2006). Specific surface area of the material equals 0.17 m^2/g using the BET method with N_2-gas[1].

Table 1 Weight percent distribution of main elements in AFS50 foundry sand used as starting material in experiments.

Component	Wt. [%]
MgO	49.14
SiO_2	41.68
Fe_2O_3	7.33
Al_2O_3	0.17
CaO	0.1
MnO	0.1
K_2O	0.02
TiO_2	0.01
P_2O_5	0.01
Na_2O	i.m.
LOI	0.33
SUM	98.56

Mechanical activation and material analysis

Mechanical activation of the olivine sand was performed using a Fritsch Pulverisette planetary mono mill. The mill is only constructed for laboratory batch experiments. The

[1] Done by Los Alamos National Laboratory, USA
[2] Done by Department of Geology and Resources Engineering, NTNU, Norway

chamber lid has two valves, thus flusing of the chamber. The closed milling chamber originally contained air at 1 atm pressure. Both chamber and balls are made of stainless steel. The volume of the milling chamber is 250 ml, and the ball dimension is 20 mm. The number of balls equals 20 with a total weight of 645,2g giving 83,8 ml of milling balls. The milling factors were chosen to investigate the importance of milling atmosphere, here air and N_2-gas were used both at 1 atm, milling time and 2 ml added deionized H_2O compared to dry milling. A constant speed of 500 rpm and continuous milling[3] was used for all samples together with 20 g of olivine sand. The weight ratio between the milled material and the steel balls was 1:32. 19 different samples were produced with different combinations of milling factors.

There has been performed different analysis for all 19 produced samples. XRF were used to determine the contamination from the milling chamber, XRD were used to study the change in crystallinity and the mineral composition, and LS coulter was used to study particle size distributions and BET for specific surface areas.

Dissolution experiment design

5 dissolution experiments were performed on both mechanically activated material and reference material. The reference sample was prepared from the olivine sand also used for the mechanical activation. The material was gently crushed by hand to minimize the structural change, sieved to a 75 µm – 150 µm fraction and cleansed with ethanol to remove fines. Two experiments were done with reference material. Three mechanically activated materials were used with the specifications 10 min dry milling, 60 min dry milling and 60 min milling with addition of 2 ml water. See Table 2 for summary of experiments.

Figure 1 flow sheet of the dissolution experiments

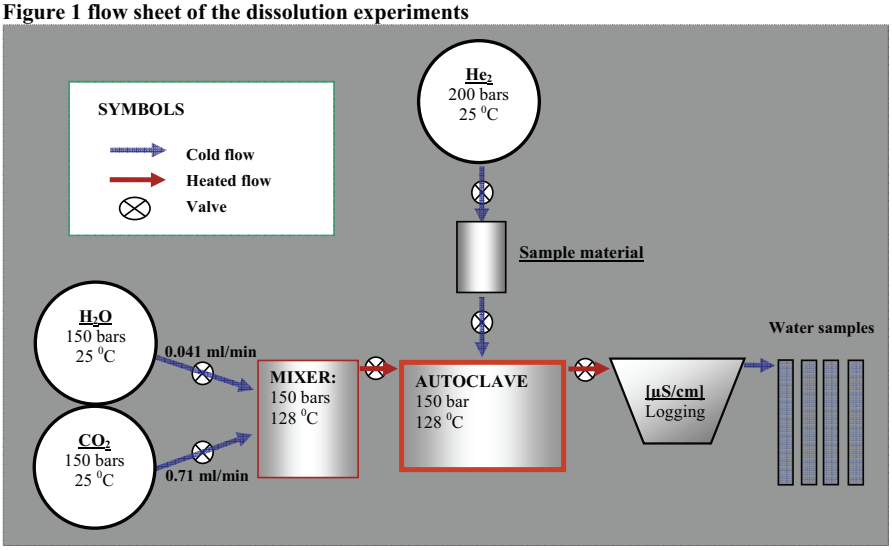

The dissolution of olivine was performed at 150 bars and 128 °C. H_2O and CO_2 was pressurized separately and combined and heated in a mixer, see Figure 1. The carbonated fluid flowed through a 50 ml autoclave at a constant flow rate of 0,798 ml/min with 2,2 mol% CO_2. This combination of H_2O and CO_2 gives a 2-phase fluid composed of both liquid CO_2 and liquid H_2O, with dissolved CO_2 converted into carbonic acid. pH is modeled to be 3,5 in

[3] For the samples milled for 60 minutes, this had to be done in 2 intervals of 30 minutes with a break of 30 min to avoid overheating of the mill.

the initial fluid. Important parameters logged during experiments were pressure to confirm steady state, the ability of the fluid to conduct electricity as a measure of the ion content and water samples with sample duration of 20 minutes, and continuously measurement of temperature. Duration of experiments ranged from 18 to 72 hours.

Table 2 Summary dissolution experiments data

Experiment	Mechanical activation of materials dissolved	Material inserted [g]
Olivine - 11	ACT_{10D}	0.4267
Olivine - 12	ACT_{60D}	0.4188
Olivine - 17	ACT_{60W}	0.1509
Olivine - 13	$REF_{75\text{-}150}$	0.134
Olivine - 14	$REF_{75\text{-}150}$	1.4266

Results/Discussion

Effects on material characteristics after mechanical activation

There are several effects of mechanical activation that can be important for the subsequent olivine dissolution process. For practical purposes, the contamination of the material from wear of the equipment will give some additions into the chemical aspects of the process. For the more technical aspects of the reaction, particle size, crystallinity as a measure of crystal lattice distortion and surface area, is also important.

The reference samples and the samples milled for 10 and 60 minutes have been analysed by XRF to quantify the main elements in the samples and the amount of contamination from the milling chamber. The element analysis revealed contamination mainly from iron. The contamination is increasing with time, and a 10 Wt% water addition during milling creates much more contamination than dry milling. The results are in agreement with the observation of wet grinding resulting in more wear on the grinding equipment than dry grinding (Tkáčová, 1989). The wear on the equipment contributes to contamination of the milled material.

One important characteristic in materials meant for dissolution processes are the crystallinity. Decreasing crystallinity increases the reactivity (Baláž, 2000, Kalinkin et al., 2003, Tkáčová, 1989) By comparing the XRD intensities, the relative change of crystallinity can be observed for the mechanically activated samples. Prolonged milling of olivine results in decreasing crystallinity, but addition of water compared to dry milling gives much more crystalline materials under otherwise equal conditions.

Specific surface area is also important in dissolution reactions, together with the crystallinity. In these specific experiments the original material has a specific surface are of 0.17 m^2/g and an increase was expected after milling. For the conditions used in these experiments there is actually a decreasing trend for dry milling after an initial increase, se Figure 2. Decrease has been observed by others also, and can be explained by aggregation of fines to bigger particles and acting as one particle (Kleiv and Thornhill, 2006). The specific surface area change over time for wet milled olivine is displaying an opposite behaviour of the dry milled olivine. There has not been observed an upper limit for the specific surface area of wet milled olivine up to 60 min milling. It is possible that the area will continue to increase even more, before is stabilizes or starts to decrease when the milling time is prolonged. The ratio between the

specific surface area of wet milled and dry milled materials ranges from 4 to 15 with wet milling giving the highest values.

Figure 2 Time dependence for dry(left) and wet(right) milled materials. Materials are milled in air.

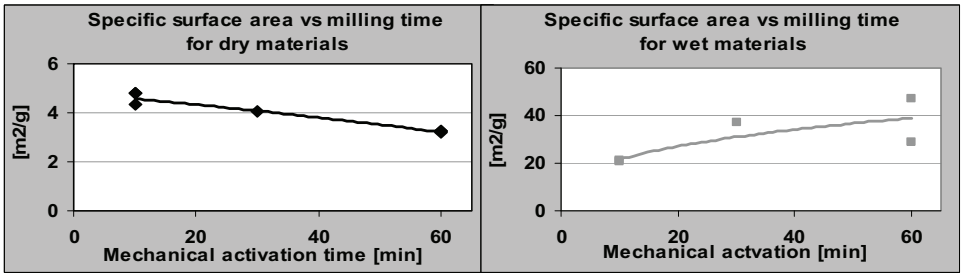

In addition to surface area and crystallinity, the particle size distributions are affected by time, atmosphere and water addition. The atmosphere in the mill is important for the activation result. When grinding in air, moisture and CO_2 can be absorbed to the surface, and prolonged grinding increases the adsorption (Baláž, 2000).

Figur 3 Effect of 10 Wt% water addition to mechanically activated materials milled for 10 minutes in air.

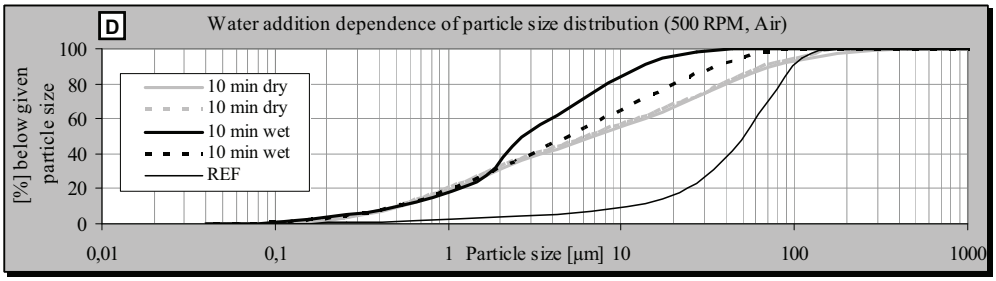

If small particles are important, milling in liquid will inhibit aggregation, see Figure 3 as example of effect of 10 Wt% water addition. Milling dry in a inert atmosphere (normally N_2 – gas) will also give small particles and also a high degree of amorphization, in contrast to liquid grinding that is less destructive regarding the crystal lattice (Baláž, 2000, Tkáčová, 1989). For dry milling N_2-atmosphere produced very fine material compared both to dry and wet milling, using the same milling time. There is also a small, but significant difference between wet and dry milling too. Mechanically activated materials added 2 ml of deionised water during simultaneously with milling, have a tendency for fewer particles in the upper particle sizes compared to the dry milled materials, and generally have a particle distribution curve moved towards finer particles.

Mineral change during milling and dissolution

The milled samples used in the dissolution experiments, the original olivine foundry sand and the dissolution products, contained no traceable serpentine. A decrease of talc from 0.5 Wt% in the original material to trace amounts in all the dissolution products was found. It might have been expected to find serpentine since the sample was milled with added water, and water is chemically bound to the material during milling. The mineral composition of the milled materials was very similar to the original material, but the XRD peaks were smaller.

The reason for fewer detectable minerals in the milled material is probably because of a decrease of the crystallinity making it harder to find minerals in small amounts.

The dissolution products from all of the 5 dissolution experiments had very similar XRD patterns. The two most converted products were the possibility to find new phases were most likely, displayed peaks probably from goethite and hematite. These are probably precipitated iron phases on the surfaces of the dissolved material, and when more material has dissolved, more will precipitate and make it possible to detect the phases with XRD. The assumption of iron phase precipitation is supported by the dark brown-red color of the residue and also the lack of iron from the water samples from all of the dissolution experiments. XRD results of the olivine sand milled 60 minutes with 2 ml of water before and after dissolution might indicate that forsterite is dissolved faster than enstatite.

Dissolution of olivine sand

In the dissolution experiments, only 3 types of different mechanically activated olivine materials were used in addition to the prepared reference material. The differences in the ion concentrations in the fluid samples and the ability to conduct electricity give indications of the influence from the mechanical activation.As a first estimate the material was assumed to be pure olivine, Fo93. The second initial assumption is that the same reactions happened in all of the experiments but with different dissolution degree depending on initial amount of material and total reaction time. These to assumptions make it easier to compare the extension and rate of dissolution.

The water sample concentrations of Mg and Si in the first hour of olivine dissolution, was not always in agreement of the stoichiometric composition of the olivine used. The reference sample experiments are approximately ideal, but the milled materials give non-stoichiometric ratios between Mg and Si. Mechanically activation of 10 minutes dry milling and 60 minutes milling with 2ml H2O have maximum Mg:Si ratios at respectively 10.5 and 2.5 and both occurring before 40 minutes reaction. Dissolution of olivine material milled for 60 minutes in air without water is the most ideal experiment regarding release of Mg and Si. As shown by XRD analysis this material is the most destroyed, and therefore probably the material with the highest number of broken crystal bonds. Since a dissolution process is essentially breaking bonds and removing ions from the crystal lattice, the deformation of the material might be one explanation for the very congruent dissolution.

The reaction rates calculated from the experiments have uncertainties resulting from different weights and some technical problems, but there is still possible to observe some indications of the mechanical activation influence. Dry milled material for 10 min is the most reactive activated sample if the rate is normalized to the measured surface area, but if the reaction rate is normalized to weight, as mol pr gram pr second instead of mol pr m^2 pr second, the wet milled material is the most reactive. The difference of reaction rates under the described conditions must be verified by additional experiments.

Conclusion

Mechanical activation of olivine has several effects of the resulting material, and these effects also influence the dissolution rates. Dry activated olivine is less crystalline than olivine activated with 10 Wt% added water calculated relative to material weight and increased milling time from 10 to 60 minutes decreases the crystallinity in general. Specific surface area increases within the same time frame for wet milling, but decreases for dry milling. When studying the release of Mg and Si ions into solution during dissolution, the mechanically

activated samples have a tendency to release Mg-ions faster than Si-ions up to 1 hour of reaction. Activation in air for 10 minutes gave up to 10.5 times more Mg than Si even though the ideal relationship is 1,86.

The specific area of the reference sample and activated samples ranged from 0.87 [m^2/g] to 47 [m^2/g]. If only surface area of the material is important for the release speed of ions into the fluid, the reaction rate normalized to area will be the same. The estimated reaction rate, R [mol/(m_2s)] of mechanically activated olivine is of the same order of magnitude as non-activated olivine, but higher specific area with in a practical process still give lower reaction times. There are however indications that dry milled materials have higher specific reaction rates given as [mol/(m_2s)], but if the total moles released within a given time frame is the most important factor, prolonged wet milling will probably give the best contribution. The performed experiments were not designed to find change in the reaction rates over time, even though that is likely due to inhomogeneous distortion of the crystal lattice in the particles or effects of changing surface area as the dissolution proceeds.

To determine the best approach to a fast reaction suitable for industrial purposes, several experiments and calculations have to be done. The importance of a high specific surface area compared to the need for lowered crystallinity has to be quantified and compared to energy consumption and efficiency of the dissolution/storage process in total.

References

APPELO, C. A. J. & POSTMA, D. (1999) *Geochemistry, groundwater and pollution,* Rotterdam, A. A. Balkema.

BALÁŽ, P. (2000) *Extractive metallurgy of activated minerals,* Amsterdam, Elsevier Science B.V.

CHEN, Z. Y., O'CONNOR, W. K. & GERDEMANN, S. J. (2006) Chemistry of aqueous mineral carbonation for carbon sequestration and explanation of experimental results. *Environmental Progress,* 25**,** 161-166.

KALINKIN, A. M., KALINKINA, E. V. & MAKAROV, V. N. (2003) Mechanical activation of natural titanite and its influence on the mineral decomposition. *International Journal of Mineral Processing,* 69**,** 143-155.

KLEIV, R. A. & THORNHILL, M. (2006) Mechanical activation of olivine. *Minerals Engineering,* 19**,** 340-347.

KOJIMA, T., NAGAMINE, A., UENO, N. & UEMIYA, S. (1997) Absorption and fixation of carbon dioxide by rock weathering. *Energy Conversion and Management,* 38**,** S461-S466.

LACKNER, K. S., WENDT, C. H., BUTT, D. P., JOYCE, J. E. L. & SHARP, D. H. (1995) Carbon dioxide disposal in carbonate minerals. *Energy,* 20**,** 1153-1170.

MARKLEY, O. W. & HURLEY III, T. J. (1983) A brief technology assessment of the Carbon Dioxide effect. *Technological Forecasting and Social Change,* 23**,** 185-201.

MCKELVY, M. J., SHARMA, R., CHIZMESHYA, A. V. G., CARPENTER, R. W. & STREIB, K. (2001) Magnesium hydroxide dehydroxylation: In situ nanoscale observations of lamellar nucleation and growth. *Chemistry of Materials,* 13**,** 921-926.

SCHUILING, R. D. & KRIJGSMAN, P. (2006) Enhanced weathering: An effective and cheap tool to sequester CO2. *Climatic Change,* 74**,** 349-354.

SCHULZE, R. K., HILL, M. A., FIELD, R. D., PAPIN, P. A., HANRAHAN, R. J. & BYLER, D. D. (2004) Characterization of carbonated serpentine using XPS and TEM. *Energy Conversion and Management,* 45**,** 3169-3179.

TEIR, S., ELONEVA, S., FOGELHOHN, C. J. & ZEVENHOVEN, R. (2006) Stability of calcium carbonate and magnesium carbonate in rainwater and nitric acid solutions. *Energy Conversion and Management,* 47**,** 3059-3068.

TKÁČOVÁ, K. (1989) *Mechanical Activation of Minerals,* Amsterdam, Elsevier Science Publishers.

TROMANS, D. & MEECH, J. A. (1999) Enhanced dissolution of minerals: Microtopography and mechanical activation. *Minerals Engineering,* 12**,** 609-625.

TROMANS, D. & MEECH, J. A. (2001) Enhanced dissolution of minerals: Stored energy, amorphism and mechanical activation. *Minerals Engineering,* 14**,** 1359-1377.

Paper II

DISSOLUTION OF MECHANICALLY ACTIVATED OLIVINE IN HYDROCHLORIC ACID - INVESTIGATING LEACHING PROPERTIES FOR CARBONATION PURPOSES

Tove Anette Haug[a]
Rolf Arne Kleiv[a]
Ingrid Anne Munz[b]

[a] Department of Geology and Mineral Resources, Norwegian University of Science and Technology, Sem Saelandsvei 1, 7491 Trondheim, Norway
[b] Institute for Energy Technology, P.O. Box 40, 2027 Kjeller, Norway

ABSTRACT

Mineral carbonation is one out of several options for CO_2 sequestration and storage. The reaction rates of appropriate minerals with CO_2, for instance olivine and serpentine with vast resources are relatively slow in a CO_2 sequestration context. The rates have to be increased to make mineral carbonation a good storage alternative. Therefore has increasing the dissolution rate of olivine been the focus of this paper. Olivine was milled with very high energy intensity using a laboratory planetary mill to investigate the effect of mechanical activation on the Mg leaching potential of olivine in 0.01 M HCl solution at room temperature and pressure. Approximately 30 % - 40 % of each sample was dissolved and water samples where taken at the end of each experiment. The pH change was used to calculate time series of the Mg concentrations, and the calculated values were compared to the Mg concentrations in the water samples. Percentages

dissolved and the specific reaction rates were estimated from the Mg concentration time series. PHREEQCi, a geochemical modelling program, was used to model the experiments and indicated that that modelling of mechanically activated materials should include factors describing the changes in the material properties related to the activation. The mechanically activated samples reacted in general faster than predicted by the theoretical models. The measured particle size distributions could not explain the rate constants found, but the specific surface area gave a nice trend versus dissolution for samples milled wet and the samples milled with a small addition of water. It was not possible to use the measured particle sice to estimate specific surface areas in agreement with the measured specific surface areas. The samples milled dry had the lowest measured specific surface areas (< 4 m^2/g), but had the highest rate constants. The crystallinity, calculated from X-ray diffractograms, was the material parameter with the best fit for the observed differences in the rate constants. Mechanical activation as a pre-treatment method was found to enhance the initial specific reaction rates with approximately three orders of magnitude for a sample milled dry for 60 minutes in a planetary mono mill compared to an unactivated sample. Wet milling in the planetary mill did not produce samples with the same maximum reaction rate as dry milling did, but wet milling in general might be easier to implement into a wet carbonation process. Mechanical activation in a planetary mill is most likely to energy consuming for a CO_2 sequestration purposes, but the increase in obtained olivine rate constants illustrates a possible potential within using milling as a pre-treatment method.

KEYWORDS

Mechanical activation, planetary mill, olivine dissolution, carbonation, geochemical modelling, PHREEQCi, specific surface area, crystallinity

1 INTRODUCTION

Mineral carbonation research is important for developing the field of CO_2 storage as carbonates. This research may hopefully also contribute to finding economical ways of using the large amount of CO_2 becoming available when CO_2 will be captured in a large scale. The IPCC Special Report on Carbon dioxide Capture and Storage (IPCC, 2005) gives a

comprehensive description of the research status until 2005 and three reviews regarding mineral carbonation can be mentioned as well (Huijgen and Comans, 2003, Huijgen and Comans, 2005, Sipilä *et al.*, 2008). The carbonation of minerals is an important natural reaction where minerals react with atmospheric CO_2 and may form carbonates. The Goldich weathering sequence states that olivine is the least weathering resistant silicate (Goldich, 1938) and hence is a promising mineral for industrial carbonation. Mineral carbonation was proposed as CO_2 storage by Seifritz (1990) and Lackner *et al.* (1995) and a range of minerals has been discussed by several others as well (Kojima *et al.*, 1997, McKelvy *et al.*, 2004, O'Connor *et al.*, 1999, Teir *et al.*, 2005). The carbonation reaction of Mg-rich olivine can be described by three steps. Firstly CO_2 is dissolved from the atmosphere in available water and carbonic acid is created with a pH around 5.6. The second reaction is the dissolution of olivine with carbonated water as described in Eq. 1. The third step is precipitation of carbonates and possibly silica.

$$Mg_2SiO_{4(s)} + 2H_2O + 2CO_2 \leftrightarrow 2Mg^{2+} + 2CO_3^{2-} + H_4SiO_2 \quad (1)$$

Olivine was chosen due to the promising natural kinetics and also due to the available amounts of olivine in Norway. The natural weathering rate of olivine is estimated to be $10^{-8.5}$ mol/(m^2s) using the average ground temperature in Norway of 6 °C and a pH = 5.6 corresponding to the acidity of rainwater. This rate is too slow for large scale industrial CO_2 sequestration operations. Several pre-treatment methods have been investigated to increase the total reaction including heat activation (McKelvy *et al.*, 2004), chemical activation (Maroto-Valer *et al.*, 2005), grinding (Summers *et al.*, 2005), additives in the reaction fluid and elevated process temperatures and pressures (O'Connor *et al.*, 2002). Mechanical activation, meaning milling with very high intensity for a short period of time, is a pre-treatment option within the grinding technology and is normally used for two purposes, mechanically alloying or increasing the leachability of metal ores in the hydrometallurgical industry. Mechanical activation used in olivine carbonation can be an effective way of increasing the dissolution kinetics in an actual process. The mills used for mechanical

activation have several times higher energy intensity than conventional tumbling mills (Baláž, 2000, Tkáčová, 1989).

Mechanical activation changes the character of the material beyond reduced particle size and increased surface area (Tkáčová, 1989). The changes in the material resulting from the mechanical activation have been found to be very important for mineral leaching properties (Eggleston *et al.*, 1989, Sangwal, 1982) and Hoberg and Götte (1985) shows how the rate constant of dissolving columbite is dependent on the degree of mechanical activation. During and after activation the crystal lattice is not in equilibrium and the excess energy caused by disordering contributes to lowering the activation energy of any following reaction of the material (Tkáčová, 1989, Tromans and Meech, 2001). Chemical reactions as an effect of introducing mechanical energy were documented as early as 1882 by M. Carey Lea (Historical review by Baláž, 2000). The effects of mechanical activation such as increased leaching rate, changes in surface area and crystallinity were published in 1968 (Szhanto, 1968). Experiments have shown that mechanical activation gives decreased crystallinity and has been measured and calculated from X-ray diffraction (Baláž, 2000, Kalinkin *et al.*, 2003, Kleiv and Thornhill, 2006, Pourghahramani and Forssberg, 2006, Tromans and Meech, 2001). Kleiv and Thornhill (2006), and Baláž *et al.* (2008) describe specific details about the effect of mechanical activation of olivine.

Enhancing the olivine carbonation rate by increasing the olivine dissolution rate was the overall motivation for the study presented in this paper. Many papers have been published regarding olivine dissolution (i.e. Chen and Brantley, 2000, Hänchen *et al.*, 2006, Liu *et al.*, 2006, Oelkers, 2001, Olsen and Rimstidt, 2007, Pokrovsky and Schott, 2000, Rosso and Rimstidt, 2000, Wogelius and Walther, 1991, Wogelius and Walther, 1992) where particle size and pH is specified and accurately controlled. In an industrial process, a strict control with the particle size is more difficult and changes in pH may occur. In this paper the mechanically activated olivine samples were used directly from the mill without further modifications of the particle size, to mimic the olivine material used in an industrial process. The dissolution experiment used is however just a screening test to differentiate between the samples, and are not designed to become an

industrial dissolution process. The batch reactions were combined with geochemical modelling with PHREEQCi (Parkhurst and Appelo, 1999) for interpretation of the dissolution experiments and comparison with crystalline olivine kinetics. In the dissolution experiments diluted hydrochloric acid was used instead of carbonic acid and assumed to behave in a comparable way for dissolution purposes, as found by Hänchen *et al.* (2006). The material properties were evaluated using crystallinity, specific surface area, and particle size distribution.

2 MATERIALS AND EXPERIMENTAL METHODS

2.1 Materials

Table 1 XRF analysis results for the original sand of olivine and the reference sample of olivine given in wt% of main elements (left) and ppm of trace elements (right).

Component	Original sample [wt%]	Reference sample [wt%]	Component	Original sample [ppm]	Reference sample [ppm]
Fe2O3	7.13	7.54	Zr	15	12
TiO2	0.01	0.03	Y	2	1
CaO	-[a]	0.4	Sr	39	6
K2O	0.01	0.06	Rb	2	1
P2O5	0.01	0.01	Zn	46	42
SiO2	41.64	42.29	Cu	10	2
Al2O3	-[a]	-[a]	Ni	3351	3593
MgO	50.62	48.39	Ba	31	-[a]
Na2O	-[a]	-[a]	Co	121.8	126.1
MnO	0.1	0.1	Cr	3005	1815.9
SUM	99.52	98.82	V	35.1	21.7
LOI	0.34	0.41	Th	1.4	1.8
			Pb	27.6	3

[a] Below detection limit

The material used in this study consisted of olivine foundry sand of the quality ASF50 provided by North Cape Minerals from their dunite deposit at Åheim in Western Norway. The AFS50 sand will be referred to as the original sample. X-ray diffraction analysis (XRD) detected forsterite, chlorite, enstatite, chromite and traces of hornblende and mica, and approximately 95 % by weight is pure olivine of the composition

$Mg_{1.86}Fe_{0.14}SiO_4$ (Osland, 1998). Another product from the same deposit, referred to as AFS80, was used to prepare a reference sample for the dissolution experiments. AFS80 had for all practical purposes, the same composition as AFS50, but the particle size of AFS80 was closer to the desired particle size distribution for dissolution. The AFS80 sand was sieved dry to retrieve the 74 – 147 μm fraction. This fraction was washed with ethanol to remove fines. Main elements and trace elements of the original sample and the reference sample, as found by X-ray fluorescence (XRF) are presented in Table 1. The original sample and the reference sample had specific surface areas of 0.47 m^2/g and 0.93 m^2/g respectively, as found by BET analyses.

2.2 Mechanical activation

Table 2 Summary of the milling combinations for the mechanically activation of the original olivine sample.

Batch name	Milling time [min]	Addition of water [ml] at 22 °C
10minDry	10	0
30minDry	30	0
60minDry	60	0
90minDry	90	0
10minW10%	10	2
30minW10%	30	2
60minW10%	60	2
10minWet	10	100
30minWet	30	100
60minWet	60	100

Mechanical activation of the olivine sand was achieved using a Fritsch Pulverisette 6 planetary mono mill by milling of 20.0 g original sample in a 250 cm^3 stainless steel mill chamber (17-19 % Cr; 8-10 % Ni). The milling was conduced at 500 rpm using twenty ∅20 mm stainless balls (12.5-14.5 % Cr; 1 % Ni) and was performed as either dry milling, wet milling by adding 100 ml of distilled water or adding 2.0 ml of distilled water as a grinding aid. At the end of each batch the final product was carefully retrieved using

a brush and a spatula. To minimize the risk of cross contamination between samples, the milling chamber and balls were washed with a brush and water, and dried with ethanol between each batch. A total of 13 samples were prepared by combining milling time and water addition as shown in Table 2. Two sets of materials were produced. The first set contained ten samples, including the nine possible combinations of 10, 30 and 60 min milling with 0, 2 and 100 ml of deionised H_2O, and also one sample milled dry for 90 min. The second set of materials was comprised of 10minW10%, 60minDry and 60minWet duplicates.

2.3 Analyses

The specific surface area was measured using the BET method with N_2 adsorption using a Flowsorb II 2300 from Micromeritics with a degasser unit. Water sample analyses were performed on the filtrated water samples using ICP-MS. Both the BET and ICP-MS analysis were done at Sintef in Trondheim, Norway. The X-ray diffraction analyses (XRD) was performed using a Philips PW1710 X-ray diffractometer, equipped with a Cu-anode operated at 40 kV and 20 mA. The samples where scanned continuously using a step size of 0.04° (2 theta) with 2 seconds per step from 2-60°. The element analyses were obtained through X-ray fluorescence analysis (XRF) using a Philips 1480 X-ray spectrometer. The XRD and XRF analysis were performed at Department of Geology and Mineral Resources Engineering, Norwegian University of Science and Technology, Trondheim. Photographs of the materials were taken with a Scanning Electron Microscope LVFESEM, Zeiss Supra, 55 VP at 2-5 kV and a WD of 5 mm at the Department of Material Technology, Norwegian University of Science and technology.

2.4 HCl dissolution experiments

Three types of dissolution experiments with varying olivine mass and HCl volume was carried out as described in Table 3. The experiments were performed by pouring the right amount of olivine into a glass beaker containing a specified volume of 0.01 M HCl. A magnetic stirrer was used to disperse the olivine sample and to avoid sedimentation throughout each experiment. The experiments were performed at 21.5 ± 1.3 °C and 1 atm in contact with air. pH was logged automatically at suitable intervals using a

Metrohm lab 827 pH-meter equipped with a Metrohm solitrode PT1000 electrode. The three experimental types had different purposes.

Table 3 Experimental specification of the three types of dissolution experiments performed. D stands for dissolution.

Experiment type	Number of experiments	Volume of 0.01 HCl [ml]	Mass of olivine [g]	Volume/ mass ratio	Stirrer speed [RPM]
D-1	18	500	0.50	1000	500
D-2	3	2000	2.00	1000	750
D-3	3	500	2.00	250	500

Volumes and masses in the experiments were determined by four criteria. 1: The pH should change from 2 to at least 3 and pH = 2 was chosen as a compromise between the pH in an diluted acid comparable to carbonic acid and obtaining a measurable reaction rate using a pH meter, 2: Approximately 30-35 % of the input olivine mass should be dissolved when approximately all acid is consumed, 3: A bench laboratory size of the dissolution experiment was applied, 4: The experimental durations should be between minimum 1 h and maximum 24 h. Within the given timeframe the experiments were terminated at a pH higher than 3.0 or at 24 h if pH never reached 3. D-1 experiments were mainly aiming at calculating rate constants for comparison of the different mechanically activated samples. Repeatability was also checked for the D-1 experiments. The solid residues from the D-1 experiments were too small for several material characteristics, and the system was up-scaled by a factor of 4 to get large enough amounts of solid residues, resulting in the D-2 experiments. The D-2 experiments also indicated whether or not increasing the volume of the system would give different results. The last combination of experimental factors was the D-3 experiment aiming at detecting the possible changes in results when the ratio between HCl volume and sample mass was decreased. 20 ml water samples were taken from the suspension at the end of each experiment using a disposable syringe. The samples were then filtered using a 0.45 μm filter and transferred to glass vials. The samples were not acidified. After the water samples were taken in the D-2 experiments, the materials and reactions fluid were filtered on 0.45 μm

filters with a vacuum pump. The filtered residuals were dried at 50 °C in a drying cabinet for several days. Specific surface analysis, X-ray diffraction and particle size distributions were performed on the dried residues.

3 RESULTS

3.1 Contamination from milling

Milling will to some extent result in contamination of the milled sample due to wear on the balls and the milling chamber. The extent of contamination is dependent of whether the milling is performed dry or wet, and also on mass ratios, energy intensity, and equipment quality and so on. Gundewar *et al.* (1990) studied ball wear and documented that wet milling created larger amounts of contamination than dry milling, which supports the contamination results for the planetary mill.

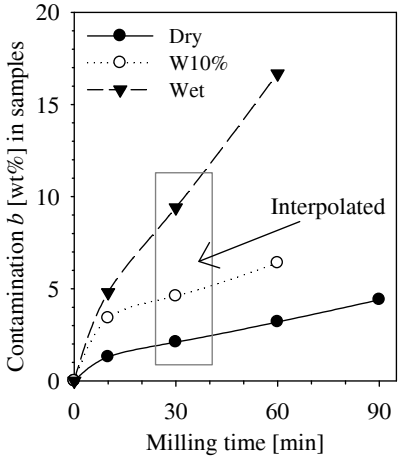

Figure 1 Estimates of milling contamination in wt% in the milled olivine samples. The values for 30 minutes milling are interpolated from the values obtained at 10 and 60 minutes assuming a linear relationship.

Contamination was visually observed as colour shadings in the mechanically activated samples, as steel particles attached to the magnetic stirrer during the dissolution experiments, and a new peak at 2-theta equals 44.6° typical for a steel alloy was detected in the XRD diffractograms. Estimates of the amount of contamination were calculated by a combination of XRF, ICP-MS of the samples, and weight measurements of the milling equipment before and after milling. Figure 1 shows how the amounts of

contamination increased with the addition of water and prolonged milling time. The main contaminating elements were found to be Fe, Ni and Cr which corresponded well with the composition of the steel balls and milling chamber. Using reflected polarizing light microscopy the contaminating was recognised as solid elongated particles.

3.2 pH as a measure of dissolved olivine

Dissolution of olivine consumes acid and the resulting pH changes were used in the calculations of both ion concentrations and rate constants. Even though the experiments were run as an open system in contact with air, the amount of CO_2 dissolving from the atmosphere was very small due to the initial pH just above 2 obtained with diluted HCl. If equilibrium with the atmosphere was reached, the concentration of $CO_{2(aq)}$ was estimated to be 10^{-4} [mol/l]. The concentration of HCO_3^- and CO_3^{2-} would be several magnitudes lower than 10^{-4} [mol/l]. Golubev *et al.* (2005) studied the influence of dissolved CO_2 on Mg and Ca silicates at higher CO_2 pressures than in air and higher pH values than in these experiments, and concluded that the dissolution of olivine was not influenced by dissolved CO_2, and thereby the effect of dissolved CO_2 was assumed insignificant.

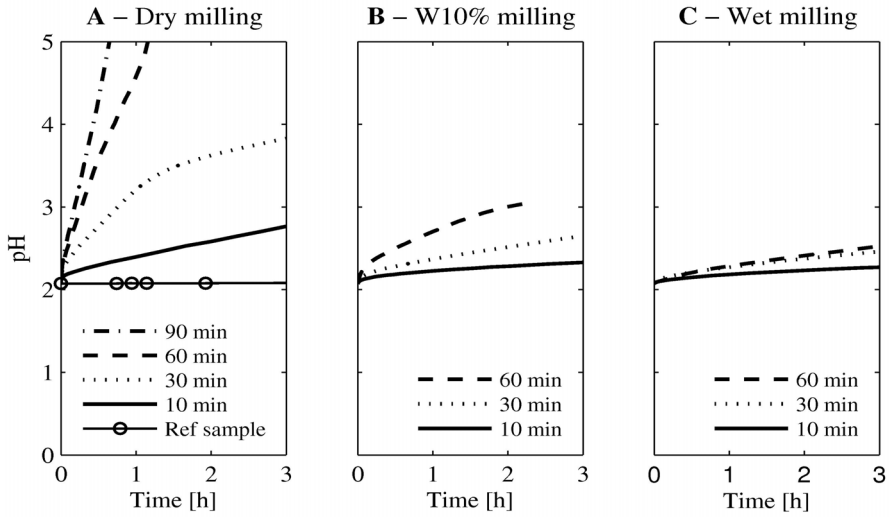

Figure 2 The main pH measurement results of the experiments of the eleven samples used in the D-1 and D-2 experiments including the reference sample. The results are divided into separate graphs by water addition alternatives used during milling.

Dissolution of 10 different mechanically activated samples, showed significant differences as shown in Figure 2 with respect to the pH changes over time as found from D-1 experiments. Replicates corresponded very well, and the full sets of the replicates are included in appendix A. The curves for measured pH were very stable even though different batches of equally activated samples of olivine were used or the system volume was changed from the D-1 experiment to D-2 experiments. The D-3 experiments used 4 times the olivine mass of the D-1 experiment and the acid consumption increased accordingly. Regarding the combinations of the milling factors, it was evident that increased milling times increased the speed of the increasing pH and that water addition during milling was a negative factor when trying to obtain the quickest pH change possible.

t_i is the reaction time from the beginning of the experiment, i.e. from the point in time when the solid sample was brought in contact with the acidic solution to the i^{th} measurement, pH_o is the initial pH and pH_i is the measured pH at t_i. The total amount of moles olivine dissolved, n_i, as a function of time, t_i, was calculated from the measured pH_i described in Eq. 2. The stoichiometric relationship between the acid consumed and the olivine dissolved equals 4. This ratio is necessary to include in Eq. 2 when converting acid consumption into moles of dissolved olivine. V is the volume of 0.01 M HCl in litres for the relevant experiment, and γ_{H+o} and γ_{H+} are the activity coefficients calculated by Davies equation respectively for the initial pH_o, and the pH_i at time t_i.

$$n_i = \frac{1}{4}\left(\frac{10^{-pH_o}}{\gamma_{H_o^+}} - \frac{10^{-pH_i}}{\gamma_{H_i^+}}\right)\cdot V \qquad (2)$$

Since the actual concentrations during the experiments were not known, an initial guess of $\gamma_{H+} = 0.913$, based on PHREEQCi modelling, was used together with a three step iteration procedure to calculate the H^+, Mg^{2+}, Fe^{2+}, and SiO_2 concentration taking into account the stoichiometry of the olivine. An iteration procedure to calculate γ is described by Appelo and Postma (1999). The calculations of the Mg^{2+} concentrations from pH was verified by PHREEQCi modelling up to a pH of approximately 4, where other reactions and phases became significant and the calculation was no

longer valid. To verify the calculations, the estimated final concentrations were compared to the measured concentrations as shown in Figure 3.

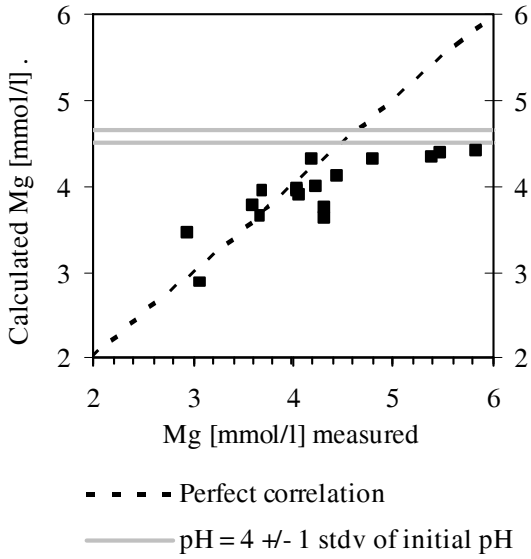

Figure 3 Mg concentrations [mmol/l] retrieved from the experimental water samples compared to the calculated Mg concentrations [mmol/l] based on pH change. The concentration of Mg in a theoretical experiment with a final pH of 4 is included since pH = 4 was found as the upper limit for the calculations from modelling. This limit is marked with horizontal lines and includes one standard deviation of the average initial pH from all of the experiments.

There is a good correlation between the calculated and measured Mg concentrations when pH < 3-4, and a change in the correlation when pH > 4, confirming the modelled results. Calculated Mg concentrations have an approximate upper limit of 4.4 mmol/l even though the actual concentrations were measured up to 5.8 mmol/l. The highest Mg concentration in a D-1 experiment, 5.5 mmol/l, was achieved with the 60minDry sample. This concentration corresponds to approximately 44 % dissolution of olivine within three hours. Below pH 3-4, the pH change was used to estimate the increasing Mg concentrations in the solution caused.

A stoichiometric approach to calculate the Fe and Si concentrations was insufficient to predict the measured concentrations of the final water samples. Fe concentrations were almost randomly distributed and very low compared to Mg concentrations. The highest Fe values, even though they

were very low, were related to the most contaminated samples. Fe measurement uncertainties can have been introduced by using ICP-MS as well. The ratio between Mg and Si in a water sample should have been 1.86 and the average ratio was 2.2. One possible explanation might be preferred dissolution of Mg or precipitation of Si-phases or adsorption of Si to the surface of the glass vials walls and water sample container walls.

$$D_i = \frac{n_i}{N_o} \cdot 100\% \tag{3}$$

$$N_o = \frac{m_o \cdot \beta}{M_m} \tag{4}$$

$$\beta = 1 - b \tag{5}$$

The percentage of olivine dissolved D_i at t_i causing the Mg concentrations to increase was calculated by Eq. 3. The parameters in Eq. 3 are n_i, given by Eq. 2, and N_o is the initial moles of olivine present in the sample, given by Eq. 4. N_o was found from the measured weight in grams of the sample m_o, the fraction of olivine in the sample, β, calculated by Eq. 5 where b was the fraction of contamination in each sample, and M_m is the molar mass of olivine = 145.1 g/mol with the given composition. Since the amount of contamination almost reached 20 %, the dilution effect was included when calculating the percentage of dissolved olivine. Using pH directly for olivine dissolution calculations presumed that olivine was the only dissolving mineral. Contamination and the dissolution of other minerals can have contributed to the acid consumption, but olivine is the most reactive mineral present. It is therefore unlikely that stainless steel or slower reacting minerals contribute significantly to the acid consumption, but cannot be ruled out since the activation will influence all the constituents of the samples.

An empirical approach to compare the dissolution of the different samples was to calculate the percentage dissolved within 30 minutes, D_{30min}. D_{30min} was found by linear interpolation of D_i for the t-values just before and after 30 min reaction time. Figure 4 shows a box plot of D_{30min} versus the ten different milling combinations and all D-1 and D-2 experiment were included.

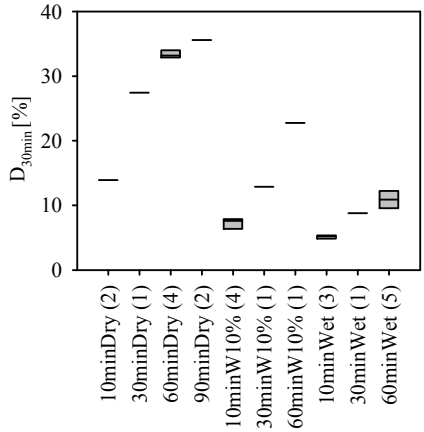

Figure 4 A summary of the results of D_{30min} for all experiments included in D-1 and D-2 are included to illustrate the variation in the duplicates. The number in parenthesis indicates the number of dissolution experiments performed for the given sample type. For samples with more than 2 duplicates, the 25 and 75 percentile was calculated and shown as the upper and lower limit of the boxes.

Dry milled samples produced the most reactive samples, W10% milled samples obtained lower results for D_{30min} than dry milled samples, and wet milled samples had the lowest D_{30min} values. The 10minDry sample dissolved 13.9 % after 30 min compared to the 60minWet sample dissolving 11.8 % indicating the positive influence of 10 min dry milling compared 60 min Wet milling. Some dissolution might have occurred during wet milling, but the concentrations in the milling fluid after 60minWet milling was 0.07 mmol/l Mg, 0.01 mmol/l Si and 0.0006 mmol/l Fe and for the 10minWet sample 0.17 mmol/l Mg, 0.012 mmol/l Si and 0.0001 mmol/l Fe, which was 2 to 3 orders of magnitude less than in the water samples after dissolution in 0.01 M HCl of the same samples. Therefore can not dissolution during milling explain the large differences between the three water addition choices found in the dissolution experiments.

3.3 Material characteristics of mechanically activated olivine and solid dissolution residues

Figure 5 shows the general results for the material characteristics after mechanical activation. Mechanical activation has three main effects on a material: decreased particle size, changes in surface topography/particle shape, and an increase in dislocations and microcracks in the crystal lattice.

Here the three effects are analysed using the particle size distribution represented by d_{10} (Figure 5A), the specific surface area (Figure 5B) and the crystallinity (Figure 5C), and were verified with SEM pictures by studying particle sizes and surface structures. d_{10} is the particle size where 10 wt% of the sample is smaller and equal this size. d_{10} were chosen due to the importance of fines during dissolution and in the contribution to SSA. The particle size distributions represented by d_{10} show large differences between the mechanically activated samples and no general trends were found with one exception The largest production of fines happens within the first 10 minutes of milling, see Figure 5A as an illustration. Using d_{50}, the average particle size, or d_{80}, representing the larger particles in the samples, did not show any trends either. The wet milled samples might also have smaller amounts of coarser particles than the dry and W10% milled samples.

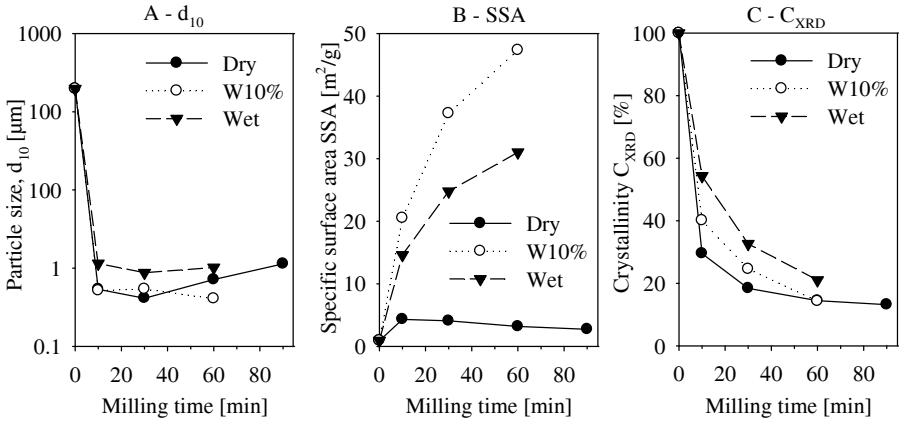

Figure 5 Summary of chosen material properties , particle size, d_{10} (A), specific surface area, SSA (B), and crystallinity C_{XRD} (C), versus milling time for dry milling, W10% milling and wet milling.

There were some uncertainties regarding the particle size distribution of the dry milled and W10% milled samples due to technical challenges. During the analysis the material flocculated to some extent due to electrostatic charge which was most evident for the dry milled samples. Ultrasound was not able to disperse the aggregates properly, hence the particle sizes were overestimated to some extent. Not only the particle sizes before dissolution were examined, but three samples were chosen for particle size distributions after dissolution as well. The 10minW10% sample

lost a large amount of fines during dissolution and the coarser particles got concentrated indicating that the fines were the most reactive particles. The 60minWet sample lost some large particles, with an even shift of the distribution curve to smaller particles with a small overweight of particles finer than 2 μm and interpreted as an even dissolution of all particles. The change in the 60minDry sample consisted mainly of a large loss of the coarsest particles, and the maximum size of the 60minDry sample shifted from 200 μm for the undissolved sample to less than 40 μm for the dissolved sample. The 60minDry sample consisted mainly of aggregates, as shown in Figure 6(A&F), and these aggregates probably dissolved along the aggregate contacts between different particles and therefore the largest particles probably were disintegrated and therefore the particle size was significantly reduced.

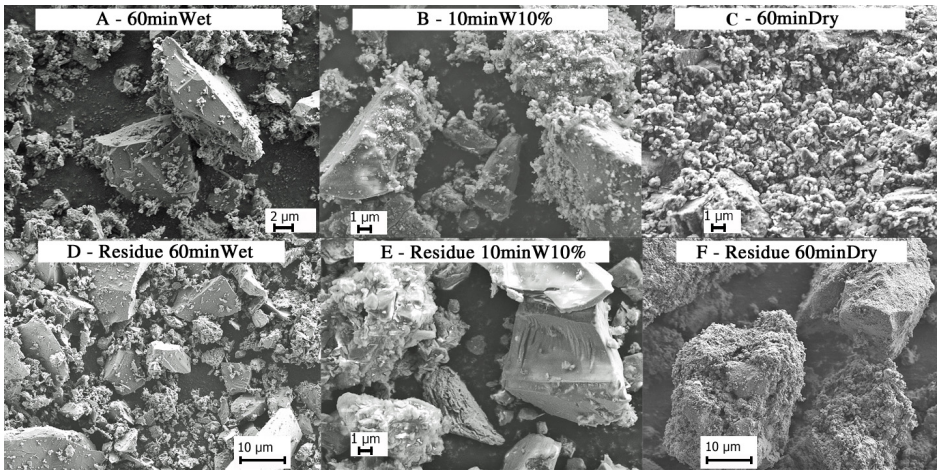

Figure 6 Electron microscope pictures of three mechanically activated samples (A, B, C) and the respective dissolution residues of the same materials (D, E, F).

SEM photographs of the materials before dissolution and the residues are presented in Figure 6. Three magnifications were used; 5000X, 10000X and 15000X depending on the feature chosen to be illustrated. For the activated materials three general types of the particles appearances were found. Very small initial particles below 1 μm (Figure 6 A-C), larger complex aggregates composed of the small particles (Figure 6 B-C), and larger particles with a typical crystalline olivine texture with smooth surfaces with some small particles attached (Figure 6 A-B). No complex aggregates were

found in the 60minWet sample and no large crystalline particles were found in the 60minDry sample. The 10minW10% sample looked like a combination of the other two samples, and the appearance was probably affected by the relatively short milling time of 10min. Milling for 10 min instead of 60 min will give a higher fraction of large crystalline grains. During dissolution the 60minWet sample did not change its appearance significantly (Figure 6 A&D). The 10minW10% sample showed both complex particles and particles with smooth surfaces almost free of fines (Figure 6 B&E). It was expected that olivine particles in the residues were going to look more crystalline. Even after approximately 35 % dissolution of the 60minDry sample, the particles still looked very complex. Only aggregates (Figure 6 F) and very small particles were observed for the 60minDry sample. Some small particles had long parallel etching cracks of nano-scale indicating direction dependent dissolution.

Not only the particle size and the observable shapes varied to a large extent, but as shown in Figure 5B there are large differences between the obtained specific surface areas, SSA. Wet milling and W10% milling increased the SSA with milling time, whereas dry milling had the lowest values and a measured maximum of 4.3 m^2/g at 10 min. The changes in the SSA due to the dissolution were checked for the same three residues that were analyzed for particle size and taken photographs of. A decrease of the specific surface areas due to dissolution were found for 10minW10% sample and the 60minWet sample, respectively 59 % and 45 % of the original values. The 60minDry milled sample had a very large increase in specific surface area from 3.2 m^2/g to 44.2 m^2/g. The large increase for 60minDry probably corresponds to the large decrease of maximum particle size for the same sample.

Deformation, reduced particle size and reduced crystallite size caused by mechanical activation influences the X-ray diffractograms and the degree of crystallinity can be calculated (Ohlberg and Strickler, 1962) based on XRD measurements. In general the background level increases and the peaks get lower and wider. These changes can also be caused by decreased particle size, decreased crystallite size, and C_{XRD} calculated by Eq.6 represents a value combining the effect of decreasing crystallite size, strain and amorphization. The C_{XRD} calculations, often used within mechanical

activation (Baláž, 2000, Ghasri-Khouzani *et al.*, 2009, Hoberg and Götte, 1985, Pourghahramani and Forssberg, 2006) were performed by measuring the average background levels, B_o and B_i, and the integral peak areas, I_o and I_i, above the background levels for all samples. Indices o and i refers respectively to the original sample representing a 100 % crystalline material and the mechanically activated sample. The resulting value of C_{XRD} is a bulk property of the sample, and cannot be translated directly into specific physical properties.

$$C_{XRD} = \frac{I_i}{I_o}\frac{B_o}{B_i}\cdot 100\% \qquad (6)$$

The peak at the diffraction angle 2-theta = 17.3° in the X-ray diffractogram for all samples was chosen to minimize the influence of surrounding peaks, in an otherwise complicated X-ray diffractogram. In part C of Figure 5 the changes in crystallinity due to milling is shown. There is a drastic decrease in the crystallinity of olivine due to mechanical activation and the largest reduction comes the first 30 minutes. Dry milling is the most destructive and wet milling is the least destructive, with W10% milling in between.

The general behaviour of dry milled olivine regarding the reductions in crystallinity and changes in specific surface area is supported by the findings of Baláž *et al.* (2008) for olivine and the general differences between wet and dry milling (Baláž, 2000). There seems be different effects on C_{XRD} of the olivine samples depending on the milling conditions. The wet milled samples had a lower destruction of crystallinity, but had large specific surface areas. The results were the opposite for the dry milled olivine, with a large reduction in crystallinity and low specific surface areas. The W10% milled samples had large surface areas as the wet milled samples, but the change in crystallinity is similar to the dry milled samples. The W10% milled samples seems to combine the effect of both wet and dry milling.

3.4 Rate constant calculations

The use of D_{30min} is one way of evaluating the dissolution kinetics of the mechanically activated samples, but rate constants describe the mechanically activated samples with a theoretical approach. The calculation of the observed rate constant is based on the moles of dissolved olivine, n_i,

found by Eq. 2, the measurement time t_i and a specific surface area adjusted to the point in time for the measurements. One rate constant is calculated for each interval, i. The i^{th} interval is defined to be the interval between the two consecutive measurements, the $(i-1)^{th}$ and the i^{th} measurement. For each interval the average pH, $\overline{pH}_i$, was calculated. The difference in using the average pH and average H+ concentration can be neglected since the intervals were small.

Obtaining a good estimate of the total surface area of the samples during dissolution is vital for the accuracy of the rate constant calculations. Three factors influenced the total surface area available: contamination reducing the olivine content, and hence the available surface area, the changes in particle size influencing the specific surface area during dissolution and the complexity of the surface due to mechanical activation. The last mentioned factor was probably crucial, but was not quantified, only photographed (Figure 6).

The estimate of the total surface area was based on the measured specific surface area of the samples multiplied by the weight of the sample in each experiment, resulting in A_o [m^2]. A_i represents the specific surface area of the solid residue assumed to be valid during the interval i. The surface area changes caused by decreasing particle size was described by a shrinking core model. The model was based on the ratio between the initial moles of olivine, N_o, and the amount of olivine still not dissolved during the i^{th} interval, N_i. N_i was calculated as the average of olivine not dissolved at the beginning and the end of the interval as shown in Eq. 7. The shape of a particle is assumed to be spherical or cubical and the shape is assumed to be preserved during dissolution since no other general model has been found for mechanically activated materials even though this is a rough assumption.

A correction for the contamination was included because some of the measured surface area originated from the contamination and not from olivine, but in general the amount of contamination was less than 3 wt% and therefore the adjustment did not change the result significantly. The measured surface area was assumed to be distributed between the contamination and olivine according to the amount of contamination. This is not exactly true since the characteristics of the contamination is not equal

those of olivine, but this approach was preferred over ignoring the presence of contamination. Better results for the specific surface area of olivine could have been obtained with measurements of the contamination. The correction factor for decreasing specific surface area in accordance to the shrinking core model is shown in Eq. 8 as η, and β from Eq. 5 corrects the surface area for the presence of contamination. Assuming olivine to be the only dissolving mineral, the observed specific reaction rate, r_i, can be expressed with Eq. 9. Even if both the remaining other minerals and the contamination is dissolved, their contribution is a small part of the total mass dissolved except for the sample 30minWet and 60minWet. The results for the last samples may therefore include noticeable uncertainties regarding the specific surface areas and a possibly an influence on acid consumption..

$$N_i = N_o - \frac{n_i - n_{i-1}}{2} \tag{7}$$

$$A_i = (A_o \cdot \beta) \cdot \eta = (A_o \cdot \beta) \cdot \left(\frac{N_i}{N_o} \right)^{\frac{2}{3}} \tag{8}$$

$$r_i = \frac{(n_i - n_{i-1}) \cdot V}{4 \cdot (t_i - t_{i-1}) \cdot A_i} \tag{9}$$

$$r = k \cdot a_{H+}^{x} \tag{10}$$

$$k_i = \frac{r_i}{\left(10^{-\overline{pH}_i} \right)^x} \tag{11}$$

Eq. 10 expresses the general reaction rate r as a function of the rate constant k, the activity of H^+ and the exponent x being the pH dependency exponential factor. The rate constant k is practically independent of pH compared to r and is therefore suitable to describe the dissolution properties of each sample during the course of each experiment. By inverting Eq. 10 and using the specific reaction rate r_i for the interval i, the average of pH within each interval i, $\overline{pH}_i$, and the pH dependency factor, then the rate constant k_i can be calculated with Eq. 11 for each interval. A pH dependency exponent equal 0.48 (Olsen and Rimstidt, 2007) obtained for unactivated olivine was used since this value was the only available option for olivine.

Dissolution experiments are often done at constant pH and measurements are performed when stable conditions have been attained. Here the system is never stable. The continuously increasing pH and the measurable decrease in mass resulted in a decrease in the reaction rate over time that maybe would not have appeared with a constant pH and approximately constant olivine mass. Therefore the comparison of obtained rate constants can only be done to some extent to published dissolution data for olivine. However, the results from all the experiments with changing pH can be compared to each other and give valuable information about the differently mechanically activated olivine samples and the effect of the milling conditions used.

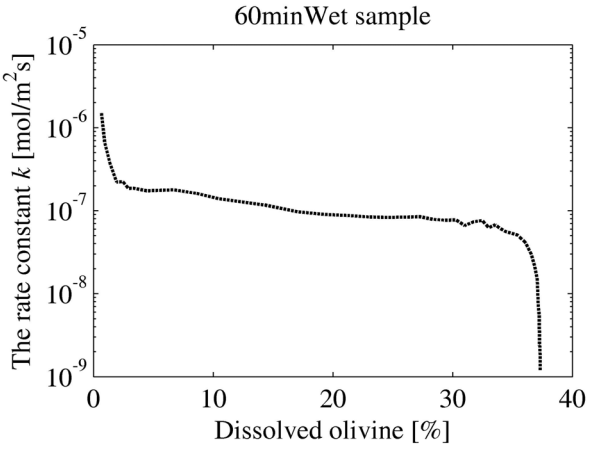

Figure 7 An example of the typical development of the rate constant with increasing dissolution, illustrated by the results for the 60minWet sample. Typical for most experimental results was the initial drop, the slowly decreasing rate constant between ~ 5 % dissolved and ~ 30 % dissolved, and the steep artificial drop when trying to approach ~ 40 % dissolution.

Figure 7 shows one example of how the rate constant k_i changes with the dissolution degree D_i for the experiment with a 60minWet sample. Figure 7 illustrates two general features found in most of the D-1 experiments. The first feature is the large decrease in k_i within the first 5 % dissolved, and the second is the significant drop at 37 %. The first large decrease is probably caused by a significant amount of fines or other initial effects. The second drop is an artificial drop caused by an error in the calculation of Mg concentration from pH du to complex formation and

buffering effects of the solution at high concentrations and increased pH. Then the calculation is no longer valid. After a certain extent of dissolution the change in pH value cannot be used to calculate the rate constant because the simplified Eq. 2 is not valid as shown in chapter 3.3 regarding measured and calculated Mg concentrations. Figure 3 compares calculated end concentrations of Mg and measured end concentrations of Mg indicates that the dissolution has gone further than the calculation indicates, and thereby supports that the limit is only a product of the inadequate calculation above approximately pH = 3-4. This artificial dissolution limit caused by the definition of the calculation appears as the vertical line to the right in Figure 7, and is not related to pH dependency of the olivine dissolution rate. The initial drop until 5 % is dissolved, and the final drop above 30 % dissolved, are excluded in Figure 8 where representative rate constants for all 11 samples, including the reference sample, are presented together with an illustration of the rate constant of unaltered olivine (Rosso and Rimstidt, 2000) appearing as a horizontal line.

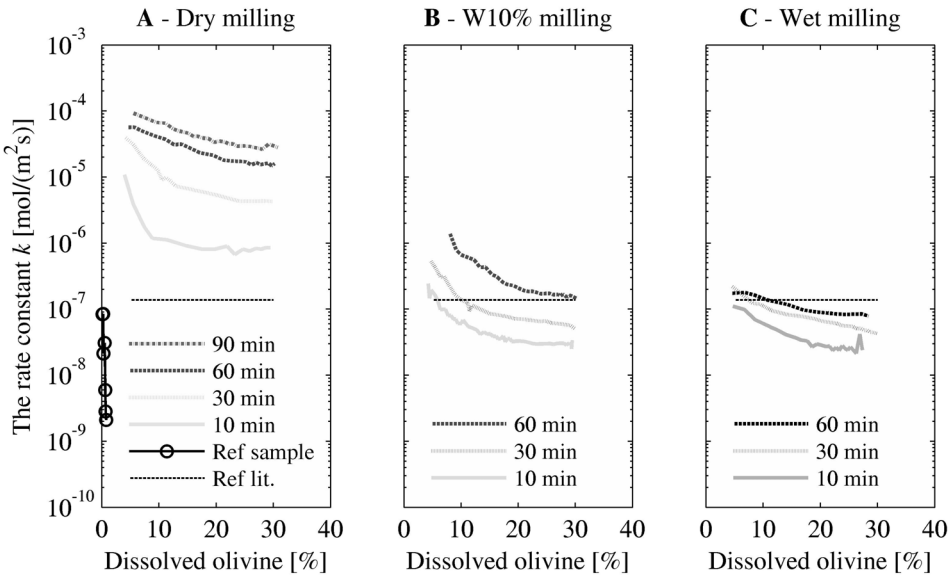

Figure 8 The calculated rate constant, *k*, for representative samples between 5 % and 30 % dissolved olivine, separated by water addition alternatives used during milling. In the case of two duplicates, the results from the earliest experiment is used, with three or more experiments the curve closest to the average is used.

There are approximately 3 orders of magnitude in difference between the highest and lowest rate constant calculated at a given D_i. A maximum rate constant of $9.2 \cdot 10^{-5}$ mol/(m²s) was obtain for the 90minDry sample at D_i = 5 % shown by the uppermost graph in Figure 8A. The lowest rate constant for the same D_i was $1.1 \cdot 10^{-7}$ mol/(m²s) found for the 10minWet sample, the bottommost graph in Figure 8C. The rate constants of the mechanically activated samples increased with increasing milling time and decreased with increasing water addition. All samples show some decline in k_i with increasing D_i, but the decline varies depending on the sample.

3.5 Geochemical modelling of the dissolution experiments

PHREEQCi is a geochemical modelling freeware from USGS (1998) described by Parkhurst and Appelo (1999) and was used in the modelling. Geochemical modelling of the D-1 dissolution experiments was performed to compare two selected published olivine kinetic data with the measured dissolution. The chosen kinetics had to be valid for the T and pH of the experiments, and a pH dependency factor of approximately 0.5. Table 4 shows a summary of the chosen kinetics and is called K1 and K2 in the following text.

Table 4 Kinetic parameters used in the PHREEQCi modelling based on the Arrhenius equation. Valid range for the temperature and pH for the parameters are included.

Kinetic model	Temp. range [°C]	pH	A_A [mol/(m²s)]	E_a [kJ/mol]	x [-]	Reference
K1	25 – 45	1.8 – 3.8	3.467	42.6	0.50	(Rosso and Rimstidt, 2000)
K2	25	< 6	13940	63	0.48	(Olsen and Rimstidt, 2007)

The rate constant applied in the models is based on the Arrhenius equation with a pH dependency included as shown in Eq. 12 where r is the forward dissolution rate far from equilibrium calculated with the Arrhenius constant A_A , E_a is the activation energy of the material, R is the universal gas constant = 8.314 ·10-3 kJ/(mol K), and T is the temperature in Kelvin. The kinetics was included in the model by implementing r from Eq. 12 together with the parameter values in Table 4, into the rate expression R_i in Eq. 13.

$$r = A_A e^{\frac{-E_a}{RT}} a_{H+}^{x} \tag{12}$$

$$R_i = (A_o \cdot \beta) \cdot \left(\frac{N_i}{N_o}\right)^{\frac{2}{3}} \cdot r \cdot \left(1 - \frac{IAP_i}{K_{fo}}\right) \tag{13}$$

Equation 13 is composed of four parts; the initial surface area related to olivine calculated with the expression in the first brackets, r the reaction rate, the shrinking core model in the second set of brackets and the last brackets expressing the reduction in reaction rate when approaching equilibrium. IAP_i is the ion activity product for forsterite at the modelling step i and K_{fo} is the equilibrium constant for forsterite assumed to be valid for the olivine used in this study. The time step size in the models was 1 min. The difference in the modelling results between the step sizes of 1 min and 1 s was less than 0.02 % using K1 kinetics and the SSA for the 90minDry. The change from 1 s to 1 min was therefore assumed insignificant. If two experiments were performed for the same mechanically activated sample, the experimental data from the first experiment was used, and with several experiments for the same sample, the experiment closest to an average result was chosen. The main output from the models was time series of the percentage of dissolved olivine and was compared to the experimental time series of D_i.

The modelling was developed in three steps, where step 1 was strictly theoretically based with reference kinetics, and step 2 and 3 included empirical adjustments to fit the experimental data. Two models were made for each experiment in step 1, using K1 and K2 and the reaction rate expression in Eq. 13 and 5 experimental parameters; the measured surface area of the material A_o [m^2], the sample mass in grams used in the experiment m_o, the fraction β of the initial sample being olivine, volume of water in the HCl solution used and the initial pH, pH_o. Both K1 and K2 estimated D_i for the reference sample to be 9.4 % compared to the measured 2.4 % after 24 h of dissolution.

There was in general a very poor agreement between the experimental results and the theoretical models from step 1. In general the experimental data was dissolving to fast in the beginning and then slowing down to rapidly. The best fit from step 1 is shown in Figure 9A and after

approximately 40 min the model only predicted half of the experimental D_i. The largest deviation between the modelled and measured D_i versus time for step 1 is shown in Figure 9B. The results from step 1 also showed that the concentrations in the solution were so far from olivine equilibrium that the dissolution rate was most likely not affected by olivine equilibrium.

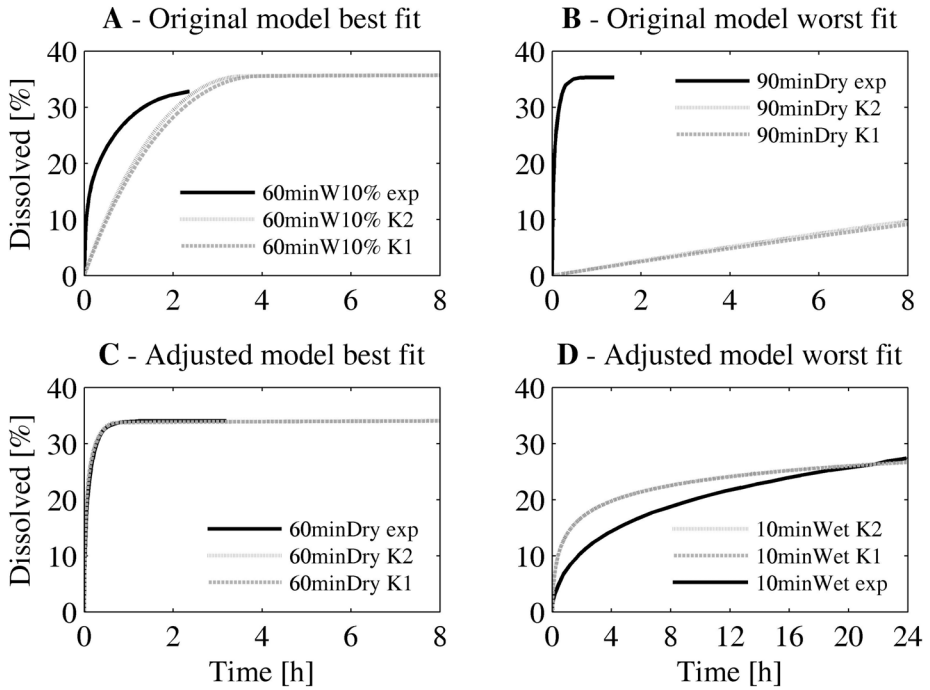

Figure 9 A comparison of the measured and modelled olivine dissolution [%]. The original model was only based on the reference kinetics, while adjusted models were fitted to the experimental data. The best and worst examples for original model using K1 and K2 from model step 1 (A – B), and best and worst fit for adjusted model after model step3 (C – D). The time scales are adjusted to the duration of the respective experiments.

The Arrhenius equation used in the model in step 1 assumes a constant k value, but the experimental k_i was found to decrease with increasing dissolution. In step 2 an attempt was made to correct for the decrease in the rate constant. The shrinking core model was modified to include the total decrease in k_i regardless of cause as an empirical approach, see Eq. 14.

$$\eta = \left(\frac{N_i}{N_o} \right)^{f_m} \tag{14}$$

The exponent in the shrinking core model was renamed f_m. This f_m value does not only correct for the change in SSA, but is an empirical value that summarized the total decrease in the calculated rate constants with dissolution degree shown in Figure 8 resulting from the mechanical activation which include preferential dissolution of fines, surface properties and changes in the crystal lattice due to activation. The rate constant found by using the f_m exponent is denoted with an asterisk. f_m was determined by substituting 2/3 with higher values, calculating k_i^* and the average of the k_i^*, $\overline{k}^*$, within the range of 0 % - 30 % dissolved olivine. f_m was found when the relative standard deviation of k_i^* was at a minimum. For an ideal setting with the shrinking core model, the value was 2/3, but f_m varied from 6.9 to 20. Inclusion of the factor f_m was helpful since the curves became more similar in shape, but still there were large deviations from the measured data.

The theoretical rate constants for olivine were $k_o = 8.87 \cdot 10^{-8}$ mol/(m^{2}s) for K1 and $k_o = 9.48 \cdot 10^{-8}$ mol/(m^2 s) for K2. The $\overline{k}^*$ values were far from these theoretical rate constants. The correction of the gap between the $\overline{k}^*$ and the theoretical k_o was done by finding the ratio, f_r, between them as shown in Eq. 15. Inserting this ratio into the final rate expression in Eq. 16, lead to step 3. f_r ranged from 4 to 1000 for both K1 and K2 indicating large differences between the rate constants of the samples compared to the theoretical rate constants.

$$f_r = \frac{\overline{k_i}}{k_o} \tag{15}$$

$$Rate = f_r \cdot (A_o \cdot \beta) \cdot \left(\frac{N_i}{N_o} \right)^{f_m} \cdot r \cdot \left(1 - \frac{IAP_i}{K_{fo}} \right) \tag{16}$$

The best and worst models from step 3 are shown in Figure 9C and D. The differences between the experimental results and the modelled results, after adjustment of the models with the empirical factors f_m and f_r, are much lower, but deviations from the measurements are found for all samples.

4 DISCUSSION

Generally in dissolution rate experiments as many parameters as possible are normally held constant, and typical examples are pH, surface areas and material masses (i.e. Chen and Brantley, 2000, Pokrovsky and Schott, 2000). Just the opposite was done in the dissolution experiments of the mechanically activated samples to simply compare differently milled samples and evaluate the effect of milling conditions and material characteristics. A significant change in the material mass during dissolution was used to discover assumed non-homogenous material properties and rate constants, since the effects of mechanical activation theoretically decrease towards the core of the particles. Such a decrease in the rate constants due to mechanical activation was observed by Hoberg and Götte (1985). The particle sizes and the specific surface areas of the materials were not constant either, but reflected the materials properties of the materials coming directly from the mill. Sieving to obtain a constant particle size of the samples prepared in the planetary mill would have introduced uncertainties influencing the evaluation of the milling parameters by excluding parts of the materials produced.

4.1 The influence of mechanical activation on olivine dissolution

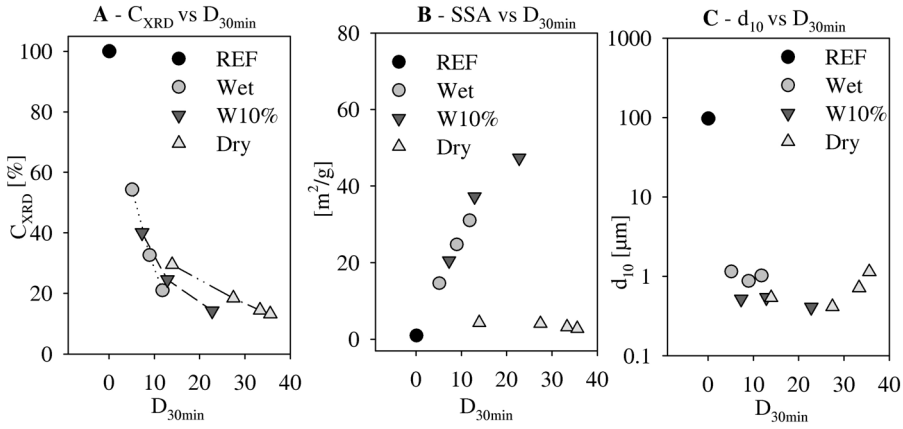

Figure 10 A comparison of the percentage dissolved after 30 min, D_{30min}, to the measured material properties of crystallinity (A), specific surface area (B) and particle size (C).

The pH measurements indicated very large variations in the dissolution rates between the mechanically activated samples. The differences between the samples were expressed by the percentage of olivine dissolved during the first 30 minutes, D_{30min}. D_{30min} was compared to the material properties in Figure 10. The particle size d_{10} was chosen to represent the particle size distributions. Small particles contributes more to the total surface area and hence the dissolving surface than larger particles and was expected to be related to D_{30min}. However, no correlation was found. One out of several possible explanations is related to how the laser diffraction measures the particle sizes. Information about the particle shape, the particle topography and the particle texture is not included and the measurements of the diffracted light are converted into particle diameters for what the instrument regards as spherical particles. The measured particle size then becomes the result of the intersection between a random section of the particle and the light. This results in a wider particle size distribution where the particles are interpreted to have a diameter close to or smaller than the true particles (Snilsberg, 2008). On the other hand many small particles preserved in an aggregate will be interpreted to have a particle size equals the size of the aggregate. Dispersing agents and ultrasound normally prevents the effect of aggregates, but the aggregates formed during mechanical activation have high tension strengths (Baláž, 2008) due to the effect of mechanical alloying, and is therefore not dispersed.

The specific surface areas of the wet and W10% milled samples seemed to have a good correlation with D_{30min}. On the other hand, the specific surface areas were very low for the dry milled samples at the same time as they obtained $D_{30min} > 37$ %. The specific surface area is a better measure of the complex particle shape and surface topography than the particle size. Even though the specific surface areas were better correlated to the D_{30min} compared to the particle size distribution, some information is lost because the specific surface area is a 2D measurement of a 3D surface. Gautier *et al.* (2001) showed that the specific surface area measured with the BET method was not correlated with the dissolution rate when studying the dissolution of quartz due to preferentially dissolution of quartz in different crystallographic directions. Awad *et al.* (2000) has shown that crystalline olivine also has preferred dissolution directions. Some examples

supporting the direction dependent dissolution of the olivine in this study were found on some 1-5 µm particles from the 60minWet and 10minW10% sample residues. These particles had long parallel etching cracks of nano-scale. As with quartz, the obtained D_{30min} measurements can not solely be explained by the measured initial specific surface area since direction dependent dissolution may be important, and can be affected by mechanical activation due to applied mechanical stress. Preferred dissolution direction is related to the importance of dissolution sites and edges and was discussed by Tromans and Meech (1999, 2001, 2002, 2003). They concluded that topographical features are actually more important than specific surface area alone and thereby support the relevance of changes in several material properties of olivine caused by mechanical activation.

During mechanical activation reduced particle size and deformation of the crystal lattice resulted in reduced crystallinity. Figure 10A shows the calculated C_{XRD} for all samples versus D_{30min}. Despite the large difference in D_{30min} for the three samples milled for 60 min with almost the same calculated crystallinity, the trend line for D_{30min} versus C_{XRD} gives a good indication of how the amount of dissolved olivine increased with decreased crystallinity. Similarities in C_{XRD} for the 60 min samples may be caused by the bulk nature of the XRD measurements and by differences in crystallite sizes of the materials. The crystallite sizes were not determined any further due to the limited analytical possibilities offered by the old XRD instrument.

Comparison of the C_{XRD} for the three samples before and after dissolution indicated that the dissolution residues were more crystalline than the initial samples. The 60minDry sample residue had a small crystallinity increase from 14 % to approximately 16-17 %, suggesting a relatively constant C_{XRD} even after 43 % dissolution. The 60minWet sample solid residue increased the crystallinity more than the 60minDry sample, from 21 % to ≈ 30 % after dissolving 39 %. The changes in C_{XRD} caused by dissolution alone indicate that the outer layers of the particles are more altered than the core or that fines were dissolved first, since fines also contributes to the decreased crystallinity. The larger increase of crystallinity during dissolution of the 60minWet sample than the 60minDry sample explains how these two samples milled for 60 min can have almost the same initial C_{XRD} and still produce differences in D_{30min} if the less

crystalline parts have a higher dissolution rate or that in fact the dry materials contain large amounts of fines that are rapidly dissolving. The specific surface area seemed to be more important for the dissolution of olivine when the crystallinity was high. With a low crystallinity the effect of variation in the specific surface area became insignificant. Mechanical activation seems to take the material – dissolution interaction beyond the surface topography and probably includes factors influencing the measured crystallinity within the particles.

4.2 Rate constants of mechanically activated olivine

For ideally behaving samples the rate constants, k_i, is pH independent and constant when implementing suitable corrections in a dissolution experiment. Hence, the rate constants of different samples or rate constants found at different dissolution degrees could be compared despite the fact that the pH is not constant. The mechanically activated samples had very varying k_i values, see Figure 8, depending on the choice of milling parameters. k_i increased with increasing milling time and decreased with water addition. k_i at 5 % dissolution varied from 10^{-7} mol/(m^{2}s) for the 10minWet sample to 10^{-4} mol/(m^{2}s) for the 90minDry sample. A second interesting feature was that k_i decreased with increasing dissolution degree. Long milling times gave an even decrease in k_i, probably indicating more uniform dissolution properties compared to shorter milling durations. The cause of non-ideal behaviour must originate from violations against the assumptions of the dissolution mechanisms or the formulation of the dissolution rate constant corrections. The main assumptions were: 1: The surface area changes of the dissolving material followed the shrinking core model, 2: The specific surface area was the only material property needed for dissolution calculations, 3: The dissolution properties were homogeneous and hence independent of dissolution degree, and 4: The k_i values calculated from an experiment with rapidly increasing pH could be compared to k_i from experiments with a constant pH.

The validity of the shrinking core model from assumption 1 was evaluated by D-2 experiments with enough solid dissolution residues to perform material characteristics analyses and compare the measured values to the modelled value. Theoretically, using the shrinking core model, the

specific surface areas should have increased with about 20 %. The specific surface area was actually reduced by 41 % and 55 % respectively for the 10minW10% sample and the 60minWet sample. The SSA of the 60minDry sample increased, but instead of a 20 % increase, the surface area increased from 3.2 m^2/g to 44.2 m^2/g, resulting in an over ten times higher specific surface area at the end of the experiment than in the beginning. This large increase can be explained by the aggregates created during dry milling which probably are solid enough to act as large particles with low surface areas during BET analysis, but during dissolution the bonds between the particles in the aggregates dissolved relatively easy and created a large amount of fines contributing to a large increase in SSA. This explanation is supported by the large decrease in the upper particle size of the 60minDry sample after dissolution from 200 μm to less than 40 μm. The simple shrinking core model was not suitable. The effect of varying pH on dissolution has been studied by Samson and Eggleston (1998), and an extra transient period of dissolution was found. Their results show the importance of pH and pH change, and therefore is the results presented here probably slightly influenced by the changes in pH and assumption 4 is probably affected.

The empirical mass change exponent f_m was used to make the average of k_i as constant as possible between D_i = 0 and D_i = 30 % dissolution. f_m included all errors connected to the assumptions 2, 3 and 4. Hänchen *et al.* (2006) found f_m, their notation was p and strictly related to surface area, to be 0.85 in their olivine dissolution experiments. For the experiments described in this paper the f_m values are not restricted to surface area, but is a bulk property including all effects of mechanical activation leading to a decrease in the rate constant. f_m were found to be between 6.9 and 20. The values of f_m seem to be larger than practically possible if only related to the surface area change and therefore these values did not correspond to the measured specific surface areas of the solid dissolution residues either. The crystallinity as discussed earlier, was found to depend on dissolution degree, and it is very likely that the cause of the observed decreases in crystallinity influenced the calculated k_i. Hoberg and Götte (1985) described decreasing rate constants with increasing dissolution degree of columbite after mechanical activation when dissolved in 10 % hydrofluoric acid, and

attributed this to decreasing density of activated phases towards the centre of the particles. In this study the amount of an activated phase in the material was indirectly measured by XRD and thereby the C_{XRD}. The results of Hoberg and Götte (1985) supports the observed decrease in the rate constant found for olivine. The change in C_{XRD} with dissolution degree was sample dependent, and hence the effect on k_i also should be sample dependent.

As can be seen in Figure 8, there seem to be both a general decrease and some initial differences between the materials. If the last part of each experiment is assumed to have a dissolution rate from the least changed sample properties and hence constant k_i. Adjustment of the decline at the end of each experiment was performed by finding the f_m* value resulting in a constant k_i after ignoring the initial higher values of k_i related to material specific properties. The k_i after introducing f_m*, shows that a large initial decrease in k_i corresponds well with a large increase in C_{XRD} after dissolution. The plausible differences in the rate constant between the outer layer and the inner core shows that the change in k_i during dissolution decreased with increasing milling time for the wet and dry milling. Longer milling times seemed to produce more homogenous samples. Just the opposite was found for W10% milling. The difference between the initial and the end properties increased with increasing milling time. The behaviour of W10% with milling time could possibly be explained by the outer layer first behaving as a wet milled sample, but after longer milling times the outer layer behaves more like dry milling with a crystalline core resembling the wet milled samples.

4.3 Interpretation of the empirical dissolution models

The two empirical factors introduced to adjust the models to the measurements cannot be directly related to the specific material properties or the experimental conditions. f_m, discussed in chapter 4.2, was applied to the models adjusting for the decrease in k_i during the dissolution, and f_r also from chapter 4.2, was a constant adjusting the theoretical rate constant to the average rate constant found in each experiment after applying f_m. Neither f_m nor f_r could be generalized, but were sample specific. Longer milling times resulted in better fits, probably due to less variation in the

sample properties both regarding surface structures and internal properties. The 60minDry sample and 90minDry samples were relatively easy to model, and had probably moderately constant material properties. For the rest of the materials, it was not possible to adjust f_m to get a constant rate constant. The main results from the modelling were that kinetics published for unactivated olivine did not fit the measured data. Models for the activated samples have to include different kinetics for each sample and have to take into account the effect of decreasing activation with increasing dissolution degree.

4.4 The importance of the results for future mineral carbonation

Two main considerations have to be fulfilled to make mechanical activation beneficial to an industrial leaching and carbonation process. Mechanical activation is a very energy intensive milling operation, but the increase in the rate constants are larger than what is possible to obtain with normal milling techniques, and may therefore be beneficial. The reaction kinetics has to be enhanced enough to outweigh the extra cost and energy penalty during milling, and the mechanical activation mill has to be dimensioned for large enough mass flows. In the experiments the influence of milling time and water addition on extensive dissolution kinetics were examined. In general, prolonged milling of each water addition alternative gave an increase in the material effects found for 10 min of milling, but the differences between the alternatives of water addition could not be generalized. The W10% water addition choice is probably neither practical for an industrial process, nor giving the best dissolution results. Therefore was milling with small additions of water as carbonation pre-treatment not considered further, even though the general effects of mechanical activation on material properties were interesting with the highest obtained specific surface areas combined with reduced crystallinity.

Often in a mineral processing plant, the solids are transported and processed wet. Wet conditions could probably be preferred for aqueous mineral carbonation due to process technical solutions. However, wet milling seems to be the worst choice regarding maximizing the dissolution kinetics of mechanically activated olivine, despite the large specific surface

areas obtained. The results show that the rate constants for wet mechanical activation are almost two orders less than dry mechanical activation for the same milling time. A 60minDry sample was able to dissolve 200 times the amount of a 60minWet sample for the same duration of dissolution. The kinetics of the wet milled samples are in the same order as the published kinetics for unactivated olivine.

Another consideration is the tolerable amount of contamination since contamination dilutes the total amount of olivine in the mass flow, and will be present in the reaction and in the wastes and products. Significant concentrations of metals from the steel alloys in solution can reduce the purity of the precipitated magnesium carbonate and silica and hence limit the product value and the markets of the products. In addition to be a direct problem in the process, contamination is also indirectly contributing to increased CO_2 emissions through extra energy consumption to produce the new equipment of steel (Musa and Morrison, 2009). The amount of contamination must be reduced to avoid process problems and avoid significant consumption of steel during milling. A reduction can be obtained by enhancing the steel quality, but then investment and maintenance cost of the milling equipment will increase. Dry mechanical activation may be a good alternative if a large increase in the rate constant is necessary due to mass flow considerations and minimizing contamination. Mechanical activation has one advantage compared to other ways of increasing the rate constant. Increased dissolution temperature and/or pressure is not necessary, hence the extra energy needed for milling is reducing the amount of energy needed for dissolution. Large scale magnesium carbonate precipitation seems to need higher temperatures, but one less element with high temperatures, might reduce the effect of total energy consumption if the mechanical activation is energy efficient enough.

The experiments were designed to have increasing pH, and the rate constants were shown to decrease. For a process with constant pH the decrease may be less than measured here, but the effect of decreasing mechanical activation with dissolution degree will still be a problem. In an industrial process, the reduced rate constants will probably require prolonged processing times if total dissolution is to be achieved, or the dissolution residues can be recycled and reactivated again. It is possible in a

carbonation process to take advantage of the pH – swing effect to further increase total reaction rate (Park and Fan, 2004).

The use of mechanical activation for an industrial process presupposes an energy favourable process. Further experiments on a larger scale are needed, and the milling energy cost versus the gain in the subsequent dissolution process has to be evaluated. The energy cost of mechanical activation is dependent on, among other things, where in the process the activation takes place. Inserting mechanical activation as an additional element in a pre-existing carbonation plant will increase the energy cost more than if the activation is considered as one of the main milling steps. To make mechanical activation a real possibility out of several pre-treatment options for mineral carbonation, it is crucial to consider the individual milling steps as a whole and evaluate the energy penalty against the gain in higher rate constants, lower mass requirements and/or faster sequestration.

5 SUMMARY AND CONCLUSION

To investigate the effect of mechanical activation of olivine, crystallinity calculations were performed based on X-ray diffraction, and specific surface area was measured together with the particle size distributions. Depending on the milling conditions, the crystallinity olivine decreased with prolonged milling times, whereas the specific surface area increased or decreased. Dry milling of olivine with a planetary mill did not produce higher surface areas than approximately 4 m^2/g after 10 min while milling with an addition of 10 wt% water gave a maximum specific surface area of 47 m^2/g after 60 min milling without any tendency to stop increasing. Wet milling gave specific surface areas between the dry and W10% milling. Dry milling was most efficient for crystallinity destruction, and wet milling seemed to preserve the original structure best. The particle size was very difficult to relate to the milling conditions, except for wet milling creating smaller particles than dry milling.

The comparison of the material characteristics to the observed rate constants, showed a correlation of both crystallinity and surface area to the total amount of dissolved olivine after 30 min of dissolution reaction, D_{30min}, but particle size distributions displayed no observable correlation. As

expected, increased milling times resulted in increased dissolution. W10% milling and wet milling showed a good linear relation between D_{30min} and specific surface area, but the dry milled samples were far from following the same trend. D_{30min} of the 60minWet sample was 12 %, the 60minW10% sample obtained 24 % and the 60minDry sample 33 %. D_{30min} increases with decreasing crystallinity, and for high crystallinity values D_{30min} correlated well with the specific surface area of the samples. The difference in the rate constant between the most rapidly dissolving sample (90minDry) and the slowest sample (10minWet) was of three orders of magnitude. The maximum measured rate constant was approximately two orders of magnitude larger than the rate constants given by Olsen and Rimstidt (2007) and references therein for untreated olivine.

Geochemical models of the experiments compared to the experimental results revealed several important characteristics about dissolution of mechanically activated olivine. A shrinking core model did not fit the material characteristics, and the resulting particle sizes and particle shapes were dependent on the choice of milling parameters. The rate constants of the materials decreased with increasing dissolution and pH. This reduction was probably related to four assumptions containing errors. The materials did not have constant dissolution properties throughout the material, the shrinking core model was not appropriate, more than one material characteristic is needed to describe the materials, and pH increase may result in a small period with transient dissolution state influencing the calculated rate constants beyond the pH dependency of olivine dissolution. The material characteristics did not succeed in explaining all the differences between the samples, and a part of the problem might be the simplifications and calculations involved in obtaining the material characteristics. The particle size is a 1D material characteristic, the specific surface area is a 2D measurement, but the mechanically activated materials have complex 3D surface characteristics and a 4^{th} dimension related to the differentiated effect of mechanically activation decreasing towards the centre of the particles.

However, the dissolution results were reproducible and the dissolution behaviour discovered is very important in an industrial setting where the milled materials are coming directly from a mill. If mechanical

activation is going to be used, the dry milled samples are the most reactive material, but wet milled materials may be more practical in a wet process despite the lower dissolution rates. If the end products are going to be sold, dry milled samples have a lower contamination degree and the products might obtain a higher purity. Mechanical activation increases the rate constant, but the application in an industrial process has to be examined further. Pilot scale mechanical activation has to be performed to get a better picture of the energy use and effects on material properties when performed on a larger scale. Pre-treatment with mechanical activation, if chosen, must be implemented as an integrated part of the total milling operation and not as an isolated additional step. When evaluating mechanical activation energy costs, the energy savings due to reduced temperature and pressure in the dissolution step can be included in the overall energy cost considerations.

ACKNOWLEDGEMENTS

Great thanks go to J. William Carey at Los Alamos National Laboratory, USA, for invaluable help with the modelling in PHREEQCi. This work was carried out as a part of the Strategic Institute Program "From waste to value: New industrial process for mineral dressing by use of CO_2" headed by Institute for Energy Technology, Norway. Funding of the program from the Research Council of Norway (Project No 158916/i30) is appreciated. Great appreciation also goes to the laboratory technicians at the Department of Geology and Rock Resources Engineering at NTNU, Norway for good support.

REFERENCES

Appelo, C.A.J. and Postma, D., 1999, *Geochemistry, Groundwater and Pollution*. 4th edn. A. A. Balkema, Rotterdam.

Awad, A., Koster van Groos, A.F. and Guggenheim, S., 2000, Forsteritic olivine: effect of crystallographic direction on dissolution kinetics. Geochimica Et Cosmochimica Acta, 64(10), 1765-1772.

Baláž, P., 2000, *Extractive Metallurgy of Activated Minerals*. 1st edn. Elsevier Science B.V., Amsterdam.

Baláž, P., 2008, *Mechanochemistry in Nanoscience and Minerals Engineering*. Springer-Verlag Berlin Heidelberg

Baláž, P., Turianicová, E., Fabián, M., Kleiv, R.A., Briančin, J. and Obut, A., 2008, Structural changes in olivine $(Mg,Fe)_2SiO_4$ mechanically activated in high-energy mills. International Journal of Mineral Processing, 88(1-2), 1-6.

Chen, Y. and Brantley, S.L., 2000, Dissolution of forsteritic olivine at 65 ^{O}C and 2<pH<5. Chemical Geology, 165(3-4), 267-281.

Eggleston, C.M., Hochella, M.F. and Parks, G.A., 1989, Sample preparation and aging effects on the dissolution rate and surface-composition of diopside. Geochimica Et Cosmochimica Acta, 53(4), 797-804.

Gautier, J.-M., Oelkers, E.H. and Schott, J., 2001, Are quartz dissolution rates proportional to B.E.T. surface areas? Geochimica Et Cosmochimica Acta, 65(7), 1059-1070.

Ghasri-Khouzani, M., Meratian, M. and Panjepour, M., 2009, Effect of mechanical activation on structure and thermal decomposition of aluminum sulfate. Journal of Alloys and Compounds, 472(1-2), 535-539.

Goldich, S.S., 1938, A study in rock weathering. The journal of geology, 46(1), 17-58.

Golubev, S.V., Pokrovsky, O.S. and Schott, J., 2005, Experimental determination of the effect of dissolved CO_2 on the dissolution kinetics of Mg and Ca silicates at 25 degrees C. Chemical Geology, 217(3-4), 227-238.

Gundewar, C.S., Natarajan, K.A., Nayak, U.B. and Satyanarayana, K., 1990, Laboratory studies on ball wear in the grinding of a hematite-magnetite ore. International Journal of Mineral Processing, 29(1-2), 121-139.

Hoberg, H. and Götte, J., 1985, The influence of mechanical activation on the kinetics of the leaching process of columbite. International Journal of Mineral Processing, 15(1-2), 57-64.

Huijgen, W.J.J. and Comans, R.N.J., 2003, Carbon dioxide sequestration by mineral carbonation: Literature Review (ECN-C--03-016), ECN Clean Fossil Fuels 52.

Huijgen, W.J.J. and Comans, R.N.J., 2005, Carbon dioxide sequestration by mineral carbonation: Literature Review (ECN-C--05-022), ECN Clean Fossil Fuels 37.

Hänchen, M., Prigiobbe, V., Storti, G., Seward, T.M. and Mazzotti, M., 2006, Dissolution kinetics of forsteritic olivine at 90-150 degrees C including effects of the presence of CO_2. Geochimica Et Cosmochimica Acta, 70(17), 4403-4416.

IPCC, 2005, Special report on carbon dioxide capture and storage. Intergovernmental Panel on Climate Change, 371.

Kalinkin, A.M., Boldyrev, V.V., Politov, A.A., Kalinkina, E.V., Makarov, V.N. and Kalinnikov, V.T., 2003, Investigation into the mechanism of interaction of calcium and magnesium silicates with carbon dioxide in the course of mechanical activation. Glass Physics and Chemistry, 29(4), 410-414.

Kleiv, R.A. and Thornhill, M., 2006, Mechanical activation of olivine. Minerals Engineering, 19(4), 340-347.

Kojima, T., Nagamine, A., Ueno, N. and Uemiya, S., 1997, Absorption and fixation of carbon dioxide by rock weathering. Energy Conversion and Management, 38(Supplement 1), 461-466.

Lackner, K.S., Wendt, C.H., Butt, D.P., Joyce, J.E.L. and Sharp, D.H., 1995, Carbon dioxide disposal in carbonate minerals. Energy, 20(11), 1153-1170.

Liu, Y., Olsen, A.A. and Rimstidt, J.D., 2006, Mechanism for the dissolution of olivine series minerals in acidic solutions. American Mineralogist, 91(2-3), 455-458.

Maroto-Valer, M.M., Fauth, D.J., Kuchta, M.E., Zhang, Y. and Andresen, J.M., 2005, Activation of magnesium rich minerals as carbonation feedstock materials for CO_2 sequestration. Fuel Processing Technology, 86(14-15), 1627-1645.

McKelvy, M.J., Chizmeshya, A.V.G., Diefenbacher, J., Bearat, H. and Wolf, G., 2004, Exploration of the role of heat activation in enhancing serpentine carbon sequestration reactions. Environmental Science & Technology, 38(24), 6897-6903.

Musa, F. and Morrison, R., 2009, A more sustainable approach to assessing comminution efficiency. Minerals Engineering, 22(7-8), 593-601.

O'Connor, W.K., Dahlin, C.L., Turner, P.C. and Walters, R., 1999, Carbon dioxide sequestration by ex-situ mineral carbonation. (DOE/ARC-99-009), Albany Research Center, Albany, Oregon, 14.

O'Connor, W.K., Dahlin, D.C., Rush, G.E., Dahlin, C.L. and Collins, W.K., 2002, Carbon dioxide sequestration by direct mineral carbonation: process mineralogy of feed and products. Minerals & Metallurgical Processing, 19(2), 95-101.

Oelkers, E.H., 2001, An experimental study of forsterite dissolution rates as a function of temperature and aqueous Mg and Si concentrations. Chemical Geology, 175(3-4), 485-494.

Ohlberg, S.M. and Strickler, D.W., 1962, Determination of percent crystallinity of partly devitrified glass by X-ray diffraction. Journal of the American Ceramic Society, 45(4), 170-171.

Olsen, A.A. and Rimstidt, J.D., 2007, Using a mineral lifetime diagram to evaluate the persistence of olivine on Mars. American Mineralogist, 92(4), 598-602.

Osland, R. 1998, *Modelling of variations in Norwegian olivine deposits: causes of variation and estimation of key quality factors*. Dr.Ing thesis, Norwegian University of Science and Technology.

Park, A.H.A. and Fan, L.S., 2004, CO_2 mineral sequestration: physically activated dissolution of serpentine and pH swing process. Chemical Engineering Science, 59(22-23), 5241-5247.

Parkhurst, D.L. and Appelo, C.A.J., 1999, User's guide to PHREEQC (Version2)—A computer program for speciation, batch-reaction, one-dimensional transport, and inverse geochemical calculations. (99-4259), U.S. Geological Survey Water-Resources Investigations, 310.

Pokrovsky, O.S. and Schott, J., 2000, Kinetics and mechanism of forsterite dissolution at 25 degrees C and pH from 1 to 12. Geochimica Et Cosmochimica Acta, 64(19), 3313-3325.

Pourghahramani, P. and Forssberg, E., 2006, Microstructure characterization of mechanically activated hematite using XRD line broadening. International Journal of Mineral Processing, 79(2), 106-119.

Rosso, J.J. and Rimstidt, J.D., 2000, A high resolution study of forsterite dissolution rates. Geochimica Et Cosmochimica Acta, 64(5), 797-811.

Samson, S.D. and Eggleston, C.M., 1998, Active sites and the non-steady-state dissolution of hematite. Environmental Science & Technology, 32(19), 2871-2875.

Sangwal, K.K., 1982, Dissolution kinetics of MgO crystals in aqueous acidic salt solutions [dislocation etching]. Journal of Materials Science, 17(12), 3598-3610.

Seifritz, W., 1990, CO_2 disposal by means of silicates. Nature, 345(6275), 486.

Sipilä, J., Teir, S. and Zevenhoven, R., 2008, Carbon dioxide sequestration by mineral carbonation. Literature review update 2005 - 2007. (2008 - 1), Åbo Akademi University, Faculty of Technology, Heat Engineering Laboratory.

Snilsberg, B. 2008, *Pavement Wear and Airborn Dust Pollution in Norway*. PhD Thesis, Norwegian University of Science and Technology.

Summers, C.A., Dahlin, D.C., Rush, G.E., O'Connor, W.K. and Gerdemann, S.J., 2005, Grinding methods to enhance the reactivity of olivine. Minerals & Metallurgical Processing, 22(3), 140-144.

Szhanto, E.v., 1968, Physikalisches und chemisches verhalten fester stoffe bei der schwingmahlung. In *Proc. VIII Internationaler Kongress für Erzaufbereitung*, Leningrad, pp.11.

Teir, S., Eloneva, S. and Zevenhoven, R., 2005, Production of precipitated calcium carbonate from calcium silicates and carbon dioxide. Energy Conversion and Management, 46(18-19), 2954-2979.

Tkáčová, K., 1989, *Mechanical Activation of Minerals*. Elsevier Science Publishers, Amsterdam.

Tromans, D. and Meech, J.A., 1999, Enhanced dissolution of minerals: Microtopography and mechanical activation. Minerals Engineering, 12(6), 609-625.

Tromans, D. and Meech, J.A., 2001, Enhanced dissolution of minerals: Stored energy, amorphism and mechanical activation. Minerals Engineering, 14(11), 1359-1377.

Tromans, D. and Meech, J.A., 2002, Enhanced dissolution of minerals: Conjoint effects of particle size and microtopography. Minerals Engineering, 15(4), 263-269.

Tromans, D. and Meech, J.A., 2003, Enhanced dissolution of minerals: Modeling conjoint effects of particle size and microtopography. Crystal Research and Technology, 38(1), 7-20.

USGS, 1998, PHREEQC Welcome Page. http://wwwbrr.cr.usgs.gov/projects/GWC_coupled/phreeqc//index.html (accessed 02.08.2008).

Wogelius, R.A. and Walther, J.V., 1991, Olivine dissolution at 25 °C: Effects of pH, CO_2, and organic-acids. Geochimica Et Cosmochimica Acta, 55(4), 943-954.

Wogelius, R.A. and Walther, J.V., 1992, Olivine dissolution kinetics at near-surface conditions. Chemical Geology, 97(1-2), 101-112.

Paper III

CARBONATION OF MECHANICALLY ACTIVATED OLIVINE

Tove Anette Haug[a]
Ingrid Anne Munz[b]
Rolf Arne Kleiv[a]
John Paul Kaszuba[c]
James William Carey[d]

[a] Department of Geology and Mineral Resources, Norwegian University of Science and Technology, Sem Saelandsvei 1, 7491 Trondheim, Norway
[b] Institute for Energy Technology, P.O. Box 40, 2027 Kjeller, Norway
[c] Department of Geology and Geophysics, 1000 E. University Avenue, University of Wyoming, Laramie, WY 82071, USA
[d] Hydrology, Geochemistry, and Geology Group (EES-6), Los Alamos National Laboratory, P.O. Box 1663, MS#D462, Los Alamos, NM 87545, USA

ABSTRACT

Energy intensive milling obtained with a laboratory planetary mill was used as pre-treatment of olivine with the purpose of enhancing the direct carbonation of olivine. The mill was run for 10 min or 60 min combining dry milling, milling with 10 wt % water, or wet milling, resulting in six combinations of milling parameters. Two carbonation experiments were performed with four reaction durations from 1 min – 45 min at 128 °C and 150 bar and 2 h and 18 h at 185 °C and 115 bar. A maximum conversion of more than 95 % was obtained after 18 h of reaction at 185 °C and 115 bar obtained for wet milled samples. Comparison of the conversion values to earlier dissolution rates for the same materials, indicated that the dissolution rate governed the conversion rate when the conversion was below ~ 10 % at 128 °C and 150 bar, whereas with conversion approaching

maximum values at 185 °C and 115 bar the rate was governed by precipitation kinetics. To take advantage of mechanical activation carbonation can be performed in two steps. The first step is dissolution, and the second step is precipitation. This separation of dissolution and precipitation can create more opportunities for optimization of the carbonation process, but will most likely introduce new challenges not associated with direct carbonation as well.

1 INTRODUCTION

Global warming concerns have resulted in large scale research focusing on CO_2 capture and storage. Mineral carbonation as one possible option for CO_2 storage, has been proposed by several researchers including Seifritz (1990) and Lackner *et al.* (1995). A range of minerals, with focus on silicates, containing Ca, Mg and Fe have been considered as feedstock because these elements form stable carbonates (Kojima *et al.*, 1997, McKelvy *et al.*, 2004, O'Connor *et al.*, 1999, Teir *et al.*, 2005). One out of several promising minerals is olivine, and the aqueous carbonation of olivine can be described by the following set of reactions. First CO_2 is dissolved in water resulting in carbonic acid, including the species formed due to dissociation, see Eq. 1. The second reaction is dissolution of olivine with acid, from the dissolution of CO_2 in water, as described in Eq. 2. The precipitation step consists of two independent reactions, i.e. precipitation of carbonate and silica (Eq. 3 and Eq. 4).

$$CO_{2(g)} + H_2O \leftrightarrow H_2CO_3 \leftrightarrow H^+ + HCO_3^- \leftrightarrow 2H^+ + CO_3^{2-} \quad (1)$$

$$Mg_2SiO_{4(s)} + 4H^+ \leftrightarrow 2Mg^{2+} + H_4SiO_2 \quad (2)$$

$$Mg^{2+} + CO_3^{2-} \leftrightarrow MgCO_{3(s)} \quad (3)$$

$$H_4SiO_4 \leftrightarrow SiO_{2(s)} + 2H_2O \quad (4)$$

Several pre-treatment methods has been investigated to increase the total carbonation reaction including heat activation (McKelvy *et al.*, 2004), chemical activation (Maroto-Valer *et al.*, 2005), grinding (Summers *et al.*, 2005), additives in the reaction fluid and elevated process temperatures and pressures (O'Connor *et al.*, 2002). Olivine carbonation has been studied up to 185 °C and CO_2 pressures of 135 bar in the laboratory (e.g. Bearat *et al.*, 2006, Giammar *et al.*, 2005, O'Connor *et al.*, 2002) and also with geochemical modelling (e.g. Bearat *et al.*, 2006, Chen *et al.*, 2006)

Mechanical activation is very intensive milling for a short period of time and represents a pre-treatment technology normally used for two purposes, mechanically alloying or increasing the leachability of metal ores in the hydrometallurgical industry (e.g. Baláž, 2000, Baláž, 2003). Mechanical activation used in olivine carbonation can be an effective way of increasing the dissolution kinetics and possibly the degree of conversion. The mills used for mechanical activation have several times higher energy intensity than conventional tumbling mills (Baláž, 2000, Tkáčová, 1989). Some carbonation experiments indicates that intensive milling might be too energy consuming (Summers *et al.*, 2005) compared to the increase in carbonation obtained, but further knowledge about the milling parameters and different mills are still valuable if the energy consumption can be reduced significantly in up-scaling or due to more efficient technology.

Mechanical activation changes the character of the material beyond reduced particle size and increased surface area (Tkáčová, 1989). The changes in the material properties resulting from the mechanical activation have been found to be very important for dissolution properties of minerals (Eggleston *et al.*, 1989, Sangwal, 1982). Experiments have shown that mechanical activation gives decreased crystallinity as calculated from X-ray diffractograms (Baláž, 2000, Kalinkin *et al.*, 2003, Kleiv and Thornhill, 2006, Pourghahramani and Forssberg, 2006, Tromans and Meech, 2001). Kleiv and Thornhill (2006) and Baláž *et al.* (2008) describe specific details about the effect of mechanical activation on olivine. Haug *et al.* (2009) showed that mechanical activation may enhance the dissolution rate of olivine in HCl-bearing solutions at conditions far from equilibrium by several orders of magnitude.

The objective of this paper was to study how mechanical activation influenced carbonation rates and mechanism. The mechanically activated olivine samples in this study were used directly from the mill without further modifications of the particle size or removal of contamination to mimic the milled materials in an industrial process where the material goes directly from the mill to the carbonation process. Batch carbonation data was modelled with the geochemical software PHREEQCi (Parkhurst and Appelo, 1999) in order to obtain saturation indices, evaluate rate limiting

processes and model conversion based on published crystalline olivine kinetics and kinetics from mechanically activated olivine (Haug *et al.*, 2009).

2 EXPERIMENTAL

2.1 Material description

The material used in the mechanical activation and direct carbonation experiments was olivine foundry sand of the quality ASF50 provided by North Cape Minerals retrieved from their dunite deposit at Åheim in Western Norway. The AFS50 sand will be referred to as the original sample. X-ray diffraction analysis (XRD) detected forsterite, chlorite, enstatite, chromite and traces of hornblende and mica. Approximately 95 % by weight is olivine of the composition $Mg_{1.86}Fe_{0.14}SiO_4$. The main elements and trace elements of the original sample as found by X-ray fluorescence analysis (XRF) are presented in Table 1. The original sample had a specific surface area of 0.47 m^2/g found by BET analysis.

Table 1 wt% of main elements (left) and ppm of trace elements (right) of the original sample as found by XRF.

Component	Original sample [wt%]	Component	Original sample [ppm]
Fe_2O_3	7.13	Zr	15
TiO_2	0.01	Y	2
CaO	-[a]	Sr	39
K_2O	0.01	Rb	2
P_2O_5	0.01	Zn	46
SiO_2	41.64	Cu	10
Al_2O_3	-[a]	Ni	3351
MgO	50.62	Ba	31
Na_2O	-[a]	Co	121.8
MnO	0.1	Cr	3005
SUM	99.52	V	35.1
LOI	0.34	Th	1.4
		Pb	27.6

[a] Below detection limit

2.2 Mechanical activation

Mechanical activation of the original olivine sand was achieved using a Fritsch Pulverisette 6 planetary mono mill, a 250 cm^3 stainless steel mill chamber (17-19 % Cr; 8-10 % Ni) and twenty 20 mm stainless steel balls

(12.5-14.5 % Cr; 1 % Ni) weighing 645 g in total. The activation was performed at ambient conditions in air using 20.0 g of the original sample. The milling was performed either dry or by adding 100 ml of distilled water (wet) or adding 2.0 ml of distilled water (10 wt% water, were the notation W10% is used) as a grinding aid. At the end of each batch the final product was carefully retrieved using a brush and a spatula. The milling chamber and balls were then washed with water and dried with ethanol to minimize the risk of cross contamination between the samples. Table 2 is a summary of milling parameters and material characteristics, including the type of carbonation experiment described in the next chapter.

Table 2 Summary of milling conditions, material properties and indications of the sample was used in the C-1 or the C-2 carbonation experiments described later.

Sample name	Milling time [min]	Water addition [ml]	Specific surface area [m^2/g], A_o	$d_{10}/d_{50}/d_{90}$ [µm]	Contamination, b [wt%]	C_{XRD} [%]	C-1 experiment	C-2 experiment
Original sample	0	0	0.47	197.2/311.9/447.7	0	100	No	No
10minDry	10	0	4.31	0.54/8.3/74.7	1.3	27	Yes	Yes
60minDry	60	0	3.19	0.71/5.9/79.8	3.1	13	Yes	Yes
10minW10%[a]	10	2	20.5	0.52/4.3/20.8	3.3	39	Yes	Yes
60minW10%[a]	60	2	47.4	0.41/3.8/39.2	6.0	14	Yes	Yes
10minWet	10	100	14.6	1.15/6.9/37.5	4.6	48	No	Yes
60minWet	60	100	31.0	1.02/10.5/27.5	16.7	21	No	Yes

[a] **W10% means that the water weight = 2 g, is 10 wt% of the material weight = 20 g.**

X-ray crystallinity (C_{XRD}) calculations were done using the dedicated software for the X-ray equipment by measuring the average background level, B_o and B_i, and the integral peak areas, I_o and I_i, above the background level for all samples, and subsequent manual calculations using Eq. 5. Indices i and o refers respectively to a mechanically activated sample, and the original sample representing the 100 % crystalline material.

$$C_{XRD} = \frac{I_i}{I_o}\frac{B_o}{B_i}\cdot 100\% \quad (5)$$

A peak at the refraction angle 2θ = 17.3° in the X-ray diffractogram for all samples was chosen to minimize the influence of surrounding peaks in a complicated X-ray diffractogram. This method was used in Haug *et al.* (2009).

2.3 Direct carbonation experiments

Table 3 Technical description of the carbonation experiments.

Exp. type	Number of valid exp.	DI water 22 °C	Mass of olivine [g]	[°C]	[bar]	Duration	Stirring
1	20	3.0 g	0.500	128	150	1/5/20/45 min	No
2	16	50 ml	7.50	185	115	2/18 h	Yes

The mechanically activated olivine samples were carbonated in two types of batch experiments performed with two sets of equipment (see Table 3 and Figure 1 for experimental details). Figure 1A presents a description of the C-1 experiments, performed at Los Alamos National Laboratory (LANL), USA. These experiments used a supercritical-fluid extractor with CO_2 as the fluid. A Teledyne Isco pump provided the pressurized CO_2 to the super critical fluid extractor. Volume of the sample cartridge was 10 ml. The cartridge was filled with the sample and then water before placement inside the supercritical-fluid extractor.

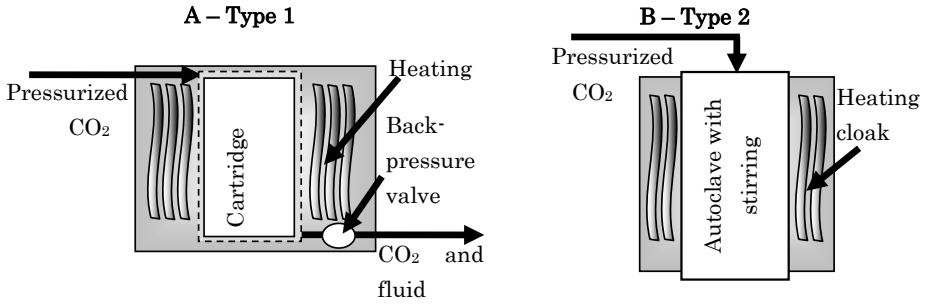

Figure 1 Illustration of the two different carbonation experiments.

Experimental temperature and pressure was obtained within less than 30 s and the experiment duration was measured from the point of application of heat and pressure. Approximately 6 ml in the cartridge was

empty and was filled with supercritical CO_2 at the start of the experiment. After the experiment about 2 ml of additional CO_2 at experimental pressure was used to displace the water and supercritical CO_2 in the cartridge. Most water samples were acidified with nitric acid, between 0.1 ml – 0.5 ml to dissolve precipitates that formed in the samples and hinder more precipitation. Samples 4B, 12B, 14, 15 and 16 were not acidified. pH was measured with pH–paper before and after acidification for several water samples and found to be less than 2 for acidified samples, and around 8 for non–acidified samples.

C-2 experiments, Figure 1B, were batch experiments, performed at Institute for Energy Technology (IFE), Norway. The equipment used consisted of 60 ml autoclaves, a HBL4570C temperature gauge with a Thyristor controller combined with heating jackets, a VS-C10 VWR magnetic stirrer with a cylinder shaped plastic covered magnet (27 mm X 7 mm), a Teledyne Isco pump, a Druck PTX – 1400 pressure manometer and a BenchLink Data Logger 3. Four batches were performed simultaneously. When the temperature was less than 3 °C away from the chosen experimental temperature, taking approximately 25 min, the autoclaves were pressurized carefully. The duration of an experiment was measured from the point in time were heat and pressure both had been applied. At the end of the experiment the heat was turned off. The autoclaves were cooled down to approximately 50 °C before depressurization. pH was measured in the opened autoclaves directly after dismantling when the immediate CO_2 degassing had stopped. A total of 15 ml water sample was taken from each autoclave with a syringe and filtered through a 45 µm filter into polyethylene bottles with airtight caps. The samples were not acidified. The reaction products and residual fluids were filtered with a vacuum pump and the products were dried in air over night. A plastic brush and water was used to clean the autoclaves. To dissolve residual precipitate inside the autoclaves, diluted HCl was added for several hours before final cleaning and drying.

2.4 Analyses

The water samples from C-1 experiments were analysed at LANL by ICP-AES to determine concentrations of dissolved Si, Ca, Mg, Na, K and B,

whereas ICP-MS was used for dissolved Al, Fe and Mn. The specific surface areas were measured using the BET method with N_2 adsorption using a Flowsorb II 2300 from Micromeritics with a degasser unit. Water analyses of the samples from C-2 experiments were performed on the water samples using ICP-MS. Both ICP-MS analyses for the C-2 experiment residues and all water samples together with the BET analyses were done at Sintef in Trondheim, Norway. XRD of the mechanically activated samples was performed using a Philips PW1710 X-ray diffractometer, equipped with a Cu-anode operated at 40 kV and 20 mA. The samples where scanned using a step size of 0.04° (2 theta) with 2 seconds per step from 2-60°. The reaction residues from selected C-2 experiments were analysed using a Bruker-axs D8 Advance X-ray diffractometer with a Cu K α anode operated at 40 kV and 40 mA. The step size was 0.02° (2 theta) with 0.5 seconds per step. The element analyses were obtained through XRF using a Philips 1480 X-ray spectrometer except for the carbonated residues where a BRUKER S8 Tiger XRF was used with a 4 kW generator. The XRD and XRF analysis were performed at Department of Geology and Mineral Resources Engineering, Norwegian University of Science and Technology, Trondheim. An analysis of the total carbon content (TC) of the residuals from experiment C-1 was performed at the Norwegian Geological Survey with a LECO SC-444 oven with a detection limit of 0.07 % of total carbon. The products from C-2 experiments were analyzed with a LECO SC632 instrument at Applied Petroleum Technology AS, Kjeller, Norway.

3 RESULTS

Table 4 A summary of all carbonation experiments with experiment type, sample choice and resulting total carbon content (TC) and obtained olivine conversion values. Experimental duplicates are marked with (I) and (II).

Exp Name	Exp. Type	Milling type	Duration	TC [wt%]	Conversion [%]
LANL 12	C-1	10minDry (I)	1 min	---	---
LANL 12B	C-1	10minDry (II)	1 min	0.37	2.4
LANL 11	C-1	10minDry	5 min	0.31	2.0
LANL 10	C-1	10minDry	20 min	0.33	2.2
LANL 16	C-1	10minDry	45 min	0.50	3.3
LANL 9	C-1	10minW10%	1 min	0.19	1.3
LANL 8	C-1	10minW10%	5 min	0.26	1.7

Exp Name	Exp. Type	Milling type	Duration	TC [wt%]	Conversion [%]
LANL 7	C-1	10minW10%	20 min	0.26	1.7
LANL 15	C-1	10minW10%	45 min	0.38	2.5
LANL 6	C-1	60minDry	1 min	0.90	6.1
LANL 5	C-1	60minDry	5 min	1.47	10
LANL 4	C-1	60minDry (I)	20 min	0.83	5.6
LANL 4B	C-1	60minDry (II)	20 min	---	---
LANL 14	C-1	60minDry	45 min	1.07	7.3
LANL 3	C-1	60minW10%	1 min	0.40	2.8
LANL 2B	C-1	60minW10%	5 min	0.27	1.8
LANL 1	C-1	60minW10% (I)	20 min	0.52	3.6
LANL 2	C-1	60minW10% (II)	20 min	0.45	3.1
LANL 2C	C-1	60minW10% (III)	20 min	---	---
LANL 13	C-1	60minW10%	45 min	0.90	6.3
IFE – 21	C-2	10minDry (I)	2 h	3.37	25
IFE – 22	C-2	10minDry (II)	2 h	3.68	28
IFE – 19	C-2	10minW10%	2 h	3.35	25
IFE – 18	C-2	10minWet (I)	2 h	2.22	16
IFE – 23	C-2	10minWet (II)	2 h	2.8	21
IFE – 20	C-2	60minDry	2 h	4.1	32
IFE – 25	C-2	60minW10%	2 h	4.64	38
IFE – 24	C-2	60minWet	2 h	4.81	44
IFE – 07	C-2[a]	10minDry	18 h	2.2	15
IFE – 11	C-2	10minDry	18 h	9.29	92
IFE – 06	C-2[a]	10minW10%	18 h	2.74	20
IFE – 10	C-2	10minW10% (I)	18 h	9.26	92
IFE – 15	C-2	10minW10% (II)	18 h	9.4	94
IFE – 17	C-2	10minWet	18 h	9.44	96
IFE – 08	C-2[a]	60minDry	18h	3.42	26
IFE – 12	C-2	60minDry (I)	18 h	8.23	77
IFE – 14	C-2	60minDry (II)	18 h	8.18	76
IFE – 16	C-2	60minW10%	18 h	8.81	88
IFE – 09	C-2[a]	60minWet	18h	3.83	34
IFE – 13	C-2	60minWet	18 h	8.61	96

[a] Experiments without stirring

A total of 36 batches of mechanically activated olivine were carbonated in two different experimental set-ups (Table 4). Milling parameters studied were water addition represented by dry milling, W10% milling and wet milling, and milling durations of 10 min or 60 min. The

products from the C-1 experiments were only analysed for total carbon content (TC) because of small products weights ≈ 0.5 g. The final weights for the products after the C-2 experiments were ≈ 10 g, thus making several analyses possible. All samples were analysed for TC, whereas XRD analyses were performed on 8 selected samples to describe changes in mineralogy and XRF-analyses were performed on 5 samples to verify the mass balance calculations. The samples chosen for the XRD analysis were selected with the purpose of covering max/min of specific surface area and max/min in crystallinity. The conversion results were used together with the results from the water analyses in mass–balance calculations.

3.1 Characteristics of mechanically activated olivine

Six samples were produced with the described combinations of milling duration and water addition. These samples were characterized by particle size distribution, specific surface area, contamination and crystallinity, C_{XRD} (Table 2). The crystallinity of the samples decreased with prolonged milling times. Dry milling was most efficient at reducing crystallinity, whereas wet milling was least destructive. Dry milling of olivine did not produce higher surface areas than approximately 4 m^2/g which was achieved after 10 min of milling, while 60 min of milling with an addition of 10 % water gave a maximum specific surface area of 47 m^2/g. The specific surface areas increased with milling time for W10% and wet milling, but decreased for dry milling. Wet milling gave specific surface areas between those obtained for dry and W10% milling. Differences in the particle size distributions were difficult to relate to the milling conditions, except for wet milling creating smaller particles than dry milling. All of the mechanically activated samples had d_{10} between 0.4 μm and 1.2 μm and d_{90} between 20 μm and 80 μm. Most samples had contamination below 6 wt%, except the 60minWet sample containing approximately 17 wt% steel. Contamination was calculated from weight measurements of the equipment and changes in composition as found by XRF and ICP-MS. In general the contamination increased with milling duration and with increasing water addition.

3.2 Particle size of carbonation products

Three initial samples and the solid reaction residues from these three samples after 2 h and 18 h of carbonation were chosen to evaluate particle

sizes of the precipitated particles by petrography and particle size distributions. The initial sample with the lowest crystallinity, 60minDry, the highest surface area, 60minW10% and the least altered, 10minWet were chosen. The reacted samples had narrower particle distributions than the initial samples. The differences in d_{10} for the products were very small ranging from 1.6 μm to 3.4 μm. In general the reaction products of the 60minW10% sample had larger magnesite grains and more euhedral magnesite grains than the other two products studied. The two carbonated 60minDry samples showed the smallest and most irregular shaped magnesite grains. The petrography revealed that the magnesite grains grew noteworthy in size from 2 h to 18 h of reaction for the products of the 60minW10% sample and the 10minWet sample. In contradiction to the results for the 60minW10% and 10minWet samples almost no change in magnesite grain size was observable for the product of the 60minDry sample.

3.3 Estimation of precipitated silica and product composition

Only magnesite was detected as a new crystalline phase in the reaction products. A low content of Si and Fe in the water samples indicated that these two elements were present in the solid phase despite the lack of minerals found from XRD or microscopy. Iron could either be present as solid solutions in magnesite, as minerals below the detection limit of the XRD instrument, or as amorphous phases. Giammar *et al.* (2005) detected only magnesite and amorphous silica even though other minerals were saturated as well, hence supporting the results from the experiments in this study. Mass balance calculations indicated large amounts of Si in the solid products with less than 0.1 % of the Si from the dissolved olivine present in the fluid phase. This was confirmed with XRF of the solid products.

An estimate of the carbonation product compositions can be calculated by Eqs. 6 through 11 assuming the contaminating steel and minerals other than olivine are inert. The total carbon content (TC) was converted to the corresponding amount of CO_2 [wt%] in the products and then used to calculate the moles of CO_2 bound, n_{CO2}, as shown in Eq. 6. Equation 6 was derived from the equation given by Huijgen *et al.* (2005) for

steel slag carbonation. n_{CO2} equals the moles of precipitated carbonate, $n_{(Mg,Fe)CO3}$, in the product. m_{aq} [%] is the weight percentage of dissolved solids relative to the total product weight m_1, M_{CO2} is the molar mass of CO_2 and $n_{(Mg, Fe)}$ is the total moles of Mg and Fe from olivine.

$$n_{CO_2} = n_{(Mg,Fe)CO_3} = m_o \cdot \frac{CO_2[wt\%]}{100 - CO_2[wt\%] + m_{(aq)}[\%]} \cdot \frac{1}{M_{CO_2}} \quad (6)$$

$$m_{steel} = m_o \cdot b \quad (7)$$

$$m_{inert} = m_o \cdot 0.05 \quad (8)$$

$$m_{(Mg,Fe)CO_3} = n_{(Mg,Fe)CO_3} \cdot M_{(Mg,Fe)CO_3} \quad (9)$$

$$m_{SiO_{2(am)}} = \left(\frac{n_{(Mg,Fe)CO_3} - \left(n_{Mg(aq)} + n_{Fe(aq)}\right)}{2} \right) \cdot M_{SiO_{2(am)}} \quad (10)$$

$$m_{(Mg,Fe)SiO_2} = m_1 - \left(m_{steel} + m_{(Mg,Fe)CO_3} + m_{SiO_{2(am)}} + m_{inert}\right) \quad (11)$$

Due to uncertainties of the chemical composition of the additional minerals present with less than 5 wt%, the contribution of these minerals to Fe and Mg is assumed negligible. The parameters included in the calculations were the contamination fraction *b* in the mechanically activated sample, the initial sample weight m_o, the final product weight m_1, the 5 wt% of other minerals present in the original olivine sand, and the molar mass of carbonate, $M_{(Mg,Fe)CO3}$, and silica, $M_{SiO2(am)}$. m_{inert} is the mass of the assumed inert minerals other than steel.

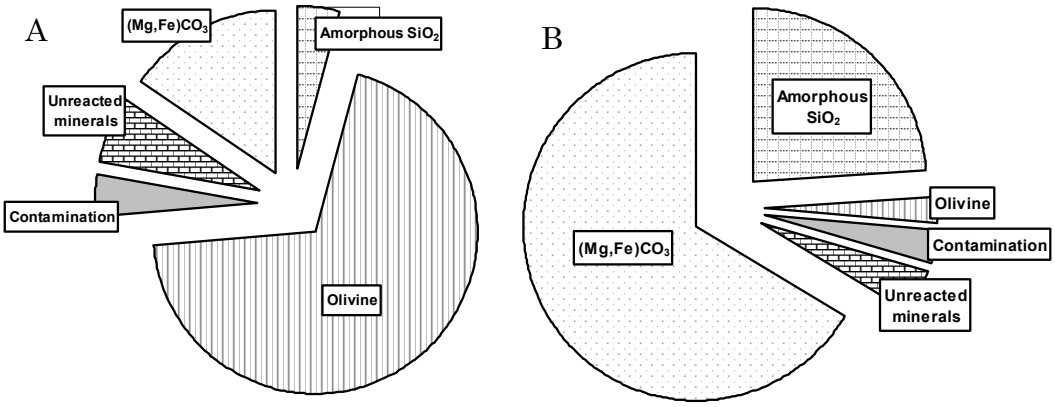

Figure 2 Composition of least (2 h carbonation of 10minWet) and most (18 h carbonation 10minWet) carbonated product at 185 °C / 115 bar.

Figure 2 shows an example of the mineral/solid phase distribution of the least and most carbonated sample at 185 °C / 115 bar. The total amount of magnesite and silica depends on the conversion, but there were in general approximately three times more magnesite than silica by mass.

3.4 Olivine conversion

Magnesite was the only new mineral detected with XRD for the 185 °C / 115 bar experiments. The original minerals present in the mechanically activated samples were detected in small amounts in the products for the samples where the mechanical activation had not destroyed the crystallinity sufficiently to hinder measurable peaks.

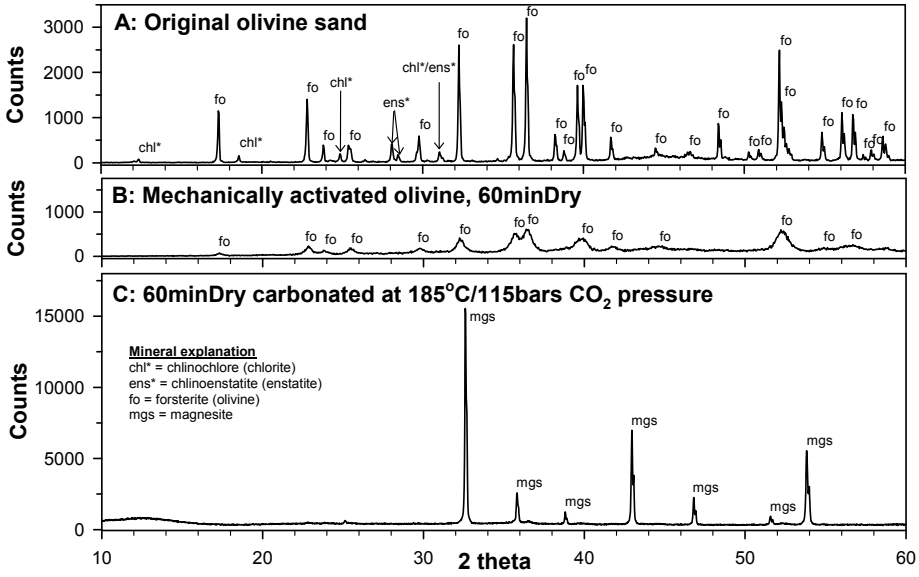

Figure 3 X-ray diffractograms of chosen materials.

Figure 3 shows the X-ray diffractograms for unactivated original olivine sample (A), the 60minDry sample (B) and the 18 h reaction product of the 60minDry sample (C) reacted at 185 °C / 115 bar. The 60minDry sample shows only magnesite peaks. No other carbonates or hydroxides were detected for any sample. Haug *et al.* (2009) found steel contamination in the mechanically activated samples that are directly comparable with the samples in this study. The steel appeared as a broad peak at approximately 2theta = 45° most evident for the 60minWet sample containing 17 wt% contamination. Both the products from 2 h of reaction and 18 h of reaction

had the characteristic peak at 2theta = 45°, but the amount was not possible to quantify. Due to the specified steel properties of the mill, and the detection of the steel peak in diffractograms of several products, the contamination has been assumed to be inert in the described carbonation reactions.

Our observation of magnesite as the only precipitate is consistent with experiments of Wolf *et al.* (2004) between 150 °C and 180 °C and 150 bar of CO_2. The products from the experiments performed at 128 °C / 150 bar were not analysed with XRD, but Hänchen *et al.* (2008) did experiments at 120 °C and P_{CO2} = 100 bar and found that under these conditions magnesite was formed directly, and under elevated supersaturation both hydromagnesite and magnesite was formed. Hence, it is very likely that magnesite or magnesite/hydromagnesite precipitated in these experiments. For the purpose of conversion calculations, magnesite was assumed to be the only precipitated carbonate. Iron from the dissolution of olivine is also assumed to have precipitated as carbonates. The stoichiometric conversion ζ [%] of available Mg and Fe present in olivine to carbonate was calculated using Eq. 12.

$$\zeta = \frac{n_{(Mg,Fe)CO_3}}{n_{(Mg,Fe)}} \cdot 100 \qquad (12)$$

Figure 4 shows the extent of conversion found for the 128 °C / 150 bar experiments (A) and the 185 °C / 115 bar experiments (B). Figure 4A shows that dry milling is much more efficient of increasing the conversion than W10% milling. In the 185 °C / 115 bar experiments (Figure 4B), the differences between the choices of mechanical activation were very small compared to the influence of reaction duration from 2 h to 18 h.

The two types of experiments can not be compared directly due to different reaction conditions, but as expected the conversion of olivine increased drastically with carbonation time for all samples. A maximum of 95.6 % was obtained for the 10minWet sample at 18 h of reaction at 185 °C / 115 bar. The detection of carbonates with a maximum conversion of 6 % for the 60minDry sample even after 1 min at 128 °C / 150 bar, including the time to reach experimental conditions and terminating the experiment, is very efficient compared to the other samples.

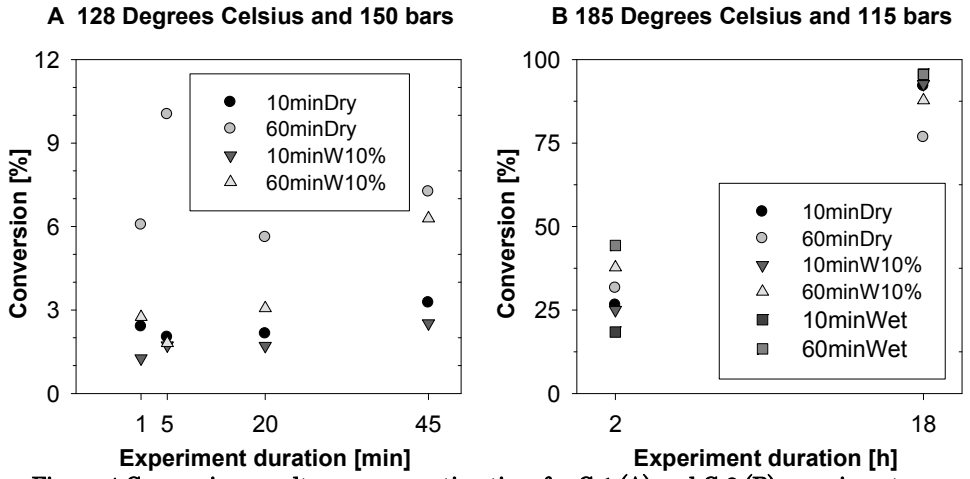

Figure 4 Conversion results versus reaction time for C-1 (A) and C-2 (B) experiments.

However, at 45 min conversion had only reached 7 %, possibly due to the absence of stirring. The reaction products were clearly more carbonated at the upper sample layer within the cartridge being in direct contact with the fluid than at the layer at the bottom of the cartridge. The effect of stirring was demonstrated in four batches from the 185 °C / 115 bar experiments carbonated for 18 h without stirring. The average conversion decreased from 90 % to 24 % without stirring.

3.5 Effect of milling parameters and material properties on conversion

Figure 4 shows the low importance of different milling conditions compared to the reaction time, but some comments can be made. For all experiments of both experiment types, the conversion was higher for samples milled 60 min compared to 10 min, except for 18 h of reaction where the samples milled 10 min reached a slightly higher degree of conversion than samples milled 60 min. In the 128 °C / 150 bar experiments the dry milled samples were always more converted than the W10% milled samples. However, in the 185 °C / 115 bar experiments there are no general trends related to the choices of milling parameters, and the conversion degree compared to milling properties are very dependent on the carbonation duration.

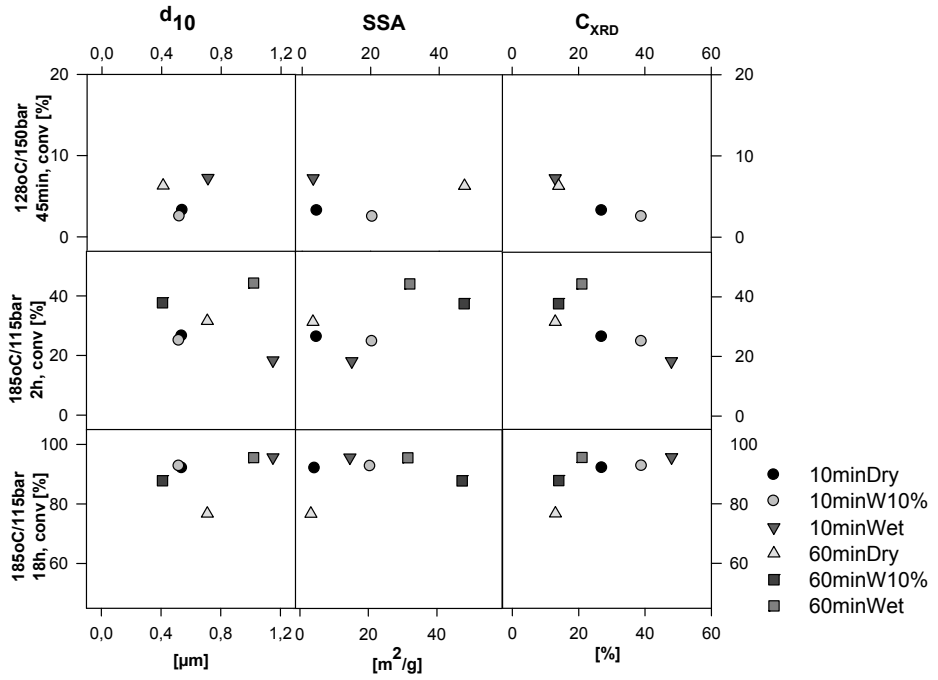

Figure 5 Plots of particle size (d_{10}), specific surface area (SSA) and crystallinity (C_{XRD}) plotted against conversion values for experimental reaction times of 45 min at 128 °C / 150 bar and 2 h and 18 h at 185 °C / 115 bar. An illustration of the lack of correlation between material properties and conversion values.

Figure 5 shows the material characteristics plotted against conversion for 45 min reaction at 128 °C / 150 bar, and 2 h and 18 h at 185 °C / 115 bar. Conversion cannot be related to the typical particle size or the specific surface areas. The materials are close in particle size and in addition the steel contamination affects both the surface area and the particle size, without actually being a part of the carbonation reaction, hence influencing the measurements and introduces errors. The 128 °C / 150 bar experiments and the 2 h experiments at 185 °C / 115 bar show how the conversion degree increased with lowered crystallinity, but for the 18 h experiments the trend is just the opposite.

3.6 Carbonation models

Geochemical modelling was carried out using PHREEQCi (Parkhurst and Appelo, 1999). To avoid underestimation of the pH due to low concentrations of dissolved CO_2, the equation of state for the pure supercritical CO_2 by

Duan and Sun (2003) was used for calculation of fugacity coefficients. The solubility was calculated using Henry's Law based on the Lichtner *et al.* (2003) method with the addition of a Poynting correction for pressure. Only pure end-members of the respective solid solution series, i.e. forsterite and magnesite were used in the modelling. No attempt has been made to include solid solutions. Models were developed both for 128 °C / 150 bar and 185 °C / 115 bar experiments in terms of molar olivine conversion versus time.

3.6.1 Model assumptions on dissolution

A reference model was based on the olivine kinetic parameters found by Hänchen *et al.* (2006) which are valid for 90–150 °C using the Arrhenius equation (Eq. 13).

$$r = A_A e^{\frac{-E_a}{RT}} a_{H+}^{n} \tag{13}$$

$$R_{ref} = \left(A_o \cdot \frac{100-b}{100} \right) \cdot \left(\frac{N}{N_o} \right)^{\frac{2}{3}} \cdot r \cdot \left(1 - \frac{IAP}{K_{fo}} \right) \tag{14}$$

$$R_{emp} = f_r \cdot \left(A_o \cdot \frac{100-b}{100} \right) \cdot \left(\frac{N}{N_o} \right)^{f_m} \cdot r \cdot \left(1 - \frac{IAP}{K_{fo}} \right) \tag{15}$$

The input values were the pre-exponential factor A_A = 854 mol/(m²s), the activation energy E_a = 52.9 kJ/mol, and the pH dependency factor n = 0.46 together with the experimental temperatures and pressures. Equation 14 defines the dissolution rate, $R_{ref,}$ used in the reference models. This equation is composed of four parts: the initial surface area of olivine in the first brackets where A_o is the available surface area of the sample, and b is the degree of contamination in the samples listed in Table 2. The second bracket implements a shrinking core model based on the initial moles of olivine (N_o) and the moles of olivine present (N). The third part is the reaction rate r. The last brackets express the reduction in reaction rate when approaching equilibrium. IAP is the ion activity product for forsterite and K_{fo} is the equilibrium constant for forsterite assumed to be valid for the reference sample and the mechanically activated samples used in this study. The time step size in the models was 1 min and the difference between 1 min and 1 s in the model was less than 0.02 % and therefore assumed insignificant. The activated carbonation models used the empirical kinetics

found for the mechanically activated samples presented by Haug *et al.* (2009) shown as a reaction rate, R_{emp}, in Eq. 15 as an extension of Eq. 14 including two new factors f_r and f_m. f_r was the ratio between the theoretical reaction rate and the initial observed reaction rate and f_m expressed an observed decrease in the reaction rate as a function of dissolution degree [%]. Table 5 summarizes the f_r and f_m included in the models (Haug *et al.* (2009) for more details). The activated kinetics were developed for 21 °C and atmospheric pressure based upon the kinetic parameters from Rosso and Rimstidt (2000) valid only for a temperature range of 25 – 45 °C and a pH range of 1.8 – 3.8 under these conditions. Their kinetic parameters were A_A = 3.467 mol/(m^{2}s), E_a = 42.6 kJ/mol and n = 0.50. These empirical parameters are directly connected to the parameters from Rosso and Rimstidt (2000), and therefore their parameters were used at the elevated temperatures and pressures despite the possible error introduced by the elevated conditions.

Table 5 Empirical factors included in the geochemical models using Eq. 15 and the empirically adjusted kinetics.

Sample	f_m	f_r
10minDry	14.5	195
60minDry	8.4	877
10minW10%	12.2	3.68
60minW10%	10.3	17.2
10minWet	15.0	6.59
60minWet	8.9	5.57

3.6.2 Model assumptions on precipitation

Precipitation of carbonates is a complex process depending on saturation indices (SI), the continuous supply of CO_2, dissolved ions, temperature, pressure and ultimately nucleation mechanisms and crystal growth. Common for all models were three simplifying assumptions: First the starting material contained pure Mg-olivine, whereas steel and minerals other than olivine were inert. The initial mass of olivine was then calculated using the estimated contamination and the fraction of olivine in the olivine sand. Second, amorphous silica was assumed to precipitate when $SI_{SiO2(am)} \geq 0$. Third, precipitation was assumed faster than dissolution, and precipitation was simplified by assuming instantaneous precipitation above

the given saturation index in each model. The reference model and the empirical models were used in three different experimental scenarios, see Table 6, with precipitation at SI = 0 for magnesite (Model A), precipitation of magnesite at SI = 1.85 (Model B), or no precipitation at all of magnesite or amorphous silica to study how fast forsterite equilibrium occurred (Model C). An SI = 1.85 for magnesite was used due to the observed supersaturation needed to initiate magnesite precipitation by Giammar *et al.* (2005). In addition to the input parameters for the reaction rates as described and the saturation limits, the total surface area and amount of olivine were input parameters in the models.

Table 6 Saturation limits for the three types of geochemical models.

Model	SI $MgCO_3$	SI $SiO_{2(am)}$	Instantaneous precipitation	Purpose
A	0.0	0.0	Above SI	Conversion with precipitation
B	1.85	0.0	Above SI	Conversion with supersaturated magnesite at precipitation
C	Increasing	Increasing	Nothing	Development of SI for magnesite, silica and forsterite ignoring precipitation

3.6.3 Results

Model A using the reference kinetics predicted full conversion of the samples within 27 min to 7 h for the highest and lowest surface areas respectively with the 185 °C / 115 bar experiments. This can be compared to the maximum measured conversion obtained at 2 h of 44 %. Figure 6A shows how model A with empirically adjusted kinetics predicts the conversion for both experiment types, and Figure 6B model B with elevated SI and empirically adjusted kinetics for the 185 °C / 115 bar experiments. The large overestimation of the conversion in the 128 °C / 150 bar experiments is most likely an effect of un-stirred conditions. With stirring in the 128 °C / 150 bar experiments the measured conversion degrees probably would have been closer to the modelled values. The results of model A at 185

˚C / 115 bar overestimated the conversion at 2 h and underestimated at 18 h.

The reduction in the predicted extent of conversion from model A to model B in Figure 6B for the 185 °C / 115 bar experiments corresponded to a minimum SI for magnesite before precipitation could begin. Saturation for both magnesite and amorphous silica, calculated without precipitation with model C, was reached within few minutes or seconds for most samples. Model A estimated a forsterite SI = -4.5 at 185 °C / 115 bar and forsterite SI = -7.1 at 128 °C / 150 bar. Hence, forsterite is very far from equilibrium if both magnesite and silica were precipitating. A SI = 2.3 for magnesite was obtained at 185 °C / 115 bar and SI = 3.0 for 128 °C / 150 bar if no precipitation occurred and forsterite stopped dissolving at equilibrium. Lowering of the temperature and increasing the pressure from 185 °C / 115 bar to 128 °C / 150 bar increased the saturation of magnesite, and hence the possibility of magnesite precipitation was increased.

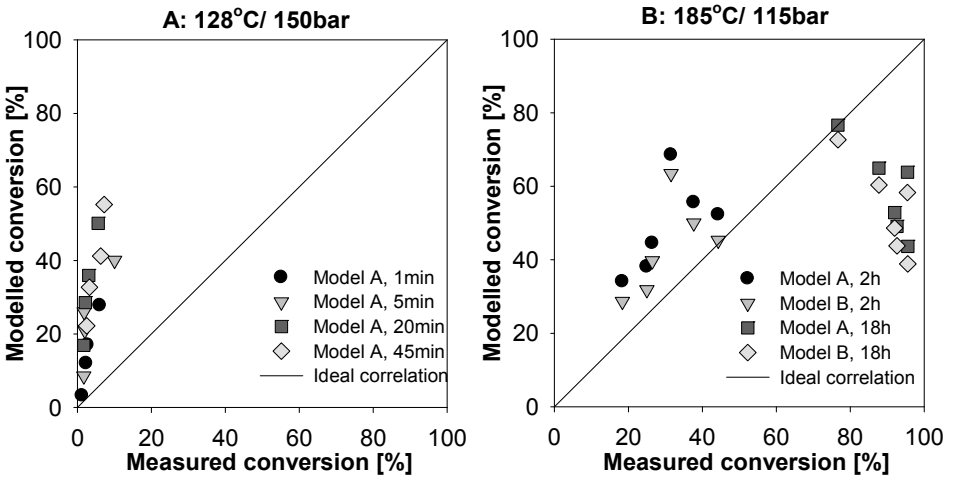

Figure 6 A – C-1 experiments with measured conversion plotted against conversion from model A with precipitation as SI = 0 and empirically adjusted kinetics. B – C-2 experiments with measured conversion plotted against conversion from model A and model B with empirically adjusted kinetics.

The maximum saturation indices achieved at the end of each experiment were estimated using the water sample with the greatest Mg or Si concentrations for each experimental and ambient condition. In general more minerals were saturated at 185 °C / 115 bar than at ambient

conditions. Magnesite was slightly saturated at 185 °C / 115 bar, but was just below saturation after lowering temperature and pressure. Several SiO_2 species and Fe-oxides-hydroxides were saturated both at 185 °C / 115 bar and room conditions. No Mg containing minerals were saturated at ambient conditions. Precipitation was observed in the water samples previously to analyses from the 128 °C / 150 bar experiments which made the modelling of SI more difficult than for the 185 °C / 115 bar experiments using measured concentrations. Estimates of Si concentration and carbonate concentrations at room temperature and pressure indicated that the precipitating phase probably was a polymorph of silica, but not an Mg containing mineral. At 128 °C / 150 bar magnesite were found to be slightly supersaturated for some samples and slightly undersaturated for other samples.

4 DISCUSSION

4.1 Olivine conversion

Several publications have results of direct olivine carbonation. The results from olivine batch experiments being very similar to the experiments described here are summarized in Table 7. The conditions and the input particle sizes vary in the published literature, but still some general comparisons can be made with the results from this study.

Table 7 Published results for direct olivine carbonation in batch experiments.

Reference	T [°C]	P [bar]	Fluid	olivine in slurry [wt%]	Time [h]	Amount of CO_2	Particle size	Conversion (Literature value)
Not mechanically activated olivine								
(O'Connor *et al.*, 2002)	185	115	H_2O	15	24	Infinite	- 37 µm	91 %[a]
	185	115	0.5 M NaHCO3 + 1 M NaCl	15	6	Infinite	- 37 µm	84 %[a]

(Giammar *et al.*, 2005)	95	100	0.25 M $MgCl_2$+ 0.50 M $NaHCO_3$	≈ 2	336	Limited	125–250 µm	45.2 wt%[b]
	95	100	0.15 M $MgCl_2$+ 0.30 M $NaHCO_3$	≈ 2	240	Limited	125–250 µm	3.5 wt%[b]
(Bearat *et al.*, 2006)	185	135	1 M NaCl + 0.64 M $NaHCO_3$	Varying	Varying	Not given	-37 µm + 37–200 µm	≈ 5 – ≈ 68 %[c]
(Summers *et al.*, 2005)	185	150	1 M NaCl + 0.64 M $NaHCO_3$	15	1	Infinite	- 75 µm[d]	≈ 5.1 %[c]
<u>Mechanically activated olivine</u>								
(Summers *et al.*, 2005)	185	150	1 M NaCl + 0.64 M $NaHCO_3$	15	1	Infinite	- 9 µm[e]	≈ 70 %[c]
	185	150	1 M NaCl + 0.64 M $NaHCO_3$	15	1	Infinite	- 9 µm[f]	≈ 84 %[c]
	185	150	1 M NaCl + 0.64 M $NaHCO_3$	15	1	Infinite	- 17 µm[g]	≈ 71 %[c]
	185	150	1 M NaCl + 0.64 M $NaHCO_3$	15	1	Infinite	Not given[h]	≈ 89 %[c]

[a] Moles of Mg from olivine converted to carbonate

[b] wt% of carbonate in product estimated from XRD

[c] Calculation not given

[d] Ground with a ball mill

[e] Ground with a Stirred media dettritor Wet

[f] Ground with a Attrition mill Wet 1h

[g] Ground with a Attrition mill Dry 1h

[h] Ground with a Attrition mill Dry 24h

The experiments given by O'Connor *et al.* (2002) were performed at 185 °C and 115 bar of CO_2 pressure, i.e. the same conditions as experiments of C-2 using mechanically activated olivine, hence the difference is the pre-treatment, solution chemistry and the technical equipment. After 18 h of carbonation of the mechanically activated olivine samples, an average conversion of 84 % was obtained, compared to 91 % after 24 h described by O'Connor *et al.* (2002). Extensive conversion after several hours is not enhanced by the introduction of mechanical activation as pre–treatment. However, a conversion of 6 % for the 60minDry sample at 128 °C and 150 bar is much more efficient than the non-activated sample used by Summers *et al.* (2005) obtaining only 5 % conversion within 1 h. It seems like mechanical activation with a planetary mill, as demonstrated here, produces olivine samples reacting very fast initially, and then the conversion rate slows down at longer reaction times and with more extensive carbonation.

The last four experiments by Summers *et al.* (2005) were based on mechanical activation of olivine performed with three other mills than a planetary mill. They concluded that intensive milling beyond a certain energy input is not efficient with respect to extensive direct carbonation. The very small differences described here at 18 h of carbonation of olivine milled in the planetary mill with different milling times and water additions are in agreement with the conclusion of Summers *et al.* (2005). Even though these experiments cannot be compared directly due to different pressures and reaction times and solutions, it appears that the planetary mill is less efficient than the method presented by Summers *et al.* (2005). There are four possible explanations. 1: Conversion increases with increased partial pressure of CO_2 (Giammar *et al.*, 2005, O'Connor *et al.*, 2002): the pressure used in this study is 115 bar compared to 150 bar (Summers *et al.*, 2005), 2: Differences in the material properties due to differences in mill performance; and 3: the use of 1 M NaCl + 0.64 M $NaHCO_3$. The addition of salts and increase in CO_2 pressure cause an increase in the magnesite precipitation to a certain extent (O'Connor *et al.*, 2002). 4: 18 hours of reaction time might have been too long to distinguish between the samples. By comparison of published conversion degrees with the obtained conversion of the mechanically activated samples, the results obtained at 1 min to 45

min at 128 °C and 150 bar were very efficient. However, the experiments for 2 h / 18 h, despite the change in temperature to 185 °C and 115 bar, do not show the same distinct conversion differences between the various milling conditions.

Normally amorphous substances dissolve faster than their crystalline counterparts. Hence, the influence of dislocations and disordering caused by mechanical activation will have large impacts on the carbonation reaction. Decreasing crystallinity was found to be related to the conversion at 128 °C / 150 bar, see Figure 5. This trend corresponds well with the trend between increasing dissolution rate with decreasing crystallinity as found by Haug *et al.* (2009) for the same materials. On the other hand the conversion degrees increases with increasing crystallinity in the 18 h experiments at 185 °C / 115 bar. If the latter experimental conditions are dominated by the precipitation rate, it might possibly indicate that crystalline materials initiate the precipitation of magnesite more than amorphous materials, but this might be related to other material properties changing during the course of reaction or the complexity of the precipitation mechanisms. Magnesite growth is governed by the available surface area of existing magnesite grains since magnesite is the preferred surface to precipitate on compared to other substances (Giammar *et al.*, 2005). There seemed to possibly be indications of a positive correlation between the amount of fines in the three mechanically activated samples studies and the size of the carbonate grains in the products from the 185 °C / 115 bar experiments.

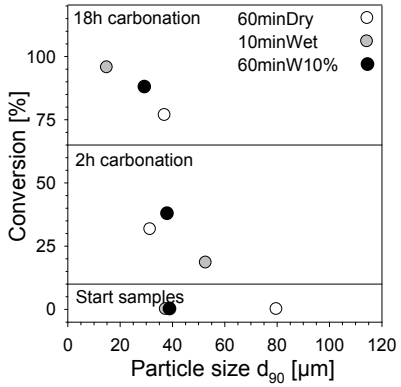

Figure 7 Conversion plotted against d_{90} for products subjected to particle size analyses.

The grain size was partially related to the conversion (see Figure 7) with increasing conversion corresponding to decreased d_{90}. This result suggests that the largest conversion was associated with the best conditions for precipitation over time. Therefore nucleation and crystal growth may possibly be the rate limiting step when performing extensive carbonation at the conditions described here.

4.2 Dissolution and precipitation

4.2.1 Rate limiting regimes and magnesite precipitation

Normally the dissolution of olivine is considered to be the rate limiting reaction during carbonation, and mechanical activation was chosen as a pre-treatment method to increase the dissolution rate up to three orders of magnitude as described by Haug *et al.* (2009).

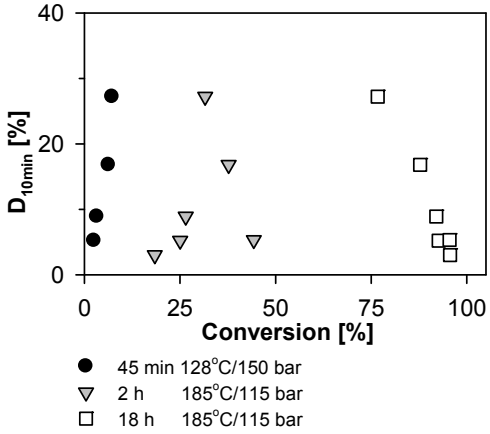

Figure 8 A comparison of dissolution and carbonation results performed on directly comparable samples. D_{10min} indicates the percentage of olivine dissolved after 10 min (Haug *et al.* 2009).

Figure 8 shows how the measured conversion degrees correlates with the extent of dissolution measured after 10 min, D_{10min}, at ambient temperature and pressure in 0.01 M hydrochloric acid. Maximum D_{10min} was 27 % obtained for the 60minDry sample. For 1 - 45 min reaction at 128 °C / 115 bar D_{10min} corresponds well with the measured conversion indicating that dissolution is the main limiting reaction. However, for 2 h reaction at 185 °C / 150 bar there is no significant correlation between the extent of

dissolution and the conversion degree, and for 18 h the conversion degree is in negative correlation with the extent of dissolution at 10 min.

The lack of correlation between the dissolution results and conversion degrees when the total carbonation time is increased indicates that other factors may have influenced the carbonation reaction in addition to the initial dissolution rate. In the dissolution experiments described by Haug *et al.* (2009), the specific dissolution rate decreased with the extent of dissolution. A decreased specific dissolution rate could be due to early dissolution of the least crystalline material, or to leaching effects of Mg leaving a silica layer, although a leached layer was not observed or silica precipitation onto the olivine grains. These two factors may be important for the carbonation experiments. The positive effect of adding $NaHCO_3$ (First observed by O'Connor *et al.*, 2002) indicates the possible importance of precipitation. $NaHCO_3$ increases the activity of the bicarbonate ion and hence the Mg-concentration needed to precipitate magnesite is lowered (Chen *et al.*, 2006) and olivine stays further from equilibrium during the carbonation reaction lowering the effect of saturation on the dissolution rate and a long reaction time.

Using basic thermodynamic analysis and magnesium ion dissolution Chen *et al.* (2006) studied key parameters affecting carbonation and found two principal reactions; dissolution of the feedstock and precipitation of carbonate from the solution. The governing reaction depends of the process conditions. Huijgen *et al.* (2006) described the carbonation of wollastonite, $CaSiO_3$, and found it to be dependent on Ca entering the solution defined by the dissolution rate at low temperatures and pressures, while at temperatures above approximately 200 °C the reaction becomes pressure dependent because the activity of the (bi)carbonate ion is reduced and nucleation and precipitation becomes the dominating reaction step. These two regimes are likely to be valid for olivine as well with slightly different temperatures and pressures dividing the reaction regimes.

Interpreting the conversions degrees for 128 °C / 150 bar in Figure 8 can indicate that conversion probably is governed by the olivine dissolution rate, while the 2 h and 18 h experiments at 185 °C / 115bar are more dependent of the nucleation and rate of crystal growth. If the two types of carbonation experiments are governed by two different carbonation regimes,

it explains why the fast dissolution rates observed in dissolution experiments (Haug *et al.*, 2009) are not reflected in the extent of conversion for the 185 °C / 115 bar experiments, but in the 128 °C / 150 bar experiments.

4.2.2 Interpretation of modelled conversion

The measured conversion of the 60minDry sample at 185 °C / 115 bar after 2 h and 18 h are compared to the modelled conversion in Figure 9 using model A with the reference and the activated kinetics. The overestimation of the conversion at 2 h from both empirical and previously published kinetics indicates that the conversion in the beginning of the experiments is not controlled not dissolution, but the nucleation and growth of crystals might be important. This supports the similarities between the published conversion degrees and the measured conversion degrees of unactivated and activated olivine materials.

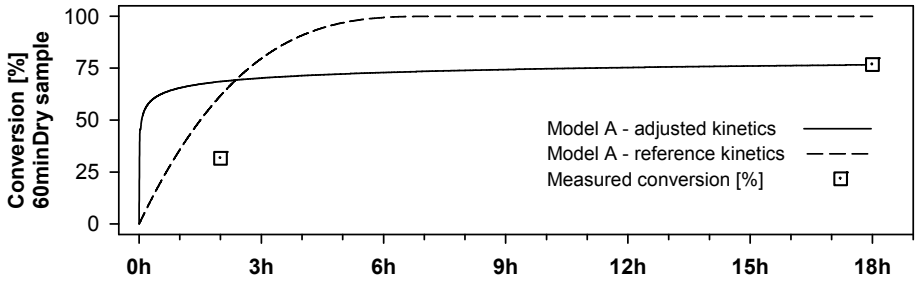

Figure 9 Comparison of the conversion model A based on reference kinetics or empirically adjusted kinetics for the 60minDry sample. Measured conversion values are included.

Giammar *et al.* (2005) observed SI = 0.25 for magnesite without precipitation in their experiments at 95 °C / 100 bar and postulated that at these conditions, nucleation was rate limiting with increasing importance of crystal growth as the amount of magnesite increased due to precipitation. The empirical model underestimated the conversion at 18 h for all samples except 60minDry, and can partially be explained by the experimental design of the dissolution experiments. Only 40 % dissolution was achieved in the dissolution experiments, and extrapolation of the results to almost 100 % dissolution might introduce large errors due to the estimated decline in the empirical reaction rate. The development of the models for 21 °C and

ambient pressure and much lower pH might also be important, since the temperature dependency was not studied.

If precipitation is the dominating rate-limiting step, then the carbonation reaction of olivine samples consists of three possible time-dependent phases. First, olivine dissolves until magnesite supersaturation has been reached and is only dependent on the dissolution properties of olivine. The second phase consists of magnesite nucleation simultaneously with olivine dissolution until maximum SI has been reached for olivine. Here, both the solution composition and the characteristics of solid material are probably important. The last phase is dissolution of olivine limited by removal of Mg and SiO_2 from the solution and thereby lowering the saturation of olivine. These three phases will possibly last and occur differently for the mechanically activated samples with varying material properties and dissolution rates. The modelled saturation indices indicated that magnesite was slightly supersaturated at the end of the experiments; hence the assumption of precipitation only above saturation was not contradicted. The saturation indices of silica phases did not confirm or say the opposite to the assumption of silica precipitation above saturation. The water samples represent the saturation indices at the end of the experiments, and they might have been much higher in the beginning of the experiment, but after 2 h and 18 h carbonation, precipitation might have been so extensive that equilibrium has been reached.

4.2.3 Occurrence of silica

Over 99 wt% of the silica originating from the dissolution of olivine was determined to be in the solid product, not in the fluid, as calculated by mass balance, using the element analyses of the solids, the total carbon measurements and the water chemistry. Silica precipitating on the surfaces of the olivine particles may inhibit further dissolution or silica may contaminate the magnesite precipitated, while direct precipitation of silica into the solution probably is not a problem. O'Connor (2002) did not find silica associated with or as a coating of the magnesite particles. In the same experiments the outer rim of the olivine particles was enriched in silica and depleted in magnesium, but this effect may have been limited to shorter experiments and silica precipitated separately from the magnesite and olivine particles was also found. Giammar *et al.* (2005) observed only a

separate precipitate of amorphous silica. A thin silica enriched surface layer has been observed by Pokrovsky and Schott (2000) for several orthosilicates and of Bearat *et al.* (2006) for olivine. There is a possibility of silica interfering with extensive olivine dissolution where Mg transport through the depleted layer or the precipitated layer is rate limiting, but neither Luce *et al.* (1972) nor Westrich *et al.* (1993) could observe a Si-rich surface layer after dissolution of olivine in acid.

It might be difficult to distinguish between a silica layer formed by Mg leaching compared to a layer formed by silica precipitation from the surrounding solution (Bearat *et al.*, 2006). Hence, the silica present in the product can occur as free silica and as thin layers on the particles. One possibly important observation of Bearat *et al.* (2006) was silica free zones on the residual olivine particles mainly associated with etch pits, indicating a stoichiometric dissolution where the olivine had dislocations or other defects. Their observation can be very important for the dissolution of mechanically activated olivine if maximising of the disordering of the structure leads to stoichiometric dissolution and avoidance of silica-layer formation on the particles. If this is valid for the carbonation of the samples presented here, silica formation can not explain why the most disordered samples have the lowest carbonation at 18 h of reaction, whereas changes in the material characteristics and precipitation limitations are more likely explanations.

4.3 Implications for a future carbonation process

Optimising a carbonation process involves balancing the dissolution of olivine versus magnesite precipitation when the carbonation reaction is performed in one step (Chen *et al.*, 2006, Hänchen *et al.*, 2008) and includes choosing suitable pre-treatment method(s) and process conditions. To make mechanical activation a practical option as carbonation pre-treatment, the milling process has to be optimized with respect to suitable material properties maximizing both the dissolution rate and the influence on precipitation rate and products.

The enhanced olivine dissolution rates observed in (Haug *et al.*, 2009) can only be taken advantage of if dissolution is the rate limiting step. If mechanical activation of olivine is going to be used, carbonation conditions

have to be adjusted to comply with the increased dissolution rates. Hänchen *et al.* (2008) stated that the pressure had to be over 60 bar to make a difference in precipitation which is in good agreement with O'Connor *et al.* (1999) saying that supercritical CO_2 is much more efficient for carbonation purposes than liquid CO_2. Therefore probably a minimum temperature and pressure would be above the supercritical conditions of CO_2 even for mechanically activated olivine. Huijgen *et al.* (2006) concluded that optimum temperature is determined by the CO_2 pressure, and at a constant pressure the carbonation rate decreases with decreasing temperature due to kinetic limitations. If a silica layer is developed during olivine carbonation several countermeasures have been proposed. Park and Fan (2004) used the effect of agitation with glass beads, stirring during carbonation can remove a forming silica layer due to abrasion (Bearat *et al.*, 2006), and in addition decreased liquid/solid ratio may be an option to increase the particle – particle abrasion.

The final reaction product contained mainly magnesite, amorphous silica, olivine traces due to incomplete conversion, traces of other original minerals and steel contamination from the milling step. For an industrial carbonation process the mass flows and equipment costs are very important. Minimum mass flows, minimum retention times, maximum conversion and minimum wear of the equipments represent the optimal condition. Minimum wear is obtained with dry milling, but the results for 18 h of carbonation seem to have wet milled materials as the material obtaining the highest total conversion. Minimum wear can in this case therefore not be achieved at the same time as maximum conversion if the same materials and conditions are used as presented here. Wet milling needs higher quality steel, and dry milling needs larger amounts of olivine to obtain the same amount of bound CO_2. The contaminating steel can be recycled by magnetic separation prior to or after the carbonation step, but this introduces a process step and increases the total cost. Here the amount of steel contamination has to be balanced against maximum conversion and importance of the contamination in the reaction.

The dissolution kinetics described by Hänchen *et al.* (2006) obtained from constant flow-through experiments overestimated the batch carbonation. Dissolution under conditions more similar to the batch reaction

with extensive dissolution of the initial materials gave much better results, even though temperature and pressure were much lower when the empirical rates were obtained in the dissolution experiments. The choice of batch or flow-through dissolution, superficial or extensive dissolution/carbonation and so on for the experiments might be important in addition to the as the temperature and pressure when performing pilot scale experiments.

5 CONCLUSION

Maximum conversion after 18 h of reaction at 185 °C and 115 bar was obtained for the wet milled samples from a planetary mill with more than 95 % conversion for both the sample milled for 10 and the sample milled for 60 min. The lowest conversion after 18 h or reaction was 77 % for the sample milled dry for 60 min. These conversion results at 185 °C / 115 bar did not correspond with the dissolution rates for the same set of samples, but the extent of conversion obtained for reaction times of 45 min or less at 128 °C and 150 bar fitted well with the dissolution rate data. These results indicate that nucleation and/or crystal growth may be rate-limiting. Carbonation of mechanically activated olivine is probably limited by the dissolution rate of olivine at 128 °C and 150 bar for reaction times up to 45 min, but for 2 h or 18 h of carbonation at 185 °C and 115 bar, the precipitation of magnesite may be significant. The results demonstrate that mechanical activation might be very efficient in increasing the dissolution rate, but then the conversion is limited by the precipitation kinetics.

Geochemical models based on empirical dissolution rate expressions found from experiments with dissolution degree up to 40 % predicted the conversion much better than olivine dissolution kinetics using only the Arrhenius equation and the shrinking core model for the decrease in particle size. The empirical model included a decrease in reaction rate with dissolution degree, which consisted of several material and experimental factors. The main conclusion from the modelling is that the conversion rate decreases with conversion degree, and the cause is probably related to material property changes and/or silica layer formation from leaching or precipitation. Material properties and silica-layer effects can be reduced by introducing abrasion and particle stress during carbonation.

To maximize the advantage of mechanical activation the temperature can be lowered to increase the dissolution of CO_2 in the fluid, thus increasing the bicarbonate activity. The rate of precipitation would then increase unless magnesite solubility due to increased temperature outweighs the effect of increased bicarbonate concentration. Several experiments have to be made before comprehensive conclusions about the efficiency of mechanical activation can be drawn. Conversion at lower temperatures and pressures is needed to study the potential of mechanical activation as a tool for energy reduction in the carbonation process. Changes in liquid/solid ratios may be important to the conversion rate as well and an evaluation of the particle interaction relationship together with flow-through experiments can give valuable insight into practical considerations for future industrial olivine carbonation processes.

ACKNOWLEDGEMENTS

This work was carried out as a part of the Strategic Institute Program "From waste to value: New industrial process for mineral dressing by use of CO_2" headed by Institute for Energy Technology, Norway. Funding of the program from the Research Council of Norway (Project No 158916/i30) is appreciated. I also appreciate very much the help from Kirk Hollis when performing experiments at the Scrub, Applied Chemical Technologies Group within the Chemistry Division (Los Alamos National Laboratory). Great gratitude finally goes to the laboratory technicians and researchers at IFE for good support during the laboratory work in their facilities.

REFERENCES

Baláž, P., 2000, *Extractive Metallurgy of Activated Minerals*. 1st edn. Elsevier Science B.V., Amsterdam.

Baláž, P., 2003, Mechanical activation in hydrometallurgy. International Journal of Mineral Processing, 72(1-4), 341-354.

Baláž, P., Turianicová, E., Fabián, M., Kleiv, R.A., Briančin, J. and Obut, A., 2008, Structural changes in olivine $(Mg,Fe)_2SiO_4$ mechanically activated in high-energy mills. International Journal of Mineral Processing, 88(1-2), 1-6.

Bearat, H., McKelvy, M.J., Chizmeshya, A.V.G., Gormley, D., Nunez, R., Carpenter, R.W., Squires, K. and Wolf, G.H., 2006, Carbon sequestration via aqueous olivine mineral carbonation: Role of

passivating layer formation. Environmental Science & Technology, 40(15), 4802-4808.

Chen, Z.Y., O'Connor, W.K. and Gerdemann, S.J., 2006, Chemistry of aqueous mineral carbonation for carbon sequestration and explanation of experimental results. Environmental Progress, 25(2), 161-166.

Duan, Z.H. and Sun, R., 2003, An improved model calculating CO_2 solubility in pure water and aqueous NaCl solutions from 273 to 533 K and from 0 to 2000 bar. Chemical Geology, 193(3-4), 257-271.

Eggleston, C.M., Hochella, M.F. and Parks, G.A., 1989, Sample preparation and aging effects on the dissolution rate and surface-composition of diopside. Geochimica Et Cosmochimica Acta, 53(4), 797-804.

Giammar, D.E., Bruant, J.R.G. and Peters, C.A., 2005, Forsterite dissolution and magnesite precipitation at conditions relevant for deep saline aquifer storage and sequestration of carbon dioxide. Chemical Geology, 217(3-4), 257-276.

Haug, T.A., Kleiv, R.A. and Munz, I.A., 2009, Dissolution of mechanically activated olivine in hydrochloric acid - investigating leaching properties for carbonation purposes (in review). Journal of Applied Geochemistry.

Huijgen, W.J.J., Witkamp, G.J. and Comans, R.N.J., 2005, Mineral CO_2 sequestration by steel slag carbonation. Environmental Science & Technology, 39(24), 9676-9682.

Huijgen, W.J.J., Witkamp, G.J. and Comans, R.N.J., 2006, Mechanisms of aqueous wollastonite carbonation as a possible CO_2 sequestration process. Chemical Engineering Science, 61(13), 4242-4251.

Hänchen, M., Prigiobbe, V., Baciocchi, R. and Mazzotti, M., 2008, Precipitation in the Mg-carbonate system - effects of temperature and CO_2 pressure. Chemical Engineering Science, 63(4), 1012-1028.

Hänchen, M., Prigiobbe, V., Storti, G., Seward, T.M. and Mazzotti, M., 2006, Dissolution kinetics of forsteritic olivine at 90-150 degrees C including effects of the presence of CO_2. Geochimica Et Cosmochimica Acta, 70(17), 4403-4416.

Kalinkin, A.M., Boldyrev, V.V., Politov, A.A., Kalinkina, E.V., Makarov, V.N. and Kalinnikov, V.T., 2003, Investigation into the mechanism of interaction of calcium and magnesium silicates with carbon dioxide in the course of mechanical activation. Glass Physics and Chemistry, 29(4), 410-414.

Kleiv, R.A. and Thornhill, M., 2006, Mechanical activation of olivine. Minerals Engineering, 19(4), 340-347.

Kojima, T., Nagamine, A., Ueno, N. and Uemiya, S., 1997, Absorption and fixation of carbon dioxide by rock weathering. Energy Conversion and Management, 38(Supplement 1), 461-466.

Lackner, K.S., Wendt, C.H., Butt, D.P., Joyce, J.E.L. and Sharp, D.H., 1995, Carbon dioxide disposal in carbonate minerals. Energy, 20(11), 1153-1170.

Lichtner, P.C., Carey, J.W., O'Connor, W.K., Dahlin, D.C. and Guthrie, G.D.J., 2003, Geochemical mechanisms and models of olivine carbonation. In *Proc. In Proceedings of the 28th International Technical Conference on Coal Utilization & Fuel Systems, March 9-13, 2003*

Luce, R.W., Bartlett, R.W. and Parks, G.A., 1972, Dissolution kinetics of magnesium silicates. Geochimica Et Cosmochimica Acta, 36(1), 35-50.

Maroto-Valer, M.M., Fauth, D.J., Kuchta, M.E., Zhang, Y. and Andresen, J.M., 2005, Activation of magnesium rich minerals as carbonation feedstock materials for CO_2 sequestration. Fuel Processing Technology, 86(14-15), 1627-1645.

McKelvy, M.J., Chizmeshya, A.V.G., Diefenbacher, J., Bearat, H. and Wolf, G., 2004, Exploration of the role of heat activation in enhancing serpentine carbon sequestration reactions. Environmental Science & Technology, 38(24), 6897-6903.

O'Connor, W.K., Dahlin, C.L., Turner, P.C. and Walters, R., 1999, Carbon dioxide sequestration by ex-situ mineral carbonation. (DOE/ARC-99-009), Albany Research Center, Albany, Oregon, 14.

O'Connor, W.K., Dahlin, D.C., Rush, G.E., Dahlin, C.L. and Collins, W.K., 2002, Carbon dioxide sequestration by direct mineral carbonation: process mineralogy of feed and products. Minerals & Metallurgical Processing, 19(2), 95-101.

Park, A.H.A. and Fan, L.S., 2004, CO_2 mineral sequestration: physically activated dissolution of serpentine and pH swing process. Chemical Engineering Science, 59(22-23), 5241-5247.

Parkhurst, D.L. and Appelo, C.A.J., 1999, User's guide to PHREEQC (Version2)—A computer program for speciation, batch-reaction, one-dimensional transport, and inverse geochemical calculations. (99-4259), U.S. Geological Survey Water-Resources Investigations, 310.

Pokrovsky, O.S. and Schott, J., 2000, Kinetics and mechanism of forsterite dissolution at 25 degrees C and pH from 1 to 12. Geochimica Et Cosmochimica Acta, 64(19), 3313-3325.

Pourghahramani, P. and Forssberg, E., 2006, Microstructure characterization of mechanically activated hematite using XRD line

broadening. International Journal of Mineral Processing, 79(2), 106-119.

Rosso, J.J. and Rimstidt, J.D., 2000, A high resolution study of forsterite dissolution rates. Geochimica Et Cosmochimica Acta, 64(5), 797-811.

Sangwal, K.K., 1982, Dissolution kinetics of MgO crystals in aqueous acidic salt solutions [dislocation etching]. Journal of Materials Science, 17(12), 3598-3610.

Seifritz, W., 1990, CO_2 disposal by means of silicates. Nature, 345(6275), 486.

Summers, C.A., Dahlin, D.C., Rush, G.E., O'Connor, W.K. and Gerdemann, S.J., 2005, Grinding methods to enhance the reactivity of olivine. Minerals & Metallurgical Processing, 22(3), 140-144.

Teir, S., Eloneva, S. and Zevenhoven, R., 2005, Production of precipitated calcium carbonate from calcium silicates and carbon dioxide. Energy Conversion and Management, 46(18-19), 2954-2979.

Tkáčová, K., 1989, *Mechanical Activation of Minerals*. Elsevier Science Publishers, Amsterdam.

Tromans, D. and Meech, J.A., 2001, Enhanced dissolution of minerals: Stored energy, amorphism and mechanical activation. Minerals Engineering, 14(11), 1359-1377.

Westrich, H.R., Cygan, R.T., Casey, W.H., Zemitis, C. and Arnold, G.W., 1993, The Dissolution Kinetics of Mixed-Cation Orthosilicate Minerals. American Journal of Science, 293(9), 869-893.

Wolf, G.H., Chizmeshya, A.V.G., Diefenbacher, J. and McKelvy, M.J., 2004, In situ observation of CO_2 sequestration reactions using a novel microreaction system. Environmental Science & Technology, 38(3), 932-936.

Paper IV

The importance of grinding solutions for mineral carbonation concepts

Tove Anette Haug[a]
Rolf Arne Kleiv[a]
Ingrid Anne Munz[b]

[a] Department of Geology and Mineral Resources, Norwegian University of Science and Technology, Sem Saelandsvei 1, 7491 Trondheim, Norway
[b] Institute for Energy Technology, P.O. Box 40, 2027 Kjeller, Norway

ABSTRACT

Olivine was milled in a ball mill, a Hicom mill, an attritor and a planetary mill, with the purpose of obtaining indications of whether or not these mills can be a part of a large scale mineral carbonation plant. Dissolution of the milled olivine samples was performed at room temperature and pressure in 0.01 M HCl, and carbonation was performed at 185 °C and 115 bar of partial CO_2 pressure. Wet milling in ball mills are probably most suited for direct carbonation since the additional energy consumption of high intensity mills were not reflected in the carbonation results at the given conditions. If it is possible to divide the carbonation reaction into dissolution with precipitation as a subsequent step, there are indications of attritors or Hicom mills to be both large enough and obtain sufficient increase in the dissolution rate of olivine if further optimization can be performed. Planetary mills are most likely to energy consuming for the purpose of CO_2 storage regardless of reaction route.

1 INTRODUCTION

Global warming concerns have resulted in large scale research focusing on CO_2 capture and storage. Mineral carbonation as one possible alternative for CO_2 storage, has been proposed by several researchers including Seifritz

(1990) and Lackner *et al.* (1995). A range of minerals, with a focus on silicates, containing Ca, Mg and Fe have been considered as feedstock because these elements form stable carbonates (Kojima *et al.*, 1997, McKelvy *et al.*, 2004, O'Connor *et al.*, 1999, Teir *et al.*, 2005). One out of several promising minerals is olivine, and the aqueous carbonation of olivine can be described by the following set of reactions. First CO_2 is dissolved in water resulting in carbonic acid, including the species formed due to dissociation, see Eq. 1. The second reaction is dissolution of olivine with acid, from the dissolution of CO_2 in water, as described in Eq. 2. The precipitation step consists of two independent reactions, i.e. precipitation of carbonate and silica (Eq. 3 and Eq. 4).

$$CO_{2(g)} + H_2O \leftrightarrow H_2CO_3 \leftrightarrow H^+ + HCO_3^- \leftrightarrow 2H^+ + CO_3^{2-} \quad (1)$$

$$Mg_2SiO_{4(s)} + 4H^+ \leftrightarrow 2Mg^{2+} + H_4SiO_2 \quad (2)$$

$$Mg^{2+} + CO_3^{2-} \leftrightarrow MgCO_{3(s)} \quad (3)$$

$$H_4SiO_4 \leftrightarrow SiO_{2(s)} + 2H_2O \quad (4)$$

Ex-situ mineral carbonation will be performed in an industrial plant, in contrast to in-situ carbonation where CO_2 is injected into geological formations. The most promising options for ex-situ mineral carbonation today are direct aqueous carbonation or indirect aqueous carbonation (Sipilä *et al.*, 2008). Direct carbonation is optimized in one process step for simultaneous dissolution and precipitation (e.g. Huijgen *et al.*, 2007, O'Connor *et al.*, 1999). Olivine carbonation has been studied up to 185 °C and CO_2 pressures of 135 bar in the laboratory (e.g. Bearat *et al.*, 2006, Giammar *et al.*, 2005, O'Connor *et al.*, 2002). The second alternative, indirect carbonation consists normally of two or more process steps. The feedstock minerals are dissolved in acids/bases and CO_2 is used in reaction with the solution in a subsequent process step (e.g. Druckenmiller and Maroto-Valer, 2005, Maroto-Valer *et al.*, 2005, Park and Fan, 2004).

Indirect carbonation introduces the possibility of optimize the dissolution and precipitation separately, but will probably need higher investments, maintenance and operational costs compared to direct carbonation. Another important difference between direct and indirect carbonation is the solubility considerations. For direct carbonation, saturation is required to initiate and sustain precipitation, while indirect

carbonation is dependent of avoiding precipitation until subsequent precipitation step(s) is reached.

In general, regardless of the choice of carbonation route, liners and grinding media are consumed by the comminution process and require substantial energy to mine, refine and to manufacture (Musa and Morrison, 2009) and has to be taken into account for the overall process costing for a full scale carbonation plant. The energy consumption of carbonation processes and costs have been studied for several minerals and industrial waste materials as steel slag (e.g. Gerdemann *et al.*, 2007, Huijgen *et al.*, 2007, Huijgen *et al.*, 2006, Huijgen *et al.*, 2005, O'Connor *et al.*, 2004, O'Connor *et al.*, 2005, Stolaroff *et al.*, 2005).

The slow carbonation rate is a main problem with ex-situ mineral carbonation. An increase in the reaction rate is normally followed by an increase in energy consumption, which has a negative contribution to CO_2 storage if the energy comes from fossil fuels. Several methods have been investigated to increase the total carbonation reaction and at the same time minimize the energy consumption. These methods include heat activation, grinding, additives in the reaction fluid and elevated process temperature and pressure (e.g. Maroto-Valer *et al.*, 2005, McKelvy *et al.*, 2004, O'Connor *et al.*, 2002, Summers *et al.*, 2005). Every mineral carbonation process will to a certain extent involve milling to obtain a given particle size distribution or specific surface area (SSA) of the material, and there may be process benefits of exploring the milling step.

Energy intensive milling, also called mechanical activation, changes the character of the material beyond reduced particle size and increased surface area (Tkáčová, 1989). Experiments have shown that mechanical activation results in decreased crystallinity (Baláž, 2000, Kalinkin *et al.*, 2003, Kleiv and Thornhill, 2006, Pourghahramani and Forssberg, 2006, Tromans and Meech, 2001). The observed changes in the material properties resulting from mechanical activation have been found to be very important for dissolution properties of minerals (Eggleston *et al.*, 1989, Haug *et al.*, 2009b, Sangwal, 1982). Haug *et al.* (2009b) showed how mechanical activation of olivine resulted in an increased rate constant, k, without direct correlation to particle size and only partially related to the specific surface area. Crystallinity was found to be the most important material property

relevant for dissolution of olivine milled in a planetary mill. The best results were obtained for dry milling which resulted in a three orders of magnitude higher rate constant compared to the rate constant of the unactivated sample in the same experiment. However, extensive direct carbonation, approaching 100 % conversion, of the same materials presented in Haug *et al.* (2009b) was found to be less dependent of mechanical activation (Haug *et al.*, 2009a). The results from these two papers resulted in the idea of looking into the choice of mills and grinding solution by comparing traditional low-intensity conventional milling with high-intensity milling. Some carbonation experiments have indicated that intensive milling might be too energy consuming (Summers *et al.*, 2005) compared to the increase in carbonation obtained. Opposing results were presented in Haug *et al.* (2009b) were significant increase in dissolution rate was obtained by changing milling parameters, indicating the relevancy of grinding solutions.

The aim of this study is to compare a conventional ball mill with three mills of higher milling intensity producing olivine samples with varying material characteristics, and try to indicate the potential of these mills within industrial mineral carbonation as CO_2 sequestration. The main focus is not to suggest the optimum milling conditions for each mill, but to illustrate the differences in dissolution and carbonation that can be obtained by varying the grinding solutions. Energy considerations are included to describe the energy consumption of each mill and compare this consumption to the maximum energy consumption available for a grinding/carbonation process used for CO_2 storage. Using data for maximum mill sizes and mass flow possibilities for these four mills, indications are also made of the possibilities of using these mills in an actual process. Energy calculations regarding the carbonation reactions are excluded beyond the results of selected relevant literature.

2 GRINDING ENERGY

There are several central parameters that can be used when trying to describe the mill power draw [kW] and energy consumption [kWh]. The operational power, P_o, is the average of the total power drawn from the power grid by the mill during operation. The net power, P_N, is the power transferred to the charge of the mill. The difference between P_o and P_N is

the power loss caused by friction in the mill motor and in the transmission from the motor to the mill, and the power used to move the mill chamber. The net specific energy consumption, W_N, can be used to compare how efficient the energy changes the material properties or carbonation results from different mills or milling conditions, while a cost evaluation will need to consider the total specific energy consumption, W_o, together with the experimental results. The total specific power, also referred to as the mill intensity I, is calculated using Eq. 5 where m_o is the mass of a sample milled. The total specific energy consumption, or milling work, W_o is calculated with Eq. 6 where t is the milling duration. Substitution of P_o with P_N yields the net specific energy consumption, W_N.

$$I = \frac{P_o}{m_o} \tag{5}$$

$$W_o = \frac{P_o}{m_o} \cdot t \tag{6}$$

$$W_N = 10 \cdot W_i \left(\frac{1}{\sqrt{\mathrm{d}_{80,\mathrm{product}}}} - \frac{1}{\sqrt{\mathrm{d}_{80,\mathrm{feed}}}} \right) \tag{7}$$

$$\text{Energetic efficiency} = \frac{W_N}{W_o} \cdot 100\% \tag{8}$$

W_N of milling in a large scale tumbling ball mill can be estimated by Bond's work index formula using Eq. 7. Here $\mathrm{d}_{80,\mathrm{product}}$ and $\mathrm{d}_{80,\mathrm{feed}}$ are the respective particle sizes corresponding to 80 wt% of the samples passing through a sieve of the given size of the product and feed materials, whereas W_i is a material constant known as Bond's work index. Bond's work index W_i is found through a standardized laboratory test (Bond, 1961a, Bond, 1961b) and is defined to be the net specific energy needed to grind a rock from an assumed infinite size to $\mathrm{d}_{80,\ \mathrm{product}}$ = 100 µm in a ball mill. W_i = 19.6 kWh/ton was found for the original olivine sand. Energetic efficiency is defined in Eq. 8 (Kheifets and Lin, 1996) and is of approximately 90 % (Kheifets and Lin, 1996) to 95 % (Musa and Morrison, 2009) for large scale ball mills, while for planetary mills the rule is 60 % - 70 % (Kheifets and Lin, 1996). Pilot scale mills or laboratory mills have lower energetic efficiencies than large scale mills.

In a mineral carbonation plant the total specific energy consumption W_o, for the milling step can be compared to the total specific energy consumption required during the carbonation step E_c. E_c is here defined to be the energy consumed pr ton of feedstock olivine obtaining a 100 % conversion. W_o and E_C will vary for different combinations of mills, the conversion degree and process conditions and these two processes must be evaluated together. The sum of W_o and E_C illustrates the total energy consumption pr ton of olivine carbonated excluding the mining and transport energy requirements. If the total conversion is held constant, then the total energy requirements of the carbonation process can be assumed to be lowered when milling increases the reactivity. The milling energy input needed to increase the olivine reactivity increases in general with prolonged milling. The highest return on the milling energy input, in terms of increased reactivity, is probably obtained in the initial phase of the milling process.

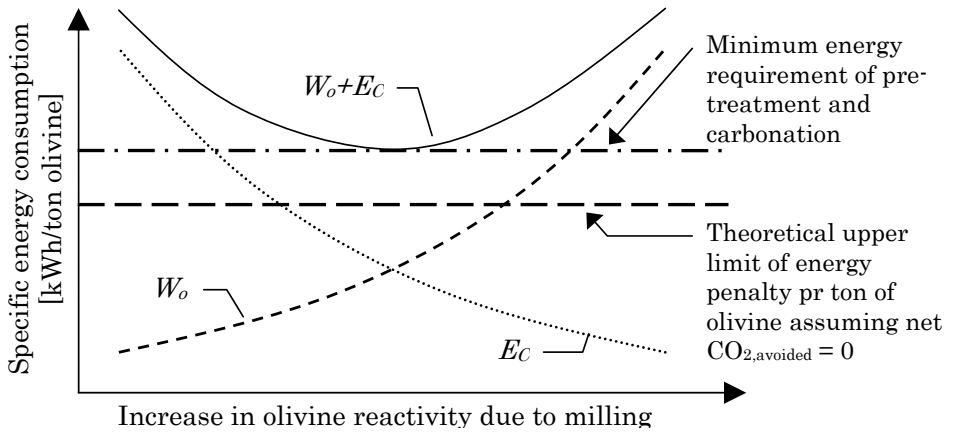

Figure 1 Illustration of how specific energy consumption during milling and specific energy consumption during carbonation can be evaluated together by assuming constant conversion of the feedstock mineral. W_0 is specific milling energy, E_c is the specific energy consumption of the carbonation process after the milling step normalized to the weight of olivine put into the process. $W_0 + E_c$ indicates the total energy consumption needed after the CO_2 has been captured and transported to the processing site. Minimum energy requirement is indicated above the theoretical upper limit because most processes today are energy consuming.

Figure 1 illustrates theoretically how milling energy can be compared to carbonation energy. The x-axis in Figure 1 represents the increase in

olivine reactivity as a consequence of increased total specific milling energy. For extensive milling to be a realistic pre-treatment option in mineral carbonation, the additional CO_2 emitted because of increased energy consumption during milling and carbonation, cannot exceed the amount of CO_2 stored. To obtain a commercially interesting milling and carbonation process, the optimized milling energy requirement given in Figure 1 has to result in a lower CO_2 emission than the amount of CO_2 bound in the process. Which is just the opposite of what Figure 1 is showing. The minimum of $W_o + E_C$ represents the optimum grinding solution if grinding is the only pre-treatment method. Measurements of energy consumption during milling, dissolution and carbonation experiments of the milled samples were performed with the purpose of evaluating the grinding solutions in the context of mineral carbonation.

3 EXPERIMENTAL

3.1 Material description

Table 1 XRF analysis results for the original olivine sample and olivine reference sample given in wt% of main elements (left) and ppm of trace elements (right).

Component	Original sample [wt%]	Reference sample [wt%]	Component	Original sample [ppm]	Reference sample [ppm]
Fe2O3	7.13	7.54	Zr	15	12
TiO2	0.01	0.03	Y	2	1
CaO	-[a]	0.4	Sr	39	6
K2O	0.01	0.06	Rb	2	1
P2O5)	0.01	0.01	Zn	46	42
SiO2	41.64	42.29	Cu	10	2
Al2O3	-[a]	-[a]	Ni	3351	3593
MgO	50.62	48.39	Ba	31	-[a]
Na2O	-[a]	-[a]	Co	121.8	126.1
MnO	0.1	0.1	Cr	3005	1815.9
SUM	99.52	98.82	V	35.1	21.7
LOI	0.34	0.41	Th	1.4	1.8
			Pb	27.6	3

[a] Below detection limit

The material used in this study consisted of olivine foundry sand of the quality ASF50 provided by North Cape Minerals from their dunite deposit at Åheim in Western Norway. The AFS50 sand will be referred to as the original sample. X-ray diffraction analysis (XRD) detected forsterite, chlorite, enstatite, chromite and traces of hornblende and mica, and approximately 95 % by weight is pure olivine of the composition $Mg_{1.86}Fe_{0.14}SiO_4$ (Osland, 1998). Another product from the same deposit, referred to as AFS80, was used to prepare a reference sample for the dissolution experiments. AFS80 had for all practical purposes, the same composition as AFS50, but the particle size of AFS80 was closer to the desired particle size distribution for dissolution. The AFS80 sand was sieved dry to retrieve the 74 – 147 μm fraction. This fraction was washed with ethanol to remove fines. Main elements and trace elements of the original sample and the reference sample, as found by X-ray fluorescence (XRF) are presented in Table 1. The original sample and the reference sample had specific surface areas of 0.47 m^2/g and 0.93 m^2/g respectively, found by BET analyses.

3.2 Milling

Table 2 Summary of mill choices for selected combinations of mill Intensity, mechanical activation and high specific surface area (SSA).

	Low intensity Laboratory scale	**High intensity Laboratory scale**	**High intensity Pilot scale**
Mechanical activation	Dry Ball mill	Dry planetary mill	Dry Hicom mill
High SSA	Wet Ball mill	Wet planetary mill	Wet Attritor

Table 2 shows the chosen mills in this study sorted by mill scale, mill intensity and the desired material properties tried to obtain from each mill. A laboratory ball mill (B) was run wet to obtain a sample close to

conventional milled olivine. To evaluate the potential for inducing structural changes in olivine at low milling intensity, dry milling was performed in a laboratory ball mill. To obtain maximum intensity a Fritsch Pulverisette 6 planetary mono mill (P) was operated in both wet and dry mode. Wet milling in a Szegvari Attritor (A) stirred ball mill of the type 1SDG was performed to maximize the specific surface area, and dry milling was performed in a pilot scale Hicom 15 nutating batch mill (H) to obtain decreased crystallinity and mechanical activation. The diameter of the planetary mill chamber was 75 mm with a volume of 0.25 L and 238 mm for the ball mill with a volume of 4.2 L. The letters in parentheses are abbreviations for each mill used in the sample names.

Table 3 Description of the milling parameters implemented in this study, including the weights and sized of the steel balls used in each mill.

Material name	Mill	RPM	Milling time [min]	Water addition [ml]	Mass olivine [g]	Part 1 Steel balls [mm]	[g]	Part 2 Steel balls [mm]	[g]
A10minWet	Attritor	350	10	1200	800	6	16000	0	0
A60minWet	Attritor	350	60	1200	800	6	16000	0	0
B2hDry	Ball mill	75	120	0	750	19.1	250	9.5	750
B8hDry	Ball mill	75	480	0	750	19.1	250	9.5	750
B2hWet	Ball mill	75	120	1200	750	19.1	250	9.5	750
B8hWet	Ball mill	75	495	1200	750	19.1	250	9.5	750
H1minDry	Hicom	900	1	0	1000	9	2011	5	10000
H5minDry	Hicom	900	5	0	1000	9	2011	5	10000
P10minDry	Planetary	500	10	0	20	10	640	0	0
P60minDry	Planetary	500	60	0	20	10	640	0	0
P10minWet	Planetary	500	10	100	20	10	640	0	0
P60minWet	Planetary	500	60	100	20	10	640	0	0

Milling was performed in air at room temperature and no measured were performed to avoid heat to be developed during milling. The chambers and steel balls used in the planetary mill and the ball mill, together with the steel balls for the Hicom mill, was washed with water and dried with ethanol to minimize the risk of cross contamination between the samples. Pressurized air and a heating cabinet were used to remove residual moisture. The Hicom mill was initially run with 1 kg of original sample and

the washed steel balls to remove any other residual material inside the milling chamber from previously run batches. The attritor was rinsed with water with a volume approximately 3 - 4 times the volume of the chamber by filling the chamber several times, rotating the stirrer for some seconds, and then letting the water out through a valve at the bottom. The cleansing procedure was finished when the water was sufficiently clear, and the procedure was repeated after each batch in the attritor. Table 3 gives a summary of the samples and the milling parameters used. The steel ball charges used in the ball mill and the Hicom mill were composed of two steel ball sizes. The steel balls in part 1 is larger than the steel balls in part 2. Size and mass of each part is given in mm and g.

3.3 Dissolution experiments

Two series of the dissolution experiments with different liquid/solid ratios were carried out, see Table 4 for experimental details.

Table 4 Specific data for the two dissolution experiments marked with a D, and the carbonation experiment is marked with C. Experiment numbers referrer to the numbering used in the paper discussing dissolution (Haug *et al.*, 2009b) and carbonation (Haug *et al.*, 2009a).

Exp. type	Number of valid exp.	Volume	Olivine [g]	[°C]	[bar]	Duration [h]	Stirring
D-1	16	500ml HCl 0.01M	0.5	21.5	1 air	1-24	500 [RPM]
D-3	10	500ml HCl 0.01M	2.0	21.5	1 air	1-24	500 [RPM]
C-2	23	50 ml DI H_2O	7.5	185	115 CO_2	2/18	Yes

The experiments were performed by pouring the defined amount of olivine into a glass beaker containing 500 ml of 0.01 M HCl. A magnetic stirrer was used to disperse the olivine sample and to avoid sedimentation throughout each experiment. The experiments were performed at 21.5 ± 1.3 °C and 1 atm in contact with air. pH was logged automatically at suitable intervals using a Metrohm lab 827 pH-meter equipped with a Metrohm solitrode PT1000 electrode. The duration of the dissolution experiments varied between 1 h to 24 h. The experiments were terminated at a pH higher than

3.0 or at 24 h if the pH never reached 3. 20 ml water samples were taken from the suspensions at the end of each experiment using a disposable syringe. The samples were then filtered using a 0.45 μm filter and transferred to glass vials without being acidified.

3.4 Direct carbonation experiments

The milled olivine samples were carbonated in batch experiments; see Table 4 for experimental details. C-2 will be used as an abbreviation for the performed carbonation experiment. Four 60 ml autoclaves were operated simultaneously including automatic logging of temperature and pressure inside each autoclave. Magnetic stirrers were used to keep the inserted sample and the precipitated reaction products in suspension. When the temperature was less than 3 °C away from the chosen experimental temperature, which occurred after approximately 25 min of heating, then the autoclaves were pressurized carefully with CO_2. Pressure was maintained with a Teledyne Isco pump. Experimental duration was measured from the point in time were heat and pressure both had been applied. At the end of an experiment the heating and pressure were turned of, and after cooling down to approximately 50 °C, the system and autoclaves were depressurized. pH was measured in the opened autoclaves directly after dismantling when the immediate CO_2 release from the fluid had stopped.

A total of 15 ml of suspension was taken from each autoclave with a disposable syringe and then filtered through a 45 μm filter into polyethylene bottles with airtight caps. The samples were not acidified. The suspension remaining in the autoclave and settled solid material were filtered with a vacuum pump and the solid products were dried in air over night. To dissolve any residual precipitate inside the autoclaves, diluted HCl was added if necessary for several hours before final cleaning with a brush and water.

3.5 Analyses

The specific surface areas were measured using the BET method with N_2 adsorption using a Flowsorb II 2300 from Micromeritics with a degasser unit. Water analyses were performed on the filtrated water samples using ICP-MS. Both the BET and ICP-MS analysis were performed at Sintef in

Trondheim, Norway. X-ray diffraction analyses (XRD) of the mechanically activate samples and the original sample were performed using a Philips PW1710 X-ray diffractometer, equipped with a Cu-anode operated at 40 kV and 20 mA. The samples where scanned continuously using a step size of 0.04° (2theta) with 2 seconds per step from 2 - 60°. For the reaction residues from selected C-2 experiments a Bruker-axs D8 Advance X-ray diffractometer was used with a Cu Kα anode operated at 40 kV and 40 mA. Step size was 0.02° (2 theta) with 0.5 seconds per step. The element analyses were obtained through X-ray fluorescence analysis (XRF) using a Philips 1480 X-ray spectrometer for all analysed samples, except for the carbonated residues where the equipment BRUKER S8 Tiger XRF was used with a 4 kW generator. The XRD and XRF analysis were performed at Department of Geology and Mineral Resources Engineering, Norwegian University of Science and Technology, Trondheim. Analysis of total carbon content (TC) for the residuals from the C-2 experiment were analyzed with a LECO SC632 instrument at Applied Petroleum Technology AS, Kjeller, Norway.

4 RESULTS

4.1 Characteristics of the mill products

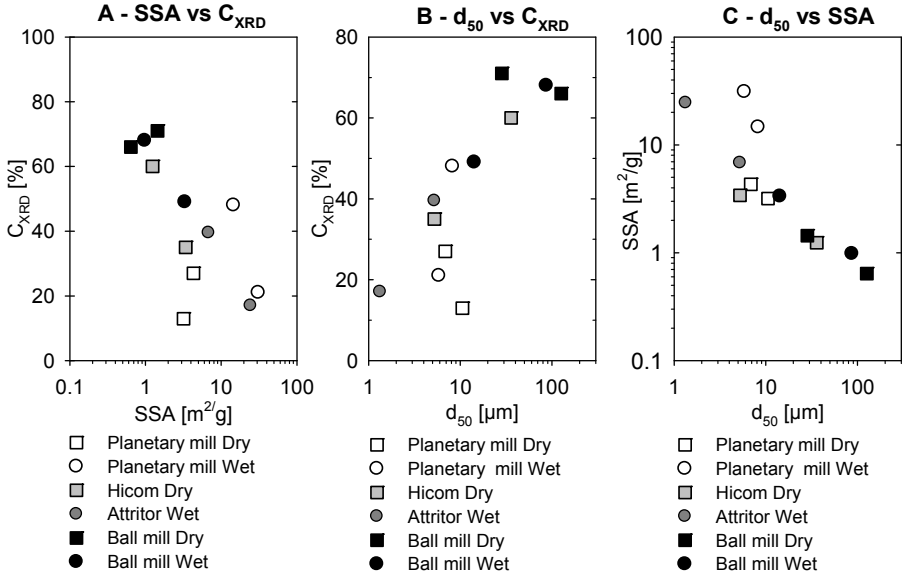

Figure 2 Plots of the relationship between SSA, C_{XRD} and d_{50}

The attritor produced the smallest particles, while the largest particles were produced by the ball mill. In general wet milling and prolonged grinding created the finest materials until aggregates were formed. Aggregates were found for the P60minDry sample consisting of coarser particles than the P10minDry sample. Figure 2 presents three plots of the correlation between the three measured material properties specific surface area, crystallinity calculated from XRD, and d_{50} represents the average particle size. The measured specific surface area (SSA), particle sizes and contamination of each milled sample is summarized in Table 5 together with references to the experiments in which they were used.

Table 5 Description the measured specific surface area (SSA), particle sizes (d_{10}, d_{50} and d_{80}) and crystallinity (C_{XRD}) together with the percentage of steel contamination of samples with a reference to the experiments in which they were used.

Material name	SSA [m^2/g]	$d_{10}/d_{50}/d_{80}$ [µm]	Contamination [wt%][a]	C_{XRD} [%][b]	D-1	D-3	C-2
Original sample	0.47	197.2/311.9/399.8	0	100	No	No	No
Ref. sample	0.93	96.8/162.9/210.5	0	57	Yes	No	No
A10minWet	6.81	0.83/5.34/13.92	2.4	40	No	Yes	Yes
A60minWet	24.5	0.30/1.34/3.01	6.8	17	No	Yes	Yes
B2hDry	0.64	9.34/126.7/224.2	1.1	66	Yes	Yes	No
B8hDry	1.44	2.14/28.43/72.32	1.5	71	Yes	Yes	Yes
B2hWet	0.98	11.6/87.1/152.8	1.6	68	No	Yes	No
B8hWet	3.33	2.20/14.31/31.82	3.5	49	No	Yes	Yes
H1minDry	1.24	2.52/36.02/92.17	1.3	60	Yes	Yes	No
H5minDry	3.4	0.30/5.22/23.91	1.3	35	Yes	Yes	Yes
P10minDry	4.31	0.54/6.87/40.99	1.3	27	Yes	No	Yes
P60minDry	3.19	0.72/10.55/48.17	3.1	13	Yes	Yes	Yes
P10minWet	14.6	1.15/8.29/24.24	4.6	48	Yes	No	Yes
P60minWet	31.0	1.02/5.88/17.54	16.7	21	Yes	Yes	Yes

[a] Estimated from ball wear measurements, ICP-MS analyses and XRF analyses.
[b] Crystallinity calculations and discussion of the materials from the planetary mill are presented in (Haug *et al.*, 2009b).

When comparing wet milled and dry milled samples with the same crystallinity, the wet milled materials displayed a much larger specific surface area, as shown in Figure 2A. Crystallinity seemed to increase with increasing average particle size, d_{50}, in Figure 2B, even though the samples

milled dry in the planetary mill and the samples milled dry in the ball mill are deviating from the shown tendency. Figure 2C shows how d_{50} decreases with increasing SSA with two exceptions. The wet milled samples from the planetary mill had larger SSA than the other samples with the same particle sizes and the H5minDry sample had a low SSA compared to the rest of the samples. In addition the wet milled samples might have had slightly higher specific surface areas than the dry milled samples when compared to d_{50}.

4.2 Energy consumption

An estimate of the total large scale energy consumption $W_{o(L)}$ can be calculated if W_o is found from a laboratory mill and used together with the energetic efficiency of the large scale mill and the net energy consumption W_N from the laboratory experiment as shown in Eq. 9. For all four mills, the power draw was measured with and without mill charge to estimate the total and net mill power applied to the samples using Eqs. 5 through 9. The results from the power and energy calculations are presented in Table 6. Figure 3 illustrates how the parameters given in Table 6 are related.

$$W_{o(L)} = \frac{W_N}{\text{Energetic efficiency large mill}/100\%} \tag{9}$$

Total energy consumption of the milled samples was estimated in two steps. The first step is common for all, and represents the energy required to produce the AFS50 sand. This total energy consumption was estimated from Bond's Work Index, W_i = 19.6 kWh/ton for AFS50 sand, and Eq. 7, resulting in 11 kWh/ton including an estimated energetic efficiency of 90 % for ball mills. This is a rough estimate because the AFS50 sand was produced by crushing and not by milling in a ball mill. The second energy consumption step represents further milling and activation, and depends on the choice of mill and milling parameters. W_o represents the total energy consumption measured for the mills in use, and $W_{o(L)}$ calculated from Eq. 9 represents an estimate for the total large scale energy consumption if these mills were used in an industrial process.

Table 6 Summary of the power draw of the mill and energy consumption. Total values and net values are included together with values normalized to the sample weights.

Sample	Operational (total) power [W], P_o	Net power [W], P_N	Total intensity [kW/ton], I	Net intensity [kW/ton], I_N	Total specific energy [kWh/ton][a], W_o	Net specific energy [kWh/ton], W_N	Energetic efficiency [%]	Large scale total specific energy, [kWh/ton], $W_{o\infty}$
Original sample					11	10		11
Ref. sample					15	14		15
A10minWet	1661	712	2076	890	356	158	44.4	226
A60minWet	1696	747	2120	934	2131	944	44.3	1348
B2hDry	163	12	217	16	474	71	14.9	78
B8hDry	163	12	217	16	1778	167	9.4	185
B2hWet	159	8	211	10	435	32	7.4	36
B8hWet	159	8	211	10	1703	92	5.4	102
H1minDry	3754	2337	3754	2337	71	49	68.6	70
H5minDry	3547	2130	3547	2130	306	194	63.4	277
P10minDry	287	106	14349	5320	2402	896	37.3	1379
P60minDry	269	88	13451	4422	13461	4431	32.9	6817
P10minWet	287	106	14349	5320	2402	896	37.3	1379
P60minWet	269	88	13451	4422	13461	4431	32.9	6817

[a] Includes the estimated energy required to produce the original sample

Large scale energetic efficiencies can be assumed to be 90 % for a ball mill (Kheifets and Lin, 1996, Musa and Morrison, 2009) and is estimated to be 65 % for a planetary mill (Kheifets and Lin, 1996), even though large scale planetary mills are not used commercially to the best knowledge of the authors. The energetic efficiency decreases with intensity (Kheifets and Lin, 1996) due to high frictional forces in the bearings and gears, generating a great deal of heat (Cho *et al.*, 2006). The attritor and the Hicom mill were assumed to have energetic efficiencies of approximately 70 %, just above the planetary mill, but significantly lower than the ball mill due to the differences in intensity. The 69 % energetic efficiency of the Hicom mill obtained in this study was within the range of the efficiency values excepted

for large scale Hicom mills. The measured energetic efficiency was 44 % for the attritor; hence, it was less efficient than large scale attritors. These two mills are pilot scale mills and hence more energetic efficient than the laboratory mills. The laboratory ball mill and the laboratory planetary mill only had respective energetic efficiencies of 10 % and 35 %.

The ball mill had the lowest energy intensity with approximately 13 kW/ton, the attritor had an intensity of 1000 kW/ton, the Hicom mill approximately 2000 kW/ton and the planetary mill had 5000 kW/ton. The mill intensities were reflected in the net specific energy consumption, ranging from 30 kWh/ton for the B2hWet sample to 4400 kWh/ton for the P60minDry and P60minWet samples.

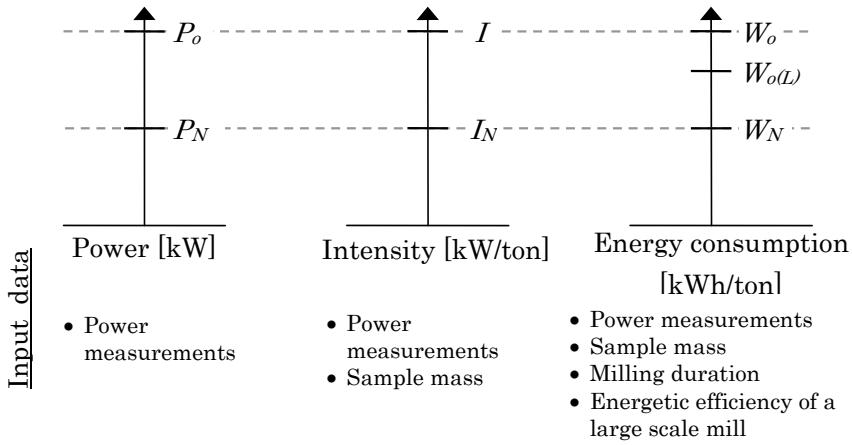

Figure 3 Relationships between power, intensity and energy parameters

4.3 Dissolution in 0.01 M HCl

The dissolution calculations are based on a linear correlation between olivine consumption and change in H^+-concentration as calculated from the pH measurements below pH = 3 using Eq. 2. The calculations of percent dissolved are described in detail by Haug *et al.* (2009b). A misleading upper limit of dissolved olivine was found when pH increases above 3 due to the influence of other reactions than Eq. 2. The value of this limit in percentage of dissolved olivine is reflected in the corresponding rate constants and is determined by the acid/olivine ratio defined in Eq. 10 where n_{HCL} [mmol] and $m_{olivine}$ [g].

$$\text{acid/olivine ratio} = \frac{n_{HCL}}{m_{olivine}} \quad (10)$$

This ratio is 10 in the D-1 experiments and an upper dissolution limit of 35 – 47 % of dissolved olivine was found, while the D-3 experiments had a ratio of 2.5 and a calculated upper dissolution limit of 8 – 10 %. The time to reach a dissolution degree of 5 % (T_5), 10 % (T_{10}), 20 % (T_{20}) and 30 % (T_{30}) were estimated to compare the difference in dissolution behaviour of the milled samples. Only T_5 were calculated for the D-3 experiments since the upper limit of calculation of olivine dissolution was 8 – 10 % in these experiments. Three samples did not reach 5 % dissolution within the experimental durations, but T_5 were estimated for the B2hDry sample and the B2hWet sample by extrapolation of the measured dissolution versus time curves. The reference sample reacted so slowly making extrapolation practically impossible. T_{10}, T_{20} and T_{30}, were found for the D-1 experiments where the dissolution had reached the respective levels within 24 h.

Table 7 presents a summary of all T values. Ball milling gave the highest T_5 values ranging from approximately 5 h for the samples milled 8 h to an estimate of 30 – 50 h for the samples milled for 2 h. For ball milling, the addition of water enhanced the dissolution properties, but for the planetary mill, addition of water gave a decrease in dissolution. T_5 decreased without exception with increasing milling time, for otherwise constant milling conditions. For the energy-intensive mills, T_5 ranged from approximately 13 s for the best result of the P60minDry sample to 3 h for the H1minDry sample, and all of them were below 40 min except for the H1minDry and the A10minWet sample.

The range of obtained T values at different dissolution degrees indicated that the samples can be divided into four groups. The P60minDry sample was the fastest dissolving sample with 30 % dissolved within 15 min. The second group was the P60minWet and P10minDry samples using approximately 4 h to obtain 30 % dissolution. A60minWet is probably in this group. The third group needed approximately 50 h to reach 30 % dissolution and here both samples from the Hicom and the P10minWet sample are included. The samples from the ball mill did not reach 10 % within 24 h and probably need much more than 50 h to reach 30% dissolution. Comparison

of a dry milled sample and a wet milled sample with an initial difference of less than one order of magnitude in T_5 indicated that the dry milled sample is only initially faster, but the wet milled sample is faster for extensive dissolution.

Table 7 Results for T_5, T_{10}, T_{20}, T_{30} for the dissolution experiments D-1 and D-3.

Sample	T_5 (D-3) [min]	T_5 (D-1) [min]	T_{10} (D-1) [min]	T_{20} (D-1) [min]	T_{30} (D-1) [min]
Ref sample	*NA*	*>1440*	*>1440*	*>1440*	*>1440*
A10minWet	81.0	*NA*	*NA*	*NA*	*NA*
A60minWet	12.5	*NA*	*NA*	*NA*	*NA*
H1minDry	186	158	678	906	3280
H5minDry	35.8	27.3	116	654	>1360
B2hDry	2580	2900	*>1440*	*>1440*	*>1440*
B8hDry	443	434	*>1440*	*>1440*	*>1440*
B2hWet	1980	*NA*	*NA*	*NA*	*NA*
B8hWet	273	*NA*	*NA*	*NA*	*NA*
P10minDry[a]	*NA*	1.02	9.46	62.7	228
P60minDry[a]	0.384	0.267	0.786	3.73	14.8
P10minWet[a]	*NA*	19.7	102	604	>1090
P60minWet[a]	7.62	6.60	19.7	71.9	232

[a] **For the samples from the planetary mill, duplicate D-1 experiments were performed and the average is shown**

The pH measurements were used to calculate rate constants, k, in addition to dissolution degree [%], and these calculations are presented in detail by Haug *et al.* (2009b). There are about 3 orders of magnitude in differences in the rate constants of the fastest and slowest sample in this study. All samples have an initial decrease in k possibly related to the dissolution of fines which would lower the available surface area more than indicated by the shrinking core model used in the calculations. In addition Haug *et al.* (2009b) suggested that increasing crystallinity of the dissolution residue due to removal of the outer layers of the milled samples probably affected the rate constant together with the amount of fines in the samples. Samples milled with the ball mill, attritor and for 10 min in the planetary mill and 1 min in the Hicom mill, all have the same initial decrease in the rate constant from approximately $1 \cdot 10^{-5}$ [mol/m^{2}s] to $1 \cdot 10^{-6} - 2 \cdot 10^{-7}$ [mol/m^{2}s] at 3 % dissolved olivine. After the initial decrease the rate constant

stabilized and the overall results of *k* reflected the differences found by studying T_5.

4.4 Influence of material characteristics on T_5

Figure 4 shows how T_5 is correlated to the measured sample characteristics. Normally total dissolution [mol/s] or time to a certain dissolution degree [%] is correlated to the available surface area.

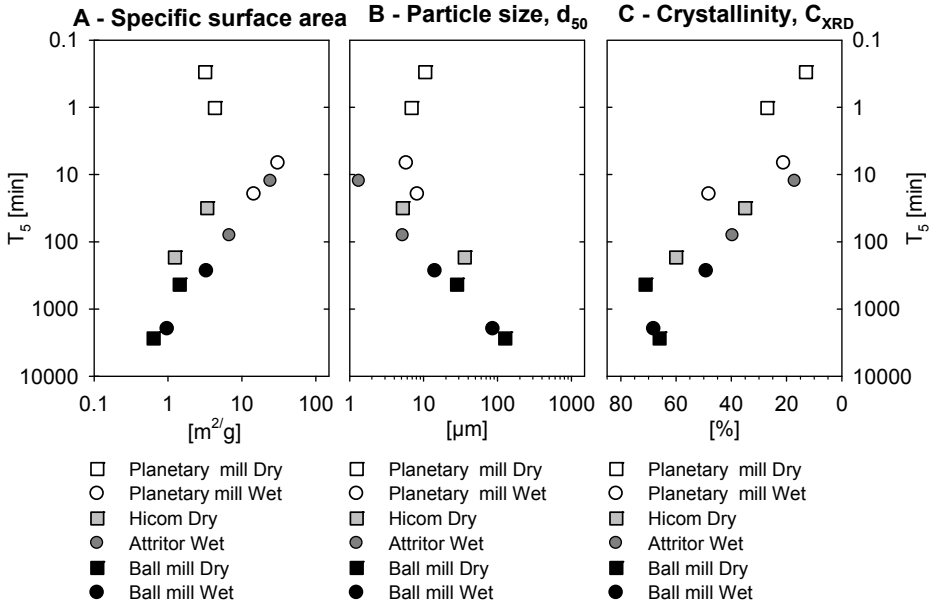

Figure 4 Correlation between material properties and the time to dissolve 5 % olivine (T_5). A – Specific surface area, B – A particle size represented by d_{50}, and C - Crystallinity.

Figure 4A shows a clear trend between the initially measured SSA and T_5 for all samples milled wet (circles as symbols). Increasing the surface area of the wet milled samples with a factor of 10 decreased the time it takes to solve 5 % with a factor of ten. The dry milled samples from the planetary mill and the Hicom mill dissolved faster than the SSA would indicate if wet milling defines the trend. Dry milled samples from the ball mill was very close to the trend between specific surface area and T_5. Dry milling performed in the Hicom mill gave a value of T_5 nearly 1 order of magnitude lower than expected. The two samples milled dry in the planetary mill had T_5 values of less than 1 min which is much faster than approximately 5 h predicted from the specific surface area.

T_5 was found to increase with increased d_{50} in Figure 4B. T_5 for the dry milled samples from the Hicom mill and the ball mill followed a linear trend relatively well, but the particle size of the samples milled dry in the planetary mill, predicts much higher T_5 than measured for the other samples. The only material property where the dry milled samples from the planetary mill follows the trend together with the other materials is when T_5 is plotted against the calculated crystallinity, C_{XRD} (Figure 4C). The crystallinity is proportional to T_5 and a 10 % point reduction in crystallinity yields approximately a 5 times reduction in T_5.

4.5 Conversion

Table 8 Experiments performed with obtained total carbon (TC) and conversion.

Exp Name	Exp. Type	Milling type	Duration [hh:mm]	wt% Carbon	Conversion [%]
IFE - 30	2	A60minWet (I)	01:34	2.28	17
IFE - 34	2	A60minWet (II)	02:00	2.55	19
IFE - 31	2	B8hDry (I)	01:34	1.30	8.8
IFE - 35	2	B8hDry (II)	02:00	1.07	7.2
IFE - 32	2	B8hWet (I)	01:34	1.62	11
IFE - 36	2	B8hWet(II)	02:00	1.55	11
IFE - 33	2	H5minDry (I)	01:34	0.55	3.6
IFE - 37	2	H5minDry (II)	02:00	0.56	3.7
IFE - 21	2	P10minDry (I)	02:00	3.37	25
IFE - 22	2	P10minDry (II)	02:00	3.68	28
IFE - 18	2	P10minWet (I)	02:00	2.22	16
IFE - 23	2	P10minWet (II)	02:00	2.80	21
IFE - 20	2	P60minDry	02:00	4.10	32
IFE - 24	2	P60minWet	02:00	4.81	44
IFE - 26	2	A60minWet	17:26	8.74	87
IFE - 27	2	B8hDry	17:26	7.98	73
IFE - 29	2	B8hWet	17:26	9.33	93
IFE - 28	2	H5minDry	17:26	3.13	23
IFE - 11	2	P10minDry	17:55	9.29	92
IFE - 17	2	P10minWet	18:01	9.44	96
IFE - 12	2	P60minDry (I)	17:55	8.23	77
IFE - 14	2	P60minDry (II)	18:01	8.18	77
IFE - 13	2	P60minWet	17:55	8.61	96

Table 8 lists all the carbonation experiments performed, the obtained TC values and calculated conversion. Figure 5 illustrate the conversion degrees obtained sorted from left to right by increasing conversion at 2 h. The

conversion calculation is discussed and described in detail in Haug *et al.* (2009a). Conversion at 2 h ranged from 3.6 % for the H5minDry sample to 44 % for the P60minWet sample, but at 18 h all samples were converted more than 70 %, with 5 out of 8 different samples above 90 %. The conversion obtained after 18 h of carbonation indicated that wet milling gives the best results. On the other hand, there were indications of dry milling producing the most converted samples after 2 h with the two following exceptions. The dry milled sample produced in the Hicom mill gave the lowest conversion, and the P60minWet sample gave the best result even though the sample was milled wet.

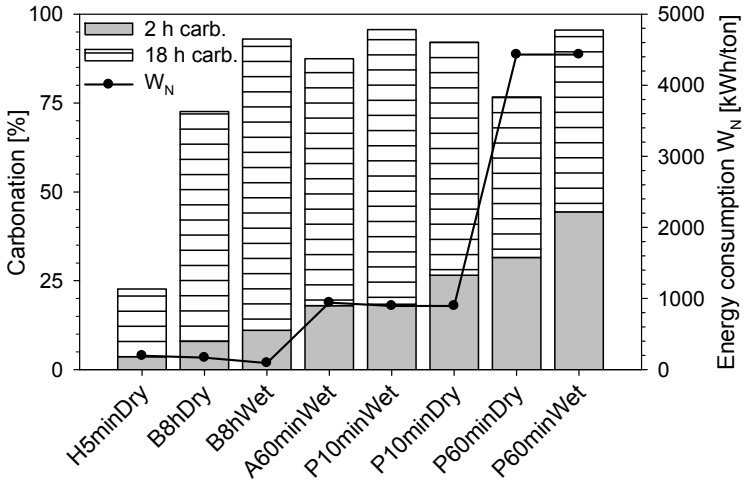

Figure 5 Obtained conversion degrees for each sample after 2 h and 18 h (left y-axis). The net specific energy consumption, W_N, is included (right y-axis).

No strong correlations were found when comparing the particle sizes, the SSA and C_{XRD} to the obtained conversion degrees as indicated by Figure 6. There is a weak trend of increasing conversion for decreasing C_{XRD} at 2 h of carbonation and no trends with C_{XRD} was found for 18 h of carbonation (Figure 6A). The samples milled in the planetary mill obtained somewhat higher conversion than the other mills for approximately the same C_{XRD}. Samples with large SSA resulted in high conversion degrees (Figure 6B) after 2 h, but the dry milled samples from the planetary mill obtained much higher conversions than the surface area would suggest. Particle size was

not correlated with the conversion degree at either 2 h or 18 h of carbonation (Figure 6C).

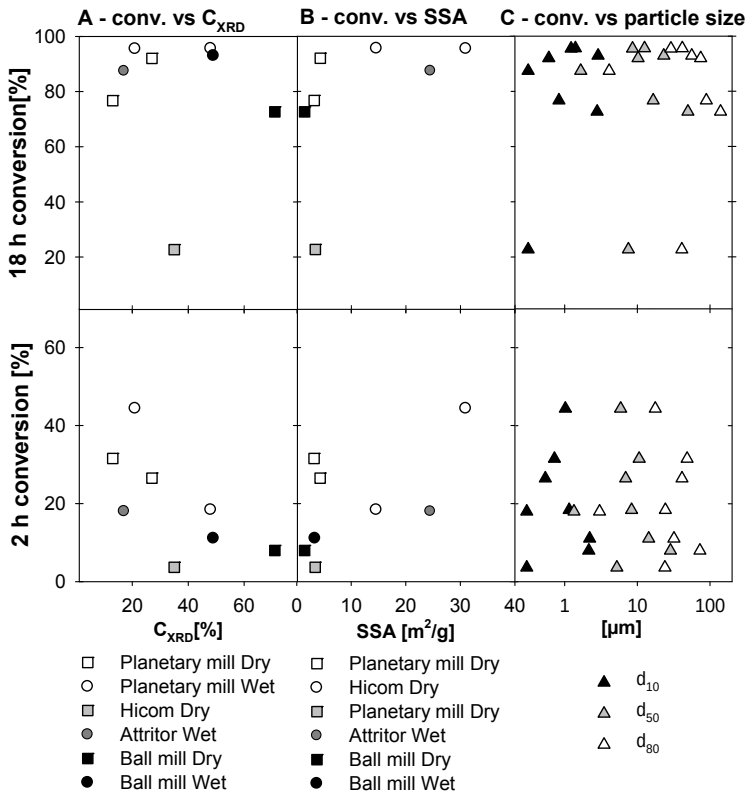

Figure 6 Correlation of the particle size (A), crystallinity (B) and specific surface area (C) with the obtained conversion after 2 h (lower row) and 18 h (upper row)

5 DISCUSSION

5.1 Carbonation in 1 or 2 steps?

Increased milling energy consumption is reflected by decreased T_5 and T_{20} indicating that the dissolution rates increased with increasing milling energy consumption (Figure 7). When the input energy was increased then the dry milled samples obtained lower T_5 than the wet milled samples. Dry milling was therefore more efficient at increasing the dissolution rate than wet milling.

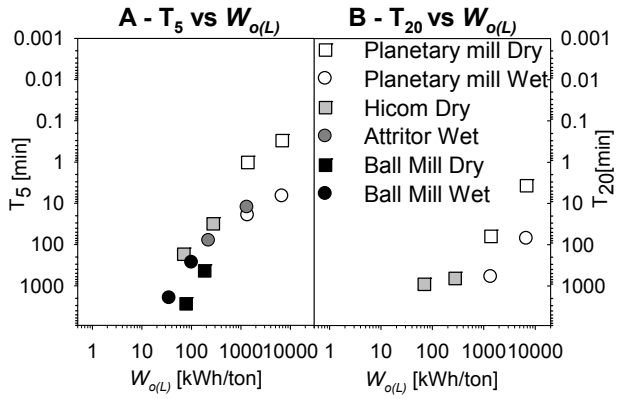

Figure 7 Correlation between the time to dissolve 5 % olivine (T_5 - A) and 20 % (T_{20} – B), and the estimated total large scale energy consumption, $W_{o(L)}$.

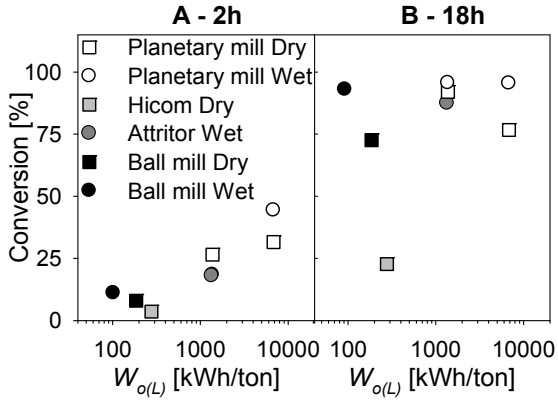

Figure 8 Illustration of how the estimated total large scale energy consumption ($W_{o(L)}$) was correlated with the conversion degrees obtained after 2 h and 18 h

After 2 h of carbonation as shown in Figure 8A, the conversion increased with $W_{o(L)}$, which corresponded well with the dissolution results. However, the conversions obtained after 18h were not easily correlated to the energy consumption, Figure 8B, or to the measured material properties in Figure 6. In Figure 9 T_5 is compared to conversion and there is a positive correlation between conversion and time until 5 % is dissolved at 2 h. The lack of correlation between T_5 and the conversion obtained after 18 h, and energy consumption and conversion after 18 h indicate that the reaction time probably has been too long to distinguish between the different samples or that precipitation and not dissolution is important. The B8hWet sample obtained an estimated large scale total energy consumption of 100

kWh/ton, the lowest total energy consumption in the study, and resulted in a conversion of 93 % after 18 h. This conversion is very close to the maximum 96 % conversion obtained for the samples P60minWet and P10minWet, with respective energy consumptions of 1400 kWh/ton and 6800 kWh/ton. The 70 times increase in energy consumption from the B8hWet sample to the P60minWet sample, is not reflected in any way when conversion is approaching 100 % in a one step batch reaction.

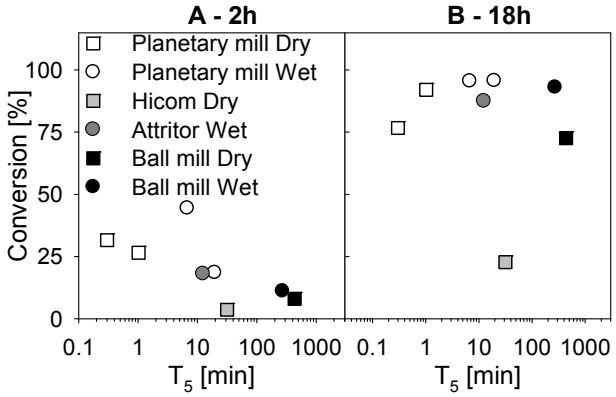

Figure 9 Correlation between conversion and T_5

The carbonation experiments illustrated a one step carbonation approach, while the dissolution experiments imitated the first step of a two step carbonation process where dissolution and precipitation are divided. Based on the findings of this study and the study described in Haug *et al.* (2009a), pre-treatment of olivine using mechanical activation with the purpose of performing direct carbonation, is probably too energy consuming. More extensive research is needed to confirm this due to the limited range of temperature, pressure and reaction times used here. These results regarding the low effect of high intensity milling corresponds well with the conclusions presented by Summers *et al.* (2005) where the milling energy consumption was not reflected in the obtained conversion. Haug *et al.* (2009a) proposed that precipitation rates and not the dissolution rate of the feedstock materials probably is the rate limiting step in direct carbonation at given conditions. The significance of precipitation observation might explain the results of Summers *et al.* (2005) as well where high intensity milling did not increase their carbonation results. Assuming extensive

conversion to be independent of the milling energy consumption above a certain level, then the best grinding solution is the mill with the energy consumption at this level. From the results presented here the ball mill seems to be the best alternative for direct carbonation.

If a two step carbonation process is used instead of a one step direct carbonation process, the dissolution results are relevant since the dissolution step is dependent on the dissolution rates. T_5 was reduced by 4 orders of magnitude together with an increase in energy consumption of 2-3 orders of magnitude. A three order reduction in T_5 is possible to obtain by increasing the specific surface area. The last decrease from $T_5 < 10$ min to $T_5 < 1$ min is only possible to obtain by dry milling in the mill with the highest milling intensity, the planetary mill. The cause of the final reduction in T_5 is not the specific surface area, but a reduction of crystallinity beneath C_{XRD} = 27 %. The same crystallinity was found for the samples milled wet for 60 min in the planetary mill and the attritor, but did not result in the same low T_5. One possible explanation to the difference in T_5, despite the same calculated crystallinity, may be a higher crystallinity in the core of the wet milled particles than the dry milled particles (Haug *et al.*, 2009b) or distribution of fines. Crystallinity is in this study an approach to measure of the activation state of the samples and the disturbance of the crystal lattice. Hoberg and Götte (1985) found indications of the mechanical activation to decrease with increasing dissolution, and their result supports the theory of decreasing rates with increasing dissolution as well as changing properties towards the core of the particles (Haug *et al.*, 2009b).

Dividing the carbonation reaction into two steps makes it possible to optimize both the dissolution process and precipitation process separately. This separation eliminates the problems with conflicting optimum pressures and temperatures for simultaneous dissolution and precipitation, but introduces equilibrium considerations including avoiding precipitation until the slurry has reached the precipitation step. The requirement of keeping secondary minerals in solution may possibly result in a much higher liquid/solid ratio than necessary for direct carbonation.

5.2 From the laboratory to the industry

The planning of a commercial mineral carbonation plant requires the laboratory experiments to be transferred to industrial scale. O'Connor *et al.* (2004), Gerdemann *et al.* (2007) and Huijgen *et al.* (2007) have discussed large scale mineral carbonation energy consumption and overall costs for conventionally milled minerals. The possibility of using Hicom mills, attritors or planetary mills have been evaluated together with a conventional ball mill in the scenario of a 100 MW power plant estimated to emit 60 ton/h or 480 kton/year of CO_2 (Huijgen *et al.*, 2007). Assuming a conversion degree of 90 % for olivine, then the given amount of CO_2 would require an approximate mass flow of olivine of 110 ton/h or 880 kton/year.

Table 9 Mill throughput and number of mills required to handle the CO_2 emissions from a 100 MW power plant.

	Ball mill (Huijgen *et al.*, 2007)[a]	Attritor C-100 (Union-Process, 2009)	Hicom 120 mill (Nesbit *et al.*, 2001)	Planetary mill (MP-8[b]) (TTD, 2009)
Max mass flow	8 ton/h	14.5 ton/h[c] (limestone)	4 – 8 ton/h (diamond refining, 17-66 kWh/ton)	25 - 50 kg/h (– 10 µm)
Mills required	14	8	15 – 30	2200 – 4400

[a] Ball mill used in cost calculation presented by the reference, not maximum available

[b] (Fokina *et al.*, 2004) mentions planetary mills taking 3-5 ton/h and the introduction page of TTD industries (TTD, 2009) mentions development of planetary mills with the capacity of 500 kg/hr.

[c] Olivine probably has a slightly lower mass flow due to a higher hardness.

Table 9 presents maximum throughputs reported for the largest continuous attritor operating in a wet mode from Union Process, the largest continuous planetary mill presented by Technics and Technology of Disintegration Ltd, results from a pilot test of a Hicom 120 Mill from Hicom industries, and the throughput of the ball mill used in an cost analysis of a mineral carbonation plant (Huijgen *et al.*, 2007). Attritors and Hicom mills most likely exist today in a large enough scale to handle the throughput of olivine needed for a carbonation plant. Using the data for the planetary mill, sufficiently large planetary mills are under development. Ball mills are

widely used in the mining industry today, and there are no problems of obtaining mills large enough to handle the necessary throughput of olivine. If experimental results later shows that prolonged milling will be required, then the throughput will decrease due to higher retention periods. Commercial ball mills, attritors and Hicom mills are most likely large enough to be implemented in a carbonation process, but then the energy consumption has to be low enough.

There is a practical cost/benefit limit of the total energy consumption pr ton of olivine given by the balance between the CO_2 stored in the mineral carbonation process and the CO_2 emissions as a result of energy consumption of the same process. There is no practical value of a CO_2 storage process that emits more CO_2 than it stores. As shown in Figure 1 in the introduction, the overall energy consumption for the mineral carbonation process normalized pr ton of olivine is the sum of the pre-treatment energy consumption and the energy consumption during carbonation. This sum determines if the combination of milling and carbonation becomes a viable option for CO_2 sequestration.

The CO_2 emissions from the energy consumed in the pre-treatment and carbonation process must not exceed the amount of CO_2 captured. Net CO_2 avoided = 0 when CO_2 from energy consumption and CO_2 captured are balanced. Approximately 500 kWh/ton of olivine is available for pre-treatment and processing purposes if all the energy produced at the 100 MW power plant was used in the sequestration process. This limit is theoretical, and for all practical purposes this limit is significantly lower than 500 kWh/ton since the amount of energy produced in the power plant has to be more than marginally higher than the energy consumed by CO_2 capture and storage.

Table 10 Published energy consumption and cost estimates of direct carbonation used for CO_2 sequestration

Ref	Grinding energy [kWh/ton]	Raw material	Conversion [%]	Cost CO_2 avoided [$/ton]	Annual CO_2 avoided in each study/area	Energy consumption [kWh/ton CO_2 avoided]	Region (Type of milling)
(Stolaroff *et al.*, 2005)	–	Slag/ concrete	70	8	32kt	–	– [a]
(Huijgen and Comans, 2005, Huijgen *et al.*, 2007, Huijgen *et al.*, 2006)	253	Wollastonite	69	102	480kt	47	–
	213	Steel slag	67	77	120kt	354	–
Table 3, Table 2 and Table 5 (Gerdemann *et al.*, 2007) together with Table II (O'Connor *et al.*, 2004)	83	100% olivine	61	78	13 Mt	415	1[b] s[c]
	13	100% serpentine	9	537	8 Mt	225	2[b] s
	13	100% serpentine	9	538	8 Mt	225	3[b] s
	13	100% serpentine	9	521	59 Mt	220	4[b] s
	89	70% olivine	61	81	126 Mt	475	5[b] s
	13	100% serpentine	12	309	187 Mt	222	6[b] s
	97	50% wollastonite	43	112	62 Mt	233	7[b] s
	233	100% olivine	81	167	7 Mt	570	1 a[c]
	339	100% serpentine	40	NC[d]	<0 Mt	NC	2 a
	339	100% serpentine	40	NC	<0 Mt	NC	3 a
	339	100% serpentine	40	NC	<0 Mt	NC	4 a
	239	70% olivine	81	173	63 Mt	646	5 a
	376	100% serpentine	92	NC	<0 Mt	NC	6 a
	167	50% wollastonite	82	110	43 Mt	311	7 a

[a] – = not specified in reference

[b] The regions were used to specify the type of minerals available for mineral carbonation. 1: Washington, 2: California/Oregon, 3: Southern California, 4: Texas, 5: North Carolina, 6: Border of Maryland/Delaware/Pennsylvania, 7: New York

[c] s = defined as standard pre-treatment and a = activated in (O'Connor *et al.*, 2004)

[d] NC = not calculated because energy consumption during mineral carbonation results in an additional CO_2 emission, and not CO_2 sequestration.

Table 10 summarizes six studies dedicated to estimate the total energy consumption of grinding and mineral carbonation together with the estimated cost pr ton CO_2 avoided for a possible industrial sized carbonation plant. Maximum sum of grinding and pre-treatment energy consumption which resulted in CO_2 storage was 253 kWh/ton. There are no pre-treatment options with energy consumption between 254 kWh/ton and 338 kWh/ton in Table 10. From 339 kWh/ton and up the pre-treatment is to energy consuming, and no CO_2 is actually stored by the process. The theoretical upper process energy consumption limit is approximately 500 kWh/ton in the 100 MW power plant, and corresponds well with ~ 340 kWh/ton as a more realistic upper limit found from the literature.

A comparison of the numbers in Table 10 to the grinding energies found in this study indicated that the Hicom mill and the attritor may have potentials for being implemented if the grinding time is kept short. Despite the good results for the planetary milled samples regarding dissolution properties, this mill is too energy consuming for the purpose of mineral carbonation since the total milling intensity was estimated to be 14000 kW/ton, and therefore is it probably very difficult to produce samples with an total energy consumption below 300 kWh/ton. The grinding solutions and choices of mills presented here illustrates a selection of possible milling environments and mills, but are not optimized for mineral carbonation pre-treatment. It exists therefore a possibility of less energy consuming grinding solutions, which may be closer to be viable as pre-treatment. Several two-step experiments have to be performed to fully evaluate the potential of the different grinding solutions and investigate the challenges of the indirect process design.

6 CONCLUSION

Pre-treatment of olivine is necessary if olivine is going to be used for ex-situ CO_2 sequestration and storage purposes. Milling as pre-treatment has been studied here through dissolution and carbonation experiments. One conventional laboratory ball mill and three high intensity mills, an attritor, a Hicom mill and a planetary mill were used to produce olivine samples with varying combinations of material properties with respect to size distributions, surface area and crystallinity. In general wet milling

produced samples with high specific surface areas reaching 31 m^2/g and dry milling produced samples with low crystallinity, down to 11 %. The estimated large scale total energy consumption to produce the samples in the study ranged from approximately 40 kWh/ton with the ball mill to 7000 kWh/ton with the planetary mill.

The decreasing time to dissolve 5 % of the olivine samples, T_5, correlated with increasing energy consumption. Energy consumption was also relatively well correlated with increasing specific surface area, with the exception of dry milling in the planetary mill, decreasing crystallinity and decreasing average particle size. The carbonation results after 2 h or 18 h at 185 °C and 115 bar could not entirely be explained by the material properties, and therefore the additional energy used to induce changes in the material properties were not efficiently utilized. The influence of precipitation kinetics during carbonation is one possible explanation for the lack of trends between conversion, material properties and energy consumption during milling.

Ball mills are the least energy consuming mills pr ton of material milled. In the case of direct mineral carbonation, these mills are probably most suited when the carbonation reaction is restricted by several other factors as precipitation rates, than increased dissolution rates obtained by milling. On the other hand, high-intensity mills may be better suited for a two-step indirect carbonation process if the challenges of divided dissolution and precipitation regarding volume flows and solved minerals in solution can be solved. Sufficiently large Hicom mills and attritor mills are most likely commercially available, and there are indications of these mills being efficient at increasing the dissolution rate of olivine with a possibly acceptable energy consumption if optimized further. Planetary mills are too energy consuming as pre-treatment for both carbonation routes. Since this study is only evaluating possible differences between the types of mills and milling conditions, less energy consuming grinding solutions with the same dissolution or carbonation properties can probably be obtained.

ACKNOWLEDGEMENTS

This work was carried out as a part of the Strategic Institute Program "From waste to value: New industrial process for mineral dressing by use of

CO_2" headed by Institute for Energy Technology, Norway. Funding of the program from the Research Council of Norway (Project No 158916/i30) is appreciated. I was very grateful for all the help from Torkjell Breivik regarding his invaluable help with the mills at NTNU, and Jan Kihle and Øyvind Brandvold's help when performing the carbonation experiments at IFE.

REFERENCES

Baláž, P., 2000, *Extractive Metallurgy of Activated Minerals*. 1st edn. Elsevier Science B.V., Amsterdam.

Bearat, H., McKelvy, M.J., Chizmeshya, A.V.G., Gormley, D., Nunez, R., Carpenter, R.W., Squires, K. and Wolf, G.H., 2006, Carbon sequestration via aqueous olivine mineral carbonation: Role of passivating layer formation. Environmental Science & Technology, 40(15), 4802-4808.

Bond, F.C., 1961a, Crushing and grinding calculations Part I. British Chemical Engineering, 6(6), 378-385.

Bond, F.C., 1961b, Crushing and grinding calculations Part II. British Chemical Engineering, 6(8), 543-634.

Cho, H., Lee, H. and Lee, Y., 2006, Some breakage characteristics of ultra-fine wet grinding with a centrifugal mill. International Journal of Mineral Processing, 78(4), 250-261.

Druckenmiller, M.L. and Maroto-Valer, M.M., 2005, Carbon sequestration using brine of adjusted pH to form mineral carbonates. Fuel Processing Technology, 86(14-15), 1599-1614.

Eggleston, C.M., Hochella, M.F. and Parks, G.A., 1989, Sample preparation and aging effects on the dissolution rate and surface-composition of diopside. Geochimica Et Cosmochimica Acta, 53(4), 797-804.

Fokina, E.L., Budim, N.I., Kochnev, V.G. and Chernik, G.G., 2004, Planetary mills of periodic and continuous action. Journal of Materials Science, 39(16-17), 5217-5221.

Gerdemann, S.J., O'Connor, W.K., Dahlin, D.C., Penner, L.R. and Rush, H., 2007, Ex situ aqueous mineral carbonation. Environmental Science & Technology, 41(7), 2587-2593.

Giammar, D.E., Bruant, J.R.G. and Peters, C.A., 2005, Forsterite dissolution and magnesite precipitation at conditions relevant for deep saline aquifer storage and sequestration of carbon dioxide. Chemical Geology, 217(3-4), 257-276.

Haug, T.A., Kleiv, R.A. and Munz, I.A., 2009a, "Carbonation of mechanically activated olivine (manuscript September 2009)." Trondheim, NTNU.

Haug, T.A., Kleiv, R.A. and Munz, I.A., 2009b, Dissolution of mechanically activated olivine in hydrochloric acid - investigating leaching properties for carbonation purposes (in review). Journal of Applied Geochemistry.

Hoberg, H. and Götte, J., 1985, The influence of mechanical activation on the kinetics of the leaching process of columbite. International Journal of Mineral Processing, 15(1-2), 57-64.

Huijgen, W.J.J. and Comans, R.N.J., 2005, Carbon dioxide sequestration by mineral carbonation: Literature Review (ECN-C--05-022), 37, ECN Clean Fossil Fuels

Huijgen, W.J.J., Comans, R.N.J. and Witkamp, G.-J., 2007, Cost evaluation of CO_2 sequestration by aqueous mineral carbonation. Energy Conversion and Management, 48(7), 1923-1935.

Huijgen, W.J.J., Ruijg, G.J., Comans, R.N.J. and Witkamp, G.J., 2006, Energy consumption and net CO_2 sequestration of aqueous mineral carbonation. Industrial & Engineering Chemistry Research, 45(26), 9184-9194.

Huijgen, W.J.J., Witkamp, G.J. and Comans, R.N.J., 2005, Mineral CO_2 sequestration by steel slag carbonation. Environmental Science & Technology, 39(24), 9676-9682.

Kalinkin, A.M., Boldyrev, V.V., Politov, A.A., Kalinkina, E.V., Makarov, V.N. and Kalinnikov, V.T., 2003, Investigation into the mechanism of interaction of calcium and magnesium silicates with carbon dioxide in the course of mechanical activation. Glass Physics and Chemistry, 29(4), 410-414.

Kheifets, A.S. and Lin, I.J., 1996, Energy transformations in a planetary grinding mill Part l. General treatment and model design. International Journal of Mineral Processing, 47(1-2), 1-19.

Kleiv, R.A. and Thornhill, M., 2006, Mechanical activation of olivine. Minerals Engineering, 19(4), 340-347.

Kojima, T., Nagamine, A., Ueno, N. and Uemiya, S., 1997, Absorption and fixation of carbon dioxide by rock weathering. Energy Conversion and Management, 38(Supplement 1), 461-466.

Lackner, K.S., Wendt, C.H., Butt, D.P., Joyce, J.E.L. and Sharp, D.H., 1995, Carbon dioxide disposal in carbonate minerals. Energy, 20(11), 1153-1170.

Maroto-Valer, M.M., Fauth, D.J., Kuchta, M.E., Zhang, Y. and Andresen, J.M., 2005, Activation of magnesium rich minerals as carbonation

feedstock materials for CO_2 sequestration. Fuel Processing Technology, 86(14-15), 1627-1645.

McKelvy, M.J., Chizmeshya, A.V.G., Diefenbacher, J., Bearat, H. and Wolf, G., 2004, Exploration of the role of heat activation in enhancing serpentine carbon sequestration reactions. Environmental Science & Technology, 38(24), 6897-6903.

Musa, F. and Morrison, R., 2009, A more sustainable approach to assessing comminution efficiency. Minerals Engineering, 22(7-8), 593-601.

Nesbit, P.Q., Du Toit, G., Mapasa, K. and Feldman, C., 2001, Evaluation of the Hicom 120 mill at Venetia Mine. Minerals Engineering, 14(7), 711-721.

O'Connor, W.K., Dahlin, C.L., Rush, G.E., Gerdemann, S.J. and Penner, L.R., 2004, Energy and economic considerations for ex-situ aqueous mineral carbonation. (DOE/ARC-2004-028), 12, Albany Research Center, Albany, Oregon.

O'Connor, W.K., Dahlin, C.L., Turner, P.C. and Walters, R., 1999, Carbon dioxide sequestration by ex-situ mineral carbonation. (DOE/ARC-99-009), 14, Albany Research Center, Albany, Oregon.

O'Connor, W.K., Dahlin, D.C., Rush, G.E., Dahlin, C.L. and Collins, W.K., 2002, Carbon dioxide sequestration by direct mineral carbonation: process mineralogy of feed and products. Minerals & Metallurgical Processing, 19(2), 95-101.

O'Connor, W.K., Dahlin, D.C., Rush, G.E., Gerdemann, S.J., Penner, L.R., Rubin, E.S., Keith, D.W., Gilboy, C.F., Wilson, M., Morris, T., Gale, J. and Thambimuthu, K., 2005, Energy and economic evaluation of ex situ aqueous mineral carbonation. In *Proc. Greenhouse Gas Control Technologies 7,* Oxford, 2011-2015.

Osland, R. 1998, *Modelling of variations in Norwegian olivine deposits: causes of variation and estimation of key quality factors*. Dr.Ing thesis, Norwegian University of Science and Technology.

Park, A.H.A. and Fan, L.S., 2004, CO_2 mineral sequestration: physically activated dissolution of serpentine and pH swing process. Chemical Engineering Science, 59(22-23), 5241-5247.

Pourghahramani, P. and Forssberg, E., 2006, Microstructure characterization of mechanically activated hematite using XRD line broadening. International Journal of Mineral Processing, 79(2), 106-119.

Sangwal, K.K., 1982, Dissolution kinetics of MgO crystals in aqueous acidic salt solutions [dislocation etching]. Journal of Materials Science, 17(12), 3598-3610.

Seifritz, W., 1990, CO_2 disposal by means of silicates. Nature, 345(6275), 486.

Sipilä, J., Teir, S. and Zevenhoven, R., 2008, Carbon dioxide sequestration by mineral carbonation. Literature review update 2005 - 2007. (2008 - 1), Åbo Akademi University, Faculty of Technology, Heat Engineering Laboratory.

Stolaroff, J.K., Lowry, G.V. and Keith, D.W., 2005, Using CaO- and MgO-rich industrial waste streams for carbon sequestration. Energy Conversion and Management, 46(5), 687-699.

Summers, C.A., Dahlin, D.C., Rush, G.E., O'Connor, W.K. and Gerdemann, S.J., 2005, Grinding methods to enhance the reactivity of olivine. Minerals & Metallurgical Processing, 22(3), 140-144.

Teir, S., Eloneva, S. and Zevenhoven, R., 2005, Production of precipitated calcium carbonate from calcium silicates and carbon dioxide. Energy Conversion and Management, 46(18-19), 2954-2979.

Tkáčová, K., 1989, *Mechanical Activation of Minerals*. Elsevier Science Publishers, Amsterdam.

Tromans, D. and Meech, J.A., 2001, Enhanced dissolution of minerals: Stored energy, amorphism and mechanical activation. Minerals Engineering, 14(11), 1359-1377.

TTD, 2009, Technics and Technology of Disintegration Ltd. http://www.ttd.spb.ru/oborud/mills/industrial/mp_8 (accessed 17.07.2009).

Union-Process, 2009, Particle size reduction equipment. www.unionprocess.com (accessed 17.07.2009).

Part 3

Appendix 1 – Calculation of C_{XRD}

Method:

1. Perform XRD analysis of an unaltered sample assumed to be 100 % crystalline, and on the altered sample(s)
2. Chose an XRD peak by minimizing the influence of surrounding peaks
3. Chose left and right limits for peak. Not necessarily exactly the same value for original and altered sample(s).
4. Use presented equations to calculate C_{XRD}. See Figure for illustration of parameters.

Equation 1 through 4 is applied the same peak for the original sample and the altered sample. The respective values of background level, B, and integral area, I_n, is denoted with the subscript o for original sample, and i for altered sample, and used in equation 5.

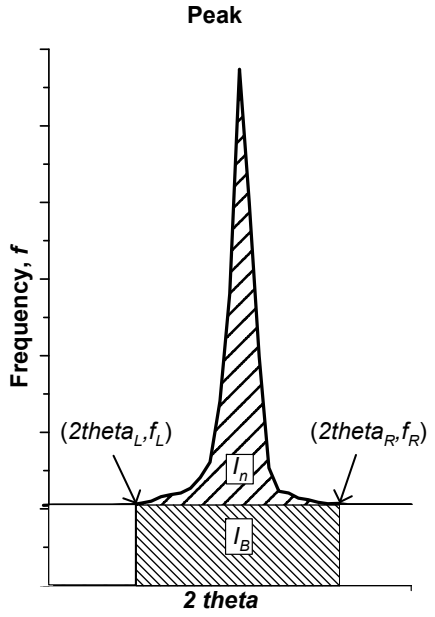

Figure Illustration of an XRD peak

Nomenclature:

$2theta_L$: left limit of peak

$2theta_R$: right limit of peak

$2theta_j$: j^{th} 2theta measurement

f_L : Frequency value of the background at the left side of the peak

f_R : Frequency value of the background at the right side of the peak

f_j : j^{th} frequency measurement corresponding to the $2theta_j$ value.

n : Indicates the number of the $2theta_L$ measurement

k : number of measurement intervals in a peak.

B : Average background level calculated from peak limits, equation 1.

I_P : Integral area of peak= area under peak of altered sample, calculated by assuming trapezes between each measurement of 2theta and frequency and summarizing all trapezes within the peak, equation 2.

I_B : Integral area under background, equation 3.

I_n : Integral area = area under peak above background, B. Found from XRD software or with equation 4.

C_{XRD}: Calculated crystallinity from equation 5.

Equations:

$$B = \frac{f_L + f_R}{2} \tag{1}$$

$$I_P = \sum_{j=n}^{n+k-1} \left(\frac{f_j + f_{j+1}}{2} \right) \cdot \left(2theta_{j+1} - 2theta_j \right) \tag{2}$$

$$I_B = \left(2theta_R - 2theta_L \right) \cdot \sqrt{\left(f_R - f_L \right)^2} \tag{3}$$

$$I_n = I_P - I_B \tag{4}$$

$$C_{XRD} = \frac{I_i}{I_o} \frac{B_o}{B_i} \cdot 100\% \tag{5}$$

Appendix 2 – Particle size distributions

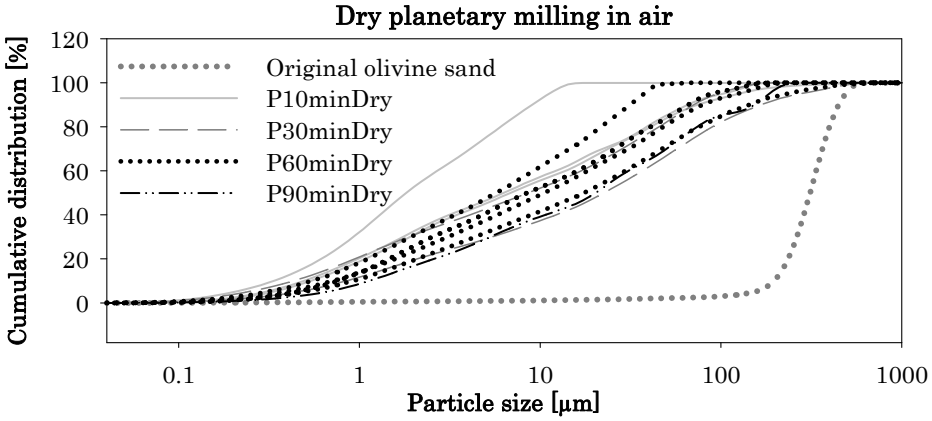

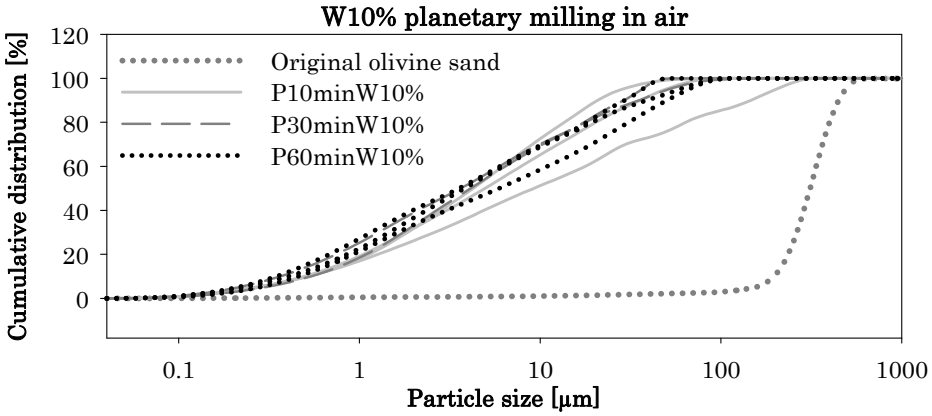

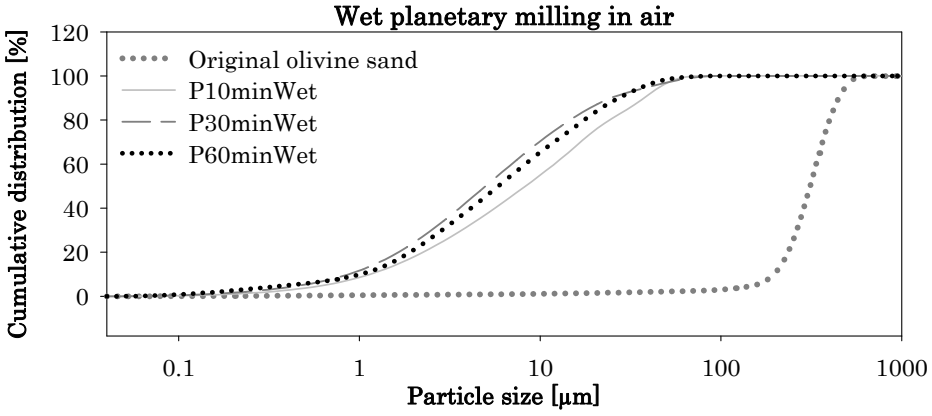

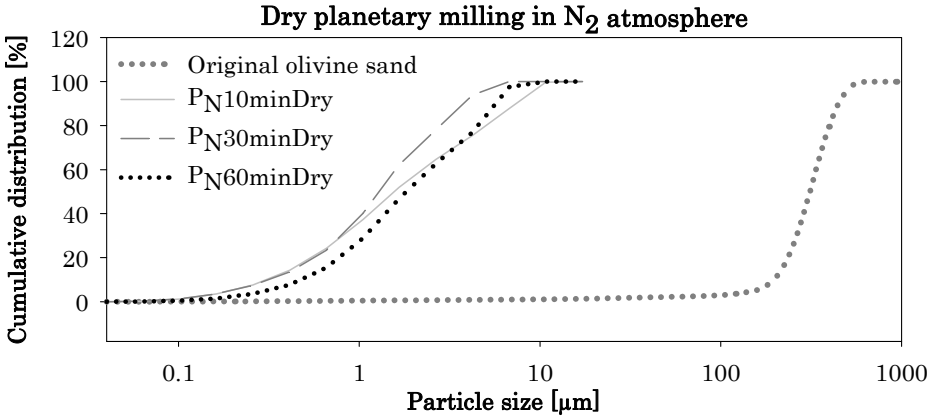
Dry planetary milling in N_2 atmosphere
Cumulative distribution [%]
Original olivine sand
P_N10minDry
P_N30minDry
P_N60minDry
Particle size [µm]

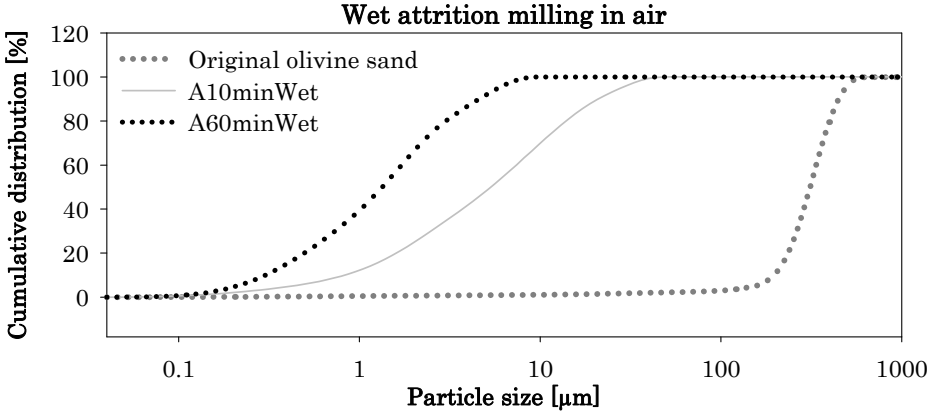
Wet attrition milling in air
Cumulative distribution [%]
Original olivine sand
A10minWet
A60minWet
Particle size [µm]

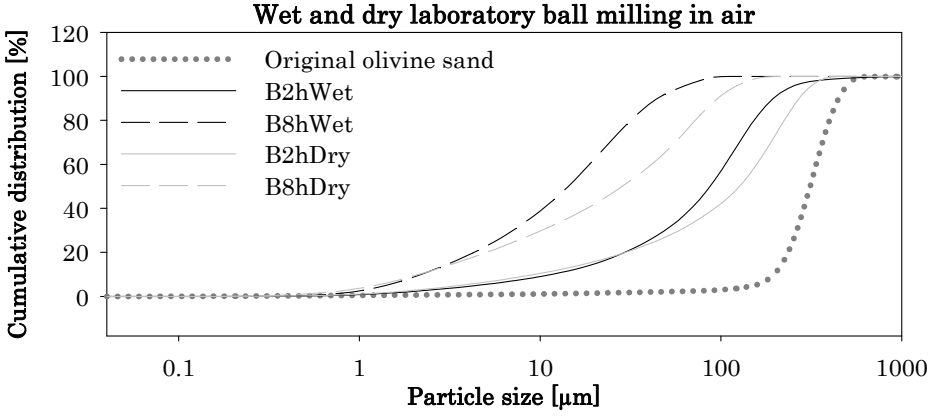
Wet and dry laboratory ball milling in air
Cumulative distribution [%]
Original olivine sand
B2hWet
B8hWet
B2hDry
B8hDry
Particle size [µm]

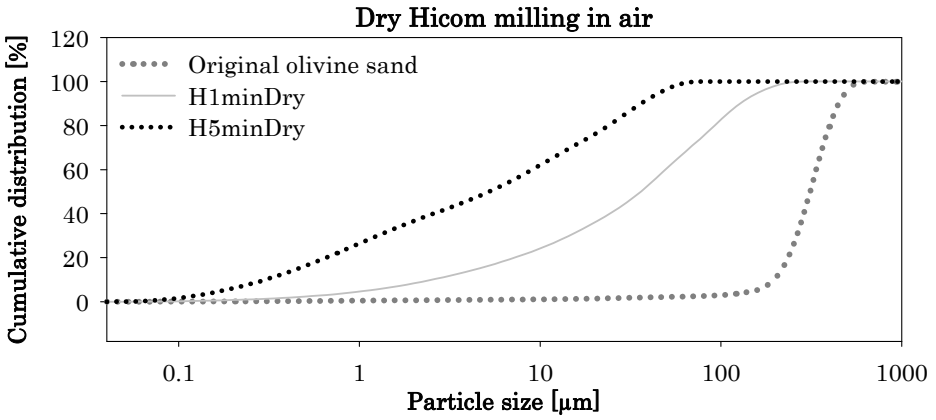
Dry Hicom milling in air
Cumulative distribution [%]
120
100
80
60
40
20
0
Original olivine sand
H1minDry
H5minDry
0.1
1
10
100
1000
Particle size [µm]

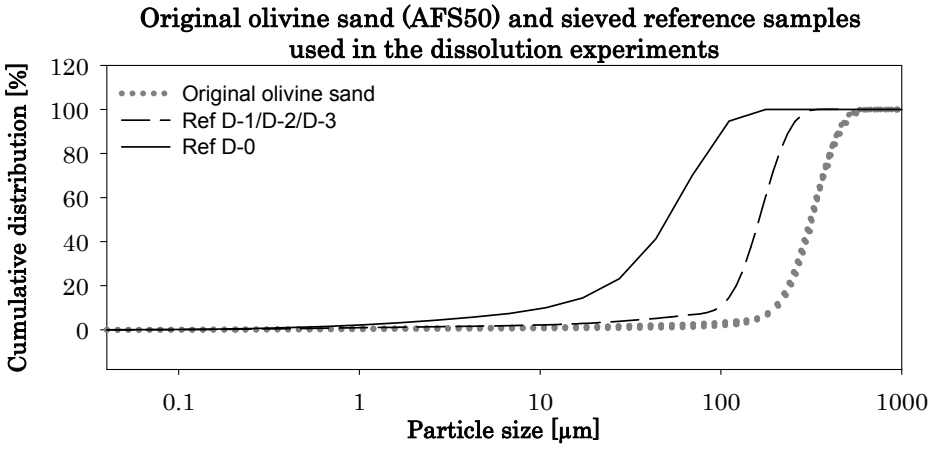
Original olivine sand (AFS50) and sieved reference samples used in the dissolution experiments
Cumulative distribution [%]
120
100
80
60
40
20
0
Original olivine sand
Ref D-1/D-2/D-3
Ref D-0
0.1
1
10
100
1000
Particle size [µm]

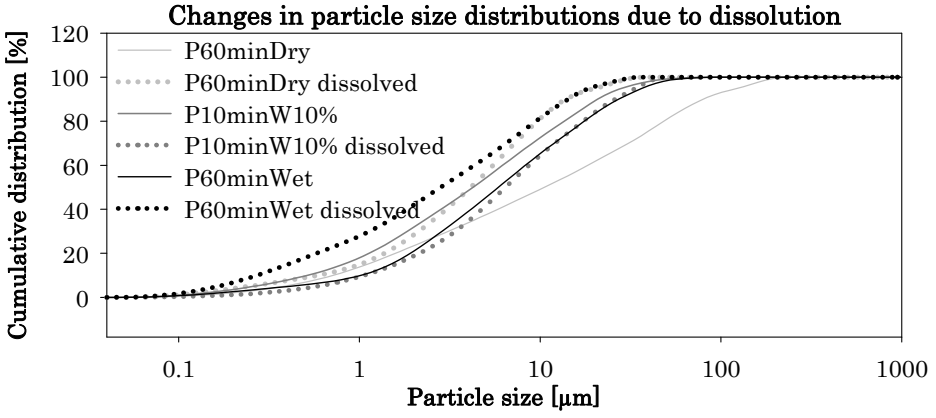
Changes in particle size distributions due to dissolution
Cumulative distribution [%]
120
100
80
60
40
20
0
P60minDry
P60minDry dissolved
P10minW10%
P10minW10% dissolved
P60minWet
P60minWet dissolved
0.1
1
10
100
1000
Particle size [µm]

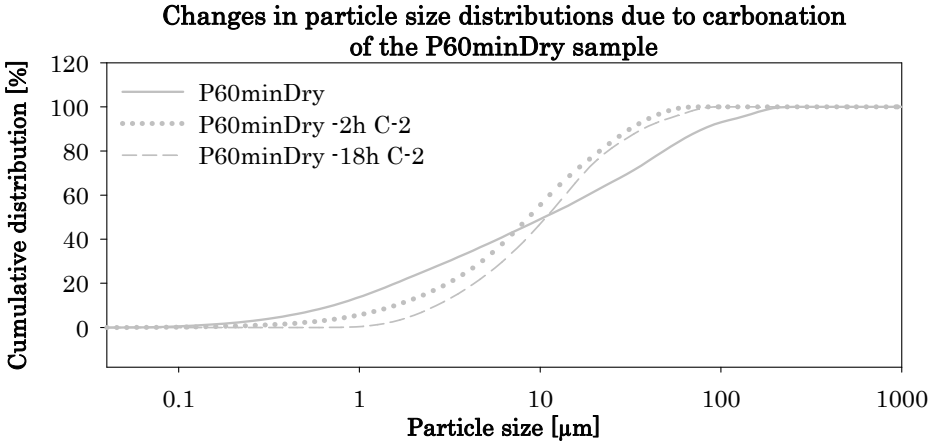
Changes in particle size distributions due to carbonation of the P60minDry sample
Cumulative distribution [%]
120
100
80
60
40
20
0
P60minDry
P60minDry -2h C-2
P60minDry -18h C-2
0.1
1
10
100
1000
Particle size [µm]

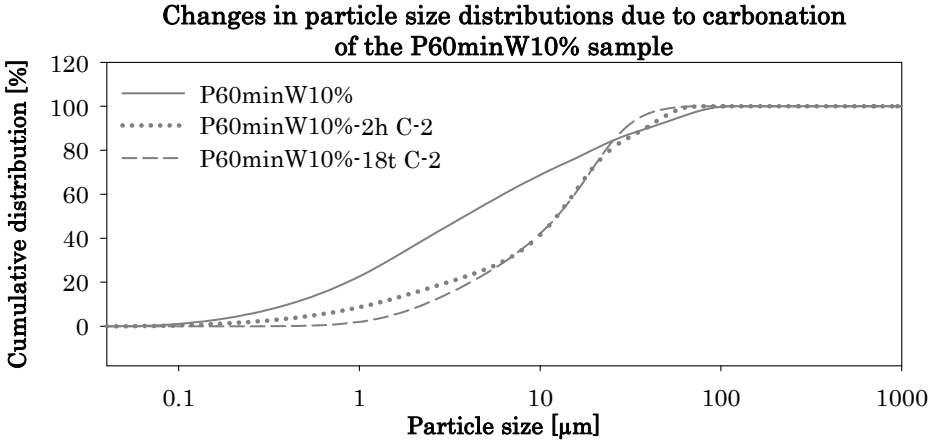
Changes in particle size distributions due to carbonation of the P60minW10% sample
Cumulative distribution [%]
120
100
80
60
40
20
0
P60minW10%
P60minW10%-2h C-2
P60minW10%-18t C-2
0.1
1
10
100
1000
Particle size [µm]

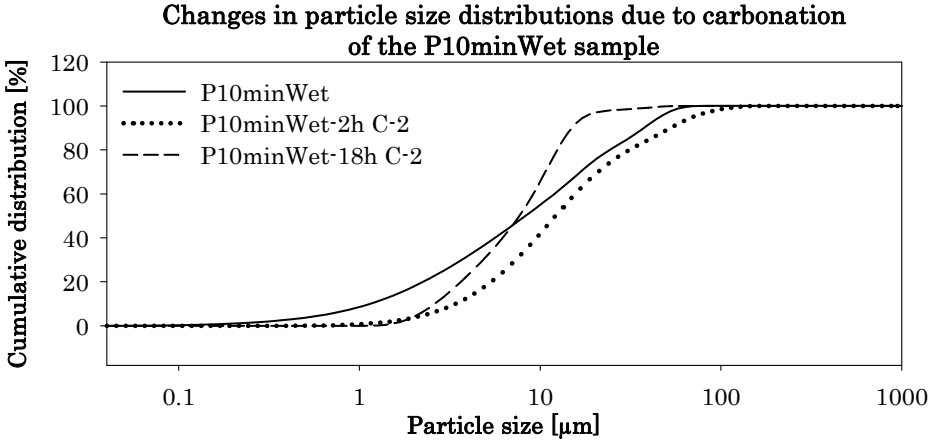
Changes in particle size distributions due to carbonation of the P10minWet sample
Cumulative distribution [%]
120
100
80
60
40
20
0
P10minWet
P10minWet-2h C-2
P10minWet-18h C-2
0.1
1
10
100
1000
Particle size [µm]

Appendix 3 – Calculation of contamination

Method:

Amount of contamination in a sample can be calculated from element analysis of an uncontaminated sample and the contaminated sample.

1. Perform e.g. XRF analysis or ICP–MS of an uncontaminated sample and contaminated sample.
2. Obtain composition of contamination from manufacturer or analyses.
3. Calculation can be done on one element, but using several eliminates the influence of uncertainties by averaging the result. Use only elements with significant concentrations. Fe is normally suitable for mill contamination purposes. Other suitable elements are defined by the composition of the steel alloy.
4. Use presented equations to calculate the contamination, X [%]. Wt% of element or wt% of oxide can both be used, if all numbers are calculated with the same unit. These two units can not be used at the same time.

Nomenclature:

P_{tot} = Total percentage of all elements in uncontaminated sample.
Ideally = 100 % but using XRF this value is normally slightly lower.

P_{Fe1} = Content of Fe before contamination [wt%]

P_{Fe2} = Content of Fe after contamination [wt%]

f_{Fe} = Fe content in contaminating steel [-], fraction between 0 and 1.

X_1 = Content of contamination compared to weight of uncontaminated sample [wt%]

X_2 = Content of contamination compared to weight of contaminated sample [wt%]

Equations:

$$X_1 = \frac{\left(P_{Fe1} - P_{Fe2}\right)}{\left(\frac{P_{Fe2}}{100} - f_{Fe}\right)},$$

$$X_2 = \frac{X_1}{\left(1 + \frac{X_1}{100}\right)}$$

Appendix 4A – Forsterite dissolution model

```
TITLE Equilibrating atmospheric CO2 with dissolving forsterite(60minW00%)
SOLUTION 1 Pure water
             temp  21.5
             unit   mol/kgw
             pH     2.084
             Cl     0.01 charge
             -water    0.5 #kg

EQUILIBRiUM_PHASES 1
       CO2(g) -3.52  1
SAVE SOLUTION 2

USER_PUNCH
       -head Time[min] Mg[mmol/kgw] Si[mmol/kgw] Forsterite[mg] olivine[%]
Area[m2] rate_pHx[mol/m2s] R_pH2[mol/m2s] rate[mol/s] deltaFo[mmol] a_corr
pH_corr SSA[m2/g]
       10 PUNCH SIM_TIME/(60)
       15 PUNCH TOT("Mg")*1000
       20 PUNCH TOT("Si")*1000
       30 PUNCH (0.003337-(TOT("Si")*0.5))*145.147*1000
       35 PUNCH GET(8)
       40 PUNCH GET(1)
       50 PUNCH GET(2)
       60 PUNCH GET(3)
       65 PUNCH GET(7)
       70 PUNCH GET(4)*1000
       80 PUNCH GET(5)
       90 PUNCH GET(6)
       100 PUNCH (GET(1)/((0.003337-(TOT("Si")*0.5))*145.147))

SELECTED_OUTPUT
      -file   60W00_HCl_rettet.sel
       -selected_out       true
       -time               false
       -ph                 true
       -user_punch         true
       -si                 forsterite
       -simulation         false
       -high_precision     false
       -state              false
       -solution           false
       -step               false
       -pe                 false
       -reaction           false
       -alkalinity         false
       -ionic_strength     false
       -water              false
       -charge_balance     false
       -percent_error      false
       -distance           false
END

USE SOLUTION 2
KINETICS 1
# Explanation:
# rate = A*exp(-Ea/RT)*ACT(H+)^-n)
#  A [mol/m2/s], Ea [kJ/mol], R [kJ/(mol*K)], T[K], reaction order n
# parms  1:surf area m2 of material 2: A 3: Ea 4: n 5:mass decrease exponent,f
# m0: initial moles of mineral# m: moles of mineral
# choose 1 gram of olivine and specific surface area of 0.08 m2/g a typical
```

```
# Fo93 145.147 g/mol, Fo100 140.6
# R = 0.008314 kJ/(K*mol), then Ea is going to be in kJ/mol also and A is in
mol/m2s.
# K1 A=0.54±0.14mol/m2s, Ea=42.6±0.8kJ/mol, n=0.50±0.004
# 86400 is seconds in 24 hours (ongest dissolution experiment).

       Forsterite
       -parms 1.55 3.467 42.6 0.5 8.4 877.17
       -m0 0.003337
       -bad_step_max 30000
       -steps 86400 in 1440
INCREMENTAL_REACTIONS true

RATES
Forsterite
-start
10 R = 0.008314
30 si_phase = SI("Forsterite")
40 sr_phase = SR("Forsterite")
50 if (M<=0 and si_phase < 0 ) THEN GOTO 1000
55 if (abs(1-sr_phase) < 0.00001) THEN GOTO 1000
60 t = 1
65 if (M0 > 0) then t = M/M0
68 if t = 0 then t = 1
80 a0 = parm(1)*parm(6)
85 area = a0*t^parm(5)
90 a0_corr = a0/area
100 n = parm(4)
110 A = parm(2)
120 Ea = parm(3)
130 pH_n = ACT("H+")^n
140 r = A*EXP(-Ea/(R*TK))*pH_n
150 pH2_corr = 0.01^n/pH_n
160 r_pH2 = r*pH2_corr
170 rate = r*area
180 moles = rate*(1-SR_phase)*TIME
184 diss_ol_pct=(M0-M)/M0*100
185 PUT (diss_ol_pct,8)
186 PUT (area,1)
187 PUT (r,2)
188 PUT (r_pH2,3)
189 PUT (rate, 7)
190 PUT (moles,4)
200 PUT (a0_corr,5)
210 PUT (pH2_corr,6)
240 if (moles > m) then moles = m
250 if (moles >= 0) then goto 1000
1000 SAVE moles
-end
END
```

Appendix 4B – Carbonation model, SI=0

```
TITLE Precipitation and solution composition of LANL carbonation experiments.
Forsterite kinetics.

SOLUTION 1 Pure water
       units  ppm
       pH     5 charge
       temp   128.0
       -water 0.003 #kg

PHASES
CO2p150(g)
       CO2 + H2O = H+ + HCO3-
       log_k -8.3570
       -analytical_expression  -1280.40497 -0.180324191 76156.3174 455.231892 -
4983328.924

EQUILIBRiUM_PHASES 1
       CO2p150(g)    2.176  10
       Magnesite     0.0    0.0
       SiO2(am)      0.0    0.0

USE EQUILIBRiUM_PHASES 1
USE SOLUTION 1
SAVE SOLUTION 2
END

USER_PUNCH #
       -head Time[h] Mg[mmol/kgw] Si[mmol/kgw] olivine(s)[mol] Ol_dissolved[%]
       10 PUNCH SIM_TIME/(3600)
       15 PUNCH TOT("Mg")*1000
       20 PUNCH TOT("Si")*1000
       35 PUNCH GET(8)
       40 PUNCH 100-GET(8)/0.003165*100

SELECTED_OUTPUT
       -file   60W00_LANL.sel
       -selected_out       true
       -temperature        true
       -time               false
       -ph                 true
       -user_punch         true
       -totals             C
       -activities         CO2 HCO3- MgHCO3+ CO3-2
       -equilibrium_phases Magnesite SiO2(am)
       -si                 Forsterite Magnesite SiO2(am)
       -simulation         false
       -high_precision     false
       -state              false
       -solution           false
       -step               false
       -pe                 false
       -reaction           false
       -alkalinity         false
       -ionic_strength     false
       -water              false
       -charge_balance     false
       -percent_error      false
       -distance           false
END
```

```
KINETICS 1
# Explanation:
# rate = A*exp(-Ea/RT)*ACT(H+)^-n)
# A [mol/m2/s], Ea [kJ/mol], R = kJ/(K*mol) [kJ/(mol*K)],T[K],reaction order n
# parms 1: surf area m2 of material present 2: A 3: Ea 4: n 5:mass decrease
exponent (f) 6:fm
# m0: initial moles of mineral# m: moles of mineral
# Fo93 145.147 g/mol, Fo100 140.6
# R=0.008314kJ/(K*mol), logA=0.54±0.14(mol/m2s), Ea=42.6±0.8kJ/mol,
n=0.50±0.004
# 3600 is seconds in 1 hour.

       Forsterite
       -parms 1.47 3.467 42.6 0.5 0.667 1
       -m0 0.003172
       -bad_step_max 30000
       -steps 3600 in 60
INCREMENTAL_REACTIONS true

RATES
Forsterite
-start
10 R = 0.008314
30 si_phase = SI("Forsterite")
40 sr_phase = SR("Forsterite")
50 if (M<=0 and si_phase < 0 ) THEN GOTO 1000
55 if (abs(1-sr_phase) < 0.00001) THEN GOTO 1000
60 t = 1
65 if (M0 > 0) then t = M/M0
68 if t = 0 then t = 1
80 a0 = parm(1)*parm(6)
85 area = a0*t^parm(5)
90 a0_corr = a0/area
100 n = parm(4)
110 A = parm(2)
120 Ea = parm(3)
130 pH_n = ACT("H+")^n
140 r = A*EXP(-Ea/(R*TK))*pH_n
150 pH2_corr = 0.01^n/pH_n
160 r_pH2 = r*pH2_corr
170 rate = r*area
180 moles = rate*(1-SR_phase)*TIME
184 mol_ol_s=M
185 PUT (mol_ol_s,8)
186 PUT (area,1)
187 PUT (r,2)
188 PUT (r_pH2,3)
189 PUT (rate, 7)
190 PUT (moles,4)
200 PUT (a0_corr,5)
210 PUT (pH2_corr,6)
240 if (moles > m) then moles = m
250 if (moles >= 0) then goto 1000
1000 SAVE moles
-end
END

USE SOLUTION 2
USE EQUILIBRIUM_PHASES 1
USE KINETICS 1

END
```

Appendix 4C – Saturation modeling

Modeling of saturation indices requires the cation distribution obtained with water analysis. Without further information of the composition of the water sample at experimental conditions, both pH and carbonate species concentrations are unknown. There are several possible approaches to determine pH and carbonate species, and two alternatives are presented here.

1: Assuming HCO_3^- to be the dominating carbonate species, charge balance with the cations in solution can be used to obtain the concentration. This alternative requires a guess of the pH. pH was obtained from the theoretical dissolution of forsterite under the same conditions and in contact with CO_2. This approach is very sensitive to the chosen pH which is dependent of the reaction path and carbonation equilibrium. Since the pH is found with an idealized olivine dissolution reaction, the obtained SI of relevant models are at its best a good estimate.

2: Using stoichiometry of the olivine dissolution and charge balance, Mg and Fe in the solution can be balanced with HCO_3^-. HCO_3^- is hence manually calculated and pH is found by automatic charge balance.

To illustrate the possibility to include several water samples in the same model 2 water samples are used in the example. Alternative two results in general in a slightly higher pH than alternative 1. Which phases to include in the selected_output section can be determined by the SI found in the output file over all possible minerals with the defined elements available.

Alternative 1

```
TITLE Saturation indices for carbonation water samples at experimental
temperature and approximately pressure using charge balance of the HCO3-
concentration and assuming pH = 2.58.
PHASES
CO2p100(g)
  CO2 + H2O = H+ + HCO3-
  log_k -8.1932
  -analytical_expression  -2121.595299 -0.291434313 126398.6965 754.9611419 -
8156166.875
CO2p125(g)
  CO2 + H2O = H+ + HCO3-
  log_k -8.2836
  -analytical_expression  -1764.152261 -0.243684483 105266.8741 627.389327 -
6842803.702
CO2p150(g)
  CO2 + H2O = H+ + HCO3-
  log_k -8.3570
  -analytical_expression  -1280.40497 -0.180324191 76156.3174 455.231892 -
4983328.924
CO2p200(g)
  CO2 + H2O = H+ + HCO3-
  log_k -8.4722
  -analytical_expression  -982.8117629 -0.143447585 57478.33779 350.1252911 -
3736812.744
END
SELECTED_OUTPUT
      -file   SI_water samples H_L_short.sel
       -percent_error
       -si CO2(g) CO2p125(g) Magnesite Quartz Siderite SiO2(am)
       -simulation       false
       -state            false
       -solution         true
       -distance         false
       -time             false
       -step             false
       -ph               true
       -pe               false
       -temperature      true
       -activities  CO2  HCO3-  CO3-2
       -totals   C  C(4)
END
SOLUTION     1
temp   185
pH     4.58
units  mmol/L
Si     7.52812
Mg     4.88631
Fe     3.937425
K      0.345644
Ni     0.36505913625
Na     0.079308603
Mn     0.0637512772
Ca     0.0268391712
C(4)   17.64747     charge

SOLUTION     2
temp   185
pH     4.58
```

```
units  mmol/L
Si     3.6517
Mg     4.91062
Fe     0.04652053675
K      0.40273
Ni     0.05304842375
Na     0.1395493
Mn     0.0042034594
Ca     0.0124736976
C(4)   9.9142810735 charge
END
EQUILIBRIUM_PHASES 1
       CO2p125(g) 2.176    10
EQUILIBRIUM_PHASES 2
       CO2p125(g) 2.176    10
REACTION_TEMPERATURE 1
       185
REACTION_TEMPERATURE 2
       185
USE SOLUTION 1
USE EQUILIBRIUM_PHASES 1
USE REACTION_TEMPERATURE 1
END
USE SOLUTION 2
USE EQUILIBRIUM_PHASES 2
USE REACTION_TEMPERATURE 2
END
```

Alternative 2

```
TITLE Saturation indices for carbonation water samples at experimental
temperature and approximately pressure
PHASES
CO2p100(g)
  CO2 + H2O = H+ + HCO3-
  log_k -8.1932
  -analytical_expression  -2121.595299 -0.291434313 126398.6965 754.9611419 -
8156166.875
CO2p125(g)
  CO2 + H2O = H+ + HCO3-
  log_k -8.2836
  -analytical_expression  -1764.152261 -0.243684483 105266.8741 627.389327 -
6842803.702
CO2p150(g)
  CO2 + H2O = H+ + HCO3-
  log_k -8.3570
  -analytical_expression  -1280.40497 -0.180324191 76156.3174 455.231892 -
4983328.924
CO2p200(g)
  CO2 + H2O = H+ + HCO3-
  log_k -8.4722
  -analytical_expression  -982.8117629 -0.143447585 57478.33779 350.1252911 -
3736812.744
END
SELECTED_OUTPUT
      -file   SI_water pH charge.sel
       -percent_error
       -si CO2(g) CO2p125(g) Magnesite Quartz Siderite SiO2(am)
       -simulation       false
       -state            false
```

```
       -solution         true
       -distance         false
       -time             false
       -step             false
       -ph               true
       -pe               false
       -temperature true
       -activities  CO2  HCO3-  CO3-2
       -totals   C  C(4)
END
SOLUTION     1
temp   185
pH     4.58   charge
units  mmol/L
Si     7.52812
Mg     4.88631
Fe     3.937425
K      0.345644
Ni     0.36505913625
Na     0.079308603
Mn     0.0637512772
Ca     0.0268391712
C(4)   17.64747
SOLUTION     2
temp   185
pH     4.58   charge
units  mmol/L
Si     3.6517
Mg     4.91062
Fe     0.04652053675
K      0.40273
Ni     0.05304842375
Na     0.1395493
Mn     0.0042034594
Ca     0.0124736976
C(4)   9.9142810735
END
EQUILIBRIUM_PHASES 1
       CO2p125(g) 2.176    10
EQUILIBRIUM_PHASES 2
       CO2p125(g) 2.176    10
REACTION_TEMPERATURE 1
       185
REACTION_TEMPERATURE 2
       185
USE SOLUTION 1
USE EQUILIBRIUM_PHASES 1
USE REACTION_TEMPERATURE 1
END

USE SOLUTION 2
USE EQUILIBRIUM_PHASES 2
USE REACTION_TEMPERATURE 2
END
```